IIMEC 2012

SUMMER SCHOOL IN ADVANCED COMPOSITE MATERIALS

International Institute for Multifunctional Materials for Energy Conversion

Composite Materials: Mechanical Behaviour & Testing

By Alkis Paipetis
University of Ioannina

Technological Education Institute of Serres, Greece. July 2 – 6, 2012


4
USA

DEFINITIONS

- COMPOSITES:

  --Multi phase materials with measurable pw fraction of every phase

- Matrix:
  - --Continuous phase
  - --Role:
    - •Stress transfer to other reinforcing phases
    - •Environmental protection
  - --Classification: MMC, CMC, PMC

metal ceramic polymer

- Reinforcement:
  - -- Discontinuous or dispersed phsae
  - -- Role:
    - MMC: increase s_y, TS, creep resistance
    - CMC: increase toughness
    - PMC: increase E, s_y, TS, creep resistance
  - -- Classification : particles, fibres, structural

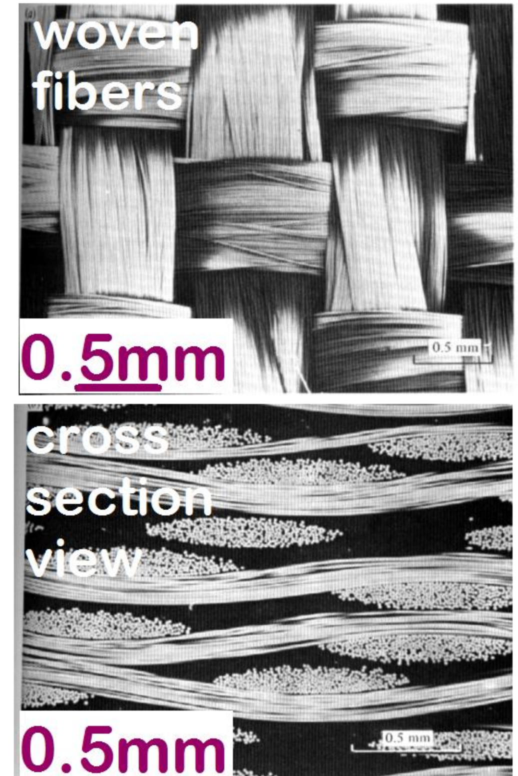

D. Hull and T.W. Clyne, *An Introduction to Composite Materials*, 2nd ed., Cambridge University Press, New York, 1996, Fig. 3.6, p. 47.

Composites

(a)

particles | fibres | Structural

- **Examples:**

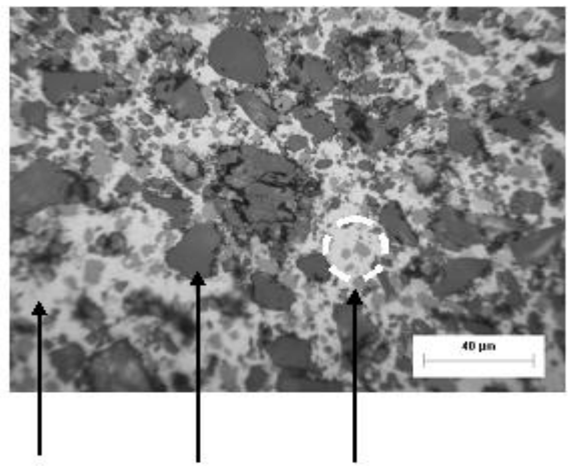

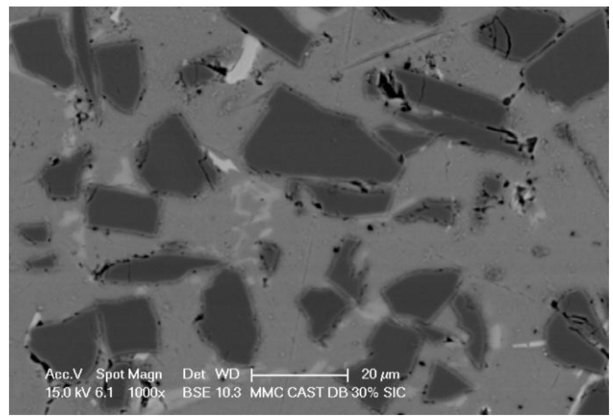

Al / SiC MMCs for aerospace automotive industry,

Reprinted with permission from D. Myriounis, University of Ioannina

-Automobile tires

matrix: rubber (compliant)

(b)

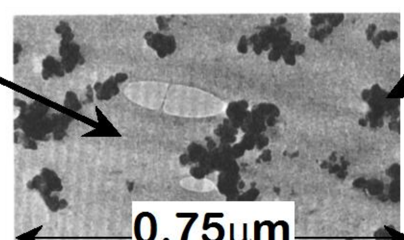

particles: C (stiffer)

Adapted from Fig. 16.5, *Callister 6e*. (Fig. 16.5 is courtesy Goodyear Tire and Rubber Company.)

Composites: FIBRES I

particles | **fibres** | structural

- **Continuous aligned fibres**
- **E.g.**

--Metals: $\gamma'(Ni_3Al)$-α(Mo)
Eutectic composition.

--Glass w/SiC fibers
E_{glass} = 76GPa; E_{SiC} = 400GPa.

matrix: α (Mo) (ductile)

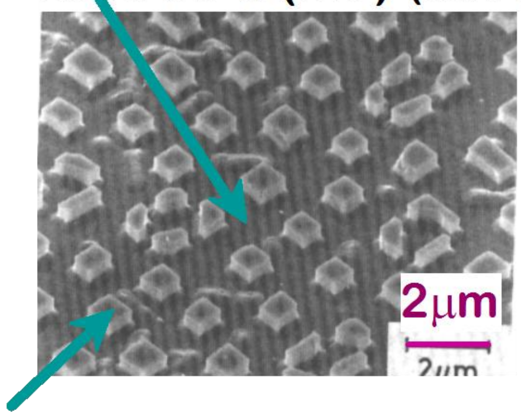

fibers: γ' (Ni_3Al) (brittle)

From W. Funk and E. Blank, "Creep deformation of Ni3Al-Mo in-situ composites", *Metall. Trans. A* Vol. 19(4), pp. 987-998, 1988. Used with permission.

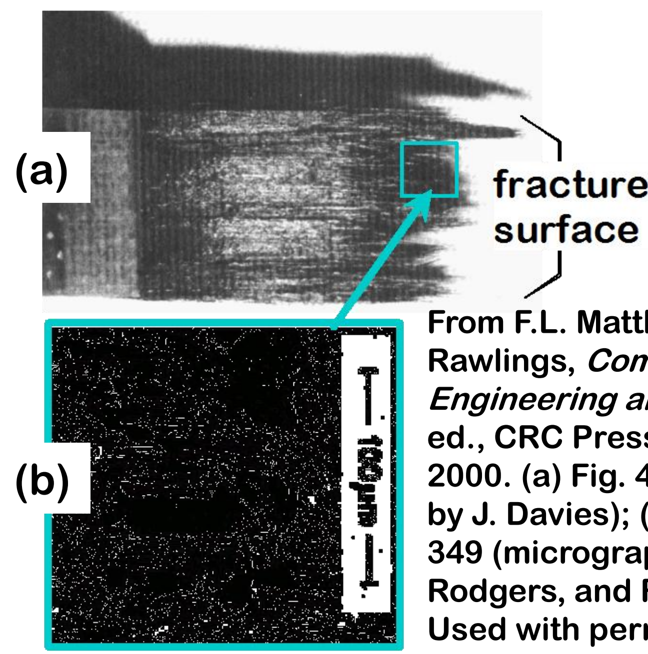

From F.L. Matthews and R.L. Rawlings, *Composite Materials; Engineering and Science*, Reprint ed., CRC Press, Boca Raton, FL, 2000. (a) Fig. 4.22, p. 145 (photo by J. Davies); (b) Fig. 11.20, p. 349 (micrograph by H.S. Kim, P.S. Rodgers, and R.D. Rawlings). Used with permission of CRC Press, Boca Raton, FL.

Composites: FIBRES II

particles | **fibres** | structural

- Discontinuous randomly dispersed 2D fibres

- E.g: Carbon-Carbon
  --manufacturing: fibre/pitch,
  and pyrolysis at 2500C.
  --use: brakes, turbines,
  protective shells

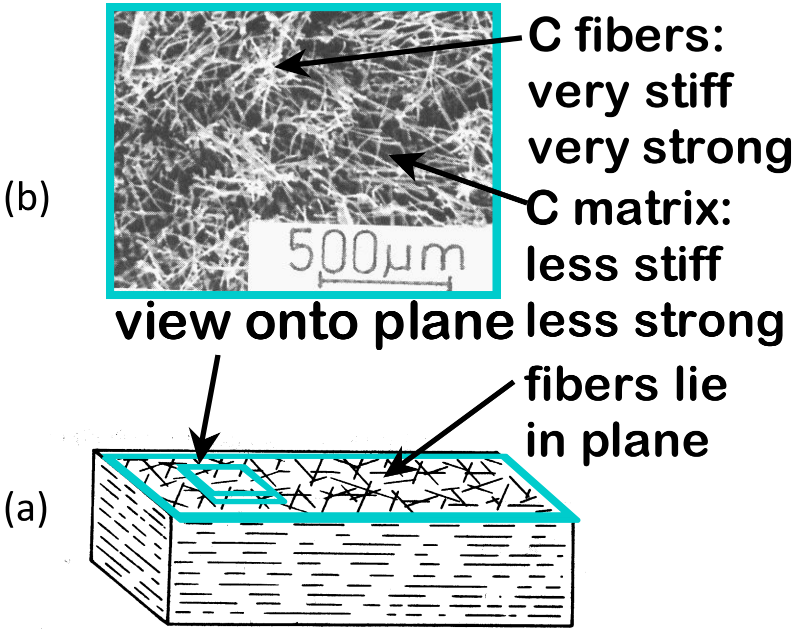

Adapted from F.L. Matthews and R.L. Rawlings, *Composite Materials; Engineering and Science*, Reprint ed., CRC Press, Boca Raton, FL, 2000. (a) Fig. 4.24(a), p. 151; (b) Fig. 4.24(b) p. 151. (Courtesy I.J. Davies) Reproduced with permission of CRC Press, Boca Raton, FL.

- Additionally:
  -- Discontinuous randomly dispersed 3D fibres
  -- Discontinuous , 1D fibres

Composites: Structural

Particles | Fibres | **Structural**

- Composite Laminates
  - -- Lamination: e.g., [0/90]s
  - -- Benefit: balanced, in plane stiffness

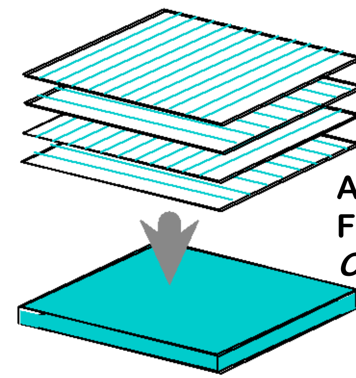

Adapted from Fig. 16.16, *Callister 6e*.

- Sandwich
  - -- Low density, honeycomb core
  - -- Benefit: weight, Flexural stiffness

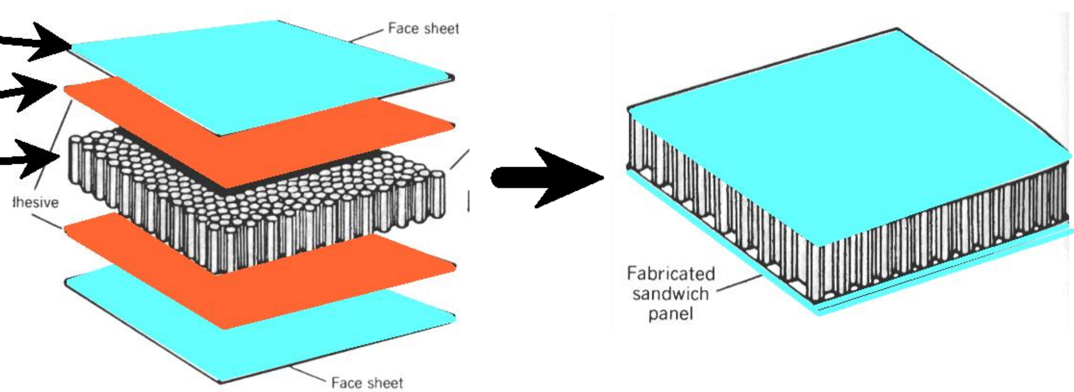

Adapted from Fig. 16.17, *Callister 6e*. (Fig. 16.17 is from *Engineered Materials Handbook*, Vol. 1, *Composites*, ASM International, Materials Park, OH, 1987.

Composites: Benefits

- CMCs: **Toughness**

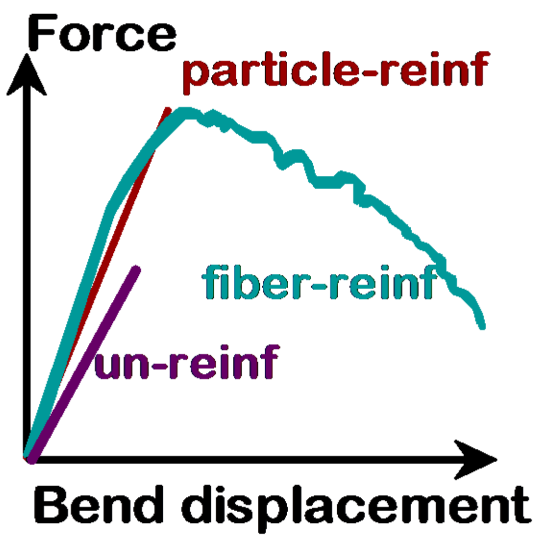

- PMCs: **Large E/ρ**

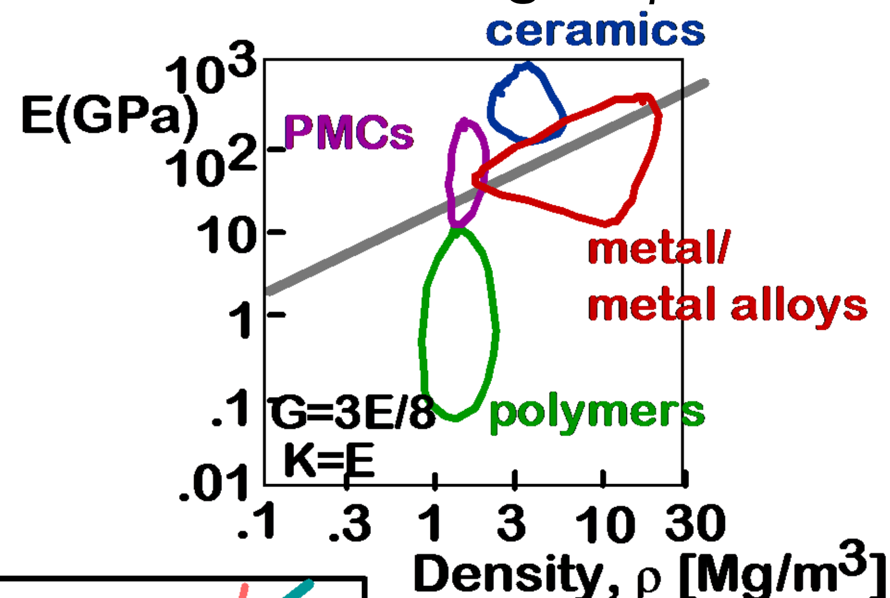

- MMCs:

  creep resistance

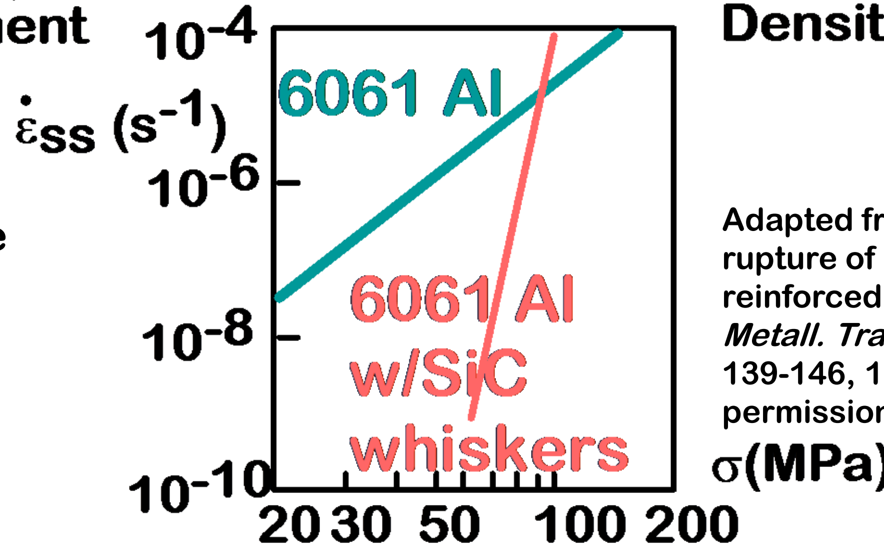

Adapted from T.G. Nieh, "Creep rupture of a silicon-carbide reinforced aluminum composite", *Metall. Trans. A* Vol. 15(1), pp. 139-146, 1984. Used with permission.

Composites: A hierarchical structure

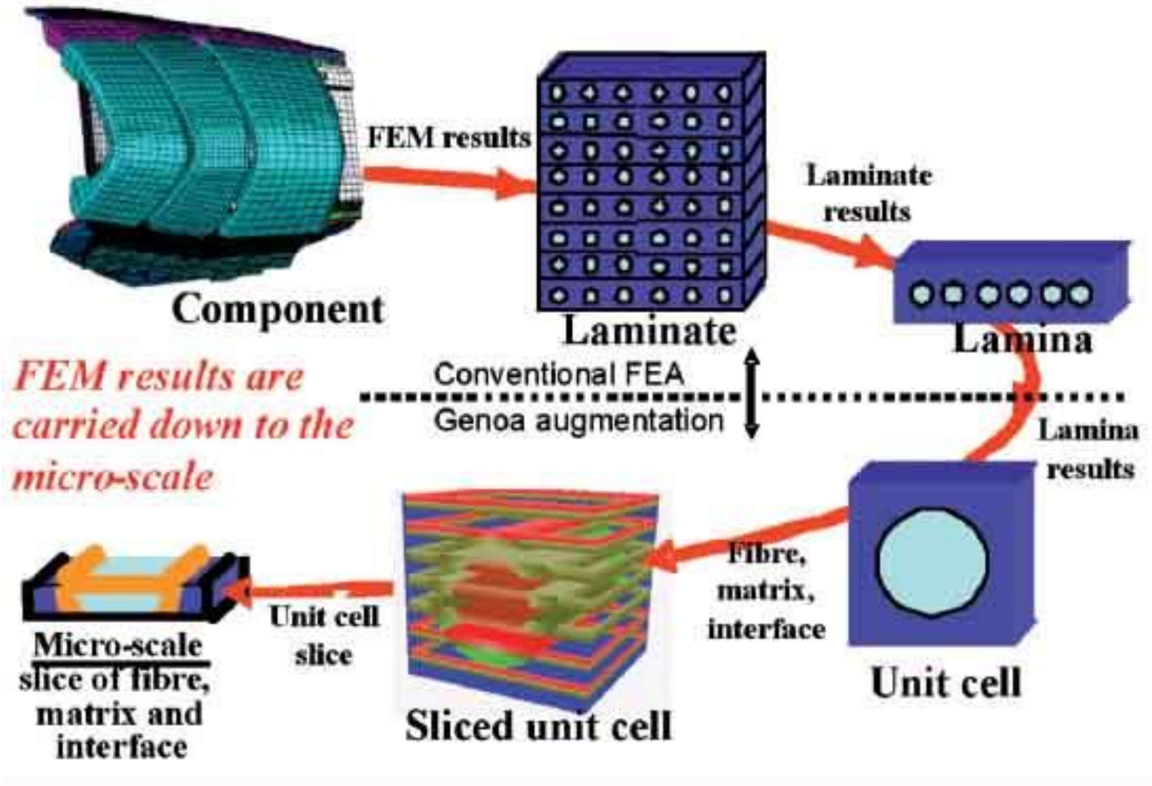

Fig. 1: Hierarchical modelling from the structural scale to the micro-scale - transmission of the FEA results at the structural scale down to the micro-scale

http://www.jeccomposites.com/news/composites-news/progressive-failure-dynamic-analysis-composite-structures

1. The interface the scale of the interface

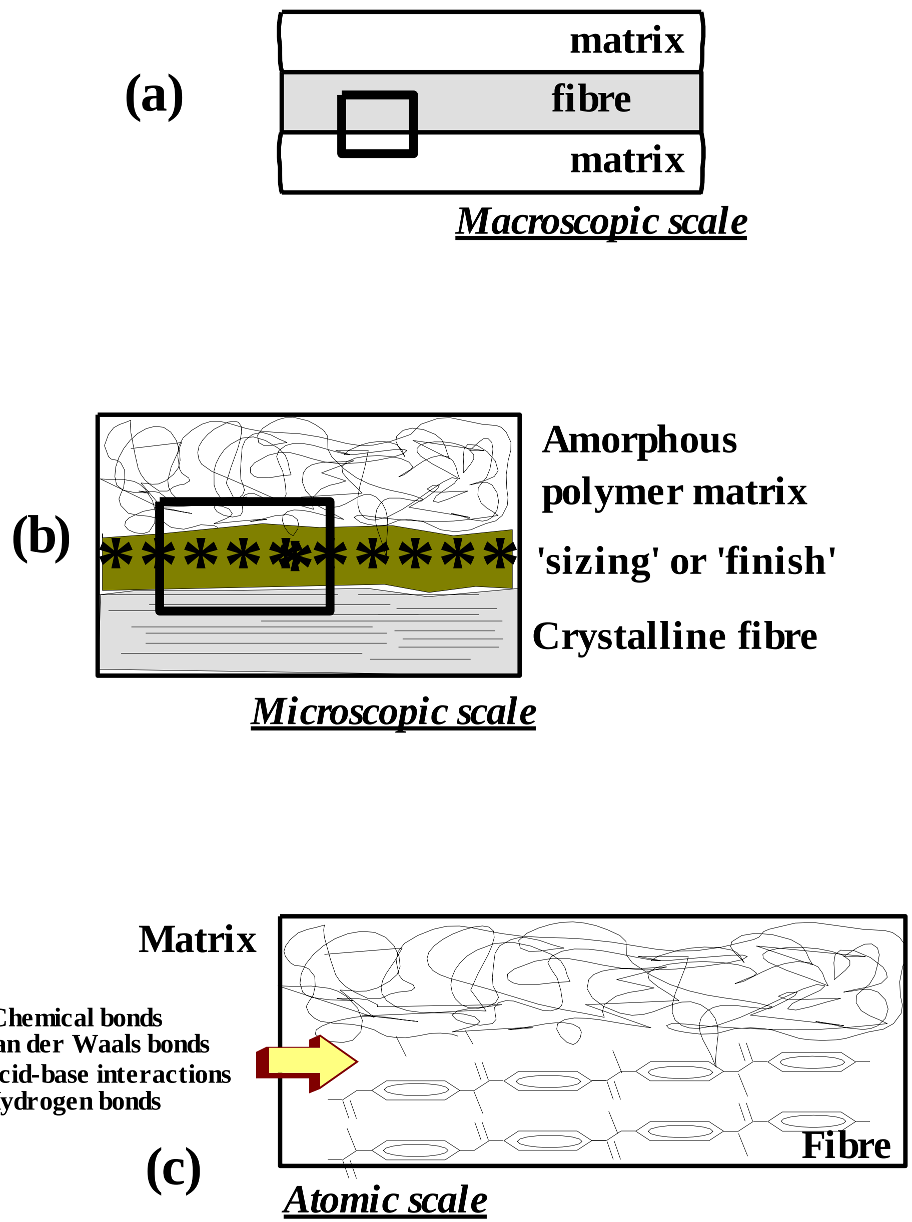

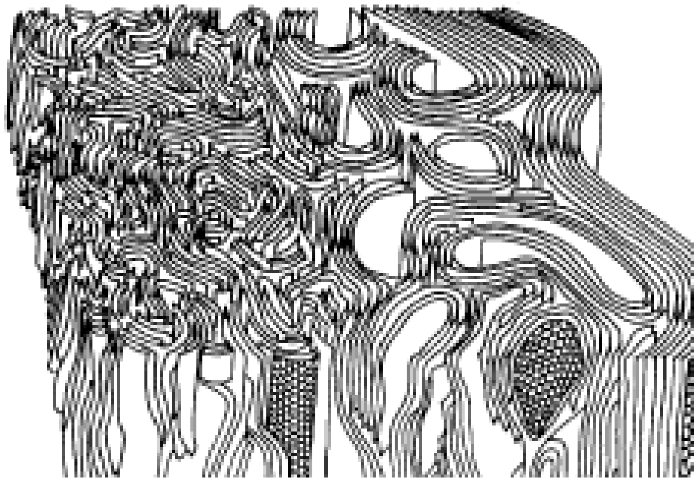

Adhesion Mechanisms: Microstructure and Adhesion

- For carbon fibres, adhesion depends on the angel of the basal plane with the symmetry axis of the fibre. The plane edges are usually the sites of chemical reaction.
    - Smaller angle means better alignment and reinforcement but worse stress transfer.
    - Oxidative treatment improves adhesion by removing exernal planes and creating edges [**Drzal, 1983**].

The nature of the interface[Drzal, 1990]

interface:
a function of thermal, mechanical and chemical environment

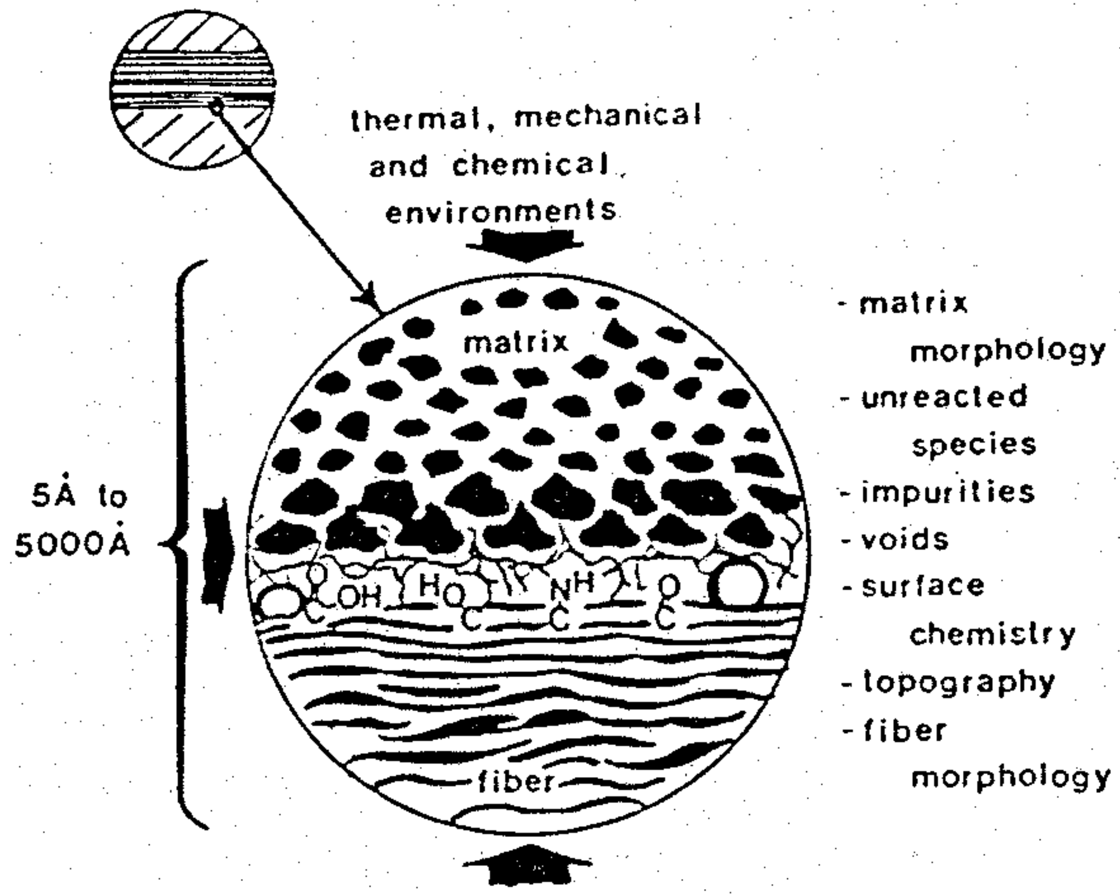

Ceramic Matrix Composites

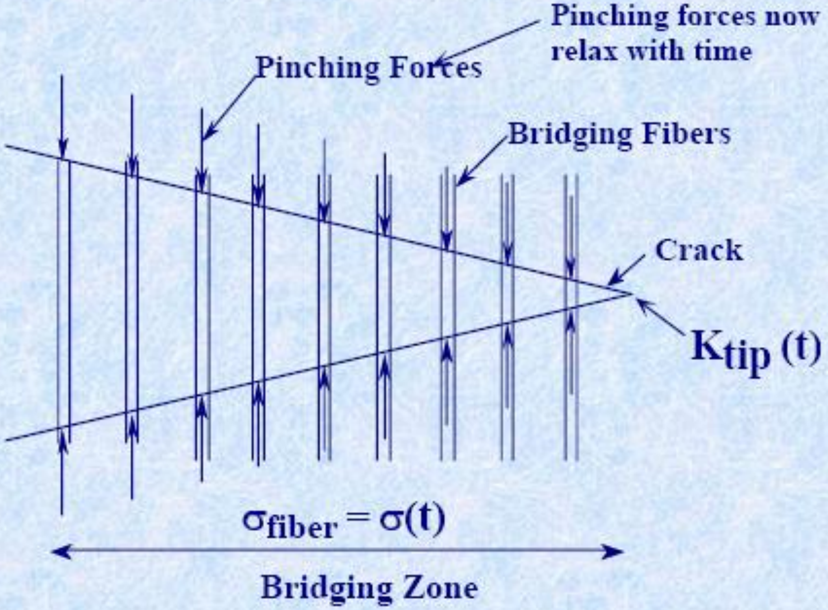

Bridged crack in SiC/SiC composite

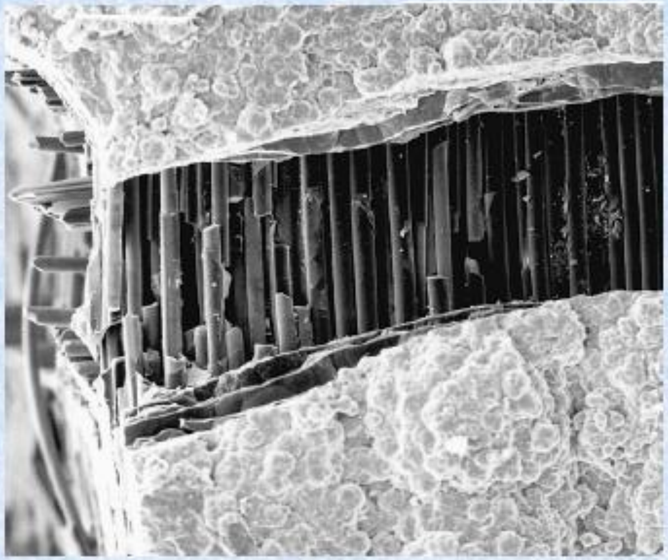

Polymer Matrix Composites (Reifsnider, 1994)

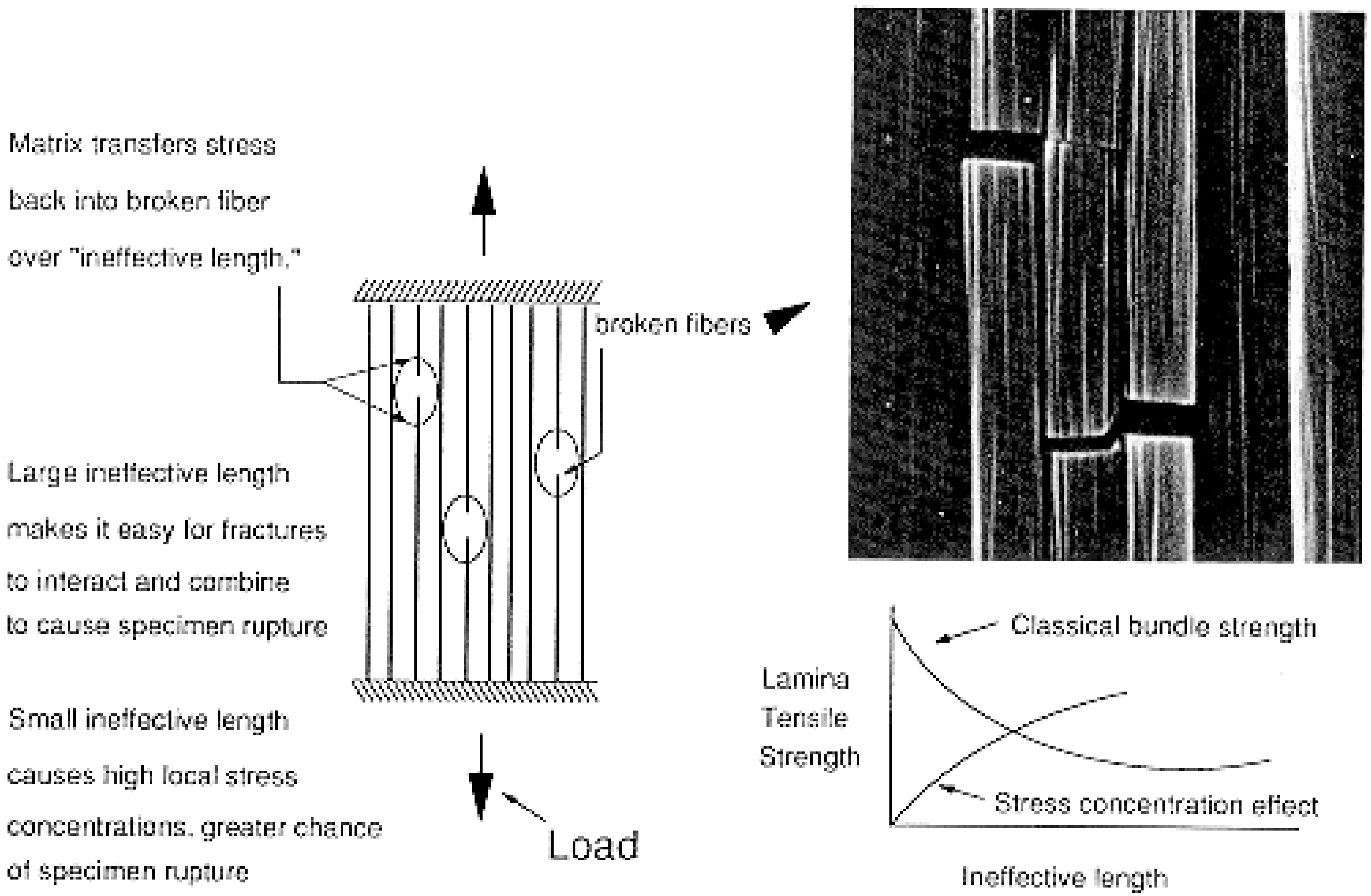

Advanced Polymer Matrix Composites

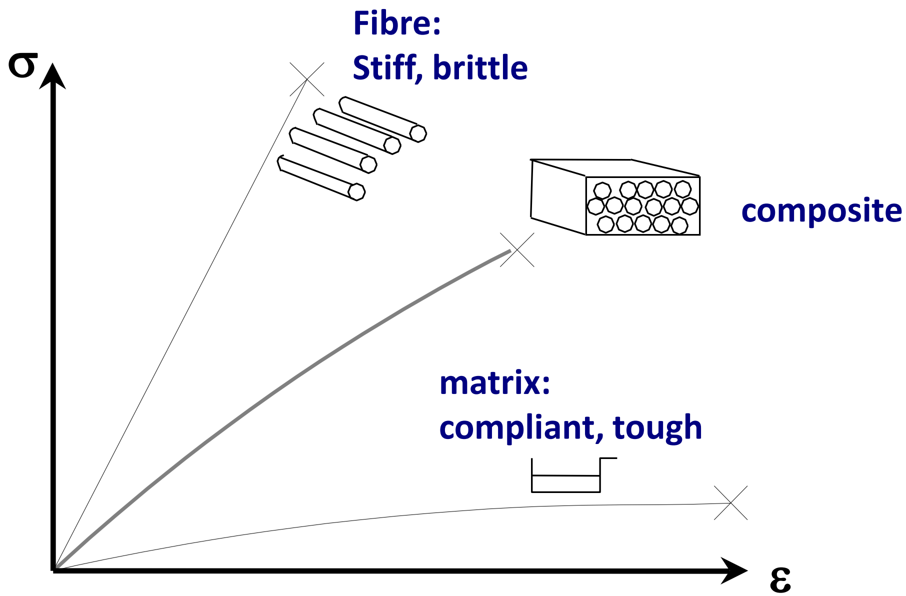

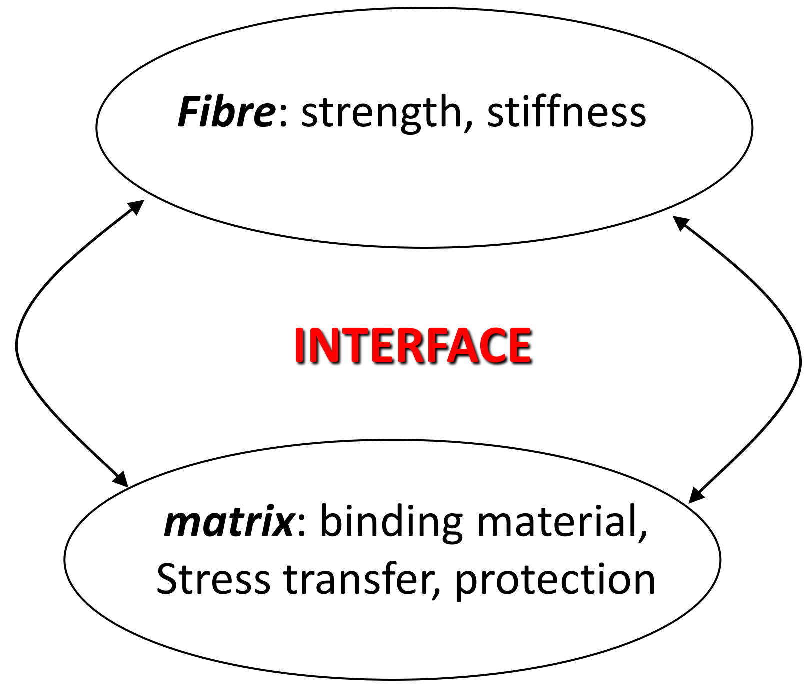

The rule of mixtures:

$$\sigma = \sigma_f V_f + \sigma_m V_m$$

Interface:
a function of mechanical thermal and chemical enviroment/history

Composites: Fracture & Stress Concentration

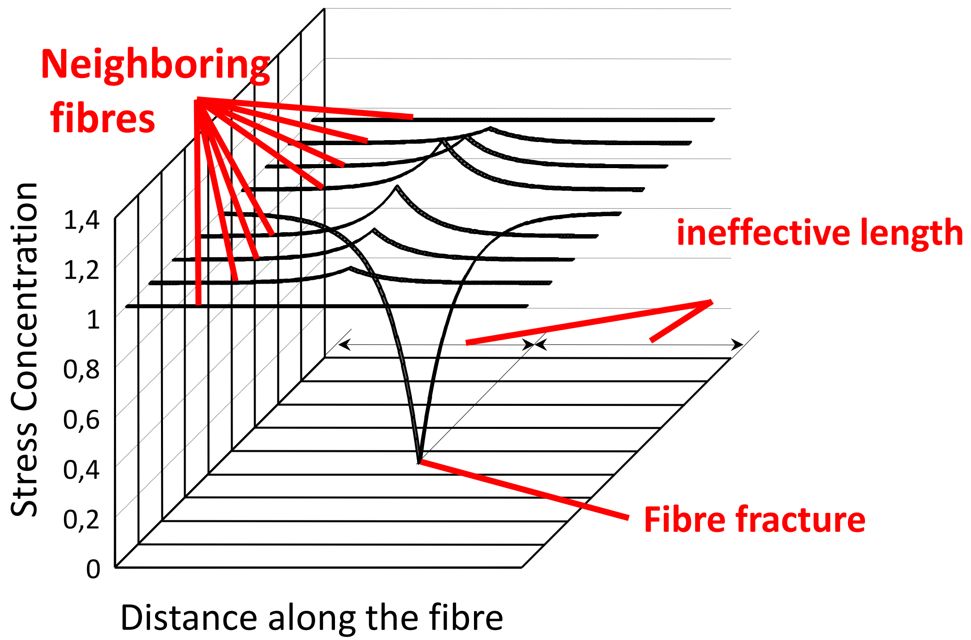

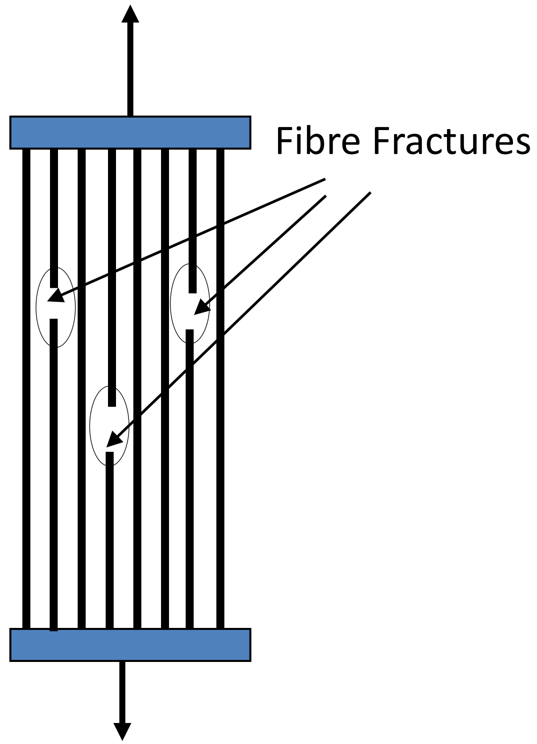

- The matrix transfers the stress through the interface along the “ineffective length”.
- Large “ineffective length” leads to the magnification of the volume of influence of the fracture and increases the possibility of multiple fracture interaction.
- Small “ineffective length” leads to high stress concentrations and brittle failure.

Interface and strength

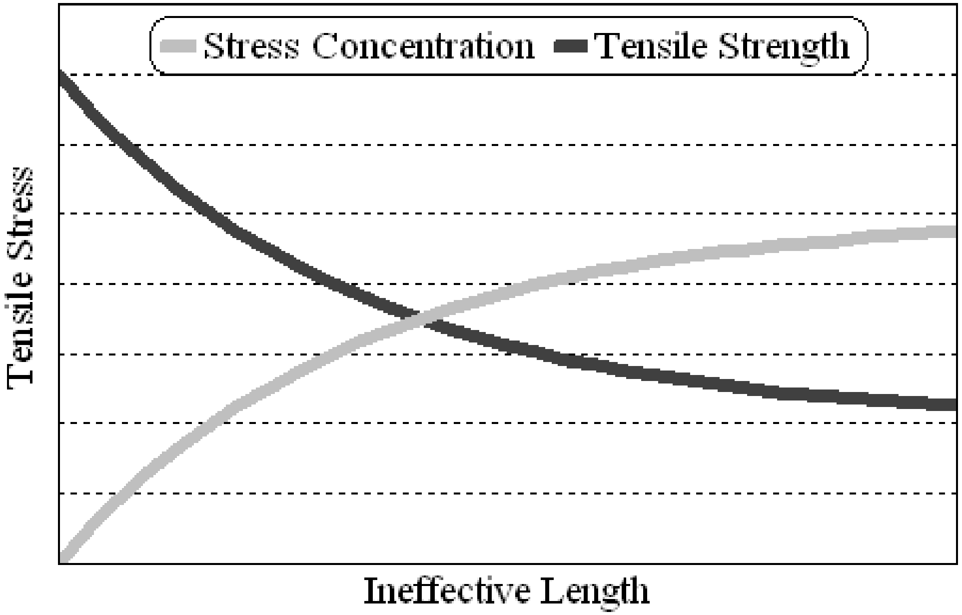

(a)

(a) Strength as a function of the transfer length

Failure of the interface

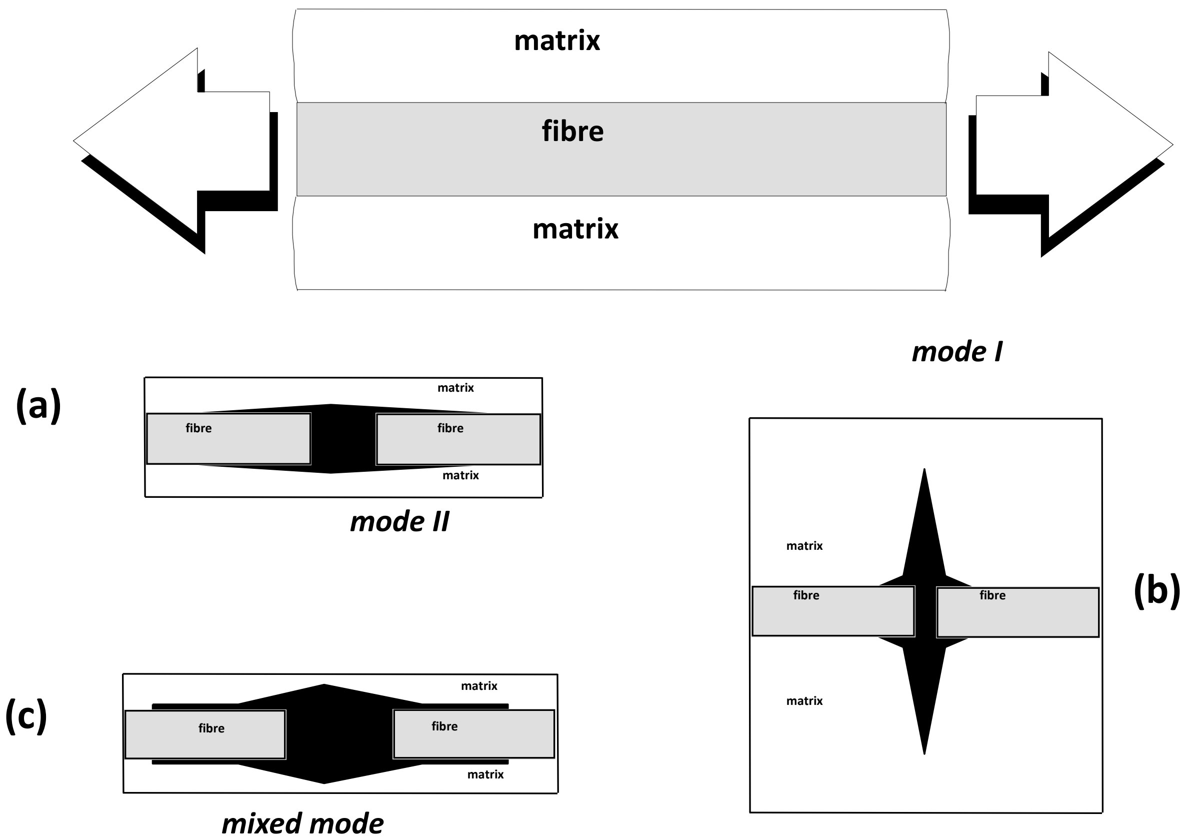

Stress transfer at the interface

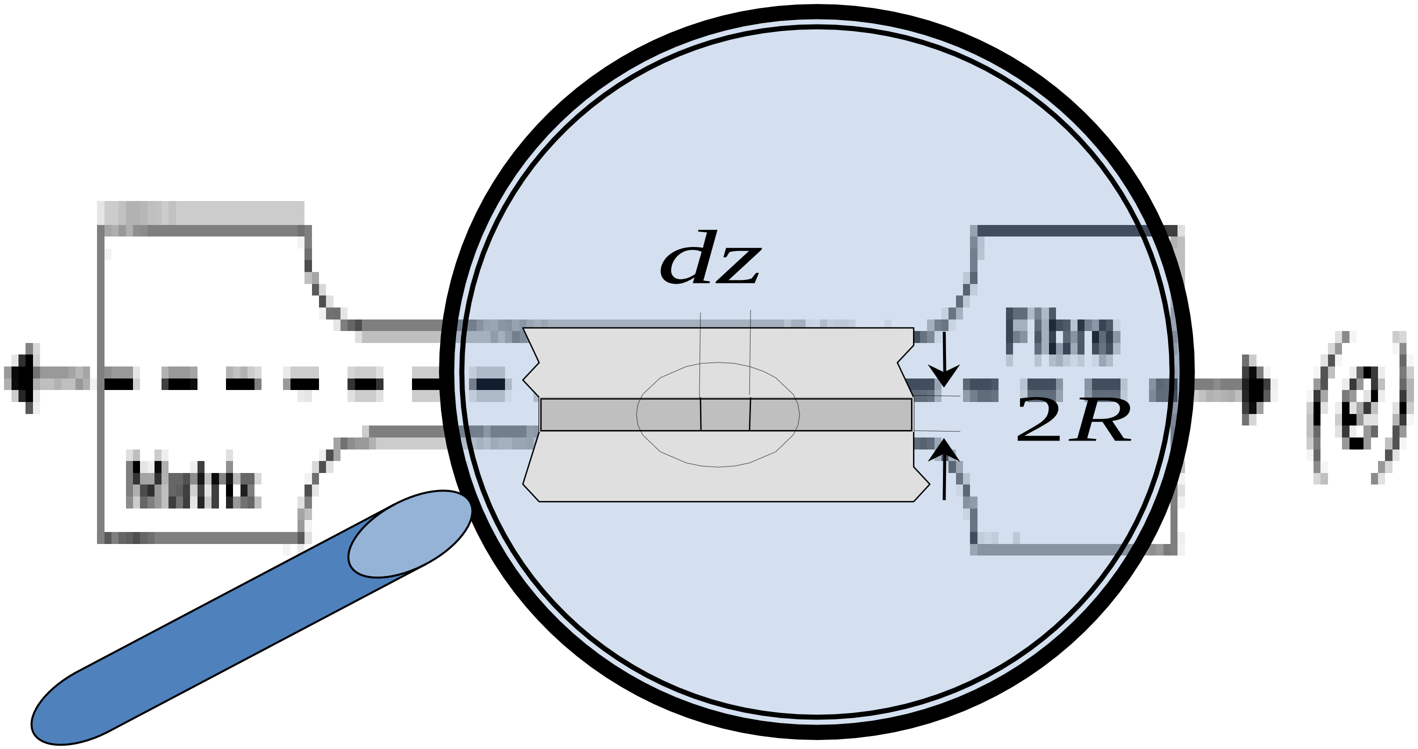

Shear stress at the interface

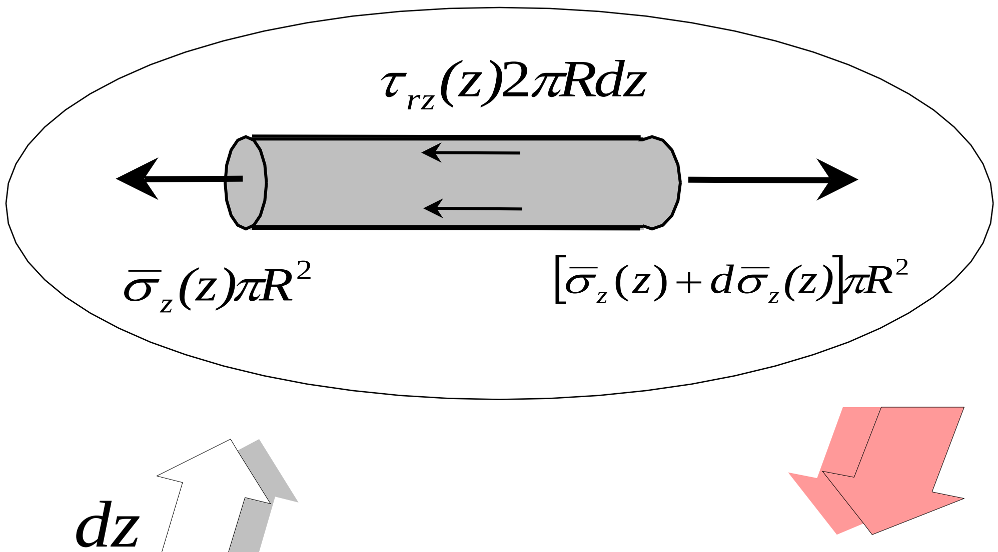

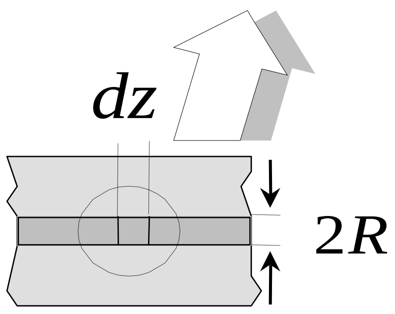

$$\tau_{rz} = -\frac{R}{2}\frac{d\bar{\sigma}_z(z)}{dz}$$

Simple models of stress transfer

- Shear lag (Cox 1952)
- Constant shear (Kelly 1965)
- Mixed models(Piggott 1980)

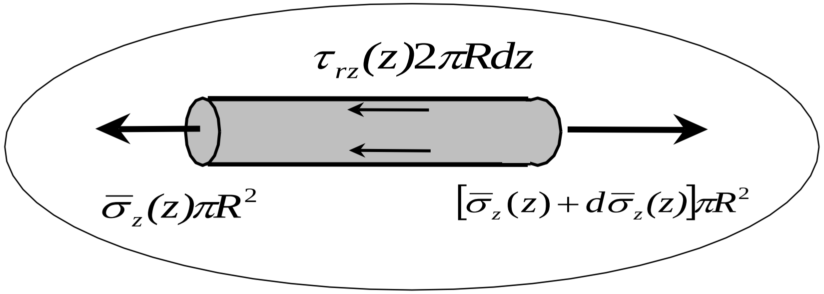

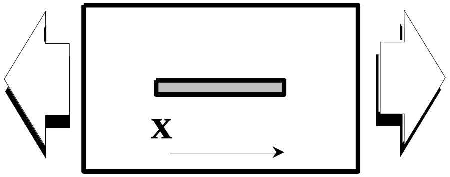

Shear lag (Cox 1952)

- Assuming that the shear force depends linearly on the difference between the actual axial translation and the one that would be if the fibre were not present:

$$S = H(w - w_\infty)$$

$$\frac{\partial^2 \sigma_z(z)}{\partial z^2} - \beta^2 \sigma_z(z) = -\beta^2 E_f \varepsilon_\infty$$

- where

$$\beta = \sqrt{\frac{2G_m^{R_\infty}}{R^2 E_f \, \boldsymbol{ln}\left(\frac{R_\infty}{R}\right)}}$$

-

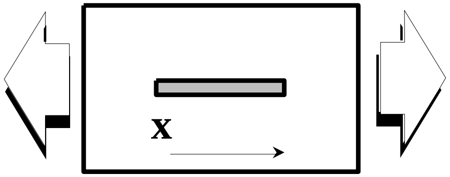

Shear lag (Cox 1952)

$$\sigma_z(z) = E_f \varepsilon_\infty \left[1 - \frac{\cosh\left(\beta\left(\frac{l}{2} - z\right)\right)}{\cosh\left(\beta \frac{l}{2}\right)} \right]$$

$$\tau_{rz}(z) = E_f \varepsilon_\infty \sqrt{\frac{G_m^{R_\infty}}{2E_f \ln\left(\frac{R_\infty}{R}\right)}} \frac{\sinh \beta\left(\frac{l}{2} - z\right)}{\cosh \beta \frac{l}{2}}$$

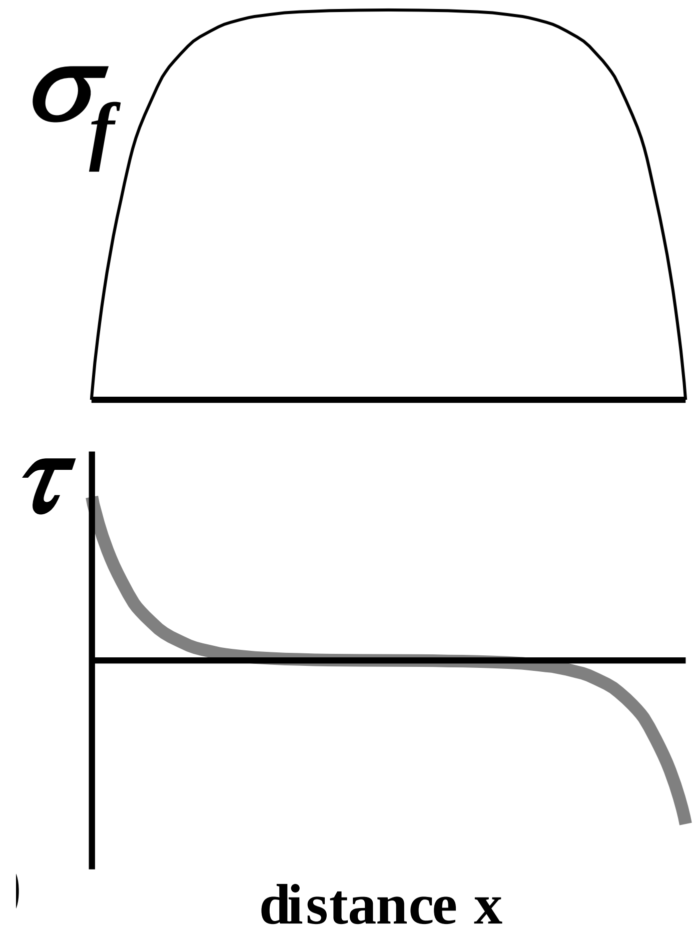

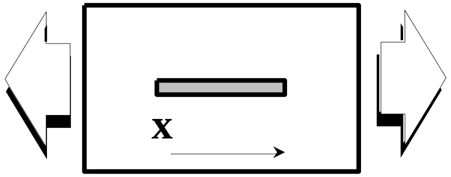

Constant shear (Kelly 1965)

•Kelly & Tyson [**1965**] assumed that shear at the interface is constant. From the equilibrium equation:

•

$$\tau_{rz} = -\frac{R\sigma_{fu}}{l_c}$$

•In this case the axial stress coincides with the strength of the fibre which is independent of z*.*

•*lc* is the critical length or the length needed to reach the strength of the fibre σ_f before fracture.

•The approach assumes a brittle fibre in a perfectly plastic matrix

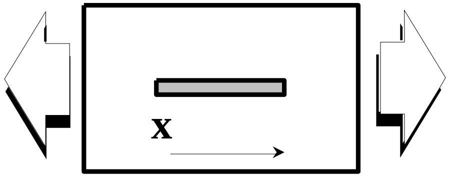

Constant shear (Kelly 1965)

$$\tau_{rz} = -\frac{R\sigma_{fu}}{l_c}$$

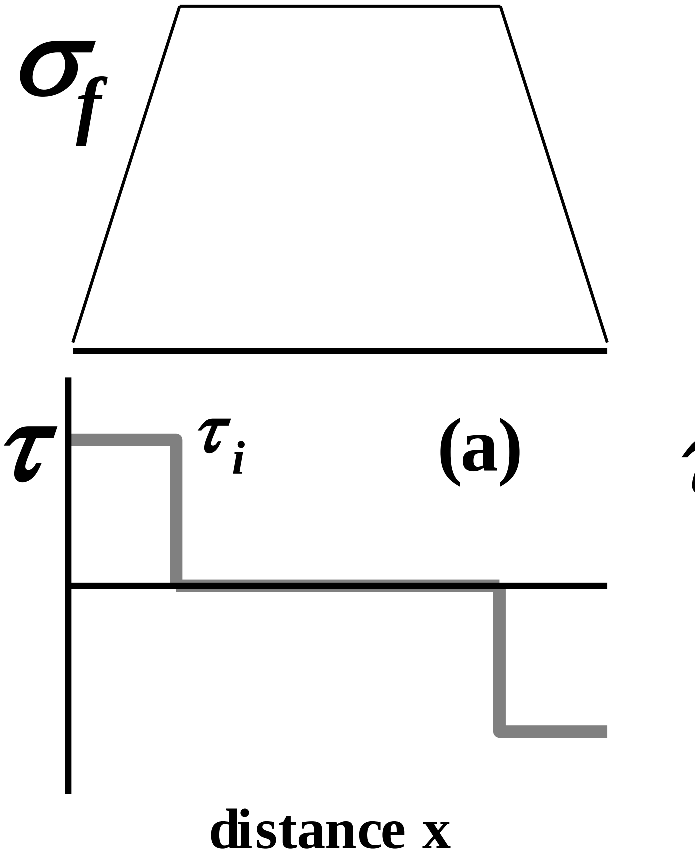

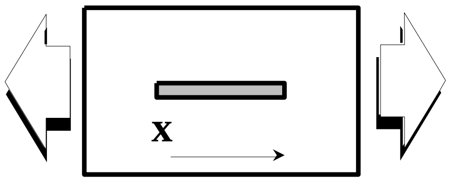

Mixed models (Piggot 1980)

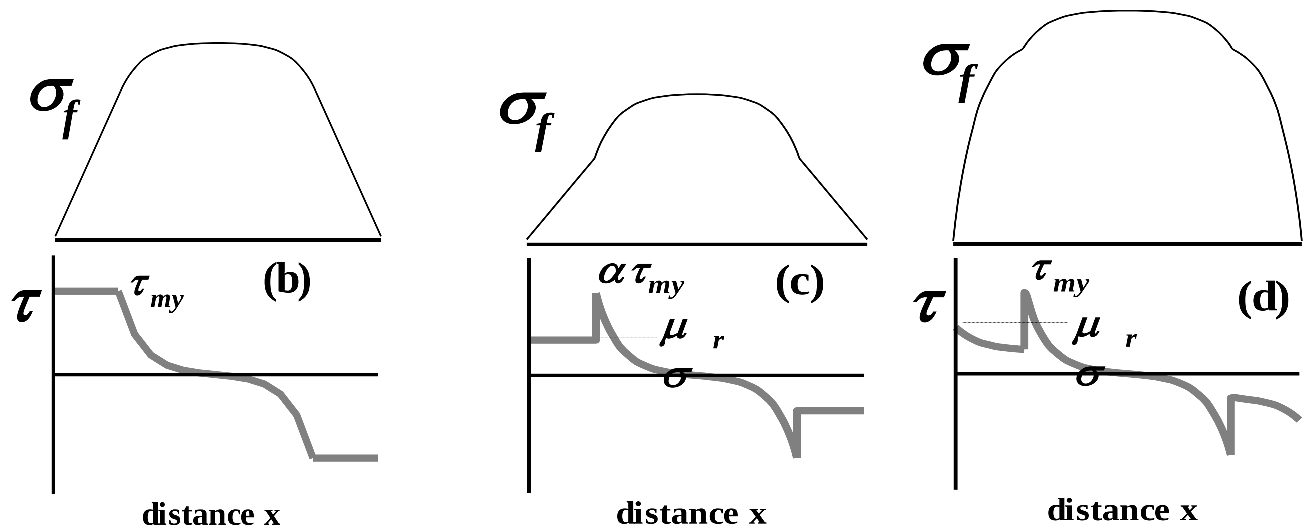

(a) (b) (c)

Experimental study of the stress transfer

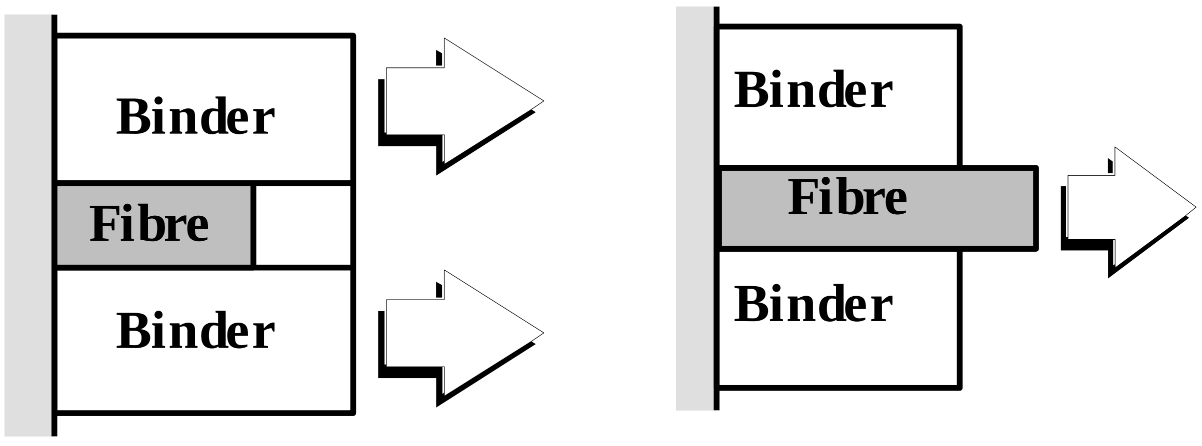

Interfacial tests

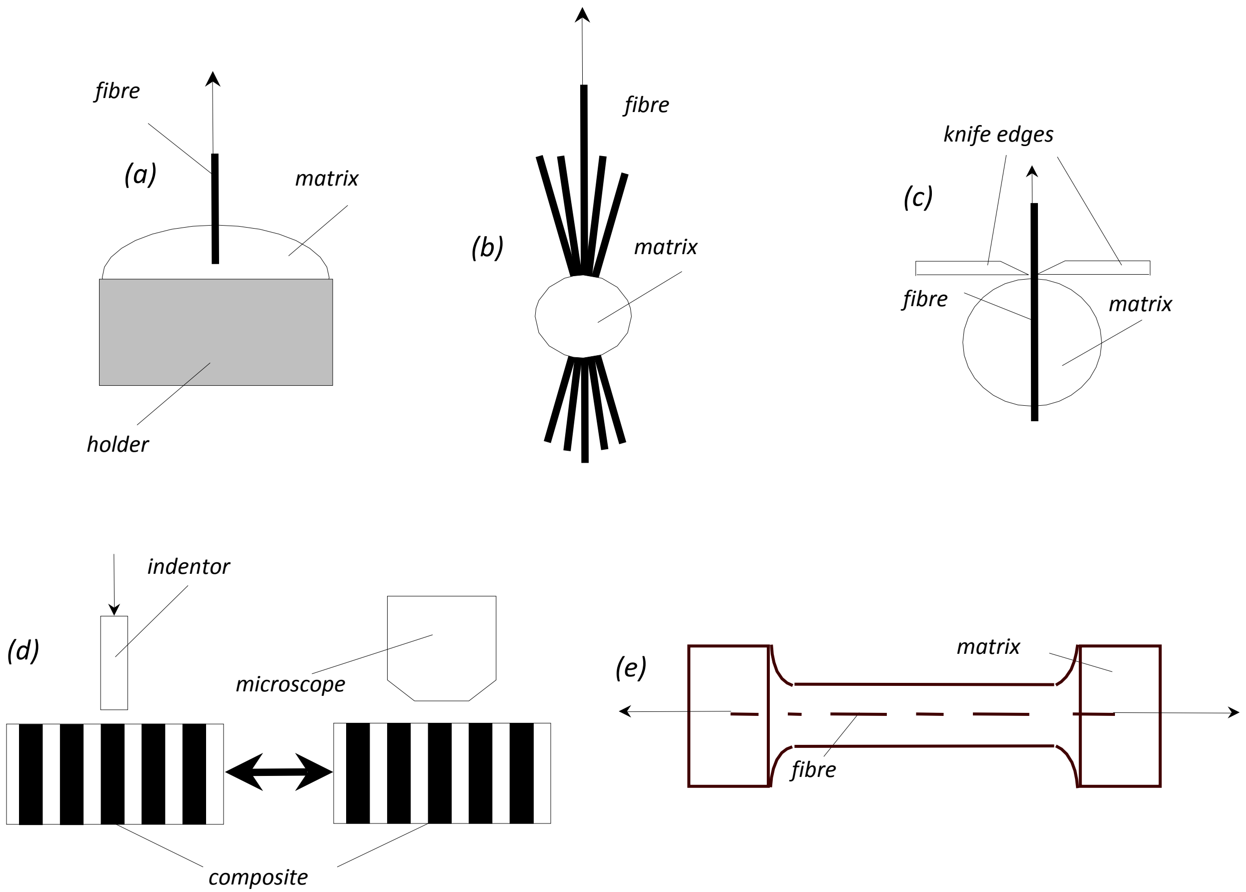

Pull out test [Shiryaeva, 1962; Favre, 1972]

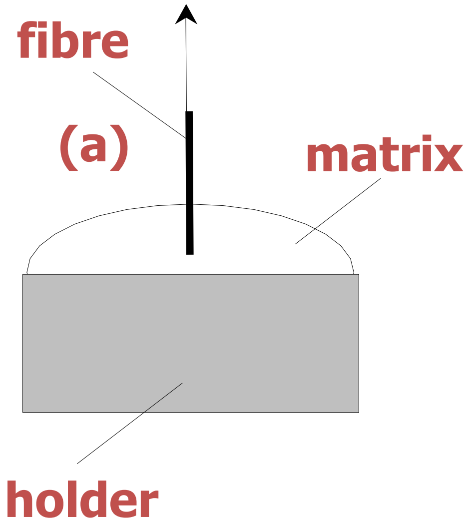

- During the pull out tests [**Shiryaeva, 1962; Favre, 1972**], a length of the fobre is embedded in the matrix.
- The loading of the free end leads gradually to the pull out of the fibre.
- The Force displacement curve may be recorded

Pull out test [Shiryaeva, 1962; Favre, 1972]

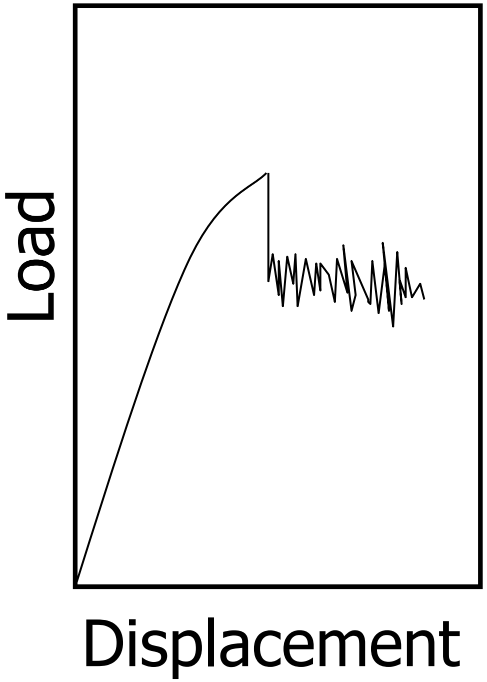

- Initially, the load increases linearly with displacement
- Matrix plasticity may lead to non linearities
- After a maximum load value, there is a sudden drop which lasts until the pull out of the fibre [**Li, 1994**].
- The interfacial strength is defined as a function of the maximum load *Pmax*.:

$$\tau = \frac{P_{max}}{2\pi R\ell}$$

- The maximum stress on the fibre σ_{max} should not exceed its strength σ_{fu} [**Broutman, 1969**] :

$$\sigma_{max} = \frac{P_{max}}{\pi R^2} \leq \sigma_{fu}$$

Pull out test [Shiryaeva, 1962; Favre, 1972]

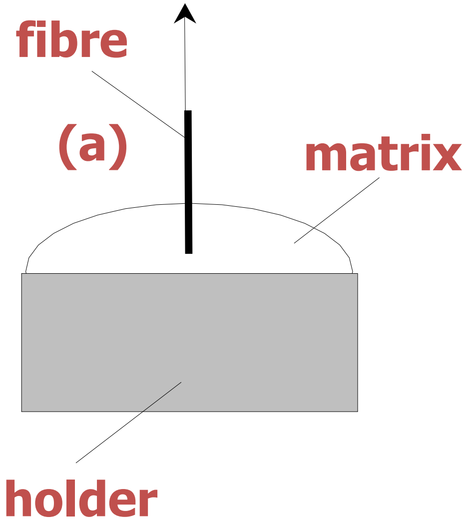

•ADVANTAGES [**Drzal, 1993**]:

- •(i) All fibre types can be tested
- •(ii) All matrix types can be tested
- •(iii) Direct measurement of interfacial strength

Pull out test [Shiryaeva, 1962; Favre, 1972]

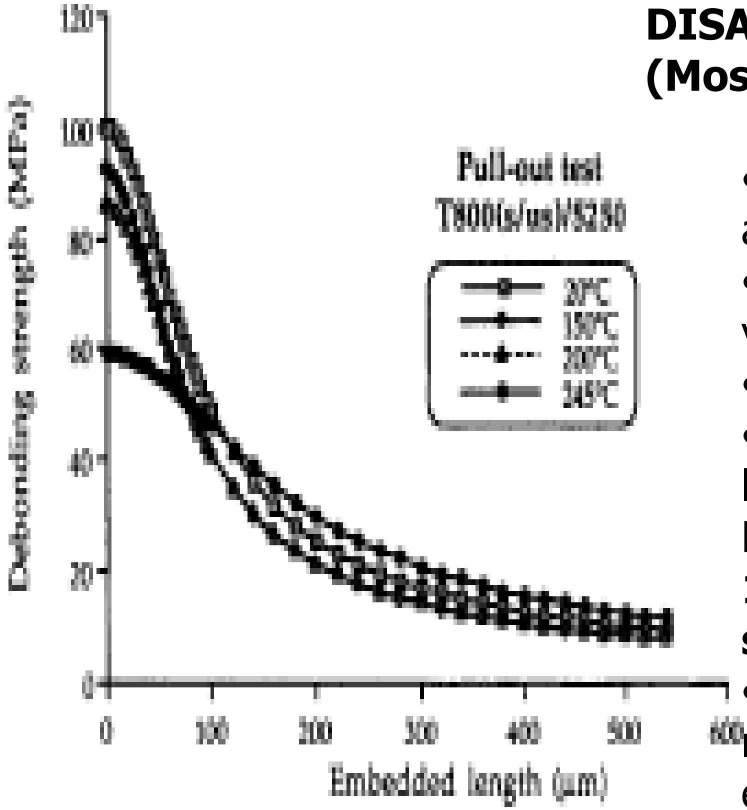

Fig. 7. Pullout tests on T800/5250.

DISADVANTAGES
(Mostly due to the test geometry)

•The wetting of the fibre may create a meniscus that affects the stress field.
•For small fibre diameters (>10 μm) the technique is vey difficult.
•The axial fibre alignment is very important
•The maximum load *Pmax* depends on the embedded length. For constant shear, the dependence is linear. However, it has been shown both theoretically [**Gray, 1984**] and experimentally [**Meretz, 1993**] **that shear is not constant**.
•The geometry does not simulate the stress field in macroscopic composites because the stresses in the entrance of the fibre may be tensile [**Drzal, 1993**].
•Many tests should be performed for statistical significance.

Pull out test: Variations

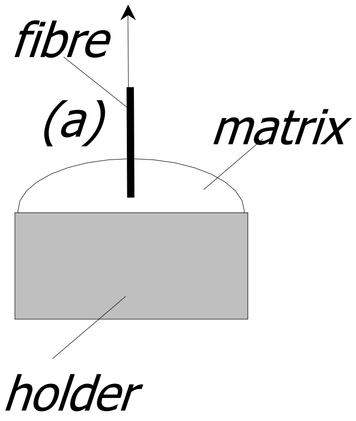

[Shiryaeva, 1962; Favre, 1972]

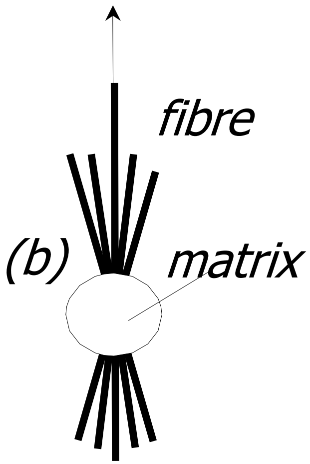

[**Qiu, 1993**]

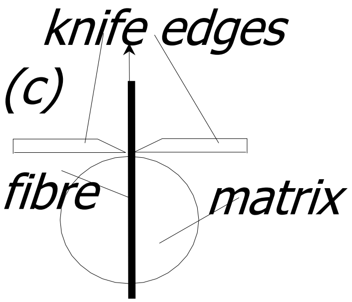

[**Penn, 1989**]

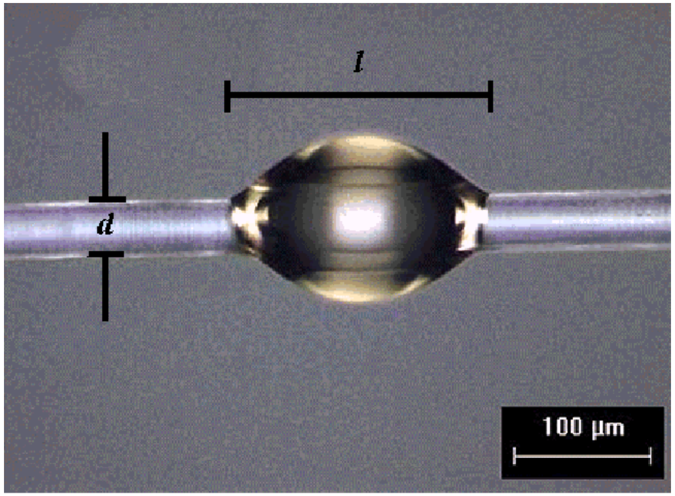

Paul J. Hogg, NOVEL TOUGHENING CONCEPTS FOR LIQUID COMPOSITE MOULDING

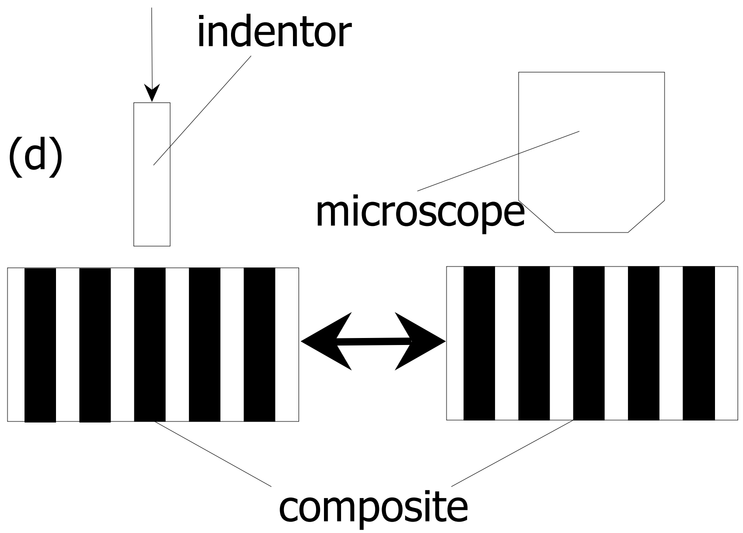

The microindentation test (MIT) [**Mandel, 1986**]

- MIT is essentially a microhardness test.
- It is performed on a grinded and polished surface
- The force displacement curve is recorded
- Specimen preparation is critical

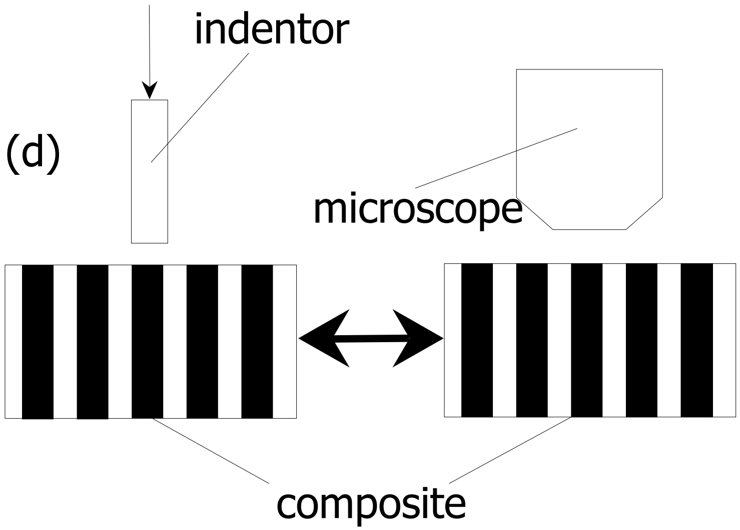

The microindentation test (MIT) [**Mandel, 1986**]

- The strength is assumed arbitrarily as the point when there is interfacial rupture of a percentage of the circumference, [**Desaeger, 1993**], the change od slope in the force displacement curve [**Netravali, 1989**], the sudden load drop [**Pitkethly, 1993**].
- Interfacial strength is derived analytically (e.g. with shear-lag) [**Desaeger, 1993**] or numerically [**Tsai, 1990**].
- The major advantage is that the test is performed in macroscopic composites but it is outweighed by the absence of a single failure criterion
- The stress concentration due to the indentor geometry may further complicate the interpretation of the data.

Fragmentation test [**Kelly, 1965**]

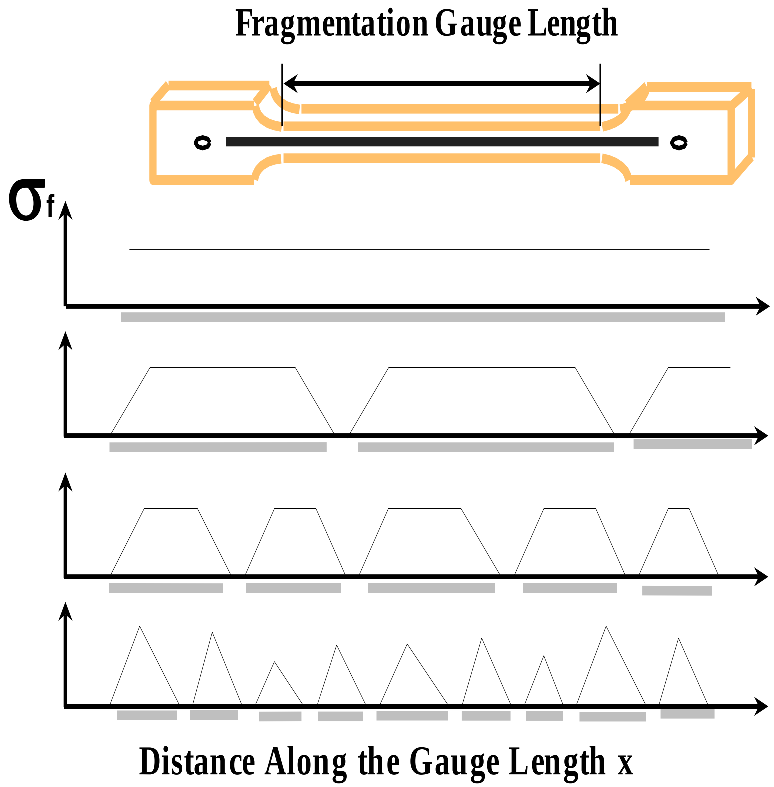

Fragmentation test [**Kelly, 1965**]

•The fibre is embedded in a polymer matrix
•The coupon in loaded in tension until the fibre starts to fracture
•Fragmentation continues until there is saturation, that is no more fractures occur. It is worth noting that if the interface did not fail, the fractures would continue until macroscopic failure of the coupon.
As a result, saturation is connected with the failure of the interface

•During the fragmentation test, fractures are recorded either optically [**Waterbury, 1991**], or with other techniques (acoustic emission) [**Favre, 1990**].
• The distribution of the fragment lengths is recorded. Interfacial strength must be derived assuming a stress transfer model.

Fragmentation test [**Kelly, 1965**]

- During tension, the fibre breaks when it reaches its tensile strength.
- If l_c is the required length for stress transfer then the distribution of fragment lengths l_f is between $l_c/2$ and l_c [**Narkis, 1988**].
- To define l_c, the strength distribution of the fibre must be known. For a normal strength distribution the transfer length l_c is defined as:

$$l_c = 4/3\ l_f$$

To derive interfacial strength, the stress field must be defined. For constant shear the problem is simplified [**Kelly, 1965**]:

$$\tau_{rz} = -\frac{R\sigma_{fu}}{l_c}$$

Fragmentation test [**Kelly, 1965**]

•ADVANTAGES

- •Symmetric stress field [**Drzal, 1990**].
- •Large measurement number per test
- •Sensitivity in different interfacial conditions
- •Direct observation of the failure events
- •Qualitative assessment of the stress field and the failure modes
- •Correlation with the fibre strength [**Gulino, 1991**]
- •Ideal geometry for advanced methods (Raman microscopy, photoelasticity, Acoustic Emission)

•DISADVANTAGES

- •Only brittle fibres in ductile matrices may be tested (at least threefold strain to failure [**Drzal, 1993**]).
- •The saturation strain is much larger than the real composite strain to failure, which instigates failure mechanisms not present in real life (debonding [**Wagner, 1995; DiBenendetto, 1996**], shear flow [**Nath, 1996**], or frictional sliding [**Piggot, 1980])**
- •Thermal stresses dominate the stress field [**Nairn 1996**]
- •The test is very difficult for small fibre diametres

Interface tests:
Interlaboratory Scatter [Pitkethly et al., 1993]

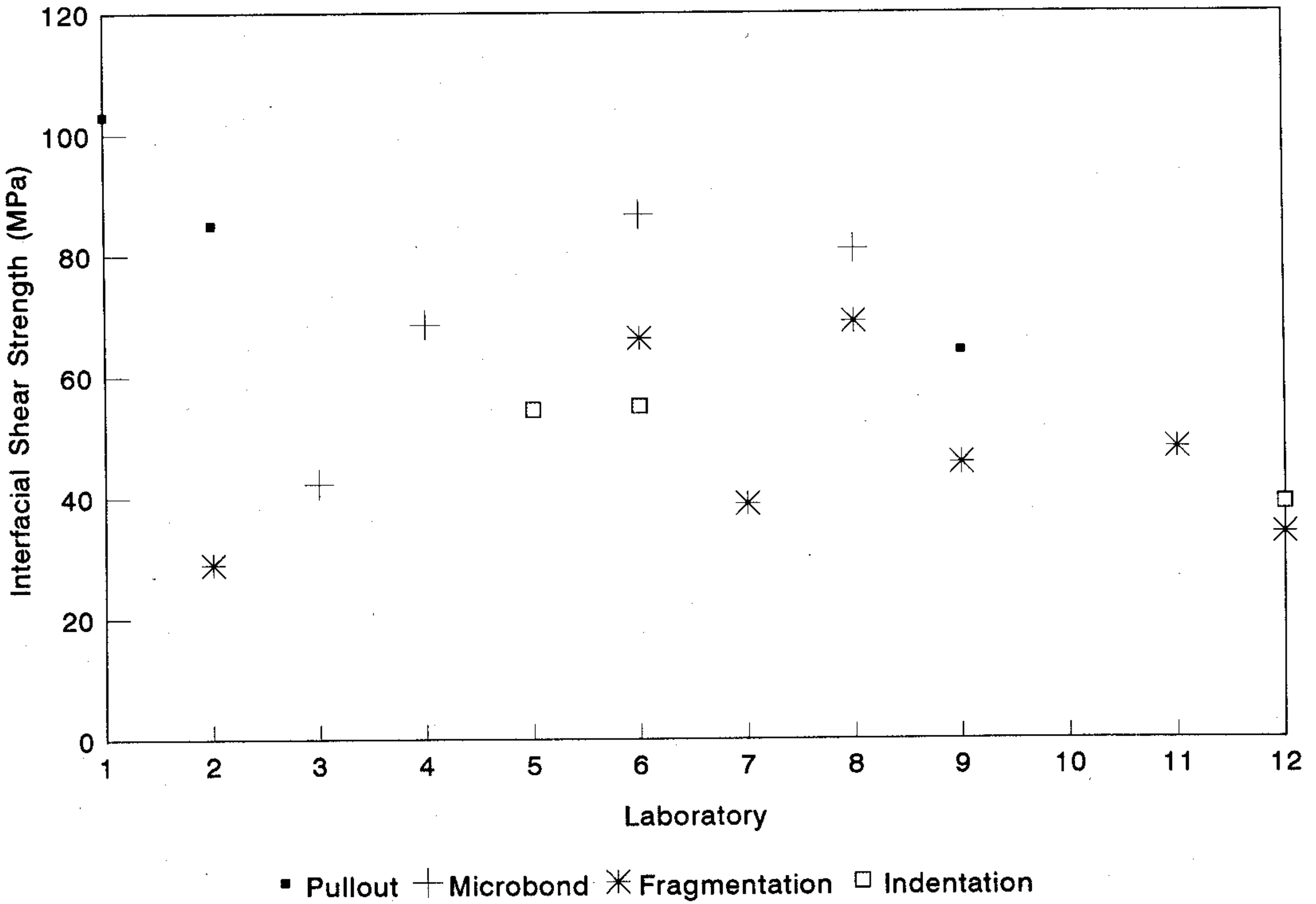

Advanced methods for interfacial testing

- Acoustic Emission
- Raman microscopy
- Acoustic microscopy
- Polarised light microscopy
- SEM

Acoustic Emission

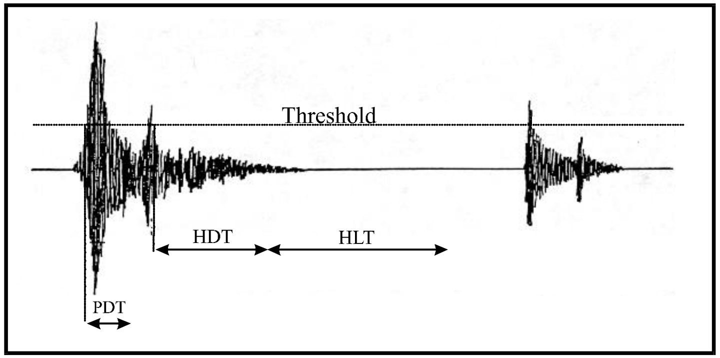

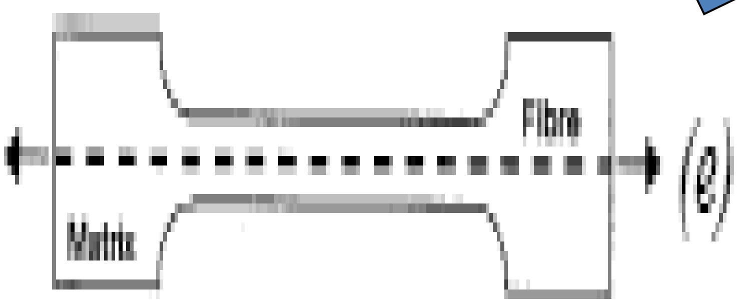

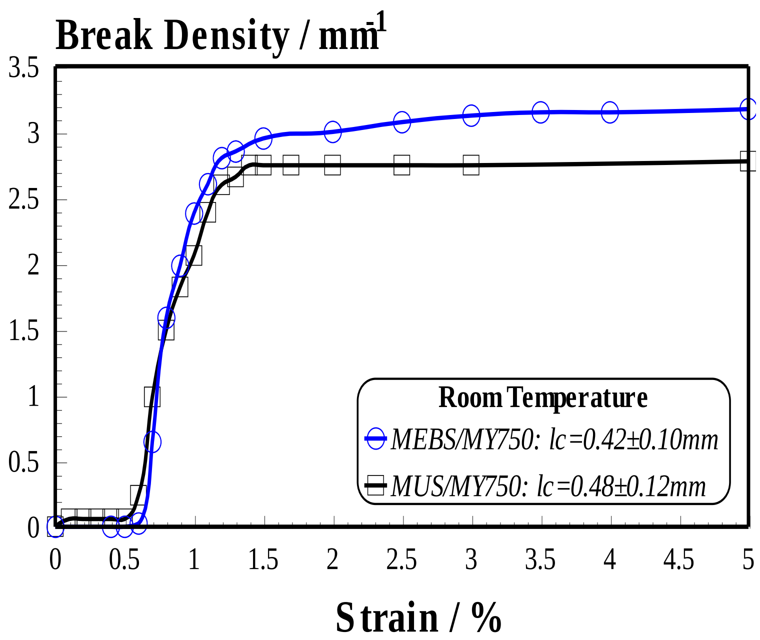

Acoustic Microscopy

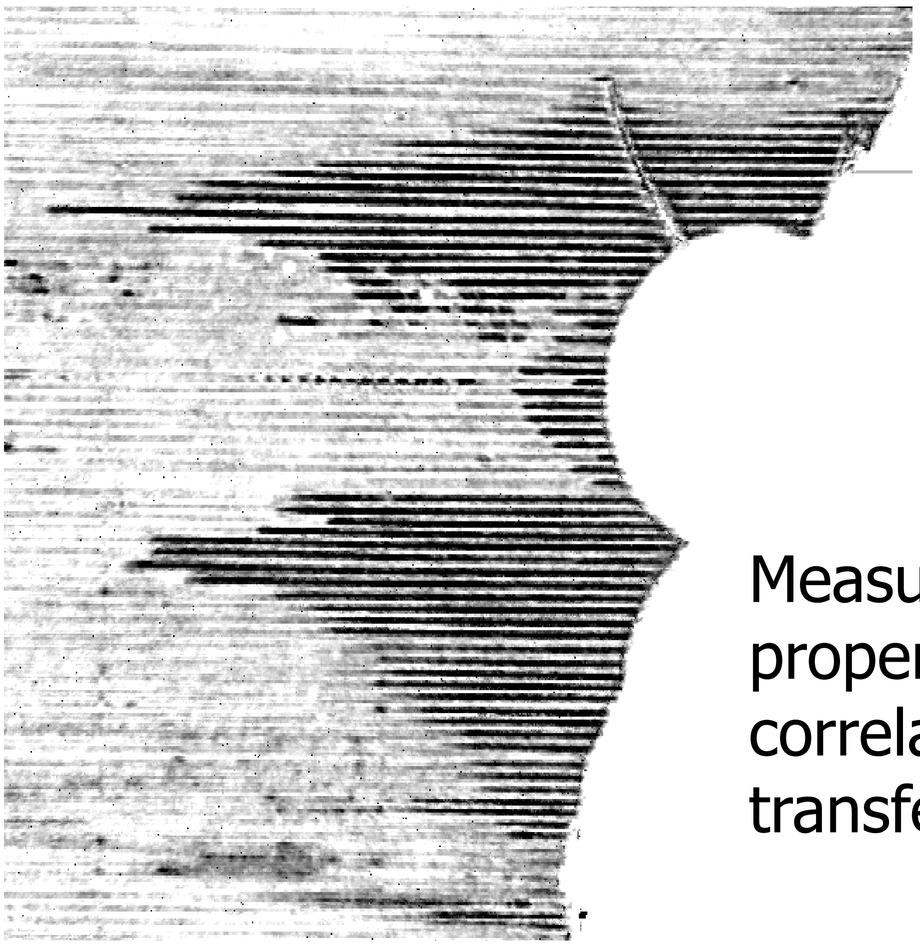

Measurement of the local elastic properties near the surface and correlation with the stress transfer

Raman Frequencies: Dependence on Applied Stress

Tension

The Raman Frequency decreases

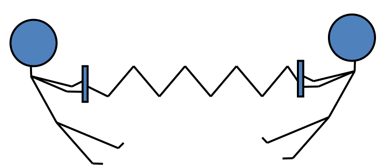

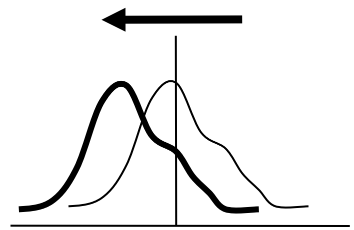

Compression

The Raman Frequency increases

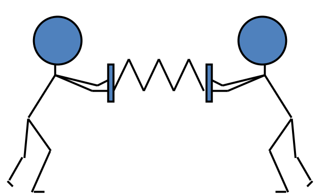

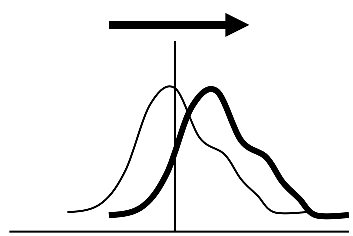

Carbon Fibres:
Raman Frequency/ stress calibrarion

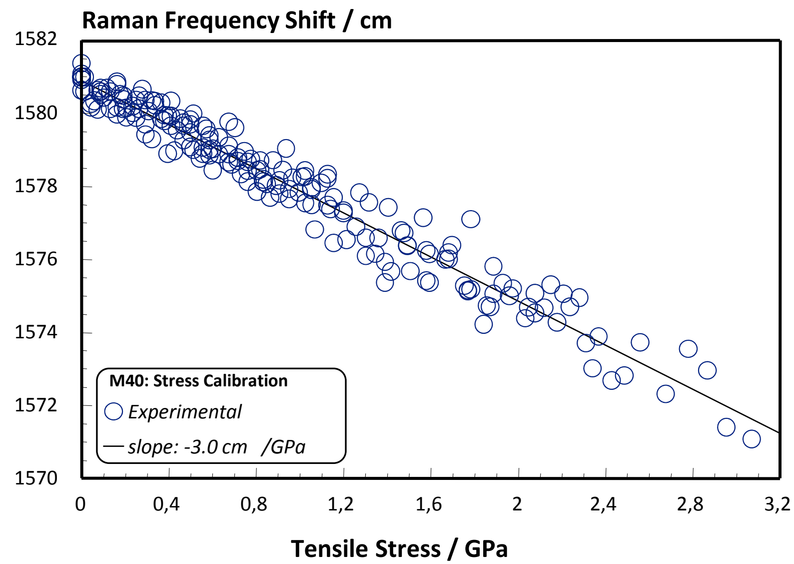

Stress transfer for different systems

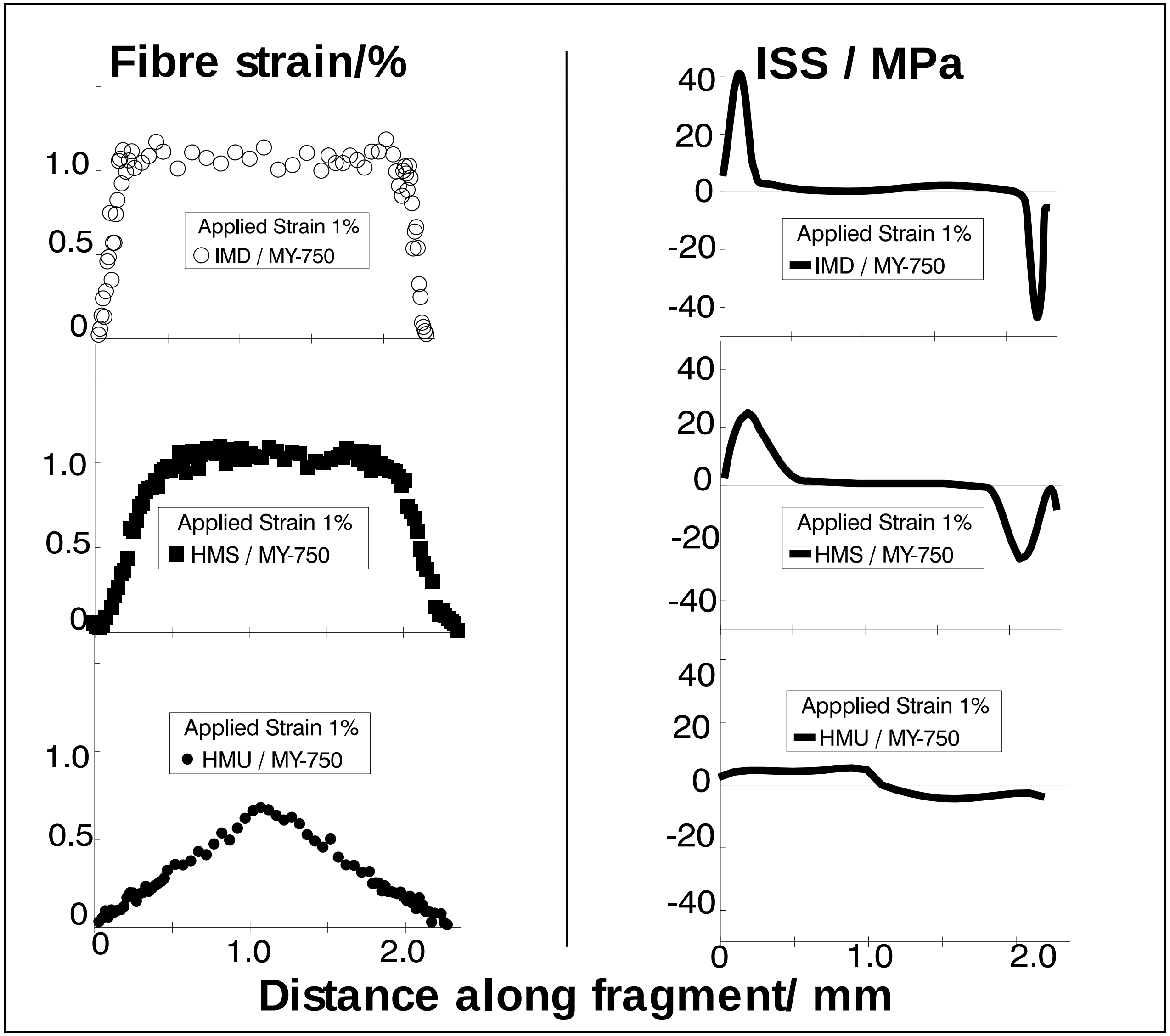

Elastic Domain: The 'β' *parametre* [Cox, 1952]

Sized fibre

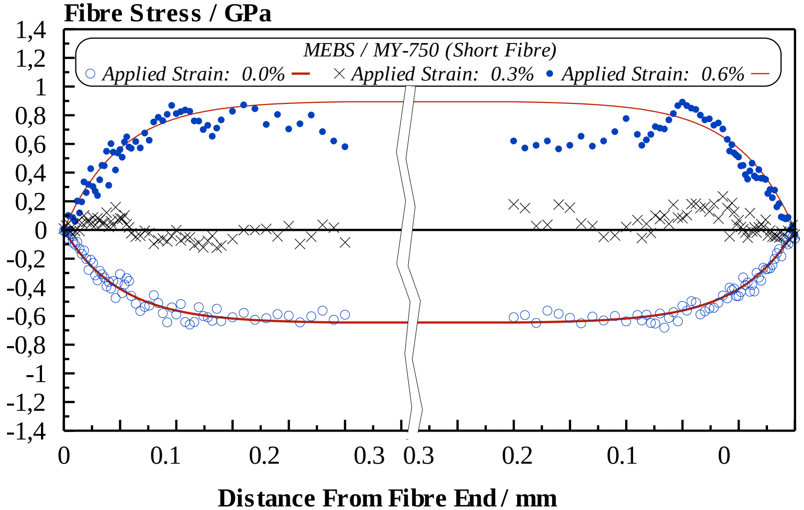

Unsized fibre

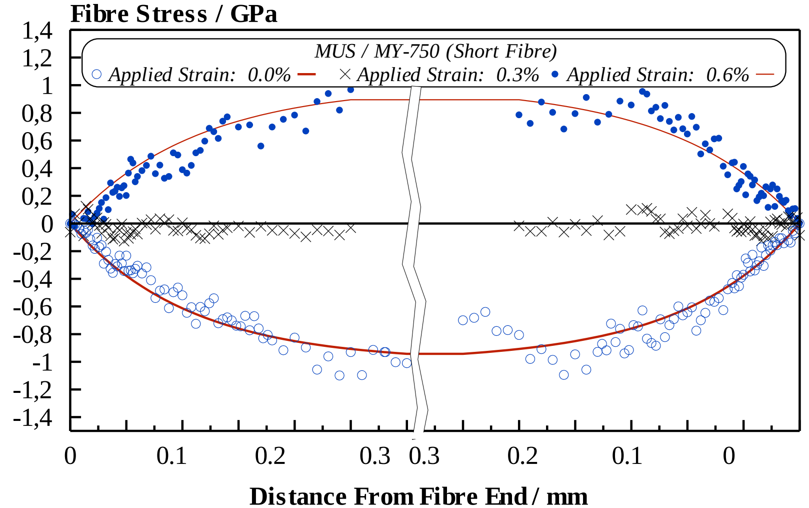

$$\sigma_z(z) = E_f \varepsilon_\infty \left[1 - \frac{\cosh\left(\beta\left(\frac{l}{2} - z\right)\right)}{\cosh\left(\beta \frac{l}{2}\right)} \right] \qquad \beta = \sqrt{\frac{2G_m^{R_\infty}}{R^2 E_f \ln\left(\frac{R_\infty}{R}\right)}}$$

E_f : fibre modulus
G_m : matrix shear modulus,
R : fibre radius,
R_∞ : Matrix shear perturbation radius

For large fibre length('shear lag' theory) **[Cox 1952]:**

$$\sigma_z(z) = \sigma_\infty\left[1 - e^{-\beta z}\right]$$

$\sigma_z(z)$: local stress on the fibre $\quad$ σ_∞ : stress at infinity $\quad$ β : constant

Polarised Microscopy

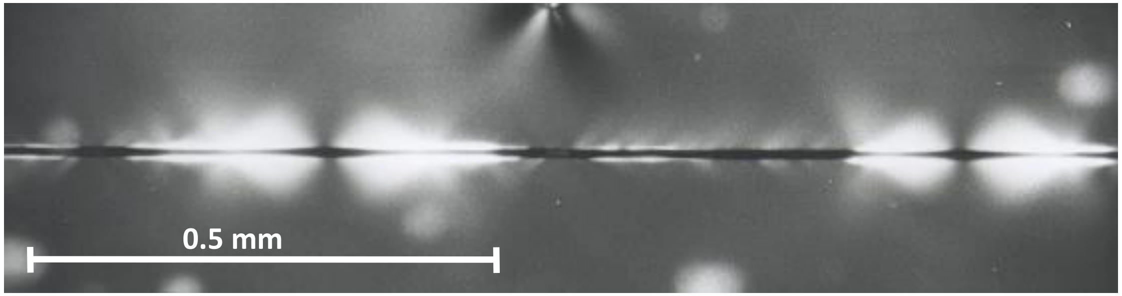

(a)

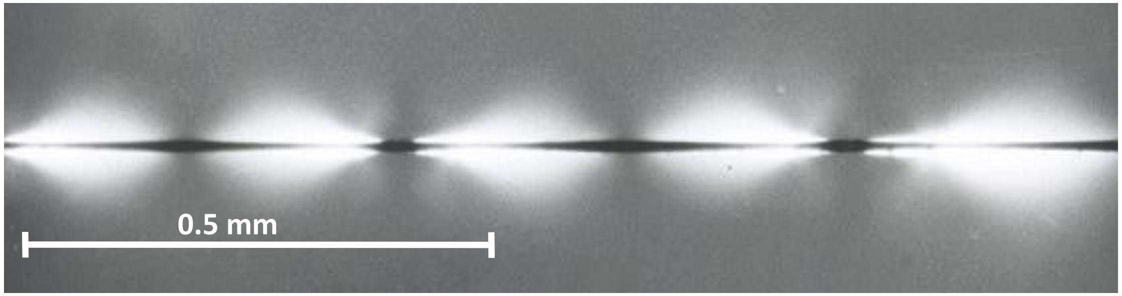

(b)

SEM (I)

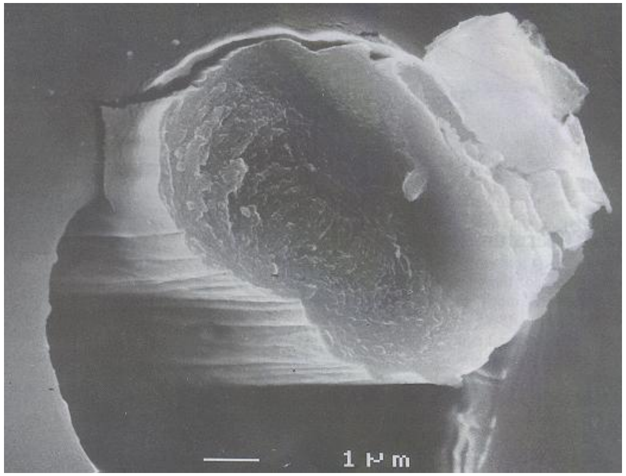

(a)

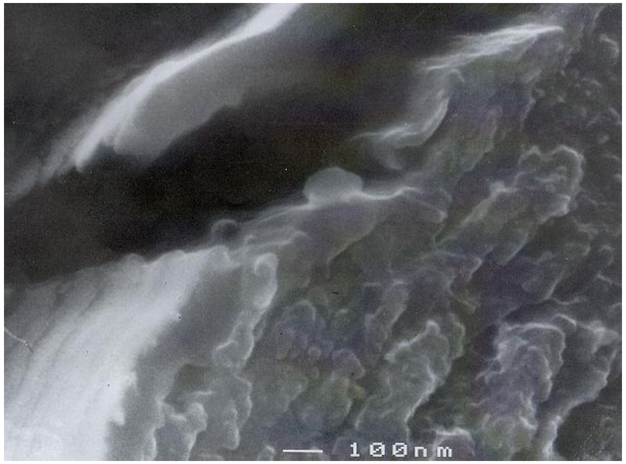

(c)

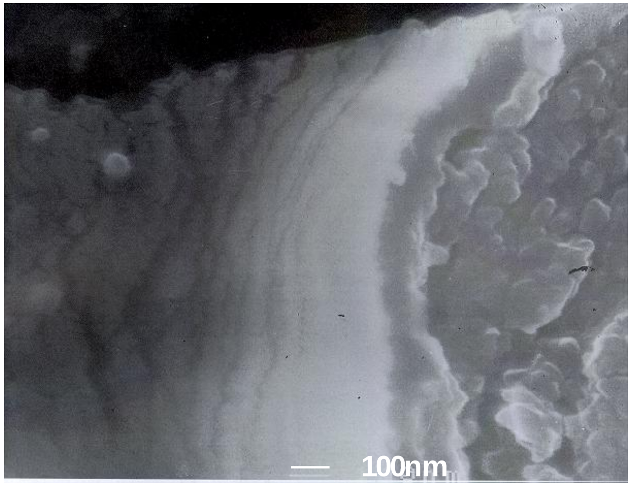

(b)

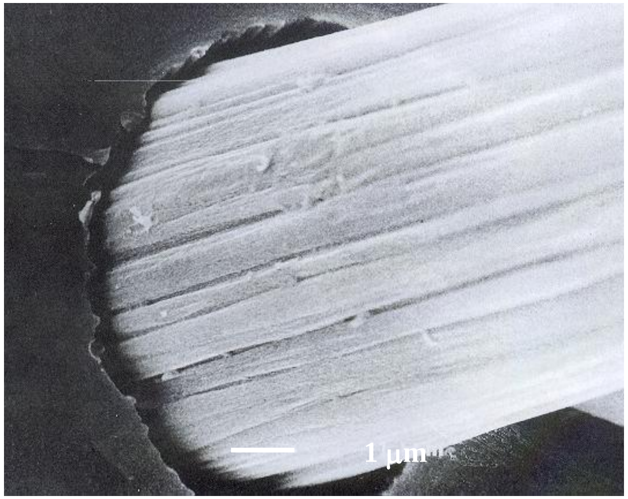

(d)

SEM II

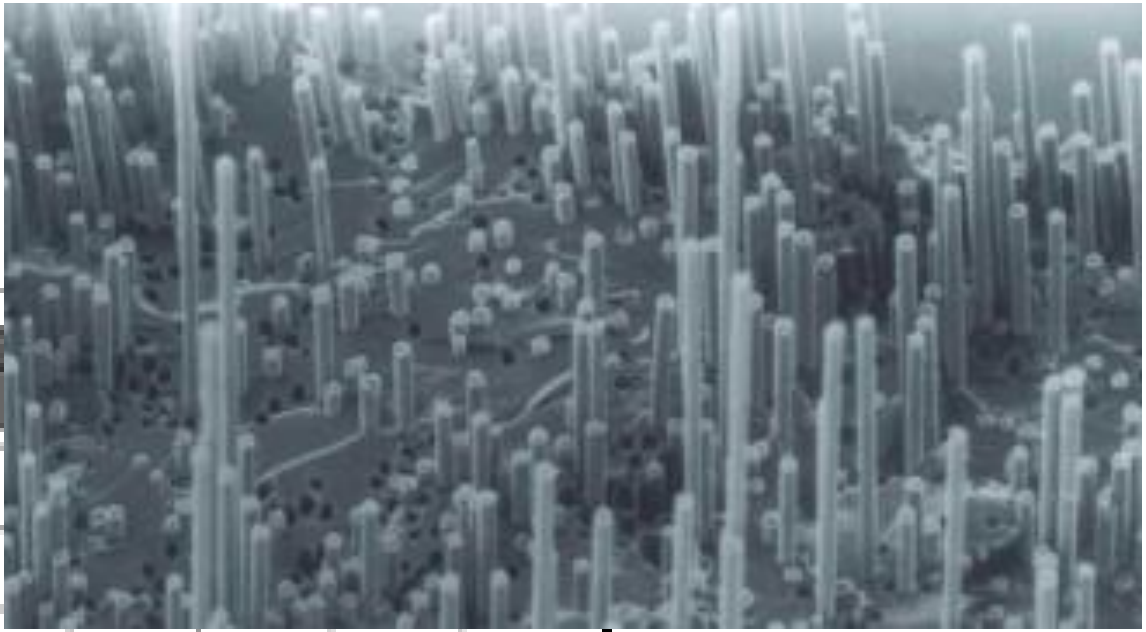

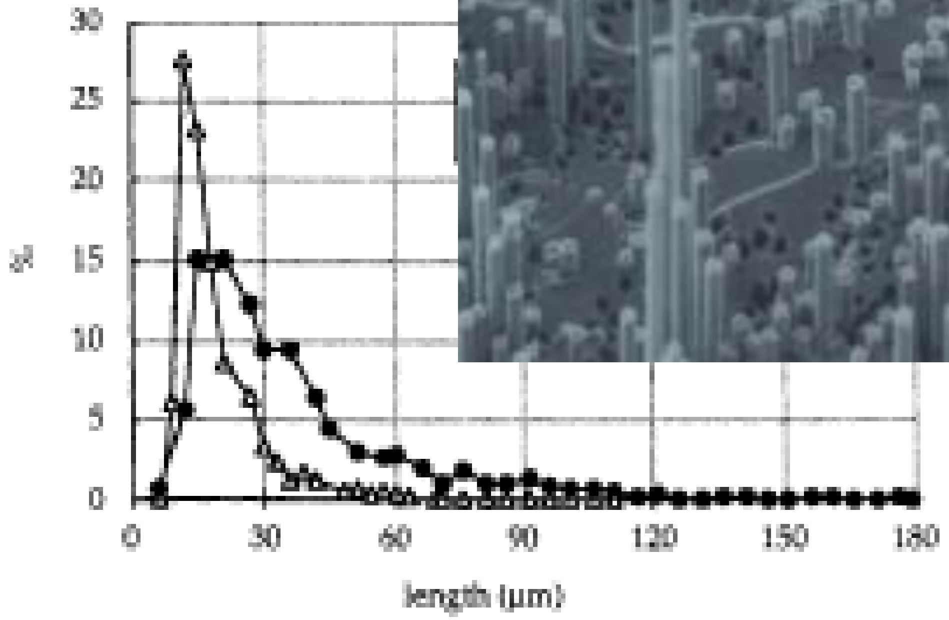

Fig. 11. SEM analysis of the fracture surface of M40 broken tows: distribution of lengths (in µm) of the pulled-out fibers. (a) Treated M40 at room temperature and 250°C; (b) treated M40 and epoxy-sized M40 at 250°C.

Macroscopic mechanical behavior of the composite lamina

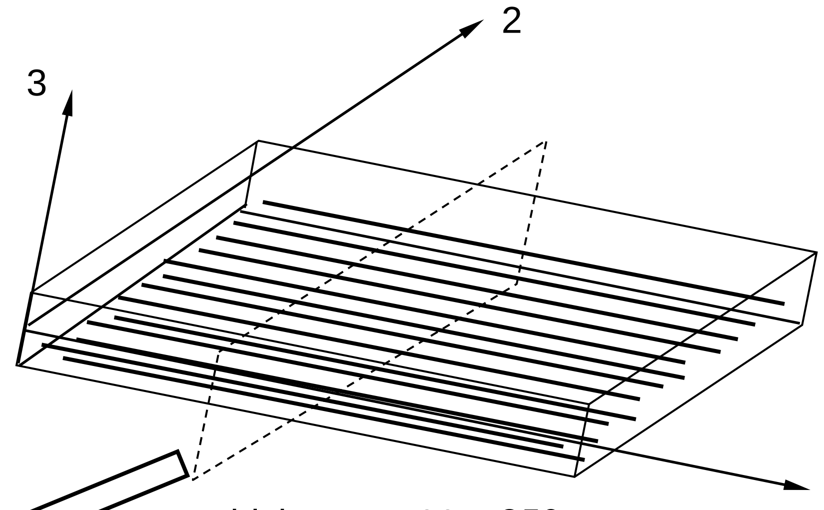

thickness: 100 – 250 μm

lamina

Typical Lamina cross section

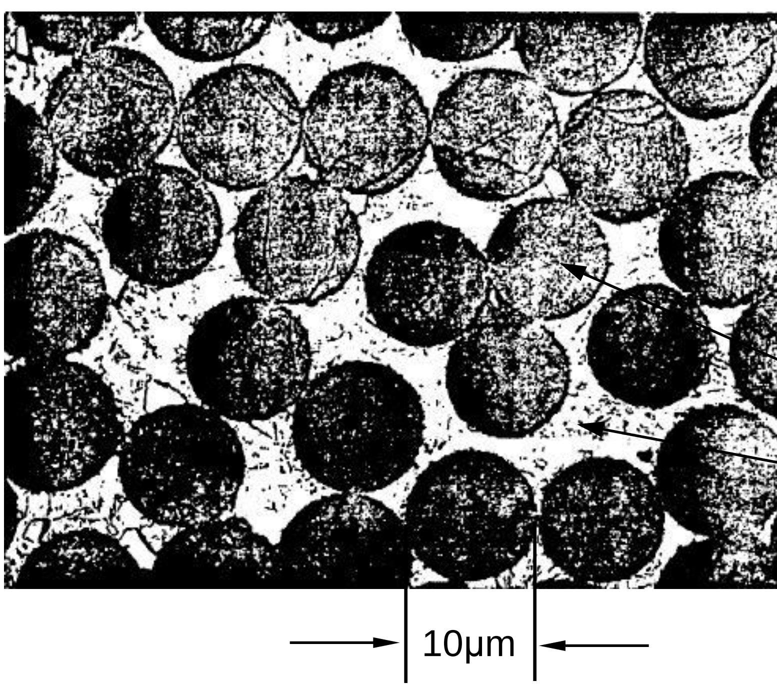

Discrete Phases:

- fibre
- matrix

Fabrics carbon, aramid, κτλ.

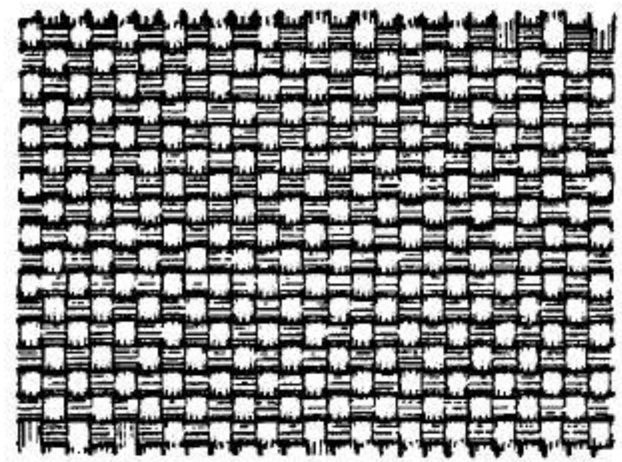

Plain weave (1 up, 1 down) glass fabric

(2) Filling yarn, running the width of a woven fabric at right angles to the warp

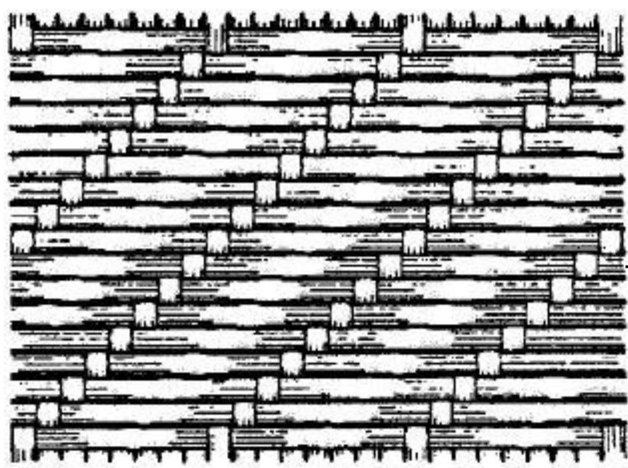

Eight-harness satin weave (1 up, 7 down)

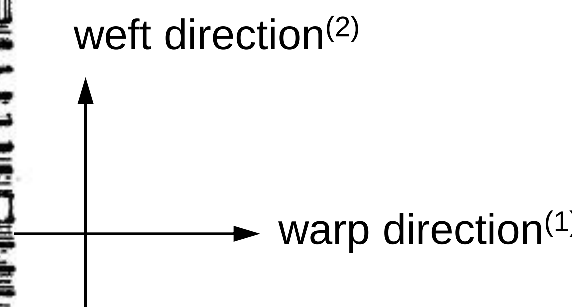

(1) In the fabric industry, those fibers or threads in a woven fabric which run lengthwise, or which are parallel to the selvedge

Composite Laminates

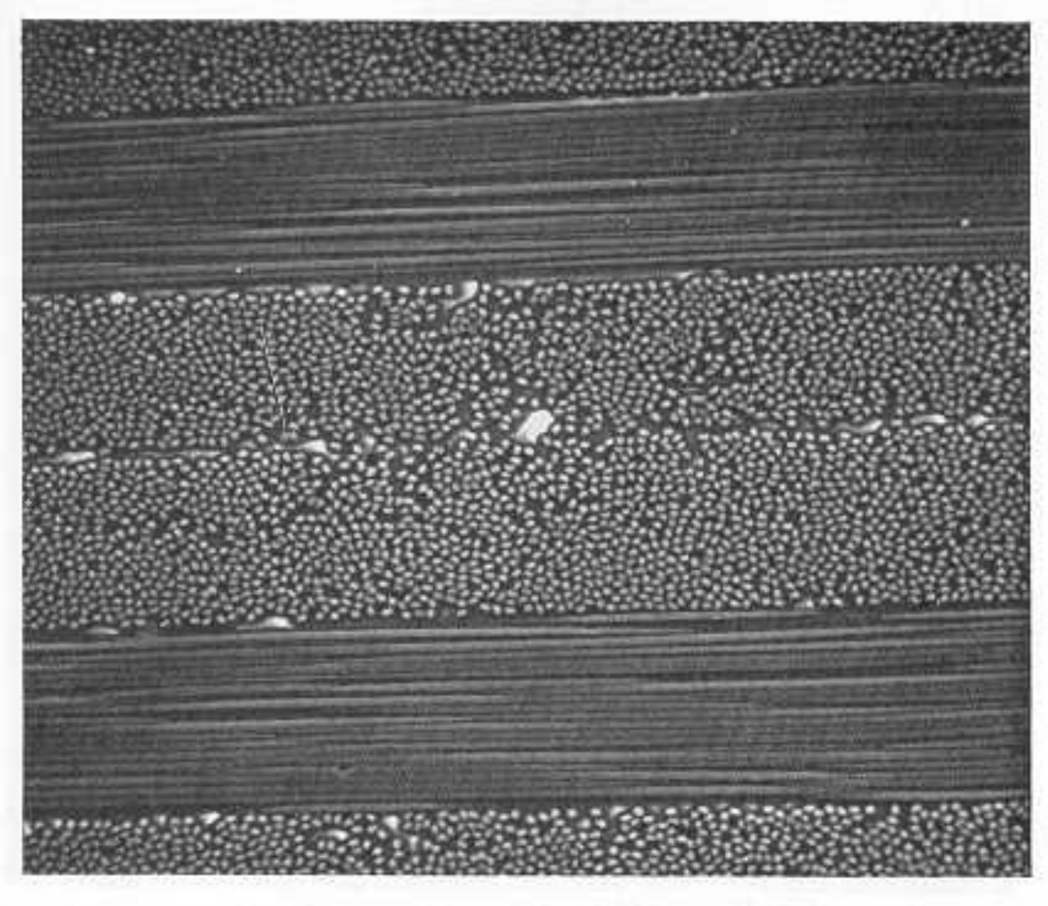

SEM photograph of a typical composite after exposure to water at 333 K for one day (c=0.59%) subjected to 45% of its UTS [O. Gillat, L.J. Broutman, STP 658 (1978)]

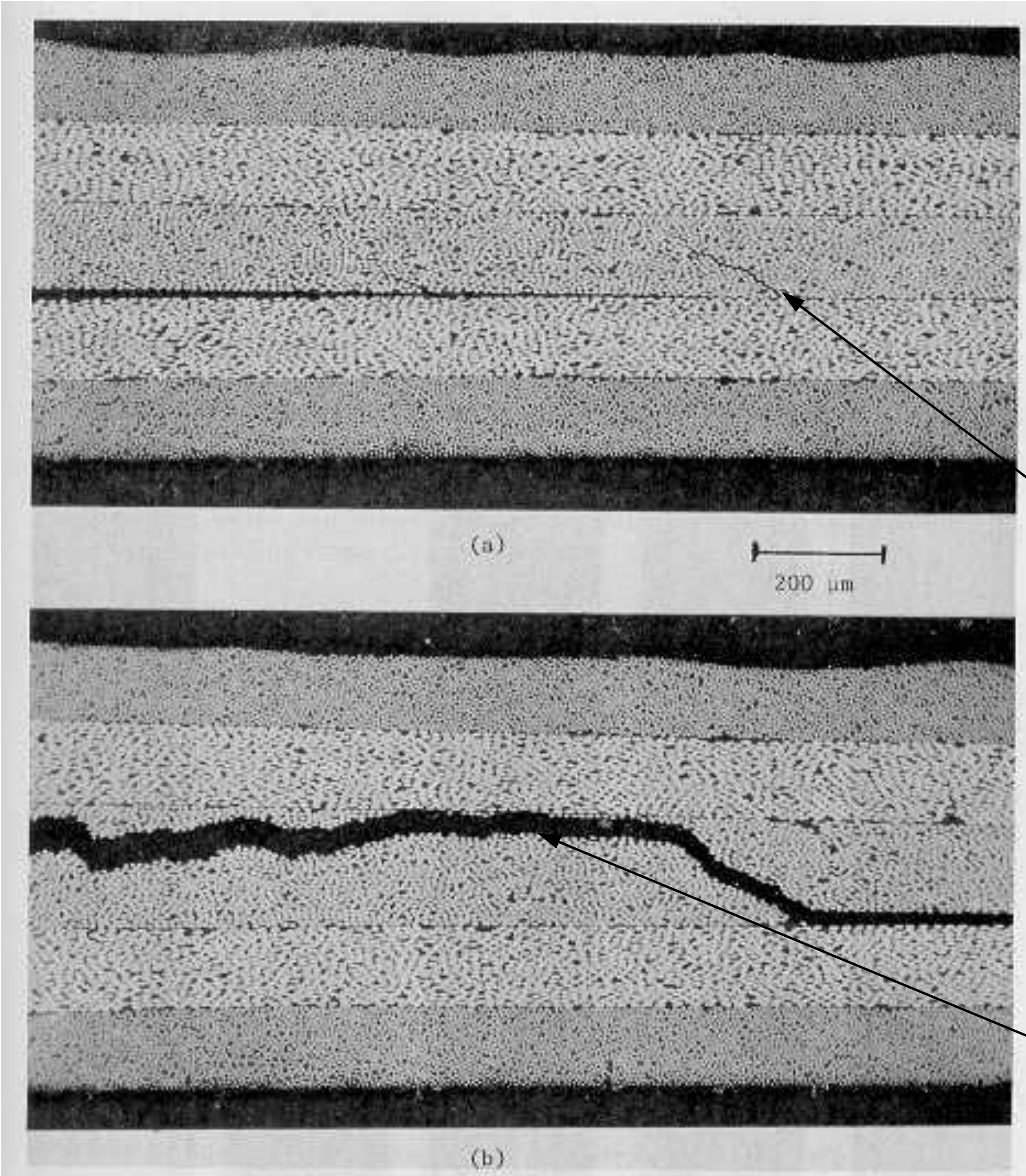

In composite laminates the composite inhomogeneity is crucial to the mode of failure

Intraply crack (matrix crack)

Interply crack (delamination)

For a UD lamina, the composite inhomogeneity (at the fibre matrix level) dominates the micro-failure mechanisms

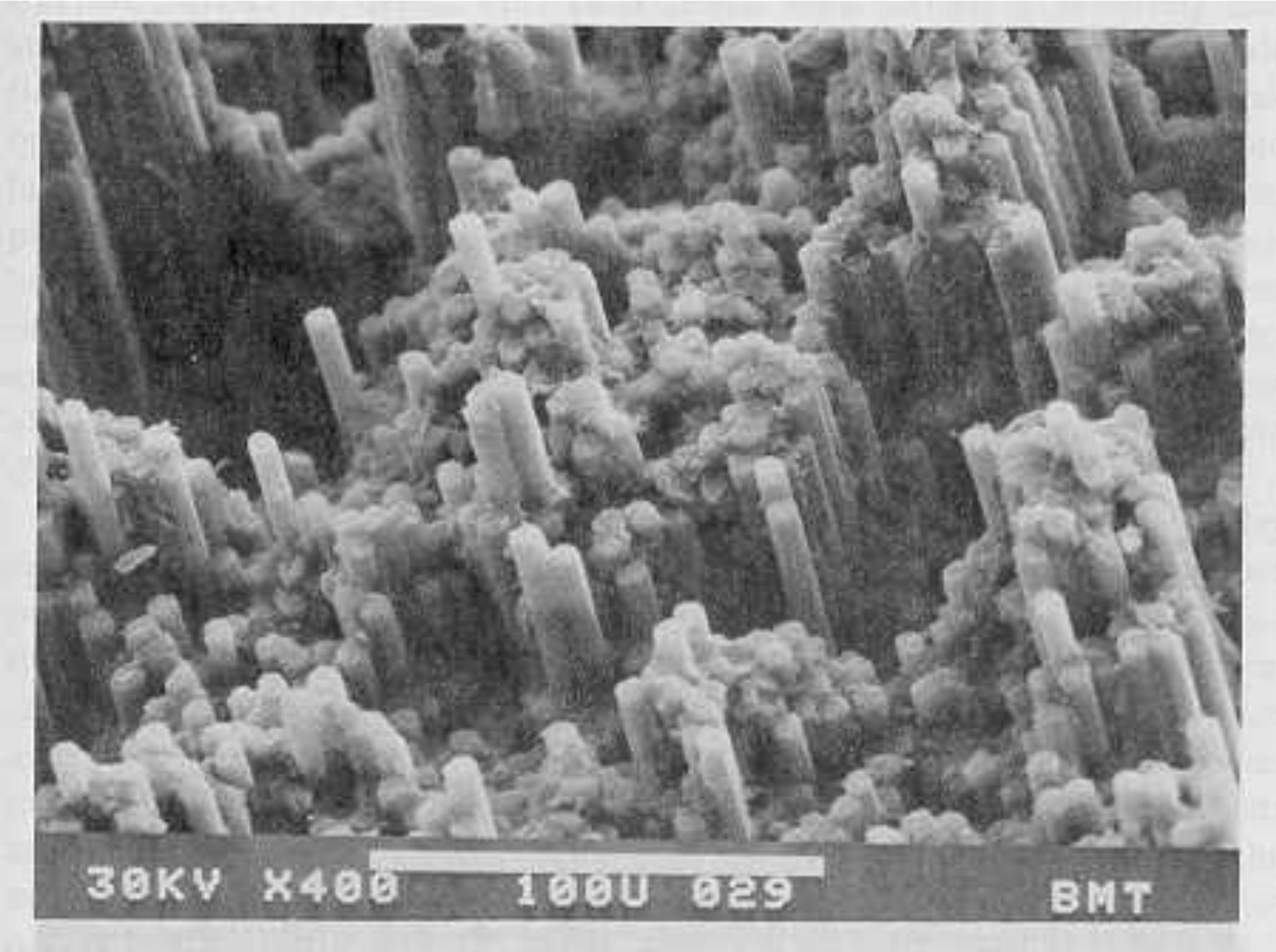

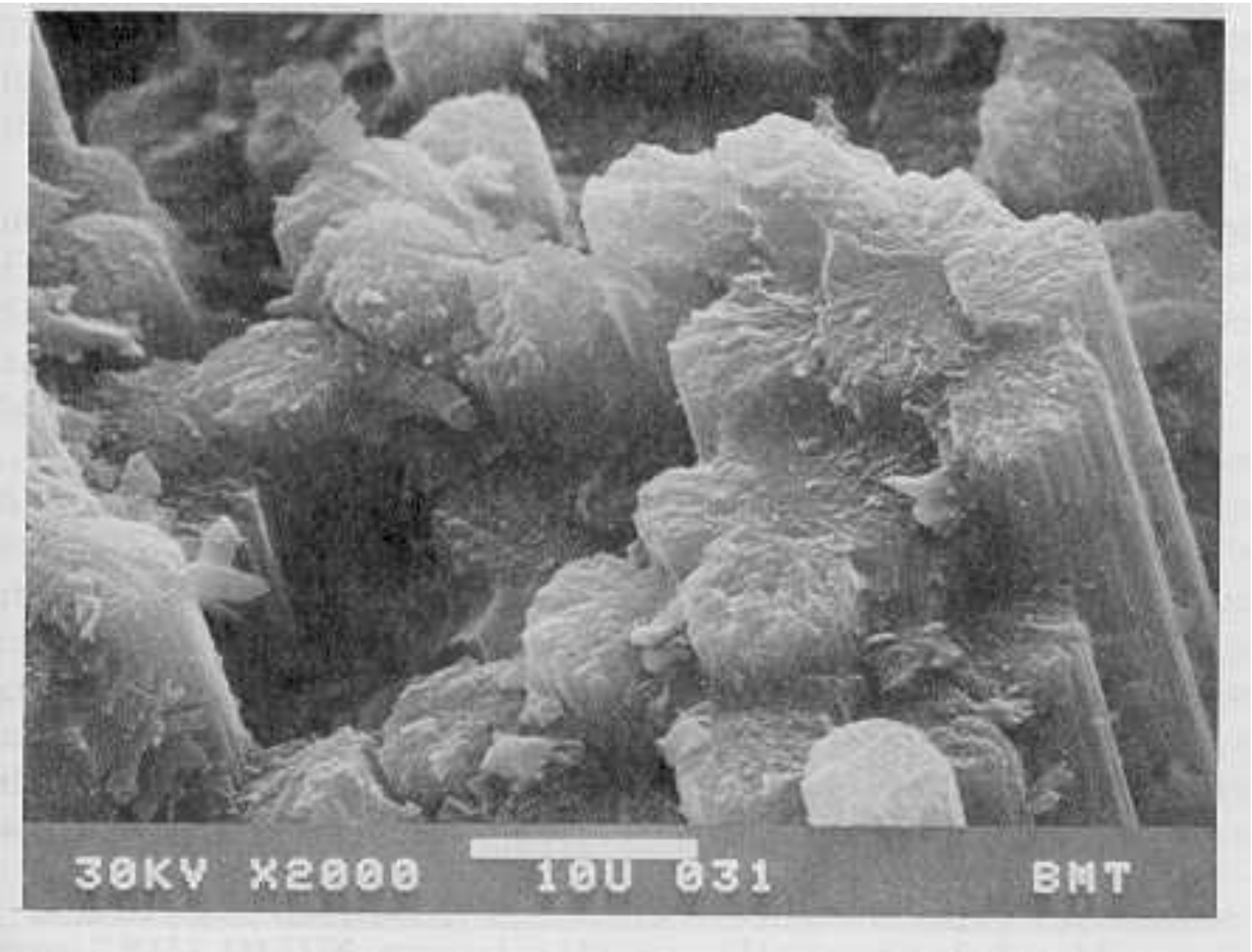

Typical microstructures of fractured specimens [A.G.Miller, A.L.Wingert, STP 696 (1979)]

Macroscopic behaviour:

The mean apparent mechanical properties of the orthotropic lamina or the laminate

The lamina is considered as ***a homogeneous anisotropic material***

(experimentally acceptable for mechanical properties such as ***technical elastic constants or strengths***)

The anisotropic composite is usually regarded as a ***linear elastic medium until***

Hooke 's Law:

- Axiom?
- Derived from energy principles?
- Empirical relationship;

Robert Hooke (1635-1703)

- “De Potentia restitutivâ” or “Of Spring” (1678)

C E I I I N O S S S T T U V

“UT TENSIO SIC VIS”

The present form of Hooke’s Law the stress tensor formulation and the equilibrium equations are expressed by:

Augustin Cauchy (1789-1875)

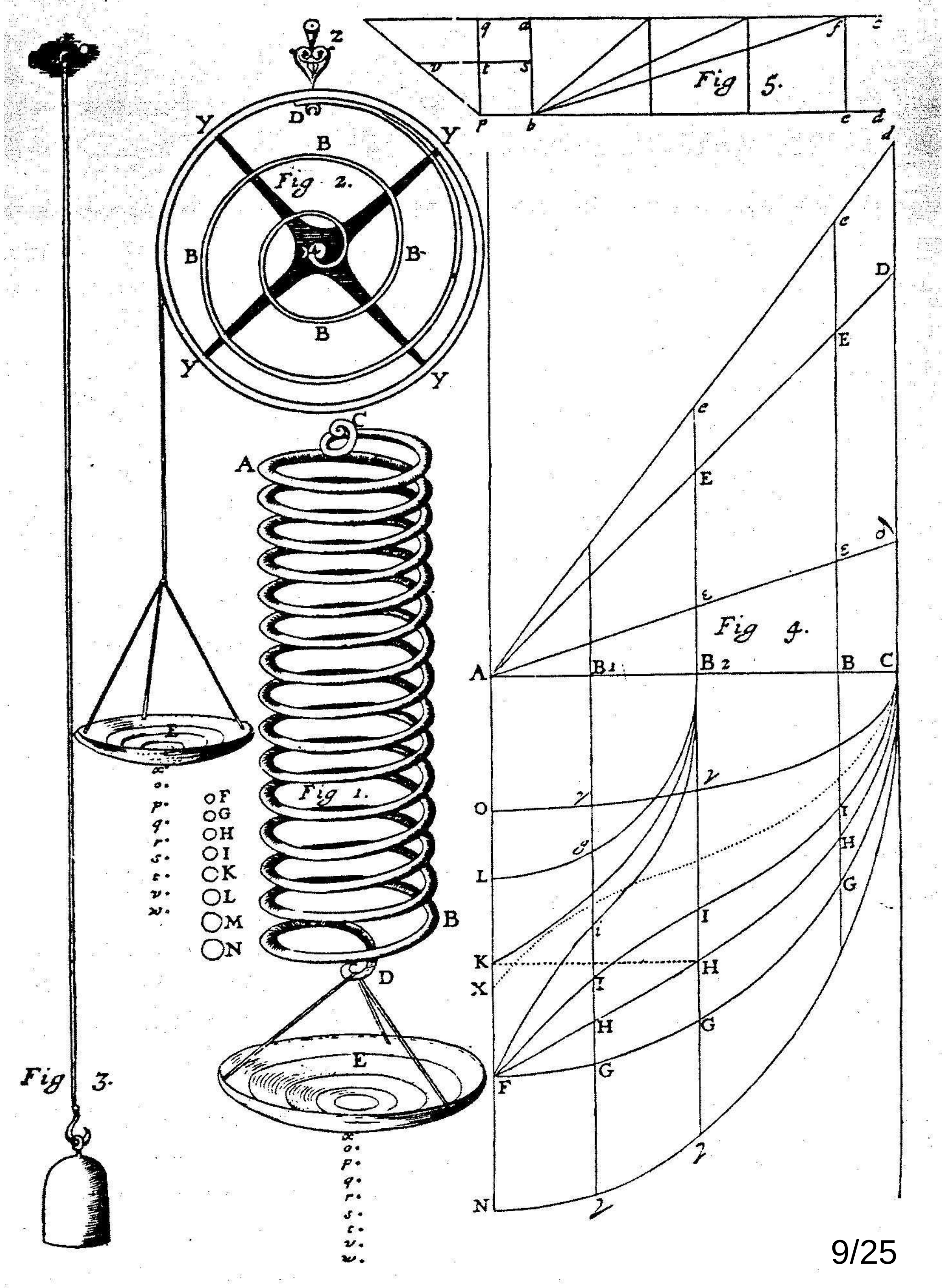

Composite Materials: Symmetries Orthotropic medium

The elastic anisotropic medium with two mutually perpendicular planes of elastic symmetry.
It can be proved that there is a third symmetry plane perpendicular to the other two..

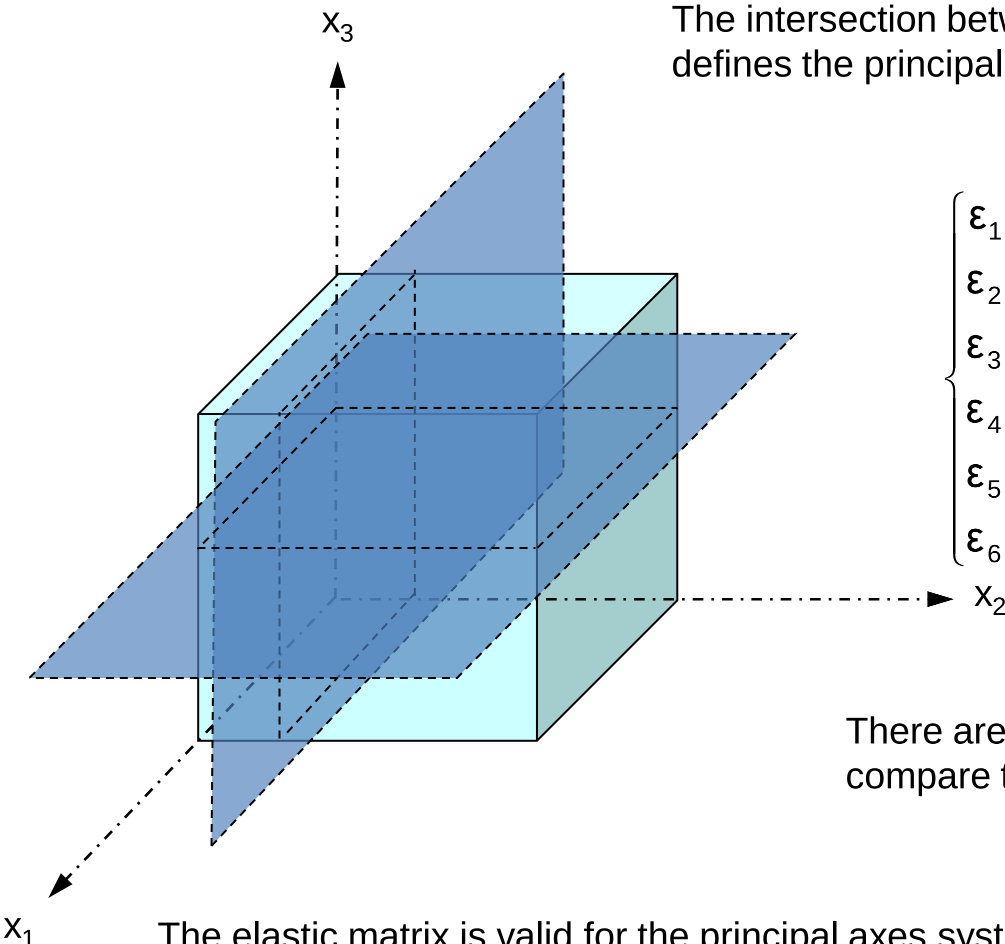

The intersection between the symmetry planes defines the principal axes of the orthotropic material.

$$\begin{Bmatrix} \varepsilon_1 \\ \varepsilon_2 \\ \varepsilon_3 \\ \varepsilon_4 \\ \varepsilon_5 \\ \varepsilon_6 \end{Bmatrix} = \begin{bmatrix} S_{11} & S_{12} & S_{13} & 0 & 0 & 0 \\ S_{12} & S_{22} & S_{23} & 0 & 0 & 0 \\ S_{13} & S_{23} & S_{33} & 0 & 0 & 0 \\ 0 & 0 & 0 & S_{44} & 0 & 0 \\ 0 & 0 & 0 & 0 & S_{55} & 0 \\ 0 & 0 & 0 & 0 & 0 & S_{66} \end{bmatrix} \begin{Bmatrix} \sigma_1 \\ \sigma_2 \\ \sigma_3 \\ \sigma_4 \\ \sigma_5 \\ \sigma_6 \end{Bmatrix}$$

There are 9 independent elestic constantsS_{ij} (or C_{ij})- compare to 21 for triclinic medium

The elastic matrix is valid for the principal axes system

Typical orthotropic medium : woven fabric

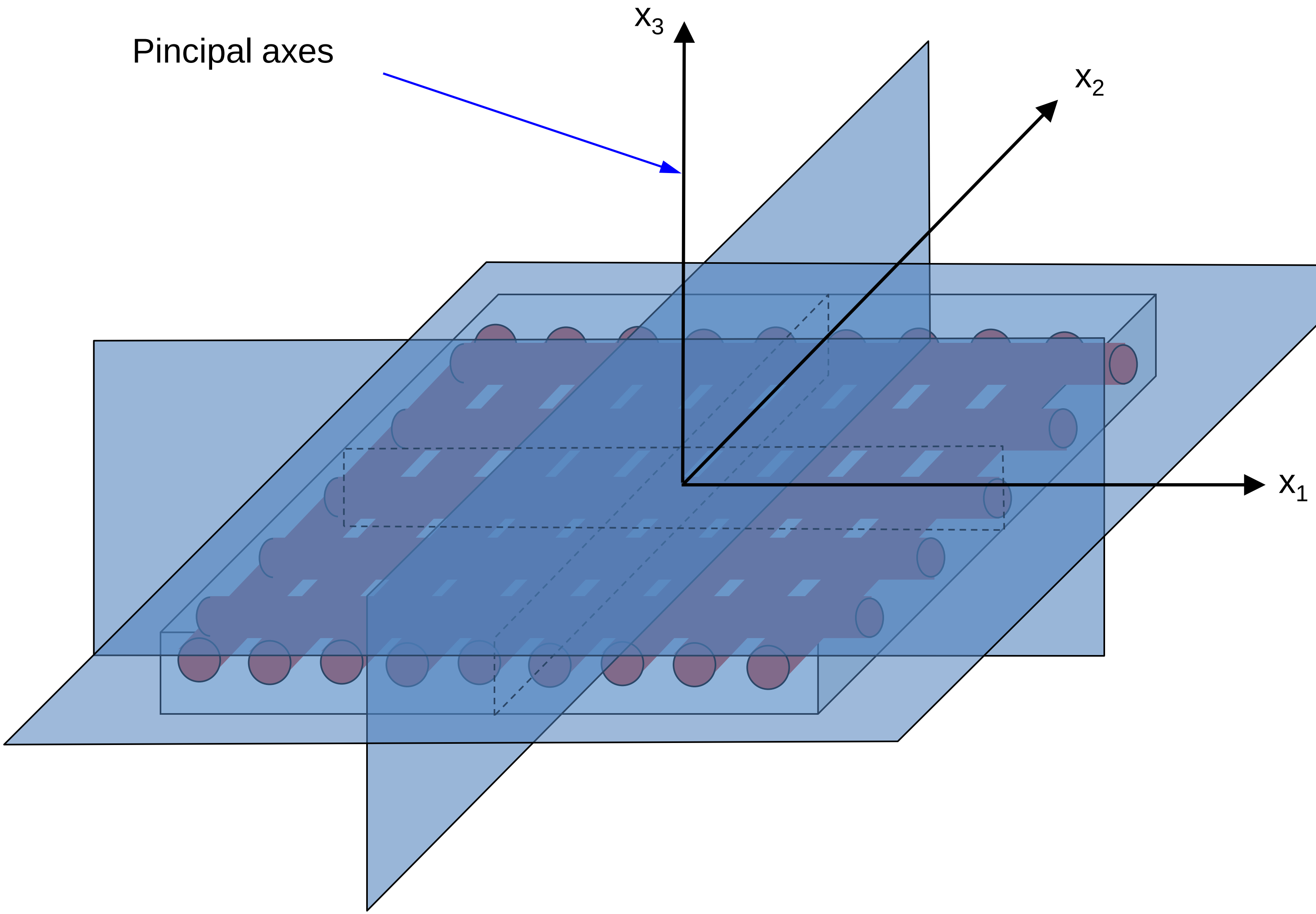

Transversely isotropic medium

It posesses an axis of ***elastic symmetry***:
All directions perpendicular to that axis are elastically equivalent
i.e all planes perpendicular to that axis are isotropic

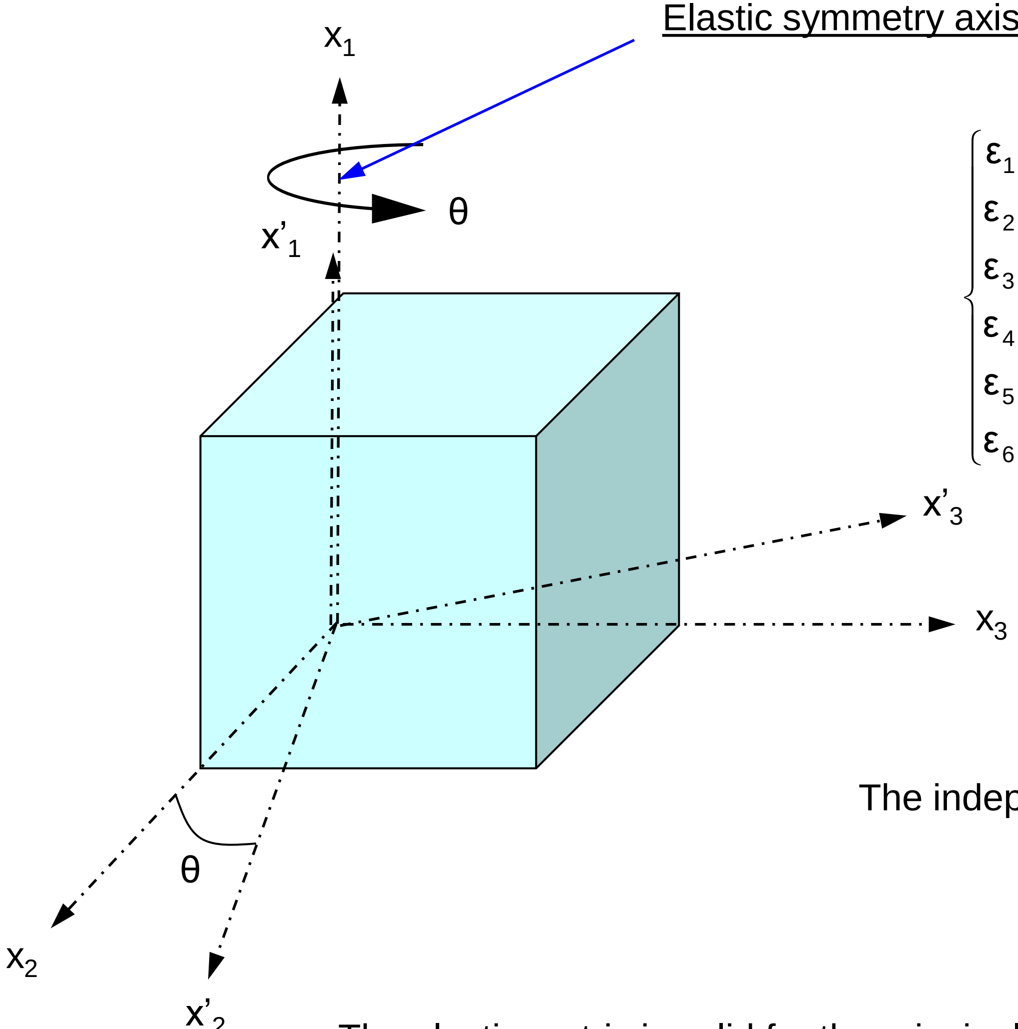

$$\begin{Bmatrix} \varepsilon_1 \\ \varepsilon_2 \\ \varepsilon_3 \\ \varepsilon_4 \\ \varepsilon_5 \\ \varepsilon_6 \end{Bmatrix} = \begin{bmatrix} S_{11} & S_{12} & S_{12} & 0 & 0 & 0 \\ S_{12} & S_{22} & S_{23} & 0 & 0 & 0 \\ S_{12} & S_{23} & S_{22} & 0 & 0 & 0 \\ 0 & 0 & 0 & 2(S_{22}-S_{23}) & 0 & 0 \\ 0 & 0 & 0 & 0 & S_{66} & 0 \\ 0 & 0 & 0 & 0 & 0 & S_{66} \end{bmatrix} \begin{Bmatrix} \sigma_1 \\ \sigma_2 \\ \sigma_3 \\ \sigma_4 \\ \sigma_5 \\ \sigma_6 \end{Bmatrix}$$

The independent S_{ij} are **5** (or C_{ij})

The elastic matrix is valid for the principal axes system

Typical transversely isotropic medium: Fibre tow

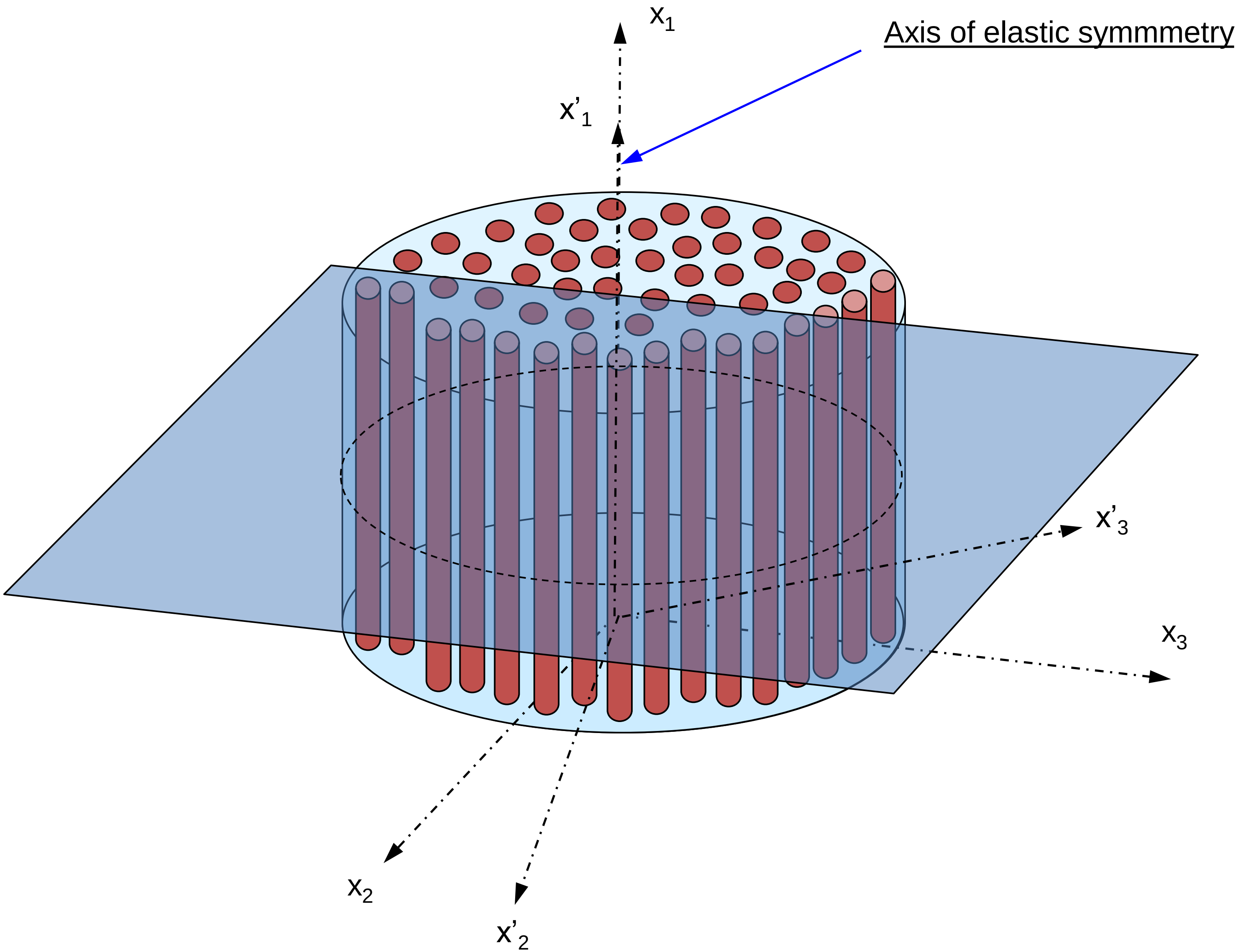

Isotropic medium

All directions are elastically equivalent

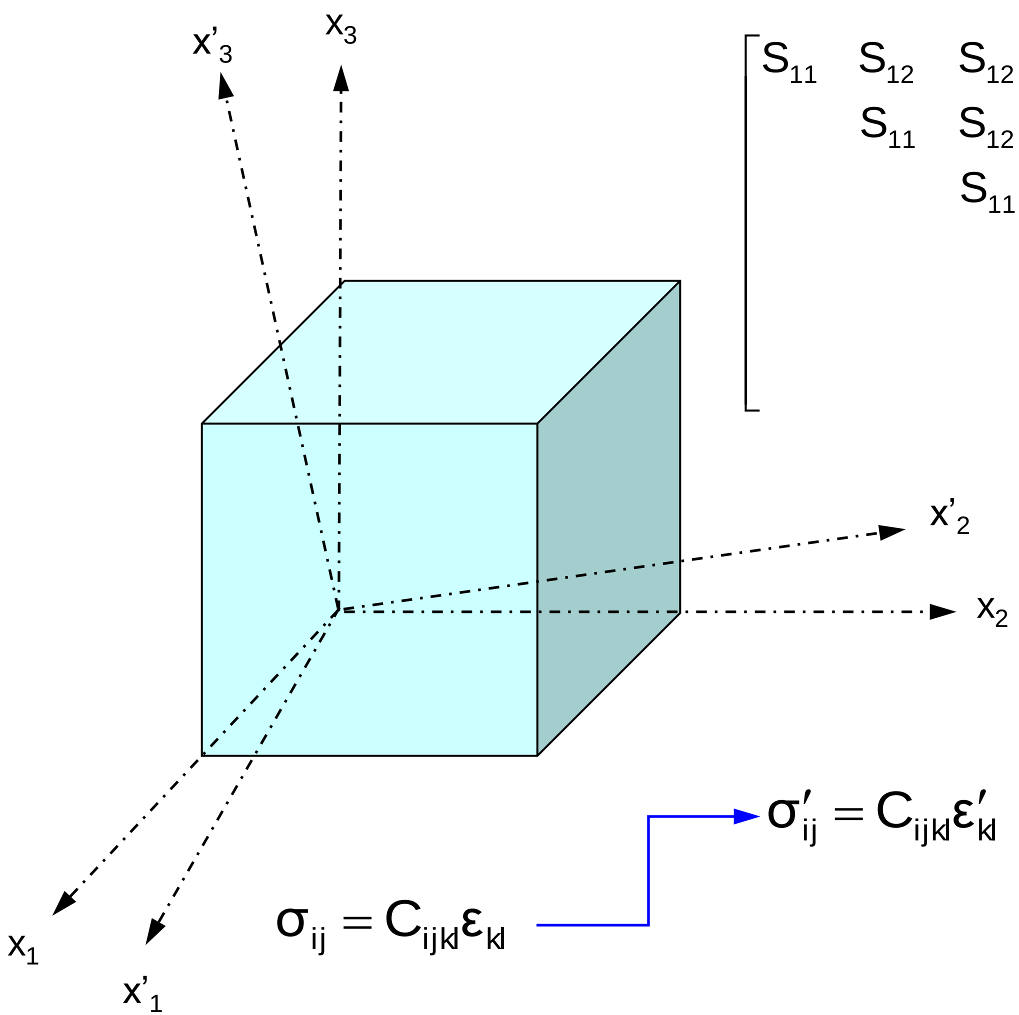

$$\begin{bmatrix} S_{11} & S_{12} & S_{12} & 0 & 0 & 0 \\ & S_{11} & S_{12} & 0 & 0 & 0 \\ & & S_{11} & 0 & 0 & 0 \\ & & & 2(S_{11}-S_{12}) & 0 & 0 \\ & & & & 2(S_{11}-S_{12}) & 0 \\ & & & & & 2(S_{11}-S_{12}) \end{bmatrix}$$

$$\sigma_{ij} = C_{ijkl}\varepsilon_{kl}$$

$$\sigma'_{ij} = C_{ijkl}\varepsilon'_{kl}$$

~~Principal axes system?~~

Typical isotropic medium: Particulate reinforced composite

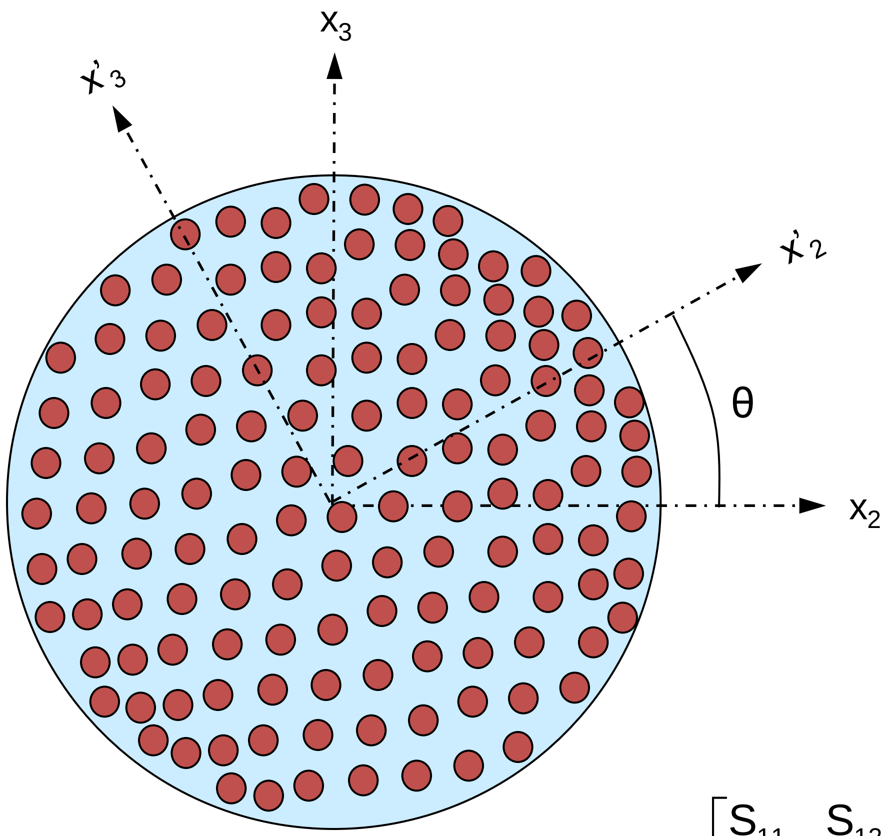

$$
\begin{bmatrix}
S_{11} & S_{12} & S_{12} & 0 & 0 & 0 \\
 & S_{11} & S_{12} & 0 & 0 & 0 \\
 & & S_{11} & 0 & 0 & 0 \\
 & & & 2(S_{11}-S_{12}) & 0 & 0 \\
 & & & & 2(S_{11}-S_{12}) & 0 \\
 & & & & & 2(S_{11}-S_{12})
\end{bmatrix}
$$

Elastic properties of a lamina

- Loading parallel to the reinforcement
- Loading perpendicular to the reinforcement
- Loading in an angle to the reinforcement

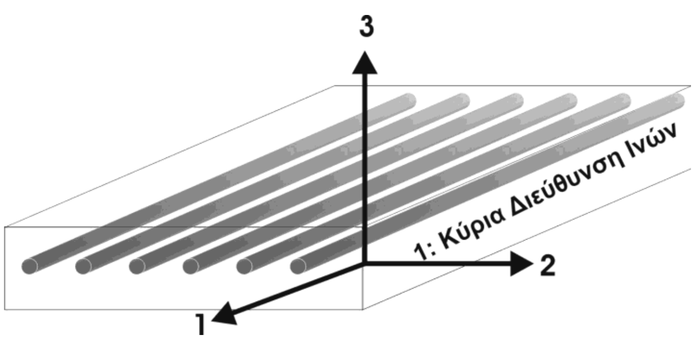

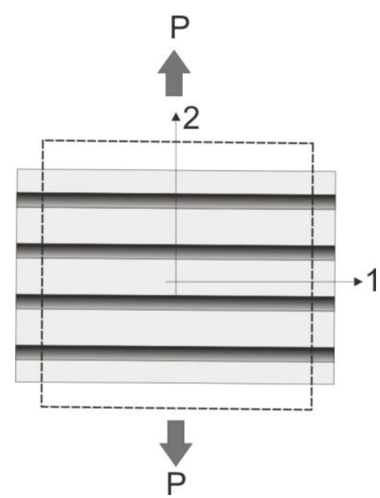

Loading parallel to the reinforcement

For a tensile stress parallel to the reinforcement assuming that:

- Interfacial bond is perfect,
- The strain ε_1 of the matrix equals that on the fibre
- The matrix and the fibre are linear elastic solids:

Which phase undertakes the maximum stress?

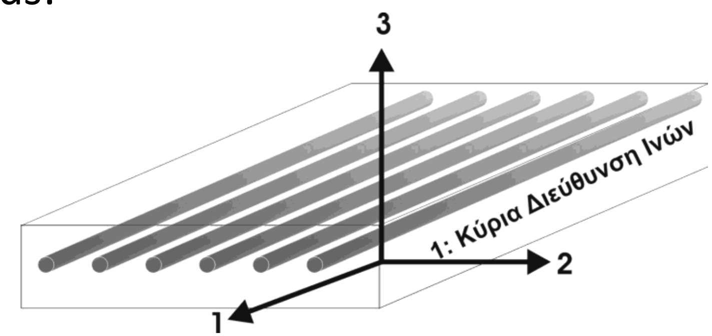

$$\sigma_f = E_f \varepsilon_1 \quad \text{and} \quad \sigma_m = E_m \varepsilon_1$$

$$P = P_f + P_m \quad \text{and} \quad P_m = \sigma_m A_m$$

$$\sigma_1 = \frac{P}{A} \quad \text{and} \quad P_f = \sigma_f A_f$$

Rule of Mixtures

$$E_1 \equiv E_{//} = E_f V_f + E_m \left(1 - V_f\right)$$

Loading perpendicular to the reinforcement

For a tensile stress parallel to the reinforcement assuming that:

- Interfacial bond is perfect,
- The strain ε_1 of the matrix equals that on the fibre
- The matrix and the fibre are linear elastic solids:

Which phase undertakes the maximum stress?

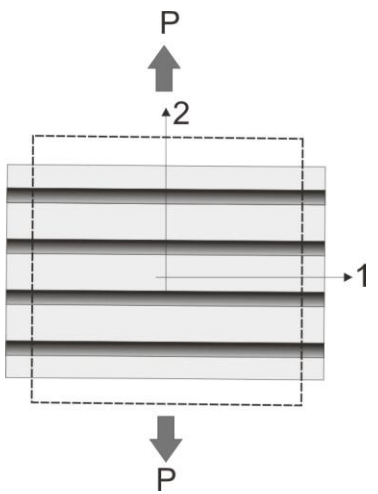

$\sigma = E_f \varepsilon_f$ and $\sigma = E_m \varepsilon_m$

Rule of Mixtures

$$E_2 = E_{\perp} = \frac{E_f \cdot E_m}{E_f \cdot (1 - V_f) + E_m \cdot V_f}$$

Corrections

Poisson effects:

$$E_2 \equiv E_\perp = \frac{E_f \cdot E_m^{'}}{E_f\left(1-V_f\right)+E_m^{'}V_f} \qquad E_m^{'} = \frac{E_m}{1-\nu_m^2}$$

Halpin Tsai:

$$E_1 = E_{//} = E_f V_f + E_m\left(1-V_f\right)$$

$$\nu_{12} = \nu_f V_f + \nu_m\left(1-V_f\right) \qquad \frac{M}{M_m} = \frac{\left(1+\xi\cdot\eta\cdot V_f\right)}{\left(1-\eta V_f\right)}$$

Where M is the composite property and ξ a parameter depending on reinforcement attributes:

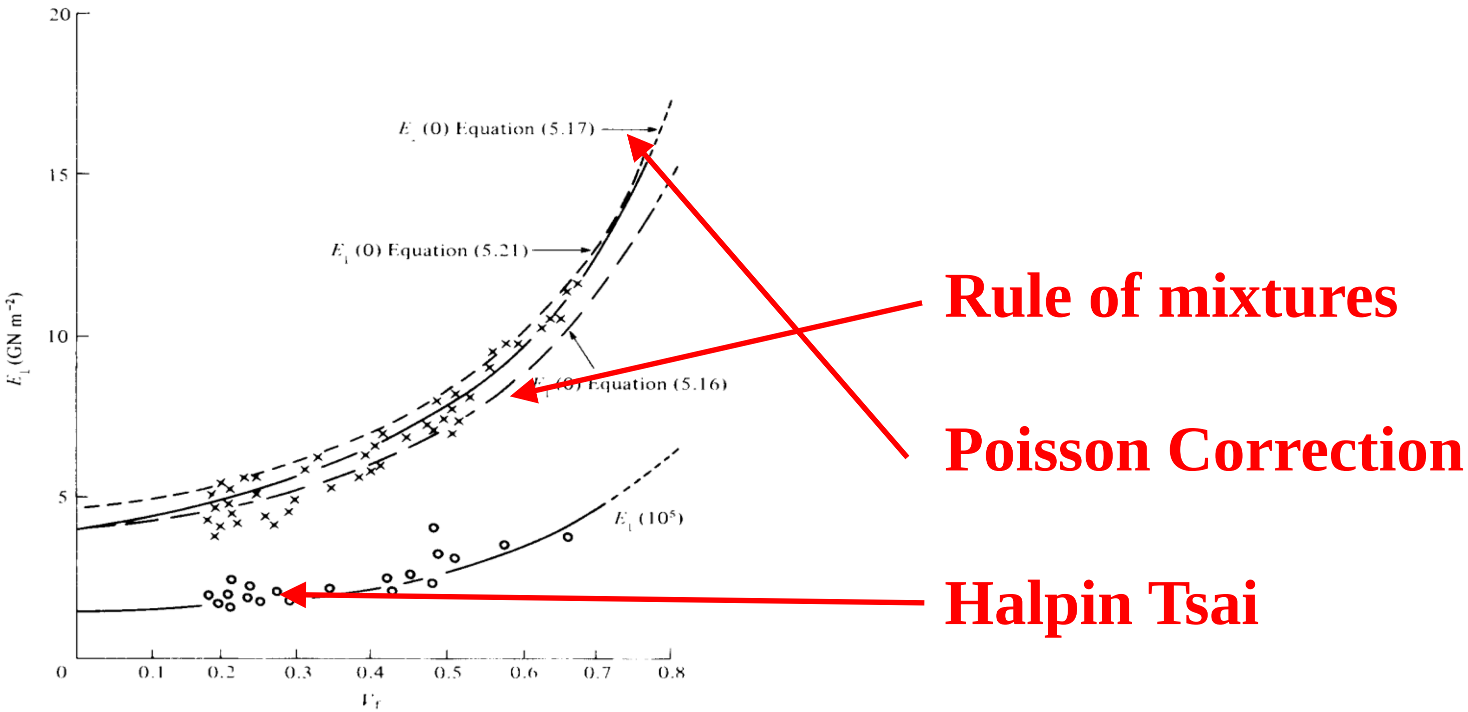

Stress concentration and strain magnification (Kies)

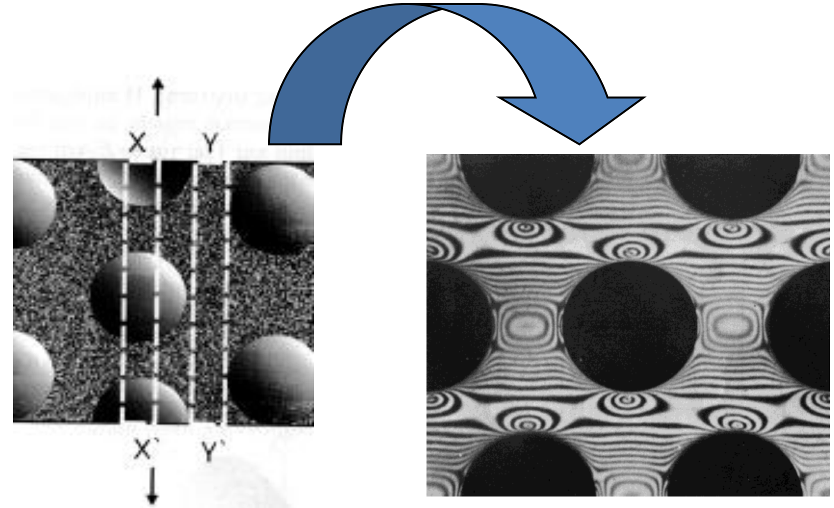

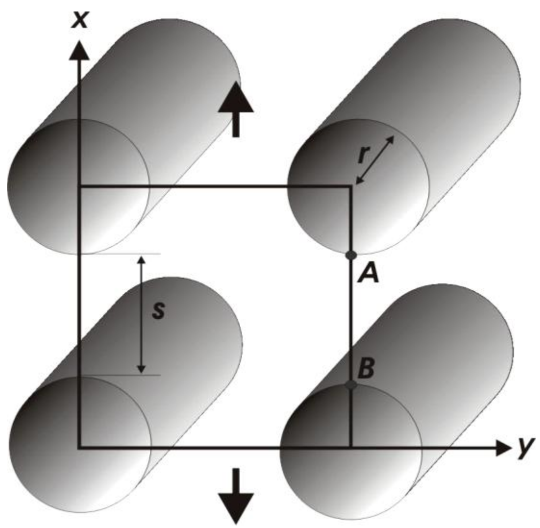

$$\frac{\varepsilon_x}{\bar{\varepsilon}_x} = \frac{\left(2 + \frac{s}{r}\right)}{\left(\frac{s}{r} + 2\frac{E_m}{E_f}\right)}$$

$$V_f = \frac{\pi}{4} \cdot \left(\frac{r}{R}\right)^2$$

$$\frac{\varepsilon_x}{\bar{\varepsilon}_x} = \frac{\sqrt{\frac{\pi}{V_f}}}{\sqrt{\frac{\pi}{V_f}} - 2 + 2 \cdot \frac{E_m}{E_f}}$$

Strain Magnification: Glass polyester

$$\frac{E_f}{E_m} = 20$$

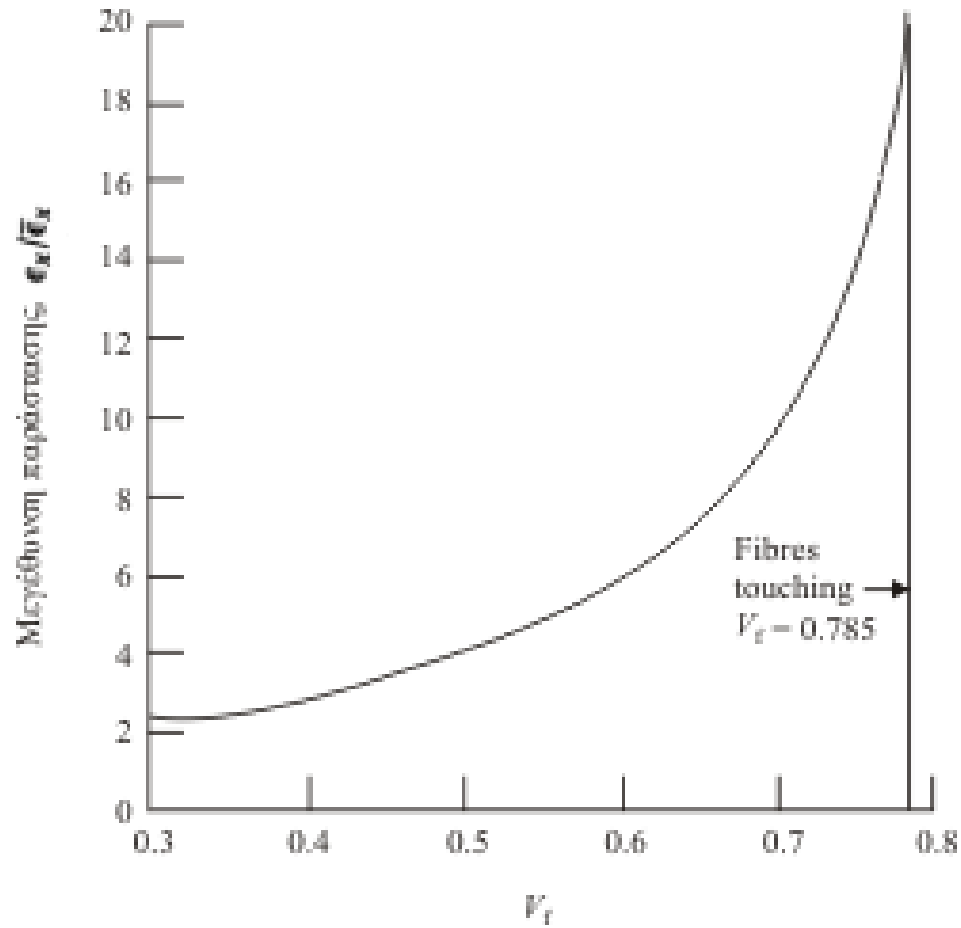

Long fibre composites with random orientation (Nielsen και Chen 1968)

$$\overline{E} = 2\pi \int_0^{\pi/2} E(\theta) d\theta$$

E(θ): Stiffness of UD lamina as a function of Theta for constant Vf.

$$\frac{1}{E(\theta)} = \frac{1}{E_1} \cdot C^4 + \left(\frac{1}{G_{12}} - \frac{2\nu_{12}}{E_1} \right) \cdot C^2 \cdot S^2 + \frac{1}{E_2} \cdot S^4$$

where: C=cosθ, S=sinθ

Long fibre composites with random orientation

- **Empirical relationships:**

$$\overline{E} = \frac{3}{8}E_1 + \frac{5}{8}E_2 \qquad \overline{G} = \frac{1}{8}E_1 + \frac{1}{4}E_2$$

The effect of V_f comes through E_1 and E_2.

Long fibre composites

Material	E_1 (GPa)	E_2 (GPa)	G_{12} (GPa)	ν_{12}
Glass-polyester	35 - 40	8-12	3,5-5,5	0,26
Type I carbon-epoxy	190-240	5-8	3 - 6	0,26
Kevlar 49 - epoxy	65 - 75	4 - 5	2 - 3	0,35

Typical E_1, E_2, G_{12} &ν_{12}
For composite types

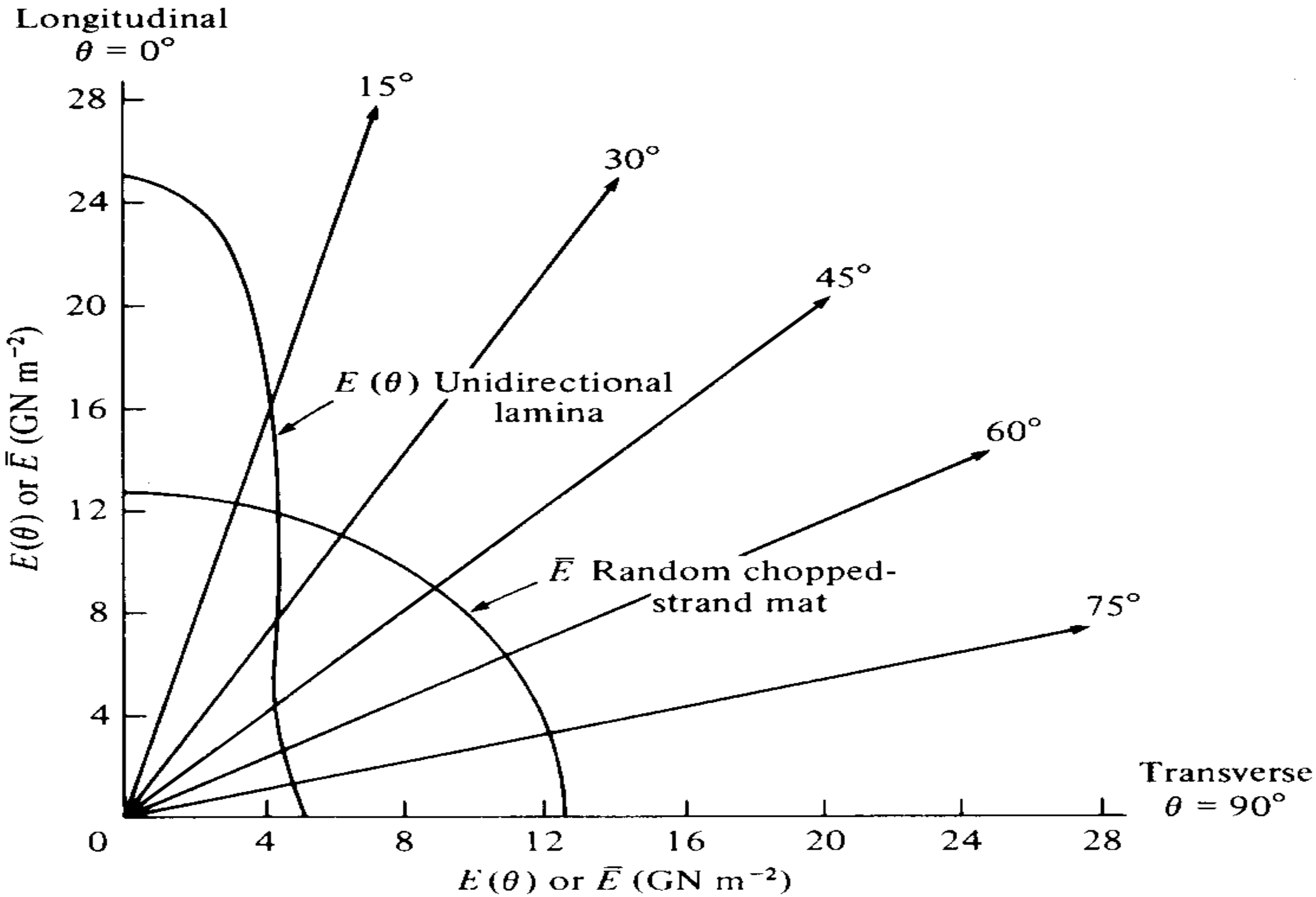

glass fibre- polyester resin with Vf=0.30 [D. Hull, 1981]

Elastic properties of short fibre composite

- Ineffective length correction (shear Lag)

$$E_1 \equiv E_{//} = \eta_l E_f V_f + E_m \left(1 - V_f\right)$$

$$\eta_l = 1 - \frac{\tanh \frac{\beta l}{2}}{\frac{\beta l}{2}} \qquad \frac{E_{short}}{E_{cont}} = \eta_l$$

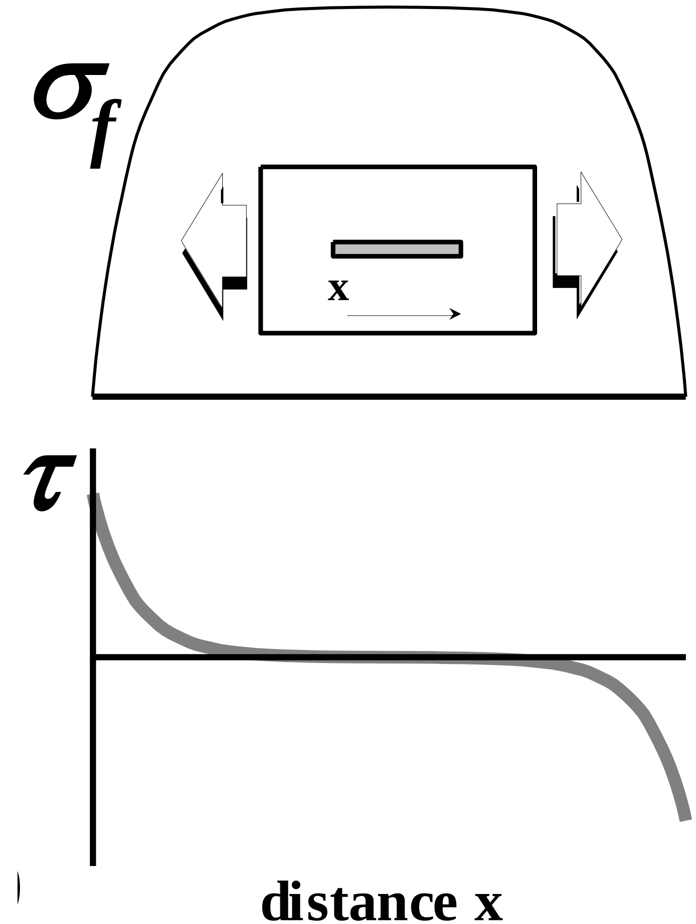

Shear lag

Υλικό	l (mm)	G_m / E_f	r (μm)	V_f	η_l
Carbon-epoxy	0,1 1,0 10,0	0,005 0,005 0,005	8 8 8	0,3 0,3 0,3	0,20 0,89 0,99
Glass-nylon	0,1 1,0 10,0	0,010 0,010 0,010	11 11 11	0,3 0,3 0,3	0,21 0,89 0,99

Elastic properties [Dingle 1974]

Fibre length 1 (mm)	V_f	$E_{//}$ Theoretical (GPa)	$E_{//}$ Experimental (GPa)	η_l
1	0,49	194	155	0,80
4	0,32	128	112	0,87
6	0,42	167	141	0,84

Tensile strength of long fibre composites

Typical strength of UD laminates (V_f 0.50)

Material	**σ*//T (MPa)**	**σ*// C (MPa)**	**σ*⊥T (MPa)**	**σ*⊥C (MPa)**	**τ*# (MPa)**
Glass-polyester	650-750	600-900	20-25	90-120	45-60
Type I carbon-epoxy	850-1100	700-900	35-40	130-190	60-75
Kevlar 49-epoxy	1100-1250	240-290	20-30	110-140	40-60

T: Tension, C: Compression

Deterministic fibre strength

From the rule of mixtures:

$$\sigma_{||} = \sigma_f V_f + \sigma_m (1-V_f)$$

$$\sigma_{||} = E_f \varepsilon_{\backslash\backslash} V_f + E_m \varepsilon_{\perp}(1-V_f)$$

Failure Possibilities:

1. $\varepsilon^*_f > \varepsilon^*_m$
2. $\varepsilon^*_f < \varepsilon^*_m$

Uniform fibre strength

1. $\varepsilon^*_f > \varepsilon^*_m$

For small V_f:

•$\sigma^*_{//}$ depends on σ^*_m.
•The matrix fails first
•The fibres take over but cannot take the load and fail

$$\sigma^*_{//} = \sigma'_f V_f + \sigma^*_m \left(1 - V_f\right)$$

For large V_f:

Since $E_f >> E_m \Rightarrow$

- The matrix undertakes a small load fraction
- The matrix fails
- The load is transferred to the fibres until they fail

$$\sigma^*_{//} = \sigma^*_f V_f$$

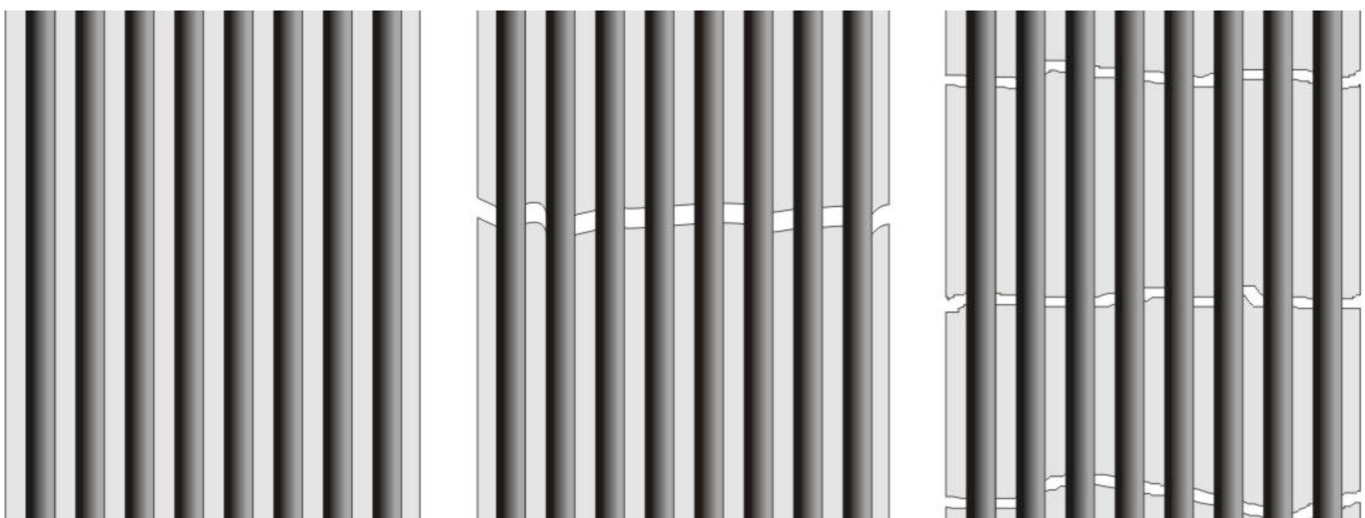

$\varepsilon^*_f > \varepsilon^*_m$: For equal V_f:

$$V_f' = \frac{\sigma_m^*}{\sigma_f^* - \sigma_f' + \sigma_m^*}$$

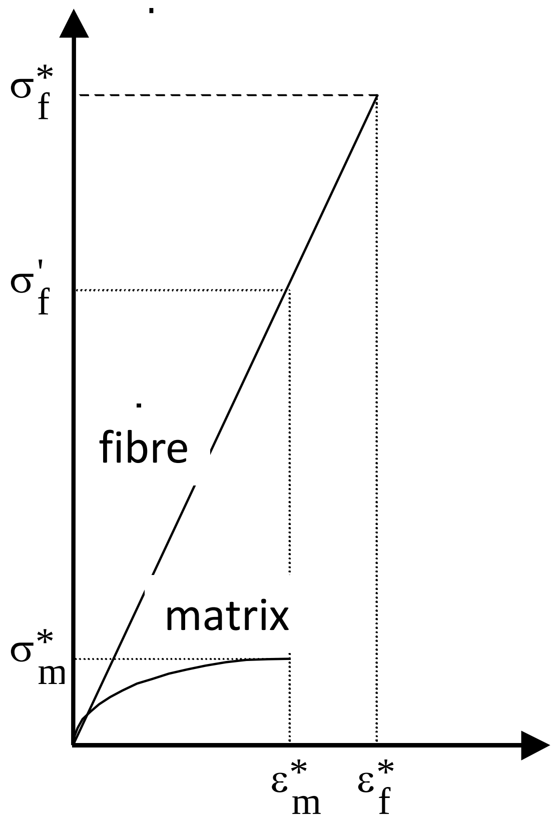

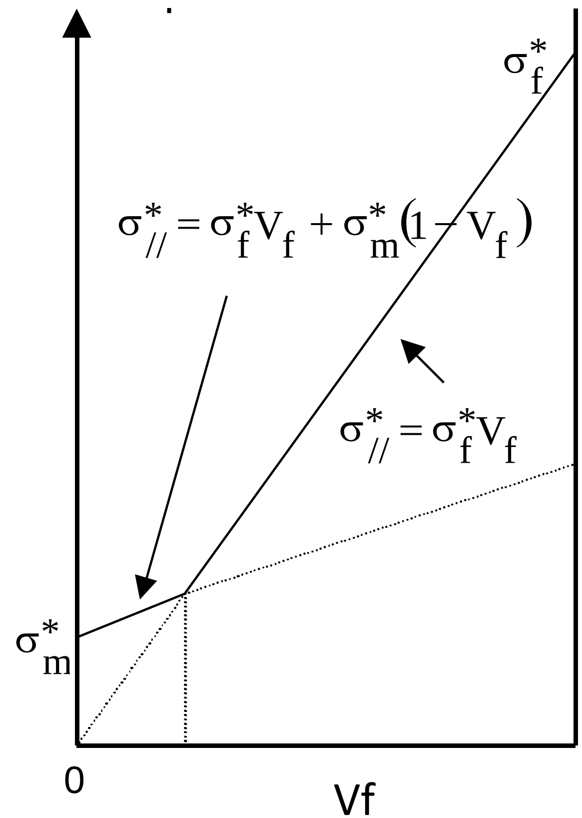

Uniform fibre strength

1. $\varepsilon^*_f < \varepsilon^*_m$

For small V_f:

- The fibres break.
- The matrix takes over the additional load
- The efficient cross section is reduced by the fibre breaks

$$\sigma^*_{//} = \sigma^*_m V_m = \sigma^*_m (1 - V_f)$$

For large V_f:

Since $E_f >> E_m \Rightarrow$

- The fibres break.
- The matrix cannot take over the additional load
- The composite fails

$$\sigma^*_{//} = \sigma^*_f V_f + \sigma'_m (1 - V_f)$$

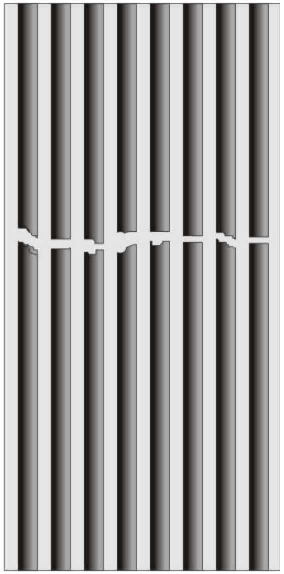

$\varepsilon^*_f < \varepsilon^*_m$: For equal V_f:

$$V_f' = \frac{\left(\sigma_m^* - \sigma_m'\right)}{\left(\sigma_f^* + \sigma_m^* - \sigma_m'\right)}$$

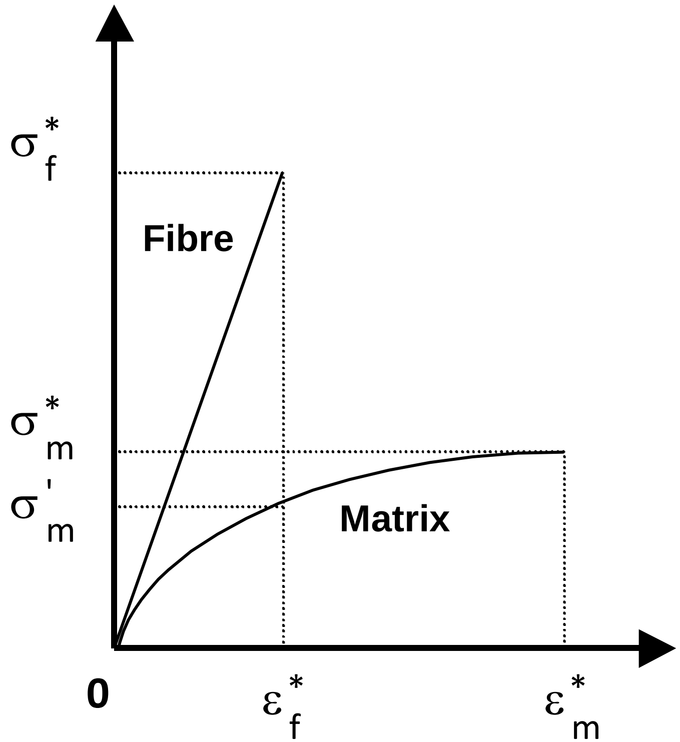

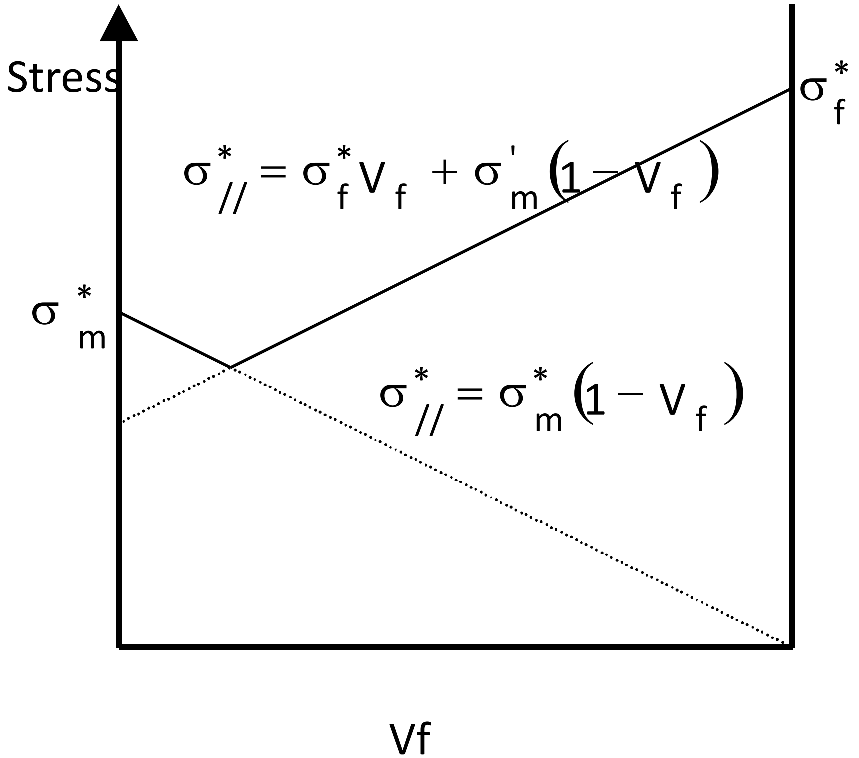

Variable fibre strength

- The fibre is brittle
  - Fracture occurs at the flaw sites where strength is reduced
  - The strength reduction is stochastic
- How does the strength depend on the fibre size? (volume or length for constant cross section);
- Experimental campaign: strength as a function of length:
- definitions:
  - σ^*_f fibre strength
  - 2r diametre,
  - l length
  - σ_1 minimum fibre strength
  - σ_u maximum fibre strength

Weibul distribution

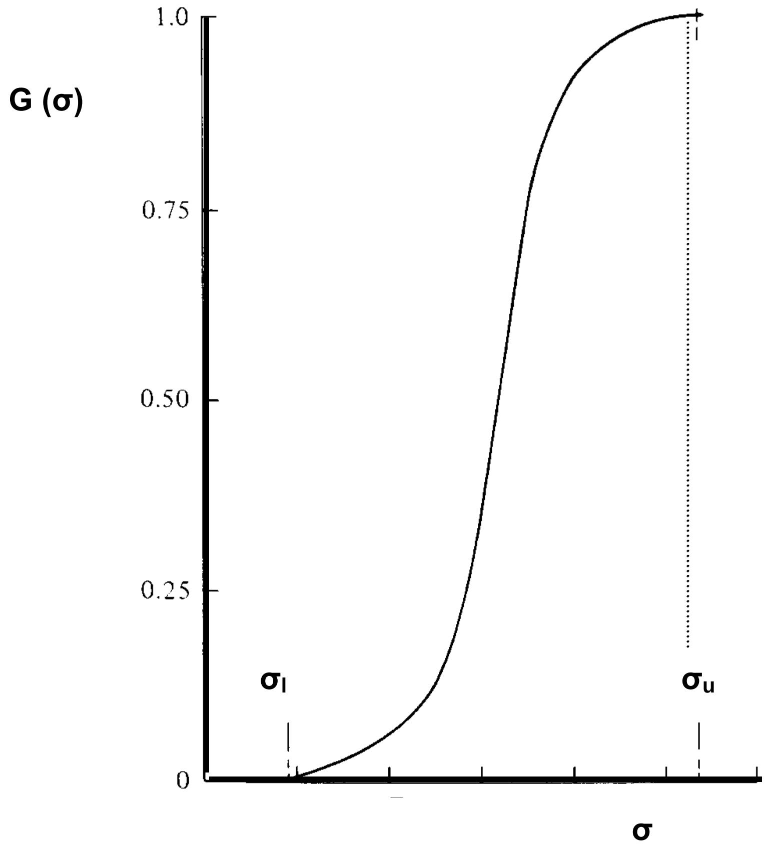

$$G(\sigma) = 1 - \left[1 - \left(\frac{\sigma - \sigma_l}{\sigma_u - \sigma_l} \right)^m \right]^\omega$$

$$\omega = \frac{l}{2r}$$ Size parameter

$$m = \frac{6\,\overline{\sigma}}{5\,\mathrm{s}}$$ Shape parameter

Where:

$$\overline{\sigma} = \sum_{i=1}^{N} \sigma_i / N \quad \text{και} \quad s = \left[\frac{\sum_{i=1}^{N} (\sigma_i - \sigma)^2}{N} \right]^{1/2}$$

For a fibre bundle (Coleman 1958)

- Assumptions:
  - α) the fibres are distinct and have equal cross sections
  - β) For stress $\sigma_{i<}\sigma_l$ the fibre deform equally and do not break
  - γ) as the load increases the weaker fibres break and the intact fibres take up the load

Fibre bundle strength(Coleman 1958)

- The maximum fracture load occurs when the developing stress on the remaining fibres reaches σ_u and the bundle fails
  - The strength, σ_b, of the bundle is less than the mean fibre strength
  - The reductions depends on the spread of the fibre strength of individual fibres:

$$\frac{\sigma_b}{\bar{\sigma}} = \left[\frac{1}{me}\right]^{1/m} \frac{1}{\Gamma(1+1/m)}$$

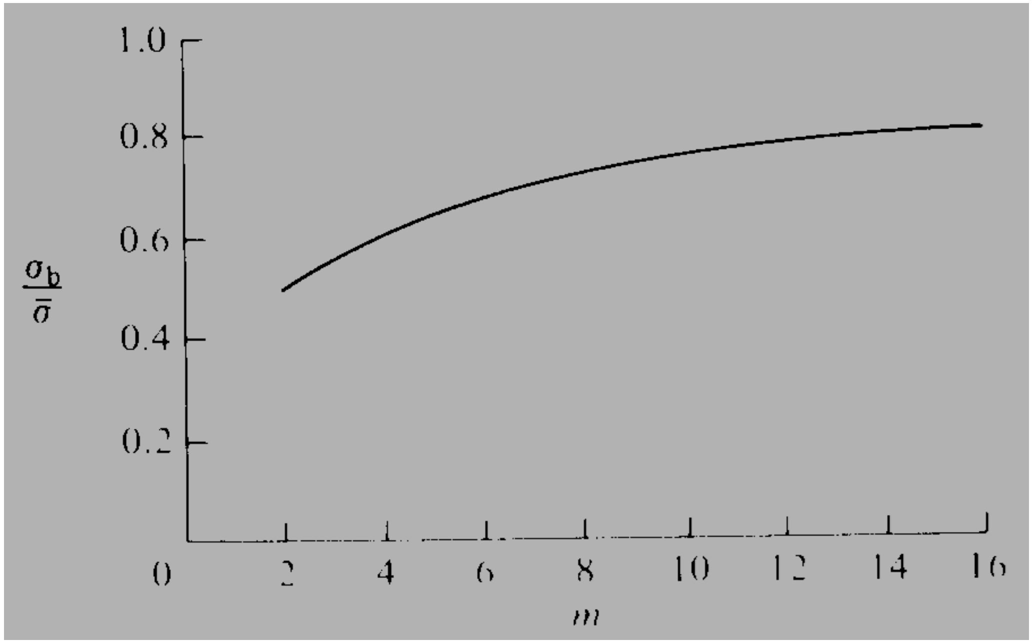

Cumulative weakening (Rosen)

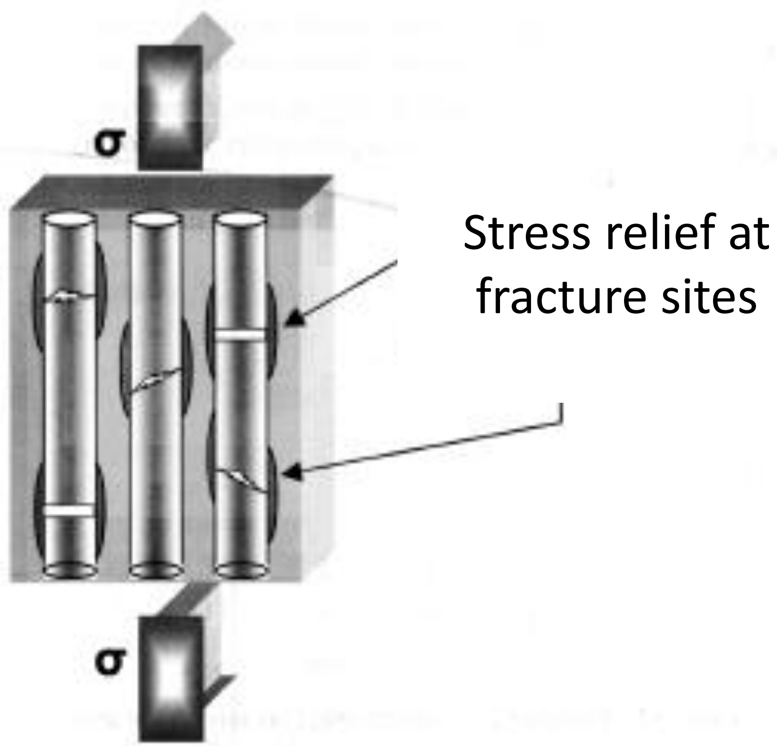

The statistical distribution of fibre strength leads to global weakening and failure:

$$\frac{\sigma^*_{cum}}{\bar{\sigma}} = \left(\frac{1}{l_c m e}\right)^{1/m} = \frac{1}{\Gamma\left(1+\frac{1}{m}\right)}$$

σ_{cum}: fibre strength

l_c: critical length

Statistical strength (Carbon / Epoxy)

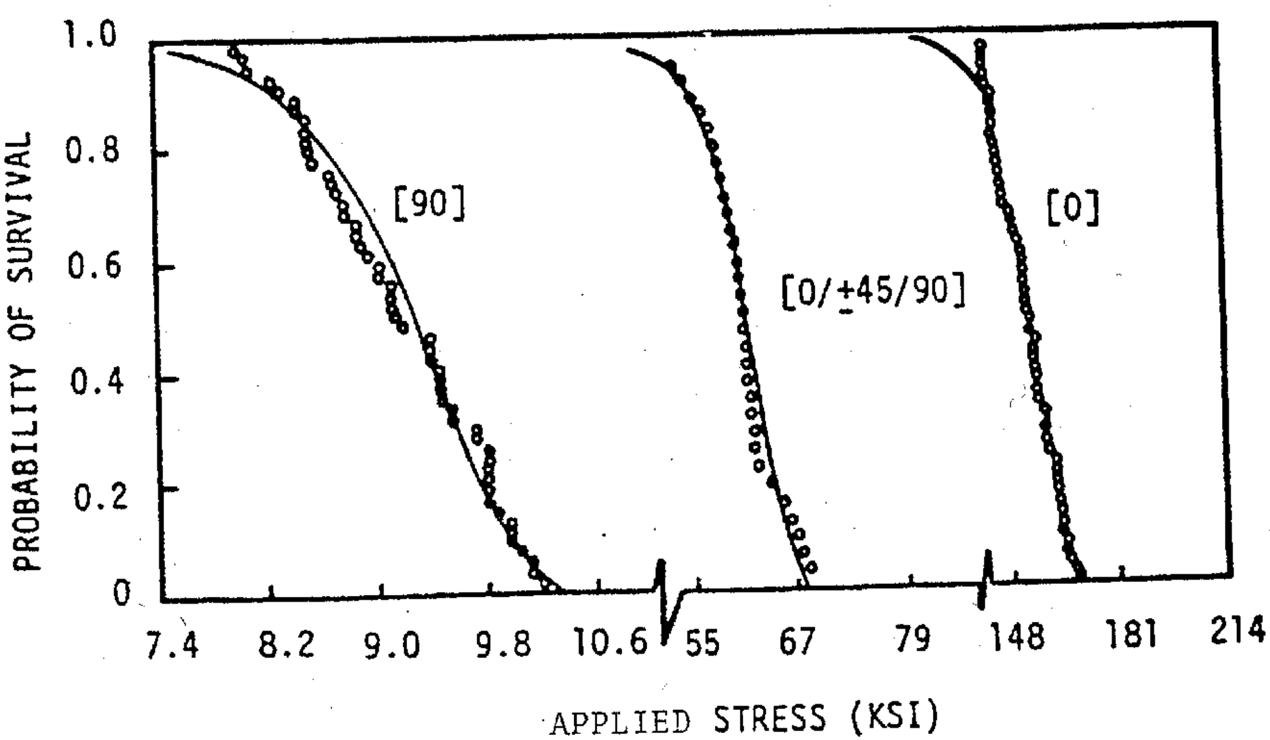

Crack propagation in UD laminates

Εικόνα 6.19 Θραύση γειτονικών ινών λόγω συγκέντρωσης τάσεων στο άκρο της πρώτης ρωγμής.

- Stress concentration leads to transverse cracking

Crack-fibre interaction

- Possibilities
  - a) The crack propagates in the matrix.
  - b) The matrix around the crack yields creating a plastic zone along the fibre.
  - c) The interface fails and the fibre retracts in the matrix.

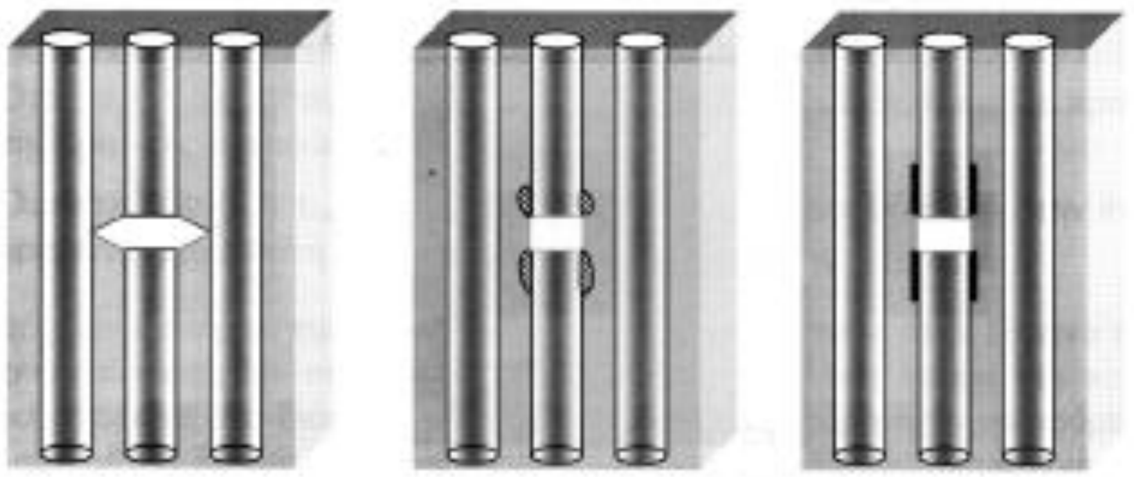

(α) (β) (γ)

Crack propagation

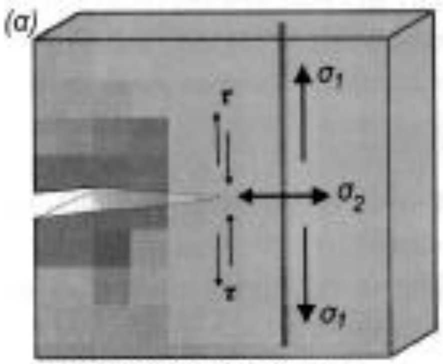

The crack propagates

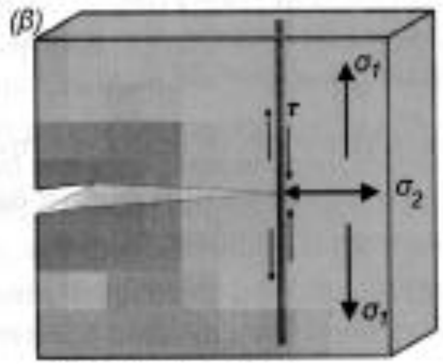

And meets the fibre

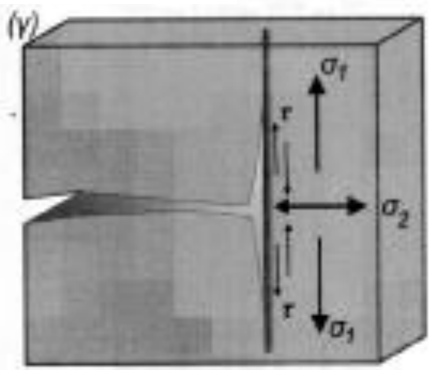

The matrix debonds from the fibre

- The stress concentration is proportional to $(c/\rho)^{1/2}$
  - ρ is the radius of curvature at the crack tip
  - 2c is the crack length

Stress field at the crack

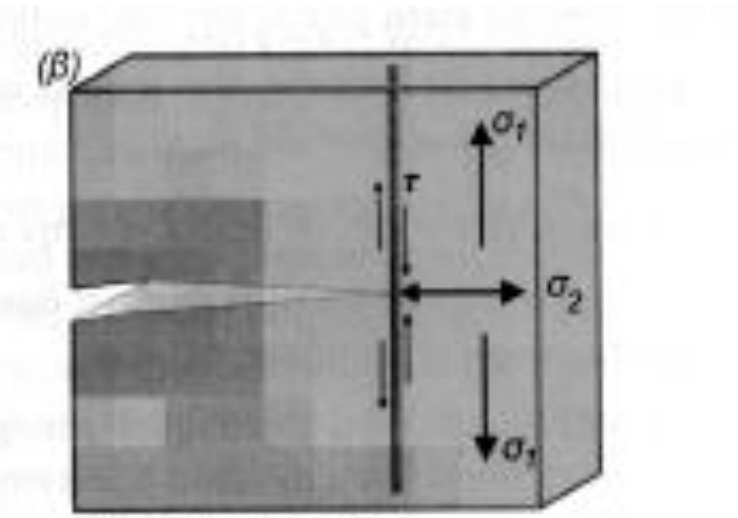

- The maximum tensile stress σ_{1max} perpendicular to the crack propagation and the maximum tensile stress σ_{2max} parallel to the crack path develop simultaneously at the crack front

Stress field at the crack

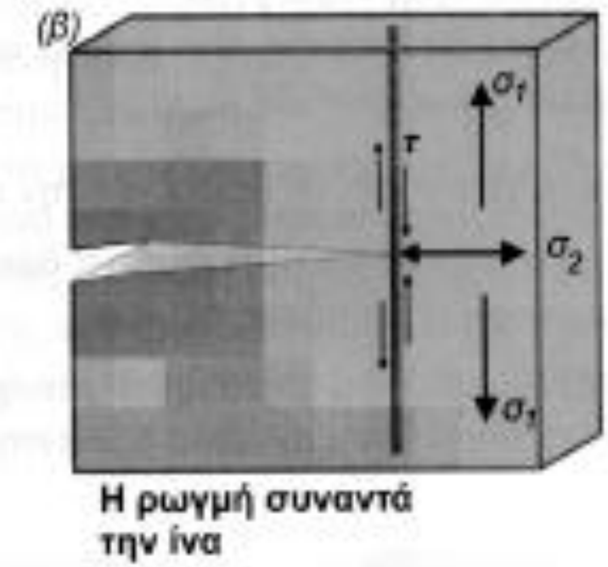

- For isotropic materials,
  - $\sigma_{1max}/\sigma_{2max} \sim 5$
- For anisotropic materials the ratio depends on the crack orientation and the degree of anisotropy.
  - For carbon fibre-epoxy with $V_f = 0.5$
  - $\sigma_{1max}/\sigma_{2max} \sim 48$
  - $\sigma_{1max}/\tau_{max}=11$
  - $\tau_{max}/\sigma_{2max} =4.4.$

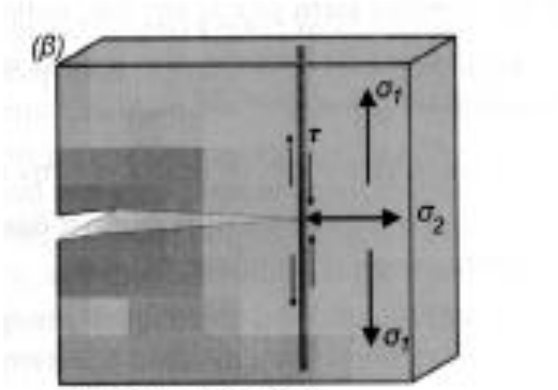

Failure at the vicinity of the crack

- The process depends on the values of σ//*, σ⊥*, $\tau_{\#}$*. :
  - α) σ//*/ σ⊥* > σ_{1max} /σ_{2max} : tensile failure parallel to the interface will precede fibre fracture
  - β) σ//* / $\tau_{\#}$* > σ_{1max} / τ_{max} : shear failure will precede fibre fracture,
  - γ) $\tau_{\#}$* / σ ⊥ * > τ_{max} / σ_{2max} : tensile failure at the interface is more probale than shear failure.

Typical values for laminates (Vf~50%)

Υλικό	$\sigma^*_{//}T$ (MPa)	$\sigma^*_{//}C$ (MPa)	$\sigma^*_{\perp}T$ (MPa)	$\sigma^*_{\perp}C$ (MPa)	$\tau^*_{\#}$ (MPa)
Glass-polyester	650-750	600-900	20-25	90-120	45-60
Type I carbon-epoxy	850-1100	700-900	35-40	130-190	60-75
Kevlar 49-epoxy	1100-1250	240-290	20-30	110-140	40-60

Transverse tensile strength

- Often, transverse strength is less than the matrix strength
  - Assumptions:
    - Zero interfacial strength at the transverse direction
    - Tough matrix (resisting crack propagation)
  - The strength is that of the matrix with reduced effective cross section

$$\frac{s}{2R} = 1 - 2\sqrt{\frac{V_f}{\pi}} \quad \Rightarrow \quad \sigma_\perp^* = \sigma_m^*\left(1 - 2\sqrt{\frac{V_f}{\pi}}\right)$$

For square distribution…

$$\sigma_\perp^* = \sigma_m^*\left(1 - 2\sqrt{\frac{V_f}{\pi}}\right)$$

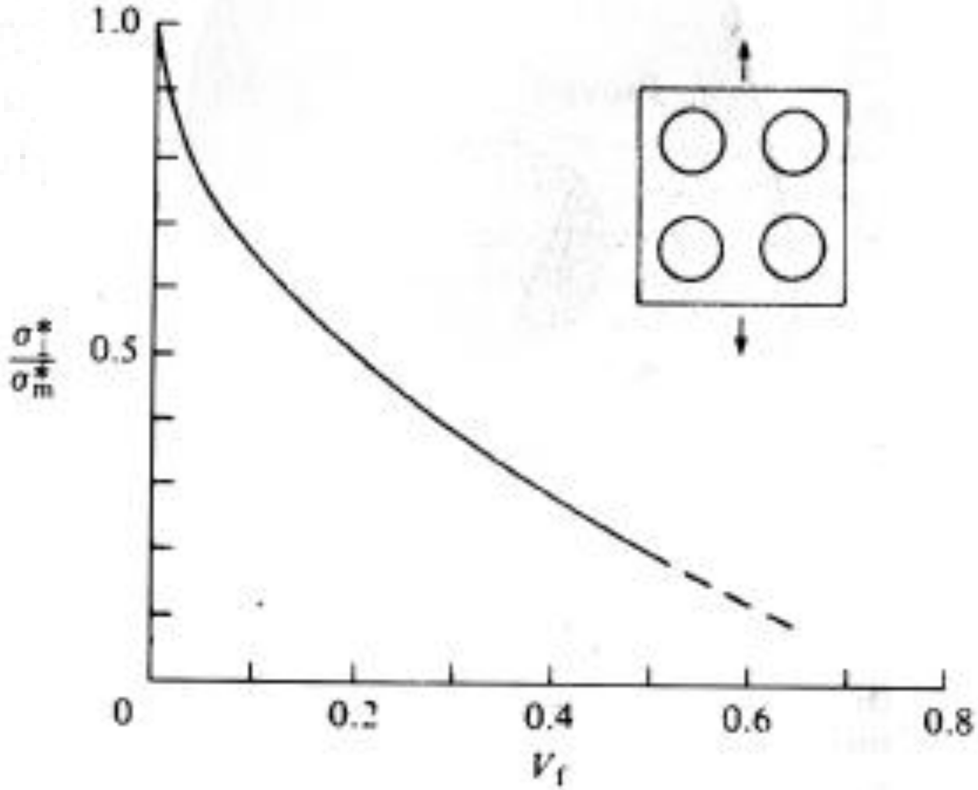

Derek Hull, 1981

Transverse tensile strength

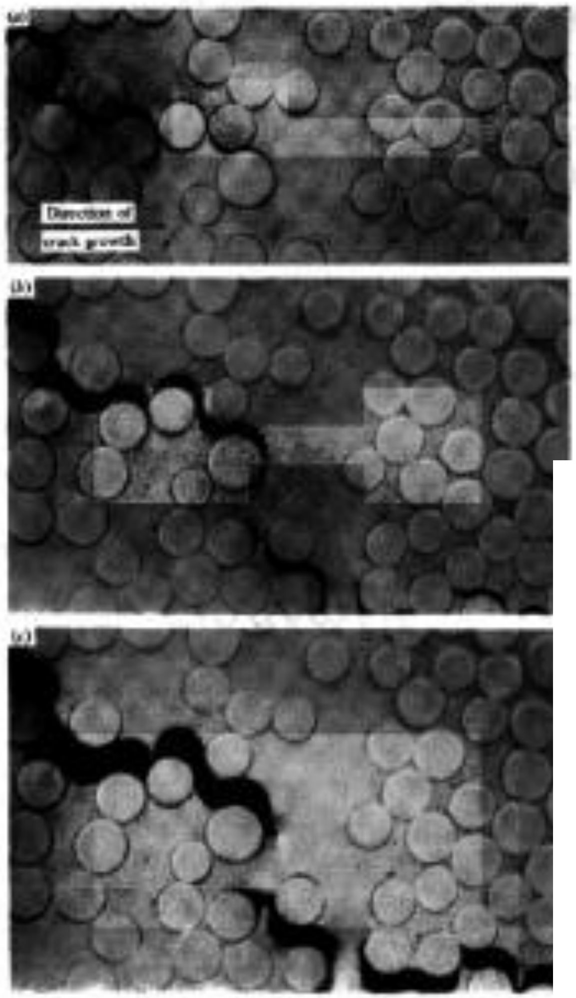

Εικόνα 6.36: Διάδοση εγκάρσιας ρωγμής σε μία στρώση glass fibre-polyester resin. Η ρωγμή έχει συναντήσει μία περιοχή πλούσια σε ρητίνη οπότε παρατηρείται διαπλάτυνση του άκρου της και ταυτόχρονα διαρροή της ρητίνης. ΠΗΓΗ: D. Hull, An Introduction to Composite Materials, Cambridge Univ. Press 1981

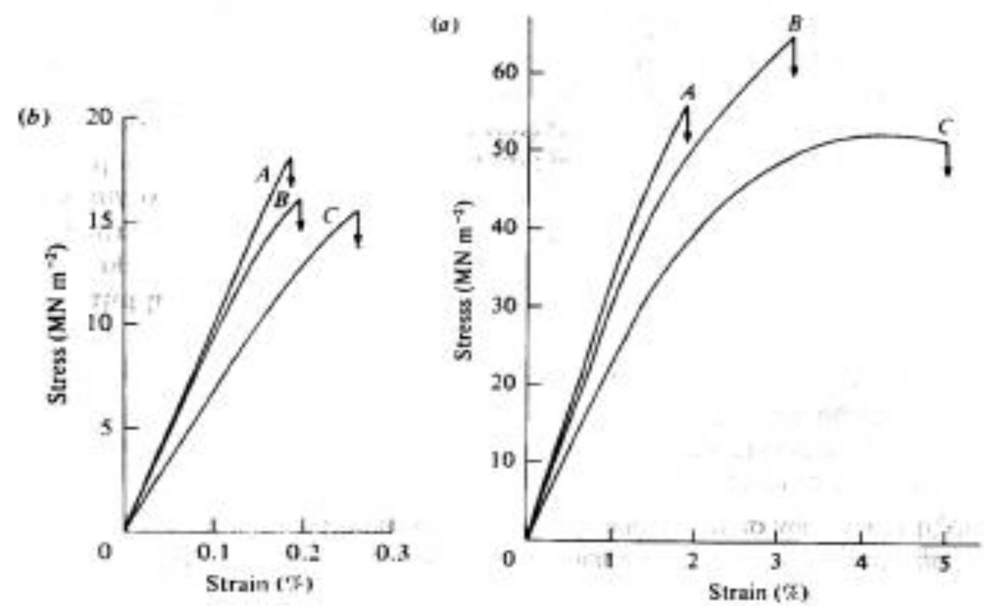

BRITISH STANDARD

BS EN ISO 527-5 : 1997
BS 2782 :
Part 3 :
Method 326G :
1997

Plastics — Determination of tensile properties

Part 5. Test conditions for unidirectional fibre-reinforced plastic composites

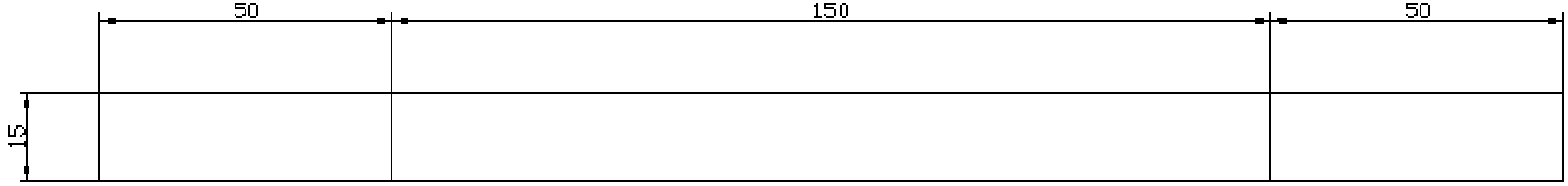

a

Geometry of test specimens

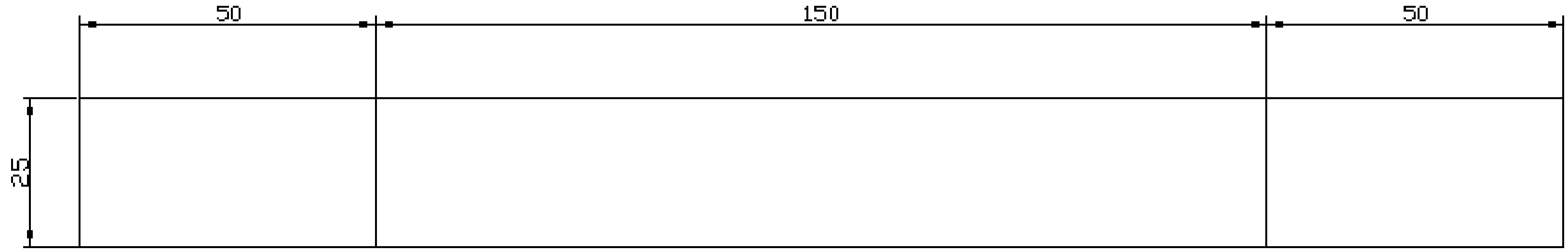

b

CRP materials

MATERIAL	CODE NAME	LAYUP
GOB	GOBU	$[0]_T$
	GOBM	$[90_2]_T$
	GOBR	$[\pm 45]_S$
HEX	HEXU	$[0_2]_T$
	HEXM	$[90_3]_T$
	HEXR	$[\pm 45]_S$

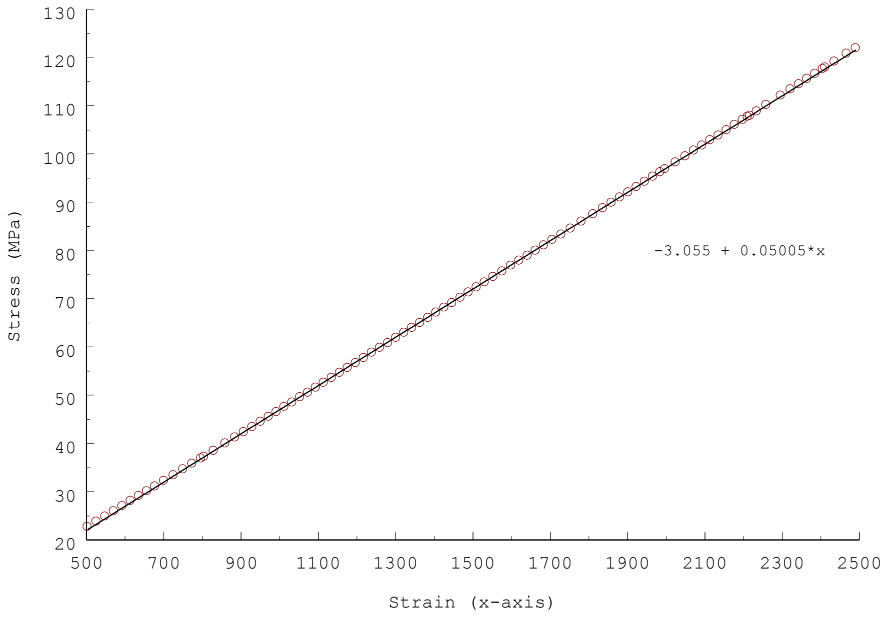

Axial stress vs. axial strain UD laminate

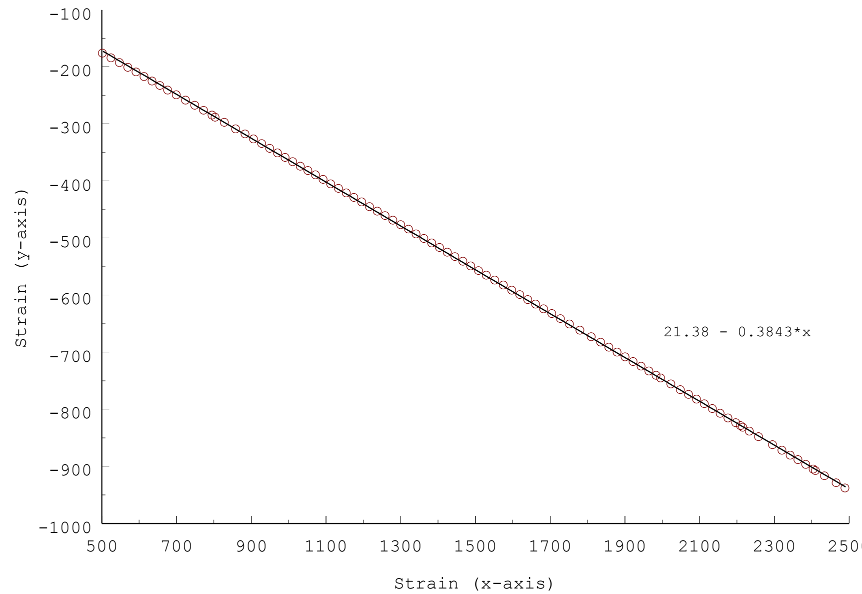

Transverse strain vs. axial strain UD laminate

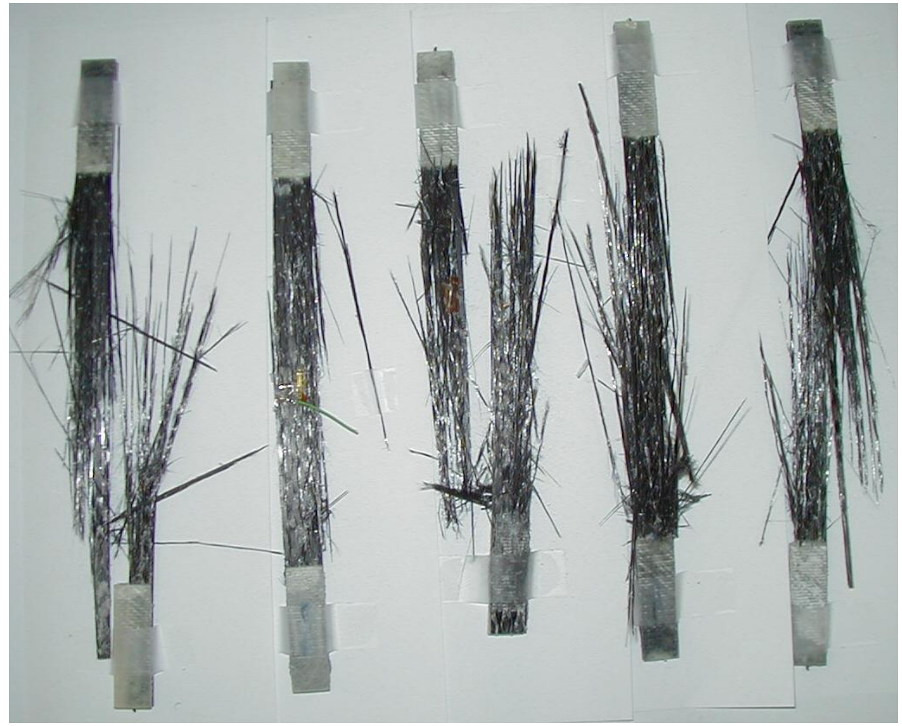

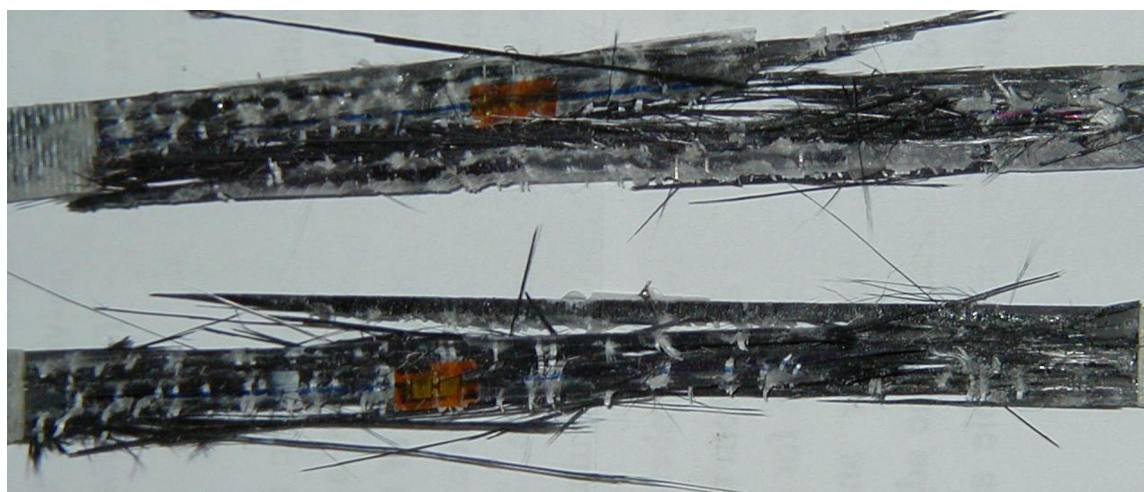

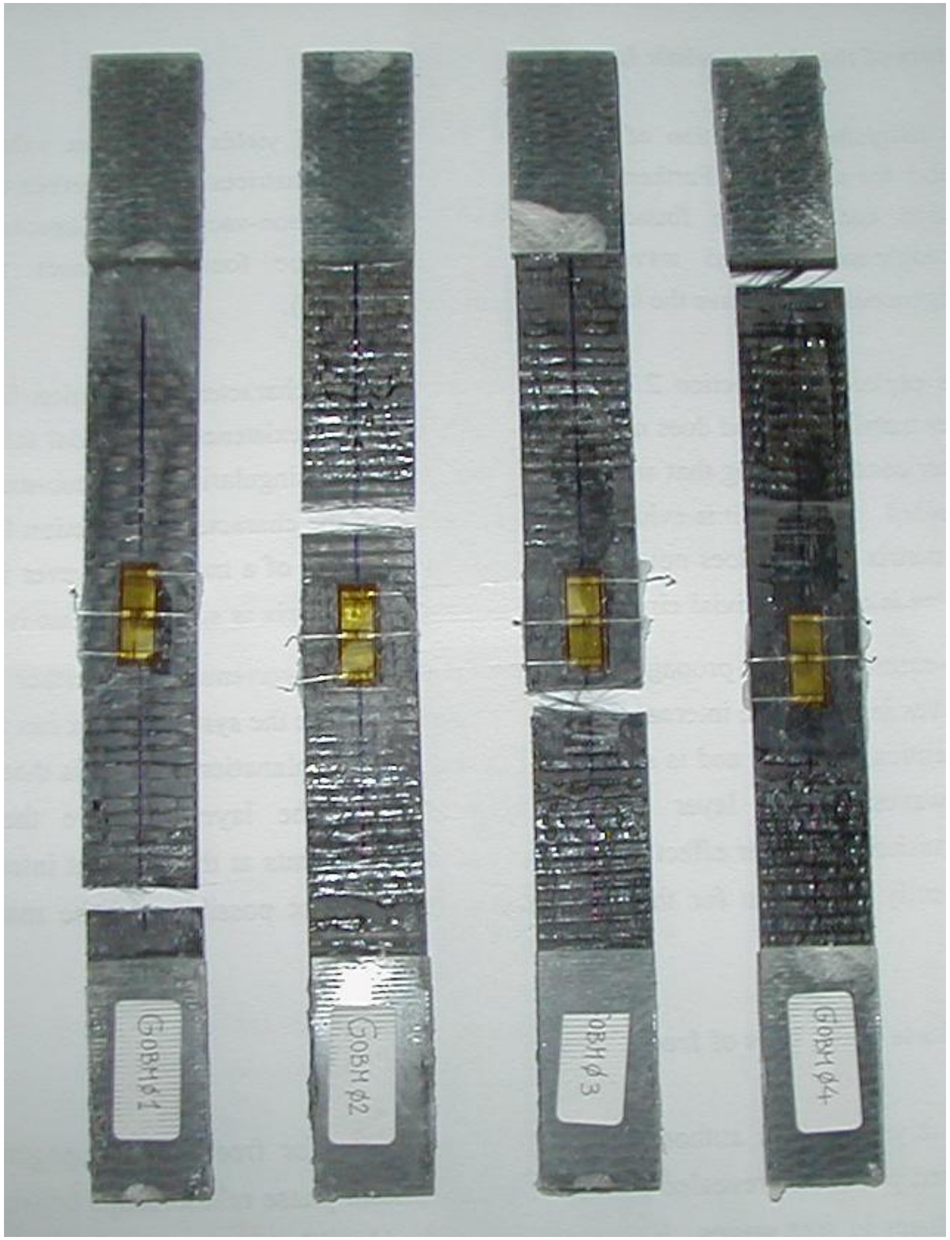

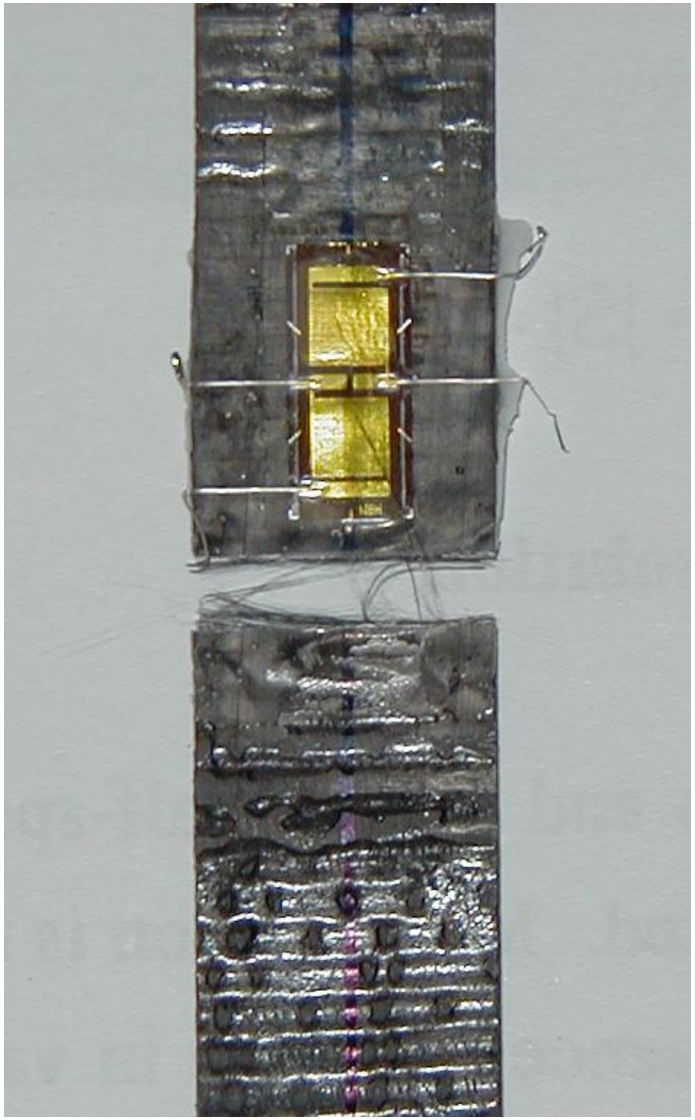

Failed HEXM coupons

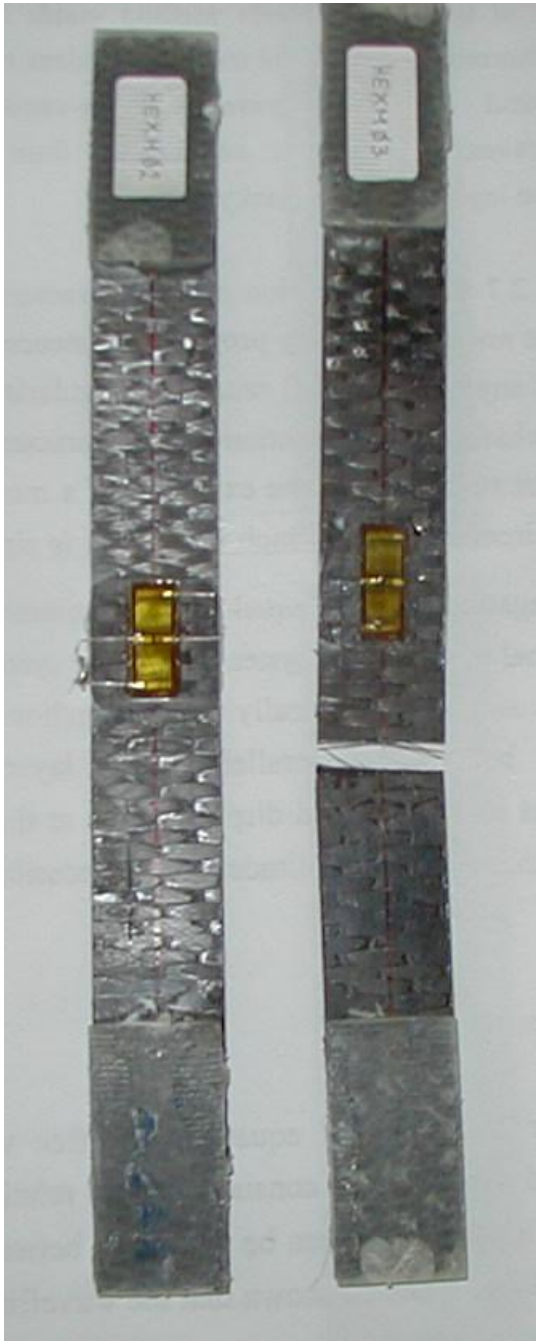

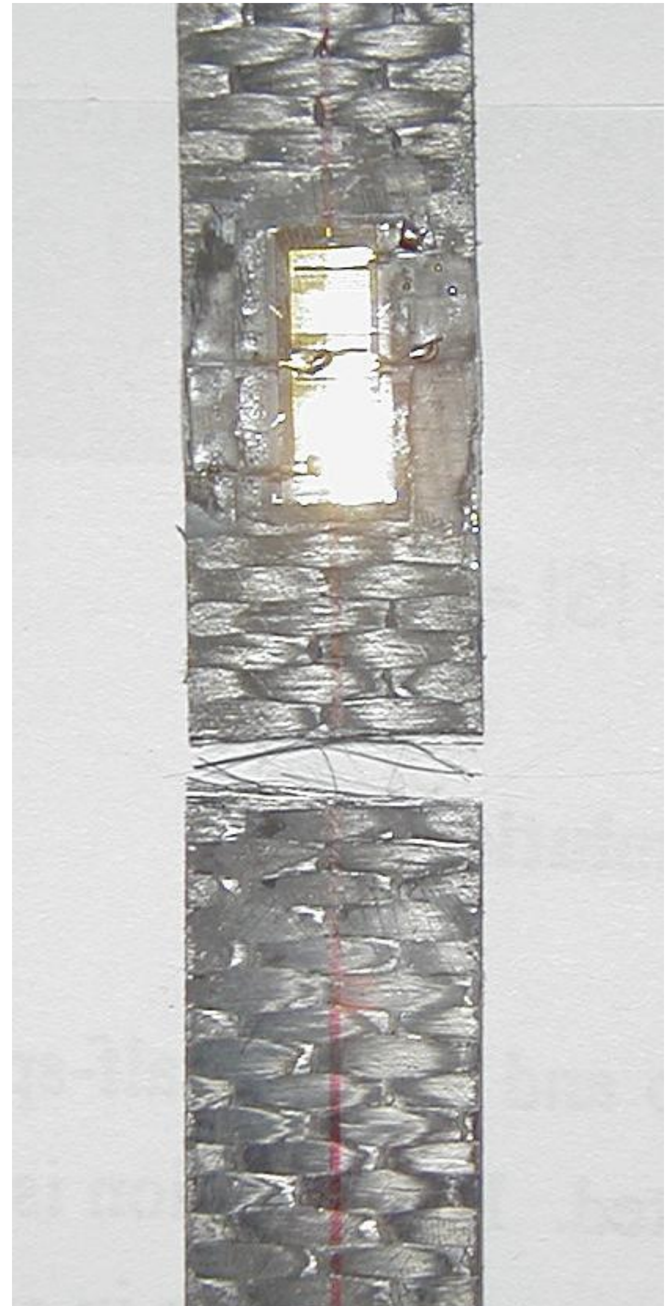

Coupons D1, failed in tension

Coupons D2, failed in tension

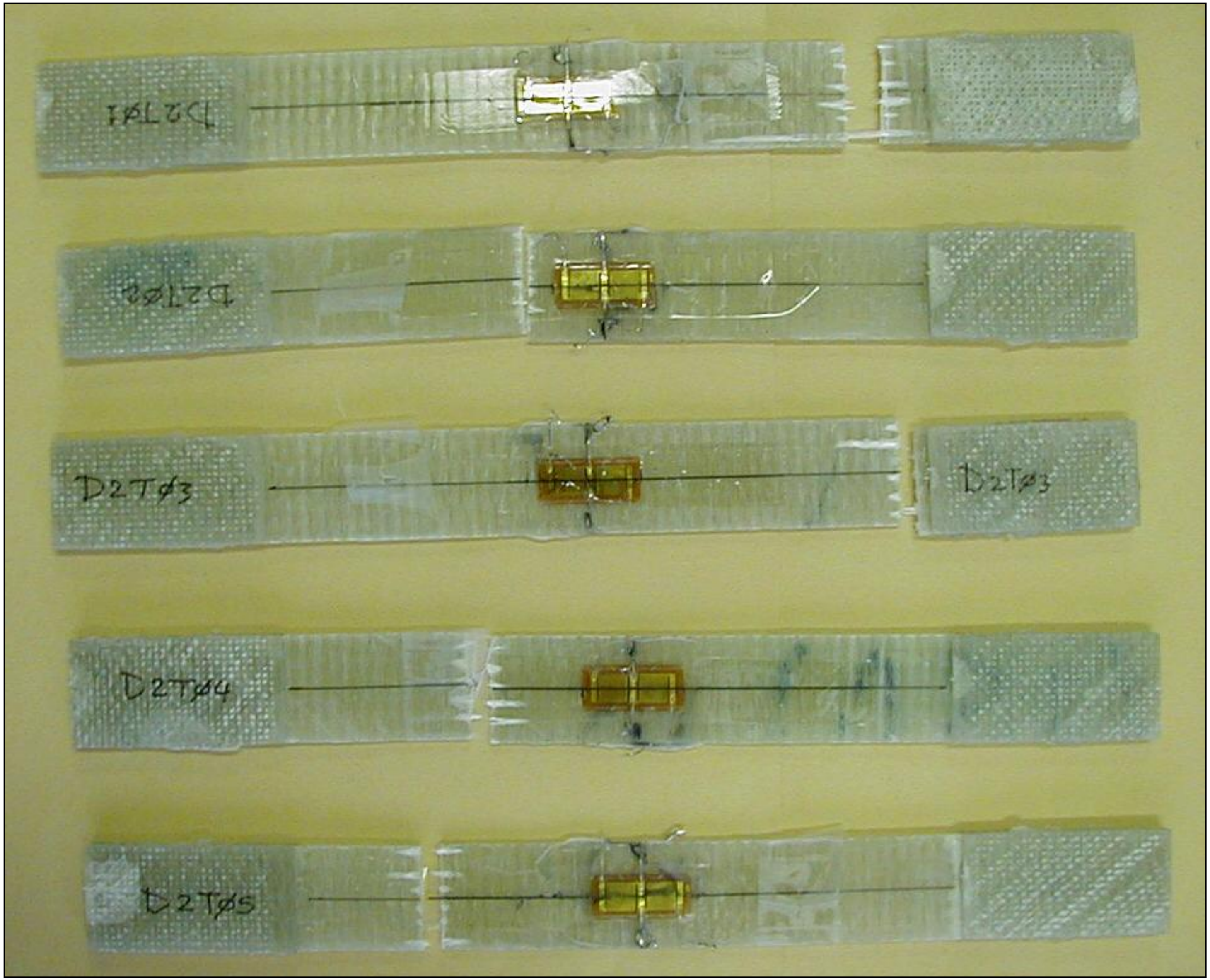

Longitudinal Compression.

Difficult to assess because it depends :

✓On the compressive properties of both fibre and matrix,

✓On the interface

✓On the void content.

The failure mode depens on

✓The lateral fibre support,

✓The volume fraction

✓The matrix properties.

Prediction of compressive strength

- The fibres are regarded as Euler columns.
- The matrix prevents buckling and increases the critical buckling load
- The elastic properties of the matrix determine the critical buckling load.
- The theoretical models are based on fibre buckling or shear matrix failure

Euler Buckling

$$EIy'' = -M$$

$$\frac{d^2y}{dx^2} = -\frac{M}{EI} = -\frac{P(y+e)}{EI}$$

$$y + e = C_1 \sin Kx + C_2 \cos Kx$$ Όπου: $K = \sqrt{P/EI}$

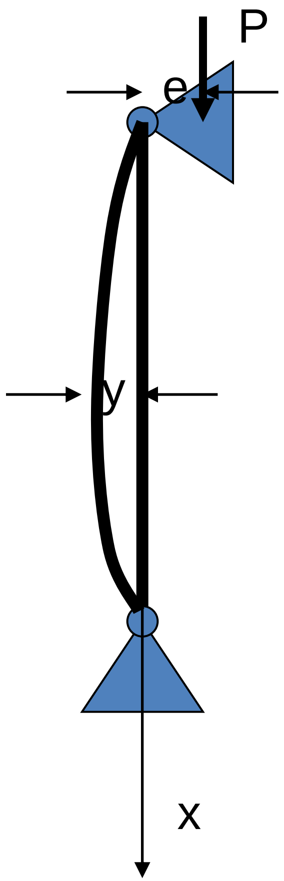

From the boundary conditions on A & B:

$$C_2 = e \qquad C_1 = \frac{e(1-\cos KL)}{\sin KL}$$

$$y + e = \frac{e(1-\cos KL)}{\sin KL}\sin Kx + e\cos Kx$$

To maximise y, the denominatior must be infinite or

sinKL=0, or KL=0, π, 2π …

$$KL = L\sqrt{P/EI} = \pi \Rightarrow \boxed{P = \frac{\pi^2 EI}{L^2}}$$ **Critical buckling load.**

The critical buckling load is less for shorter columns, stiffer materials and open cross sections!

Out of phase failure

- The fibres buckle out of phase
- The matrix is subjected to tension and compression in the transverse direction
- Failure depends on critical buckling load
- Assumptions:
  - Strain in the y direction is independent of y
  - The matrix is essentially unloaded in comparison to the fibres

"Extension" mode

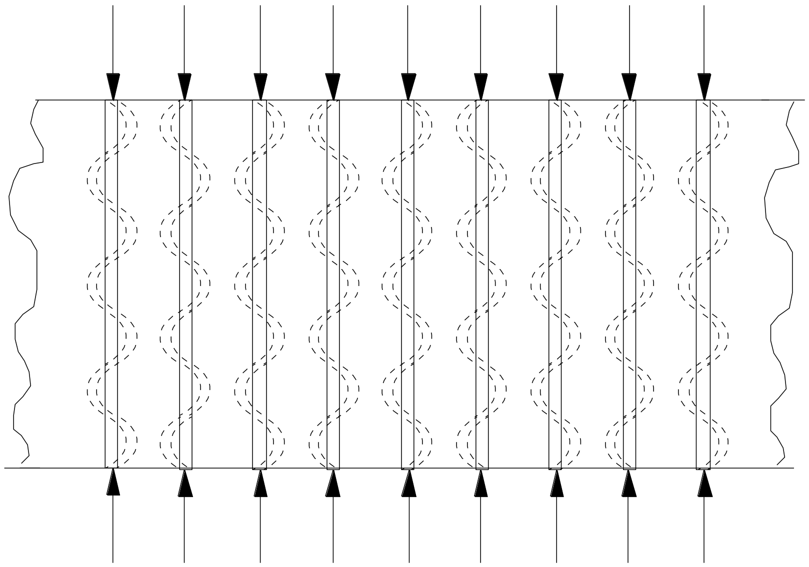

In phase failure

- The fibres buckle in phase
- The matrix is subjected to shear
- Failure depends on the shear strength of the matrix
- Assumptions:
  - Strain in the y direction is independent of y
  - Gf >> Gm or the fibres essentially remain undeformed

"Shear" mode

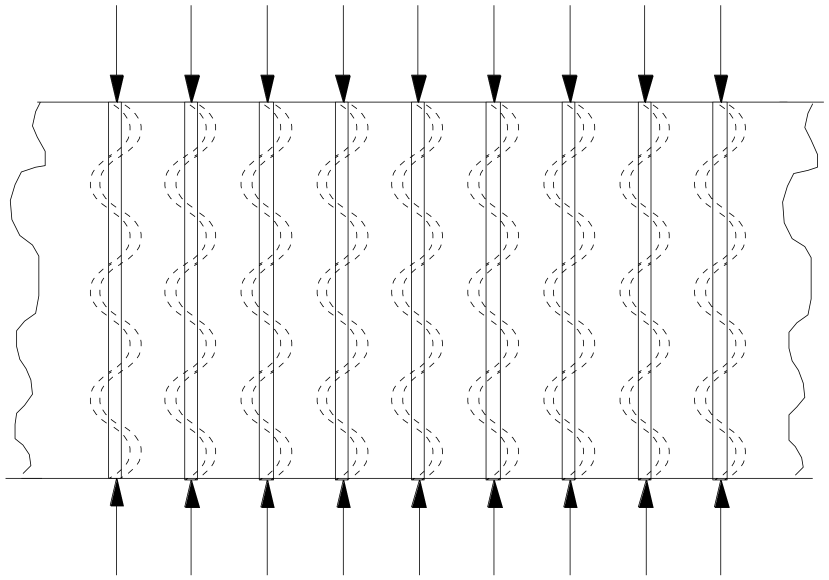

Out of phase failure

$$\sigma_c = \left(V_f + (1-V_f)\frac{E_m}{E_f} \right) \sigma_{f_{cr}} \quad (2.1)$$

$$\sigma_{f_{cr}} = 2\sqrt{\frac{V_f E_m E_f}{3(1-V_f)}} \quad (2.2)$$

σ_c : compressive strength

V_f : volume fraction of the fibres

E_m : matrix elastic modulus

E_f : fibre elastic modulus

"Extension" mode

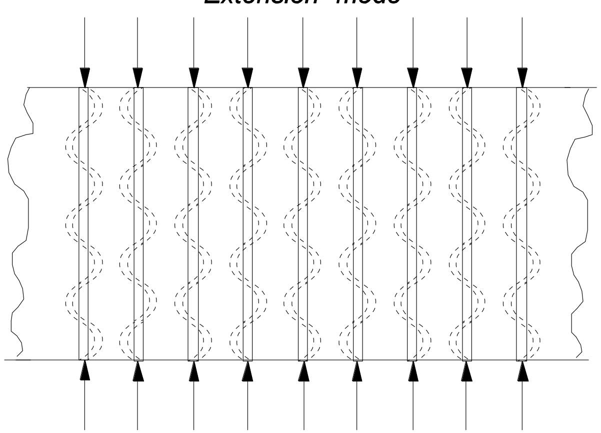

In phase failure

$$\sigma_c = \frac{G_m}{1-V_f} \quad (2.3)$$

$$\varepsilon_{cr} = \frac{1}{V_f(1-V_f)}\left(\frac{G_m}{E_f}\right)$$

"Shear" mode

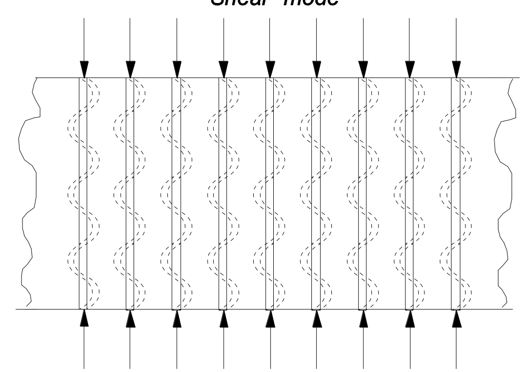

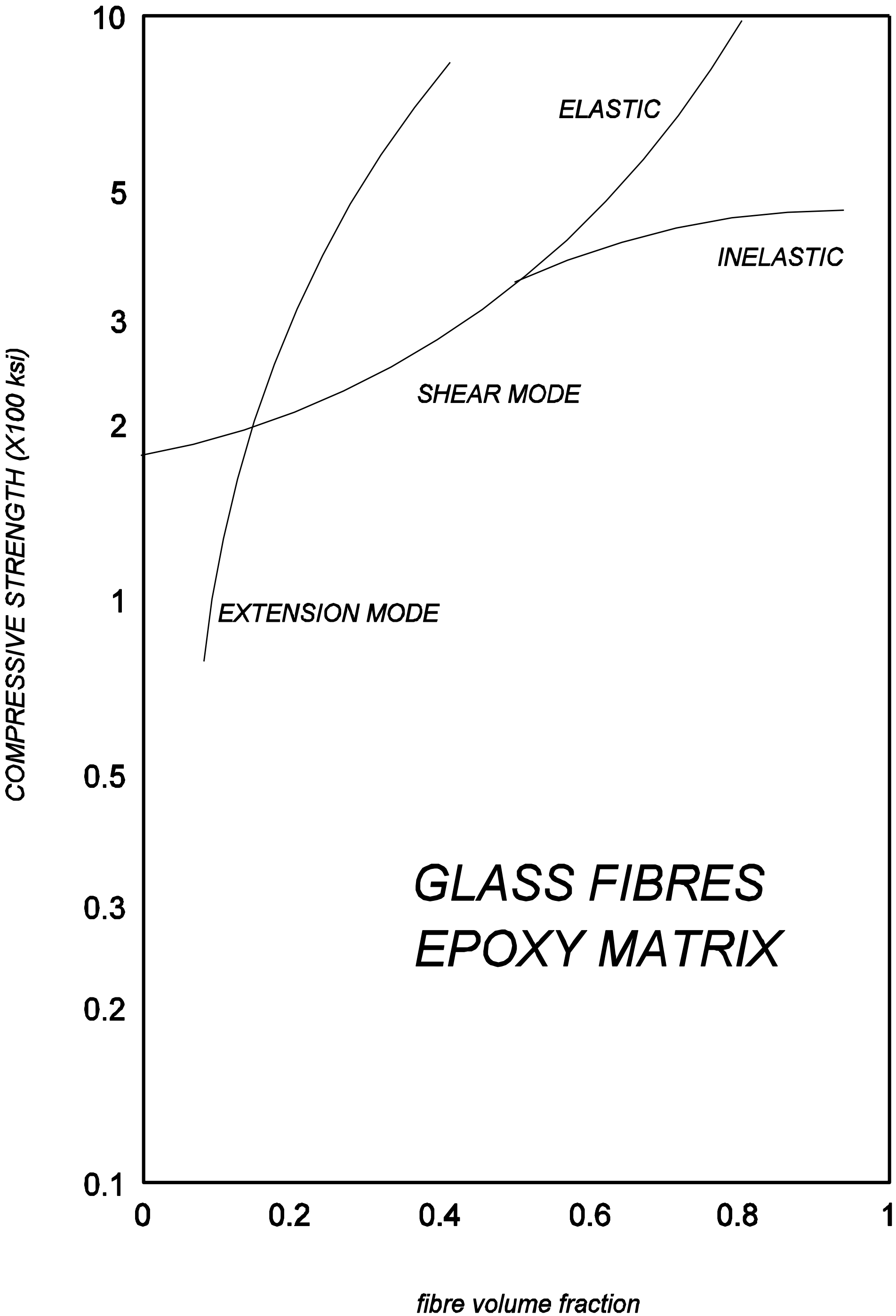

Compressive strength of unidirectional glass/epoxy composites

σ_c as a function of V_f

Out of phase failure is valid for low V_f.

For typical $0.6 < V_f < 0.7$ the strength is calculated between 450 & 600 Ksi (3100 & 4150 MPa), at a strain to failure > 5%!

Compressive failure

- Other affecting parameters:
  - Local inhomogeneities in the fibre Vf,
  - Void and defect content.,
  - Fibre misalignment and curvature,
  - Weak or bad interface which instigates debonding and decreases critical buckling load,
  - Viscoelastic matrix behavior, or reduced Gm,
  - Anisotropic fibres with weak transverse properties (carbon or Kevlar) or non linear compressive behavior.

Compressive Failure Modified models

σ_c as a function of V_f

- Gm is a linear function of compressive strain (Dow & Rosen)
- The matrix is perfectly plastic (Lager & June) $\sigma_c = c \dfrac{G_m}{1\text{-}V_f}$ (2.5)
- Shear controlled model (M.R.Wisnom) $\sigma_c = \dfrac{G_m\,\gamma_m}{V_m\,(\gamma+\alpha)}$ (2.6)
- Curvature and misalignment (Hahn & Williams)

$$\sigma_c = V_f\ G_{LT}\ \frac{\gamma_{LT}}{\gamma_{LT} + \dfrac{\pi f_o}{e}} \quad (2.7)$$

σ_c : compressive strength.

V_f : volume fraction.

G_{LT} : shear modulus of the composite.

γ_{LT} : shear strain.

f_o/e : initial fibre deflection to wavelength.

Effect of fibre misalignment on predicted compressive strength of unidirectional XAS/914, [7].

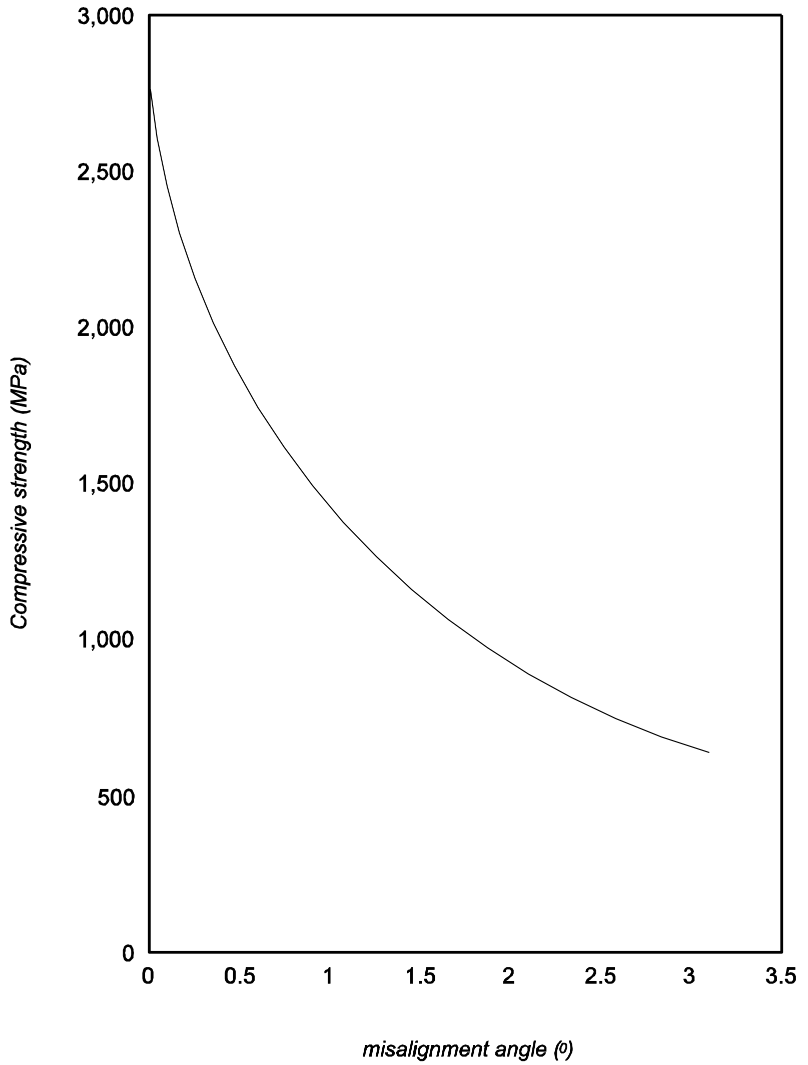

Compressive failure (mechanisms)

- Fibre buckling leads to their failure.
  - Buckled fibres are both subjected to tension and compression
  - Brittle fibres (e.g. carbon fibres) fail when their strength is reached locally creating a characteristic failure zone
  - Viscoelastic or plastic fibres create a plasticity zone when the yield stress is reached

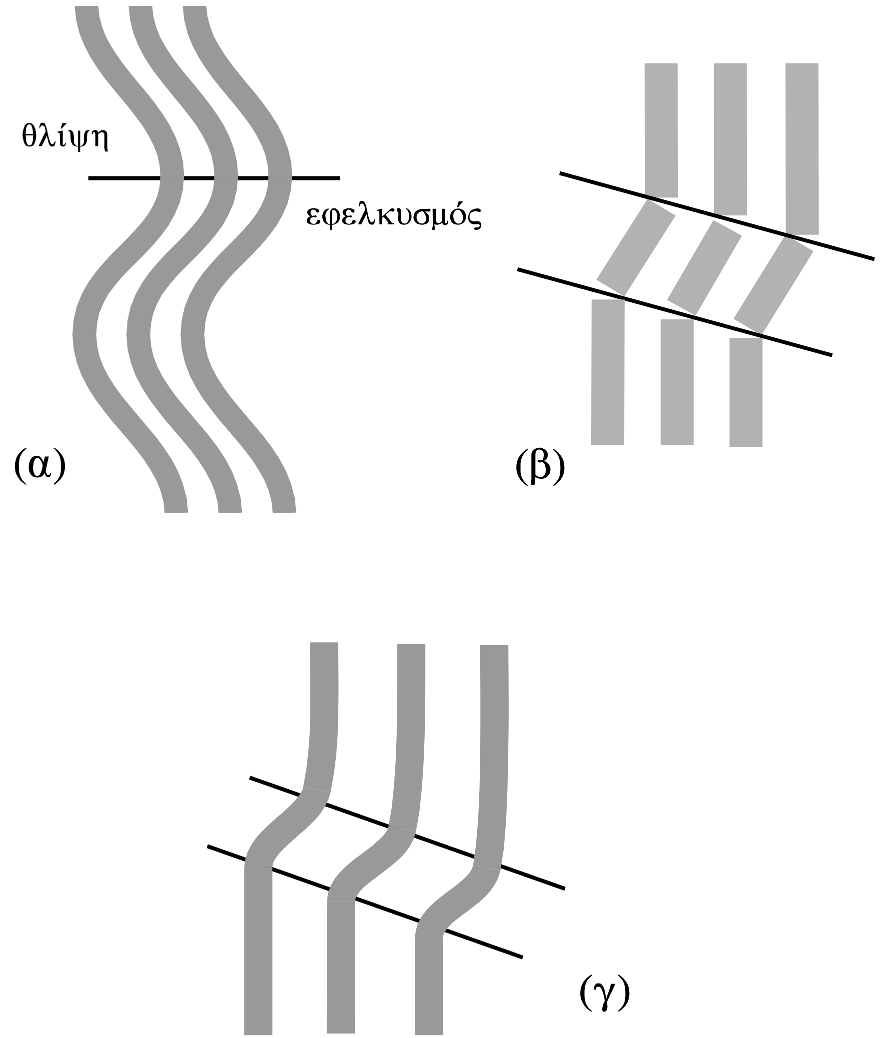

Maximum Shear

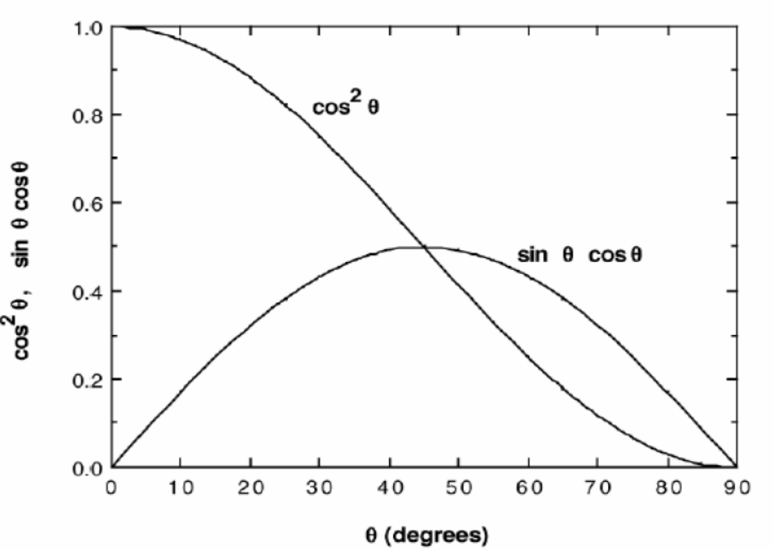

- If Shear failure precedes buckling Failure: For shear stress τ: $\tau = \sigma_{||C} \sin\theta \cos\theta$
- Shear is maximum for θ=45°, $\tau_{max} = \sigma_{||C}/2$
- From the rule of mixtures:
  - $\sigma^*_{||C} = 2\,[V_f\,\tau^*_f + (1-V_f)\,\tau^*_m]$

Where τ^*_f και τ^*_m the shear strength of the fibre and matrix respectively

$$\sigma' = \sigma \cos^2\theta = \sigma\left(\frac{1+\cos 2\theta}{2}\right)$$

$$\tau' = \sigma \sin\theta \cos\theta = \sigma\left(\frac{\sin 2\theta}{2}\right)$$

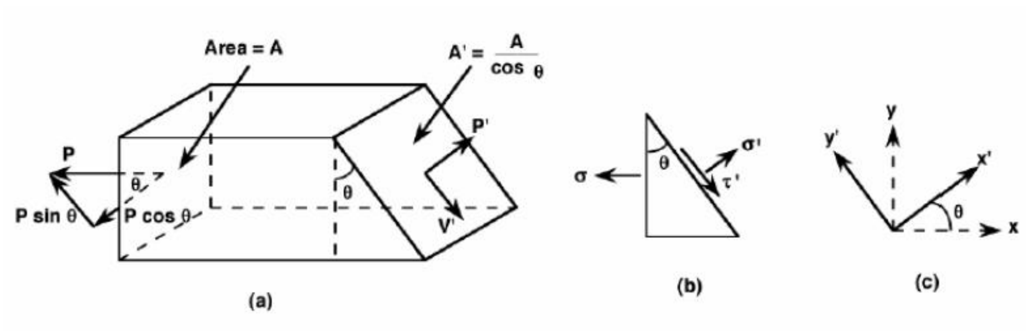

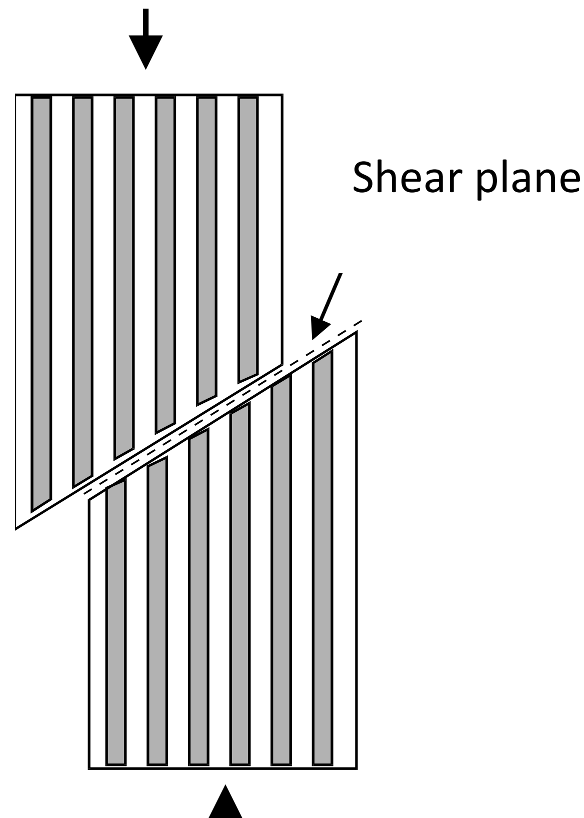

Compression

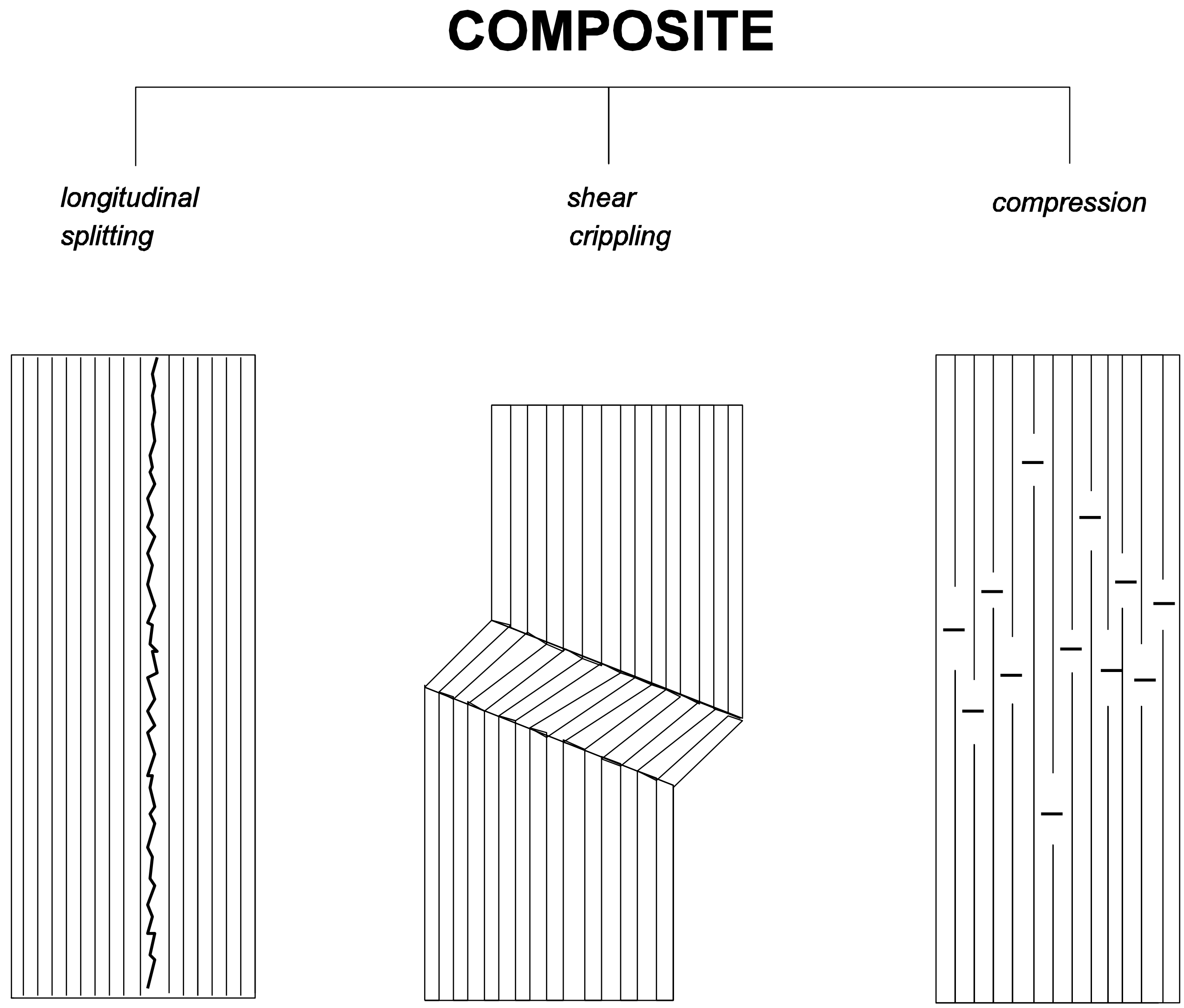

A. Paipetis, Mechanics of composite materials Lecture Notes

Compression

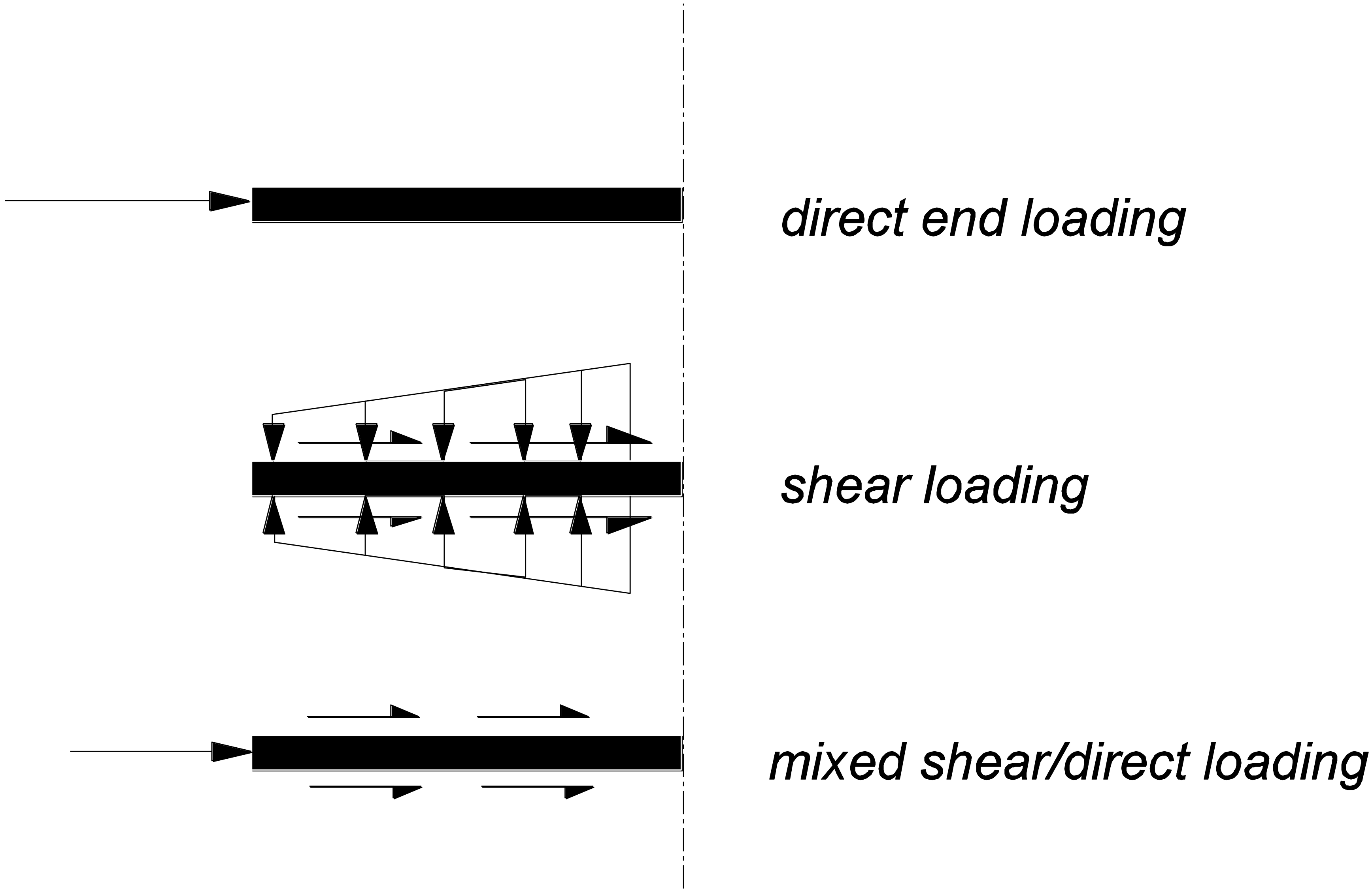

A. Paipetis, Mechanics of composite materials Lecture Notes

Compression

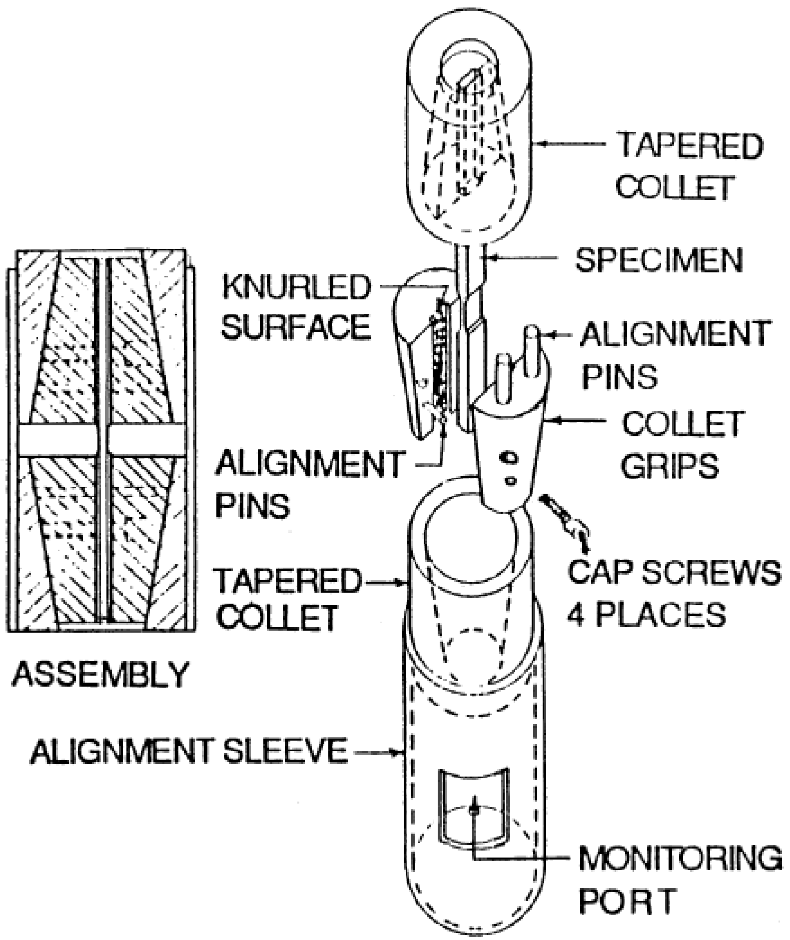

Figure 2 Celanese compression test fixture (ASTM D 3410).

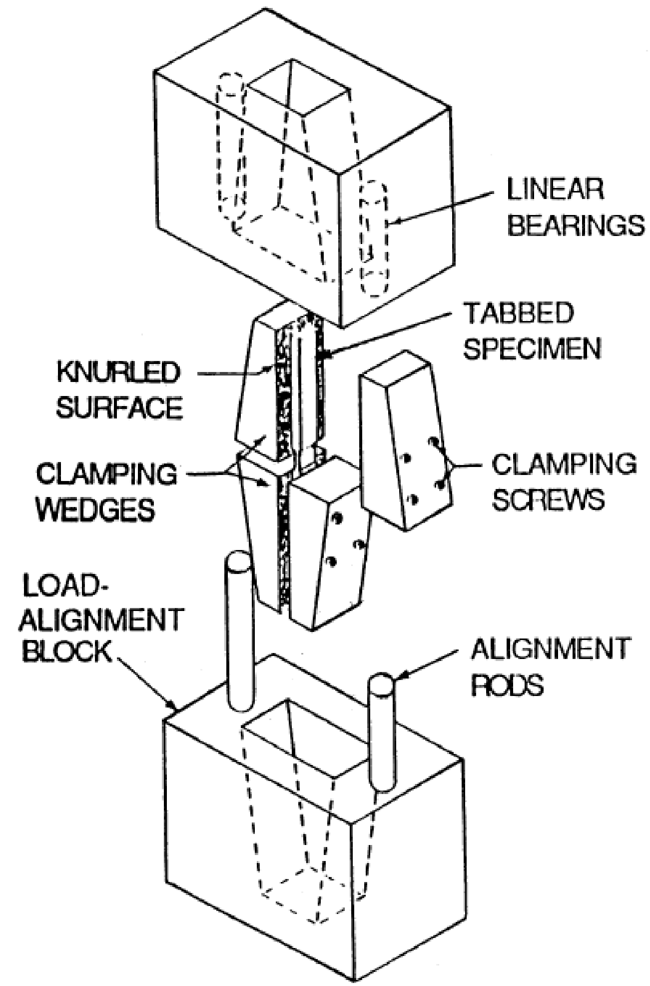

Figure 4 IITRI compression test fixture (ASTM D 3410).

DONALD F. ADAMS, University of Wyoming, Laramie, WY, USA, Volume 5, Ch 5.05 of Comprehensive Composite Materials

Compression

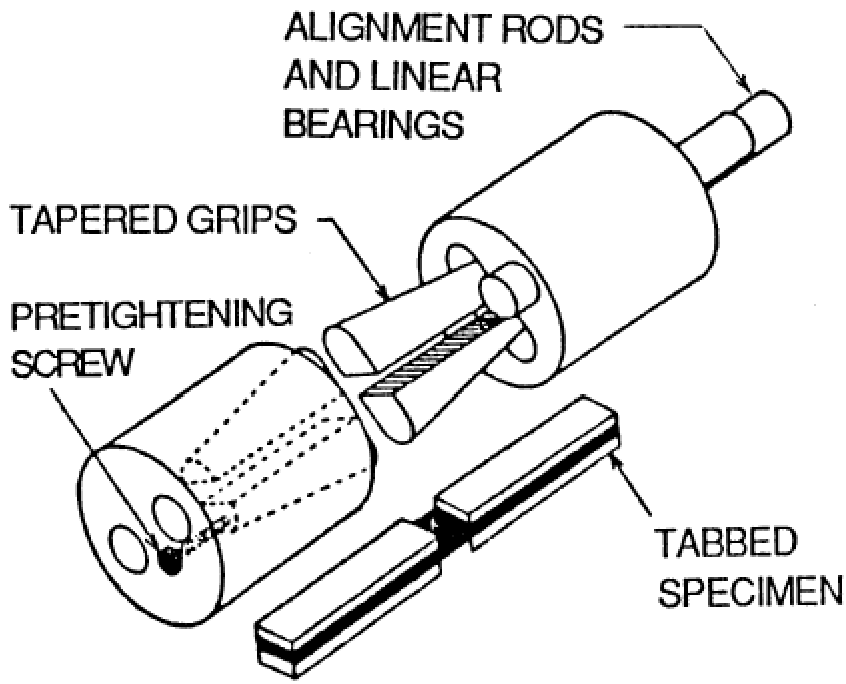

Figure 6 Wyoming modified celanese compression test fixture.

DONALD F. ADAMS, University of Wyoming, Laramie, WY, USA, Volume 5, Ch 5.05 of Comprehensive Composite Materials

ASTM Standard D695 compressive test fixture for rigid plastics, [17]

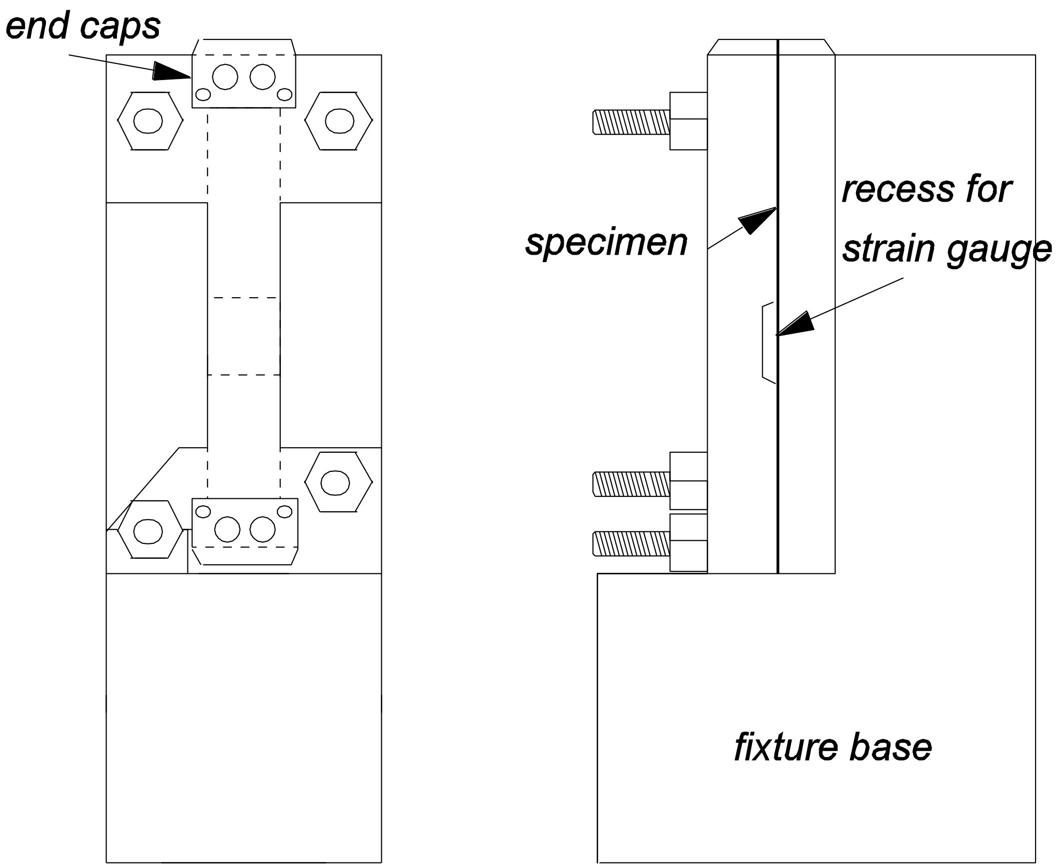

Imperial College compression test rig and specimen

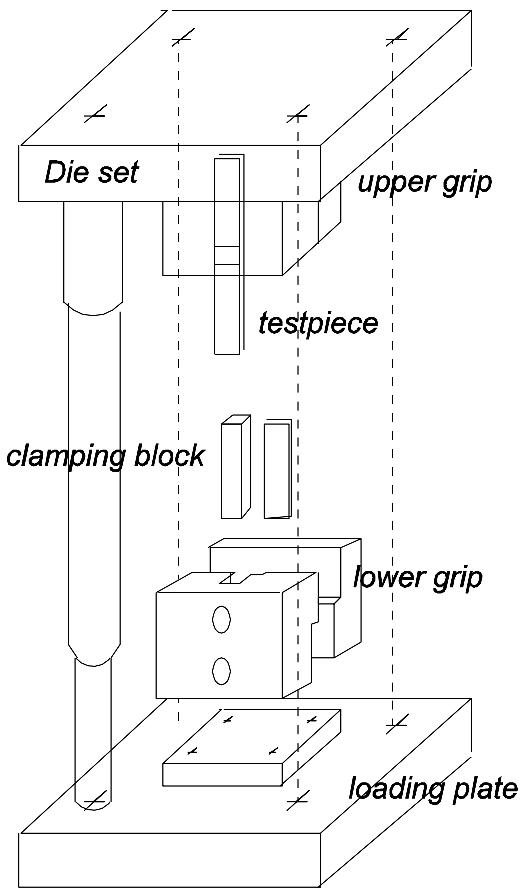

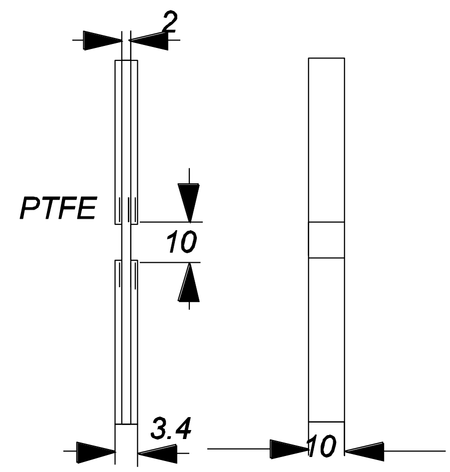

Compression

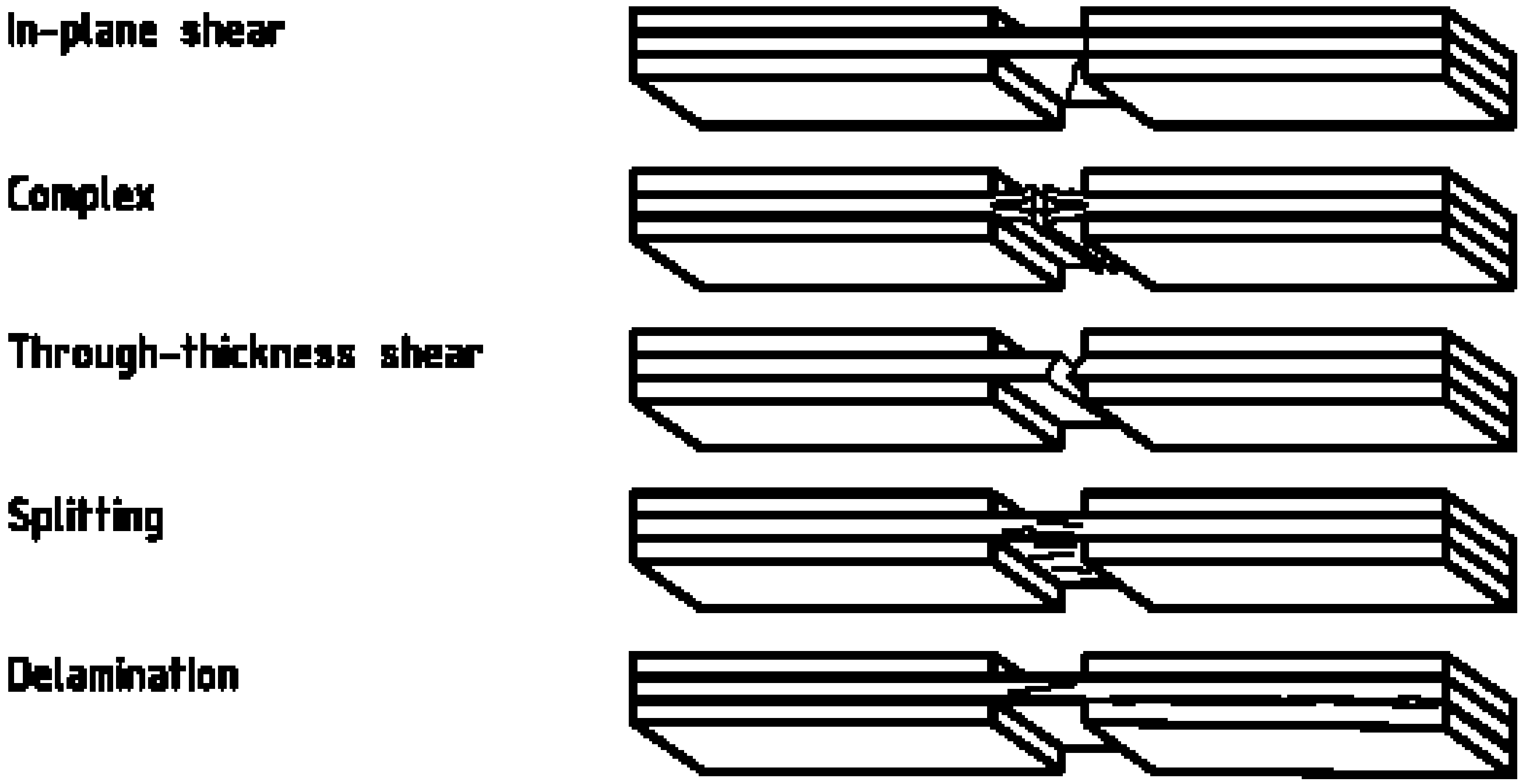

Typical failure modes under static compressive load.

Compression

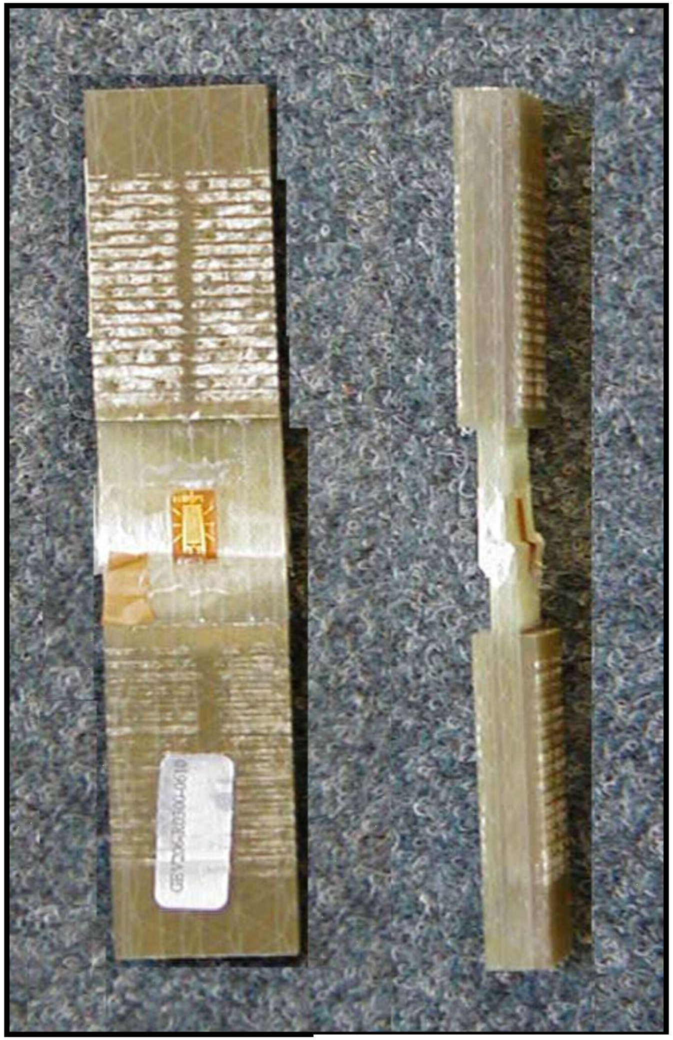

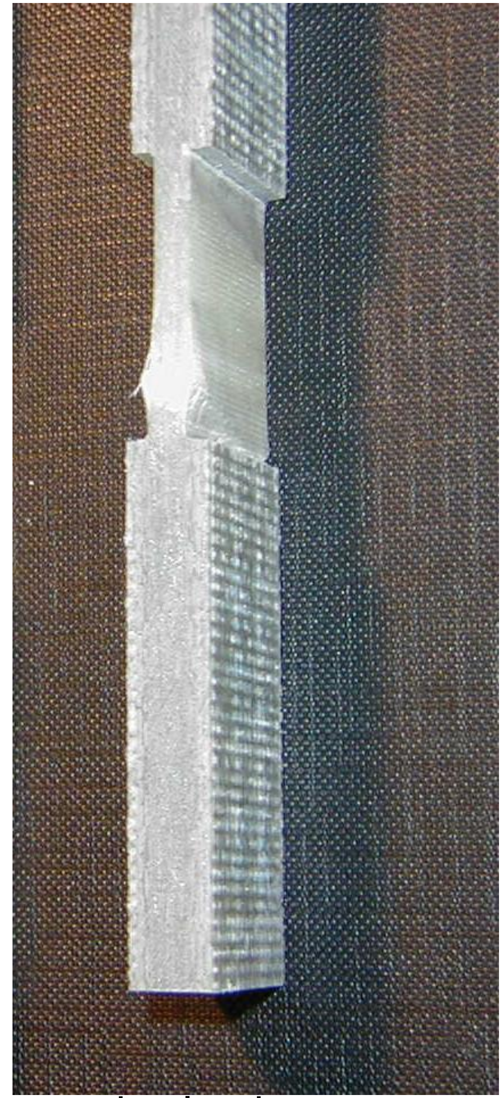

Typical failure mode under static compressive load

Compression

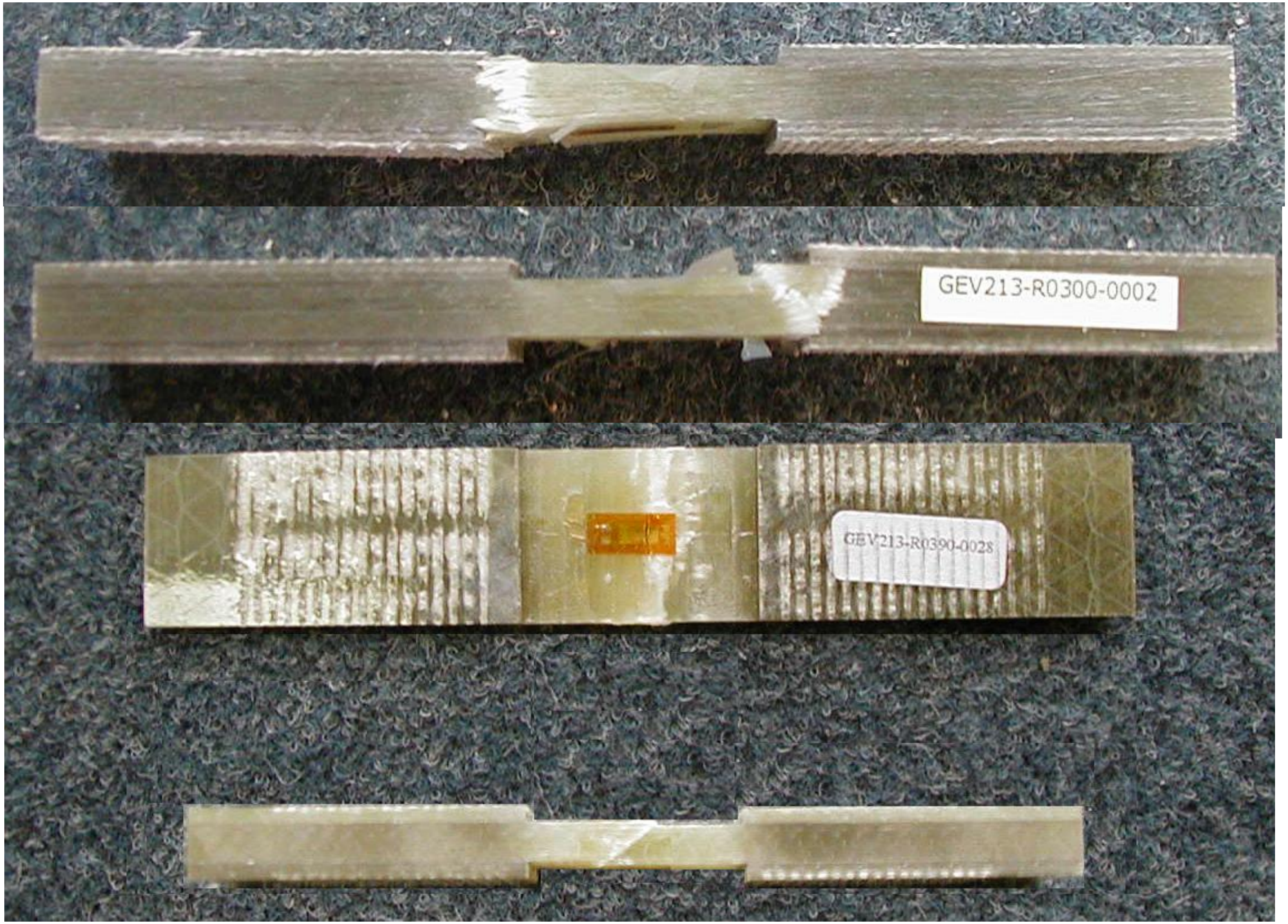

A. Paipetis, Mechanics of composite materials Lecture Notes

Weibul distribution of experimental results (XAS/914 UD composite laminate).

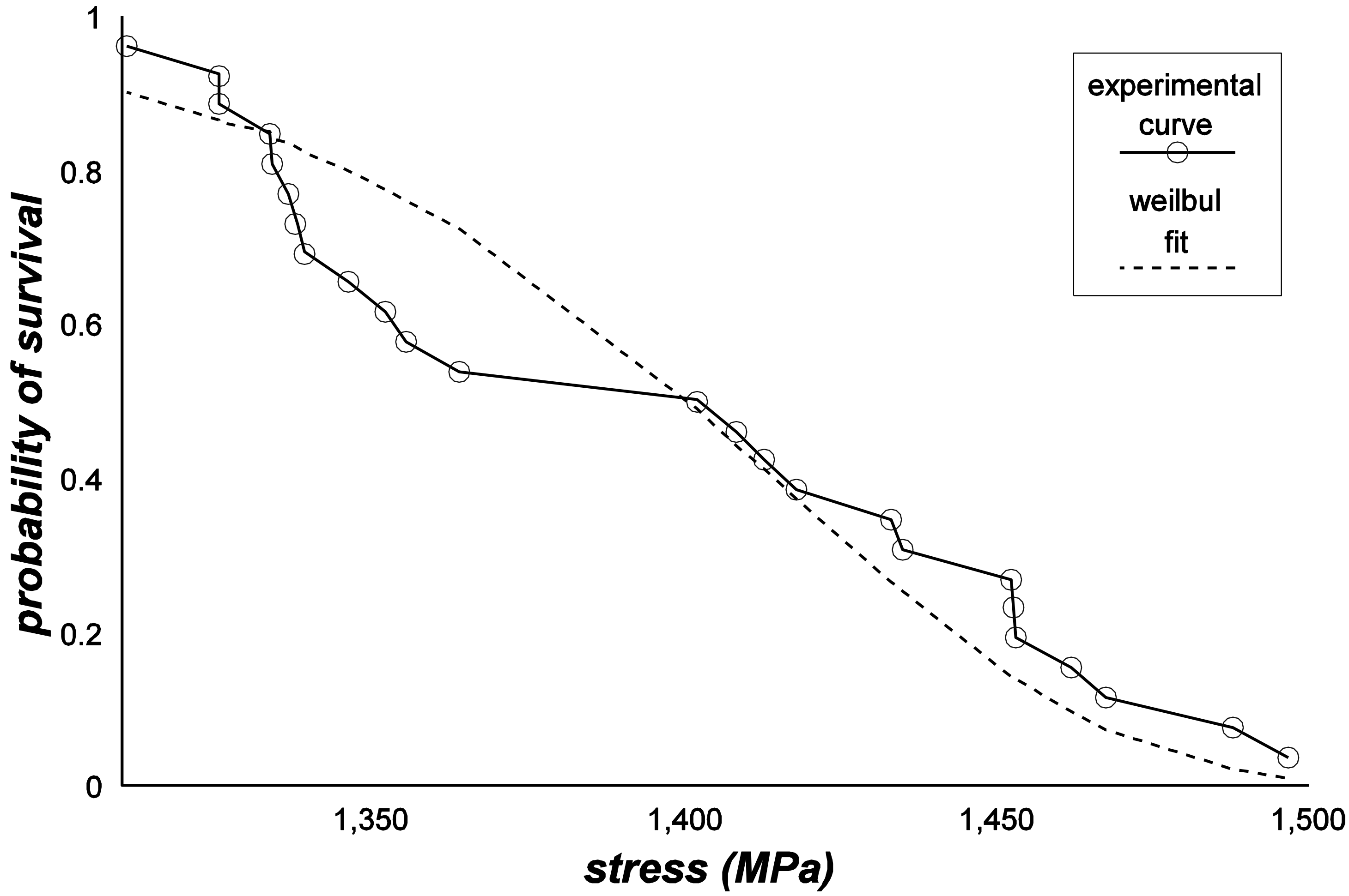

Macrobuckling of the specimen prior to failure.

"negative" side

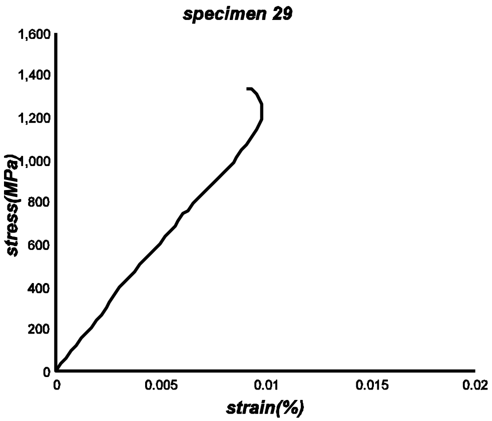

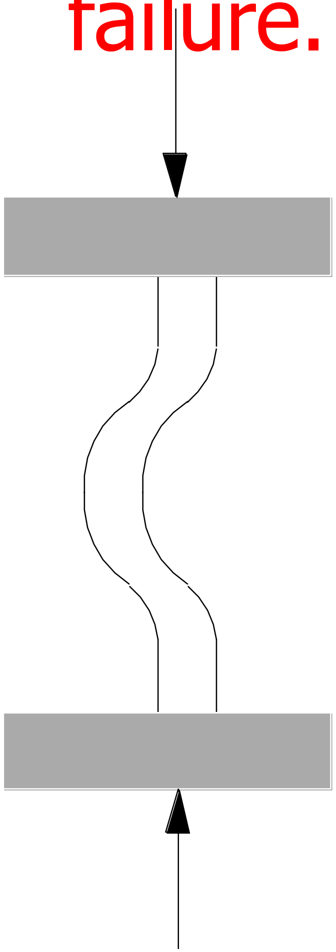

"positive" side

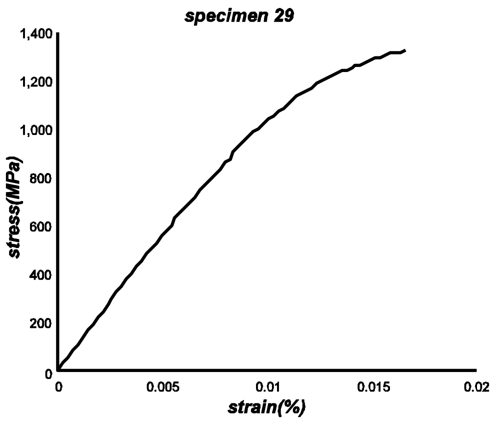

Modulus reduction with increasing strain.

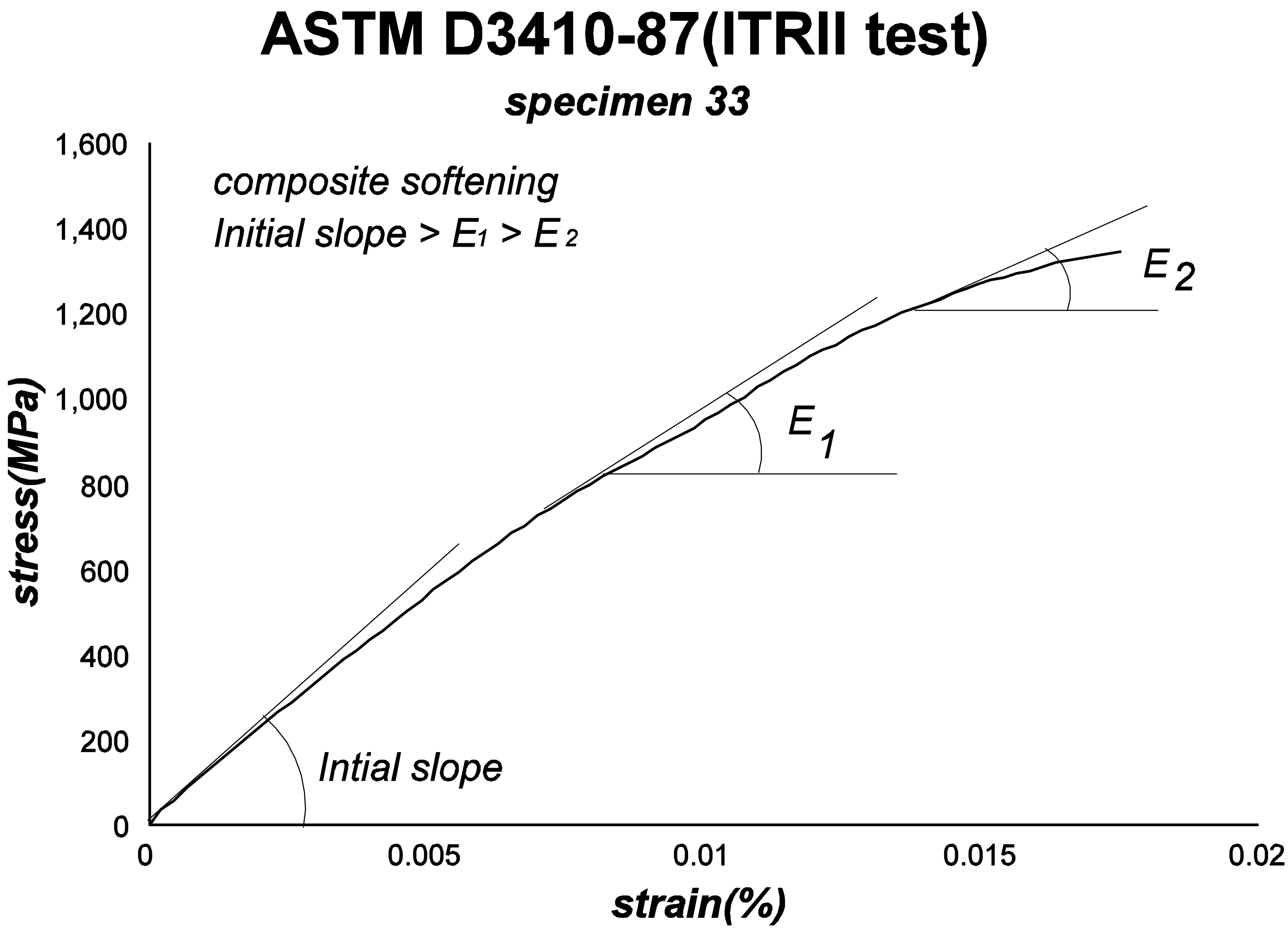

Shear Properties.

The shear properties are

(I): Shear modulus

(II): Shear strength

- ✓Composites are anisotropic:
- ✓Three types of shear
  - ✓ interlaminar
  - ✓ in plane longitudinal
  - ✓ intralaminar

Shear in principal planes:

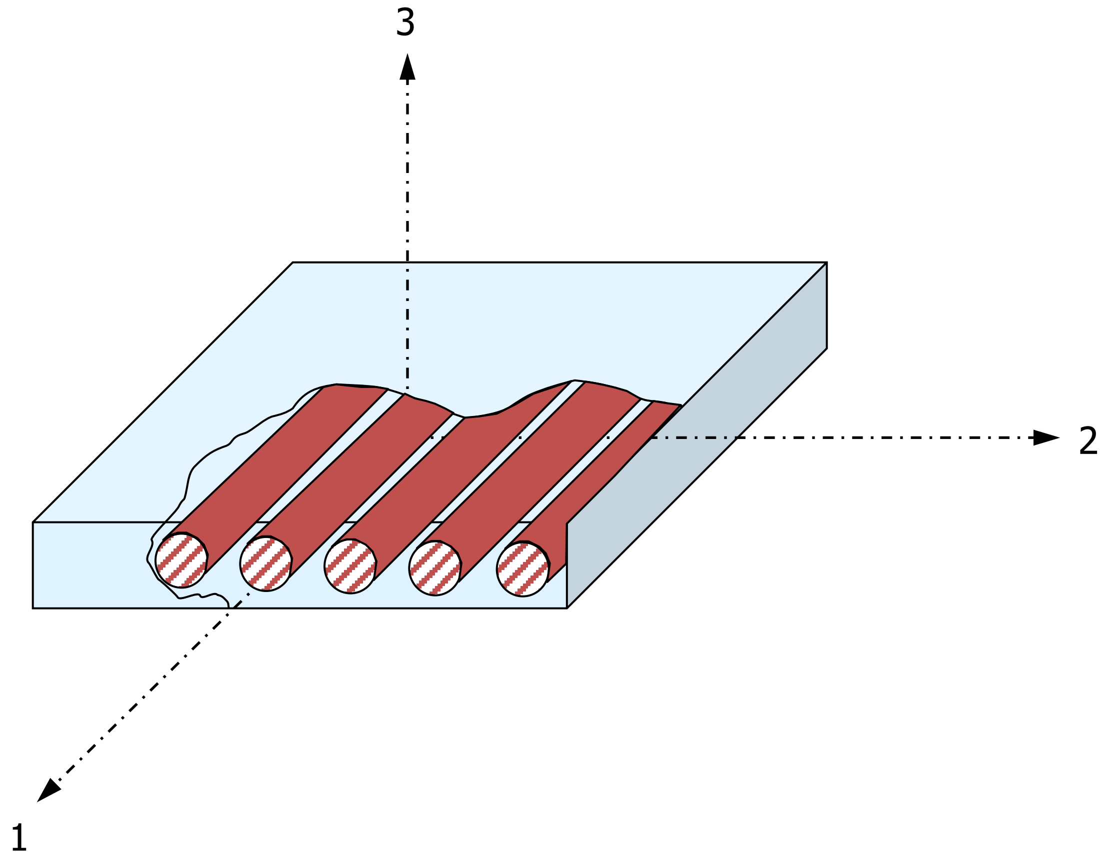

Shear planes: (2-3), (1-3) και (1-2)

Shear testing.

✓interlaminar(τ_{13})

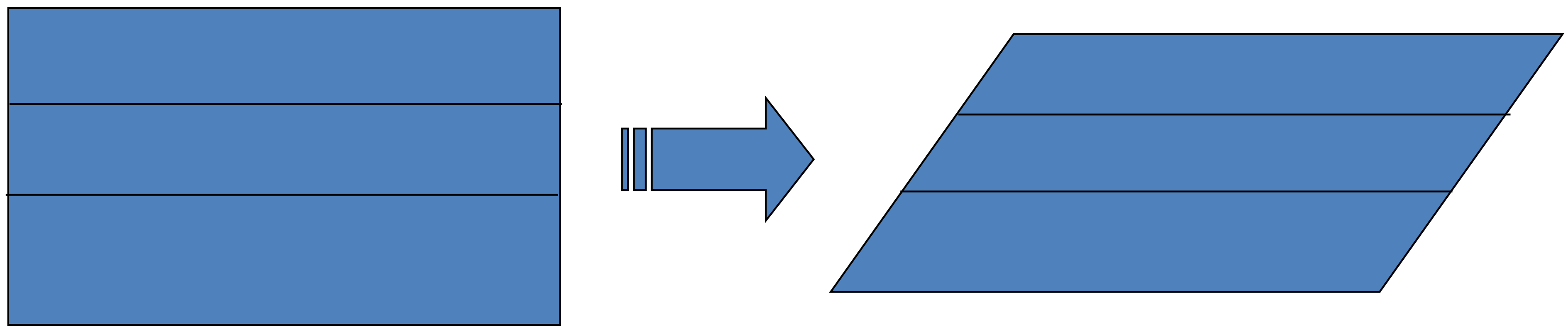

Shear testing.

✓In plane (τ_{12})

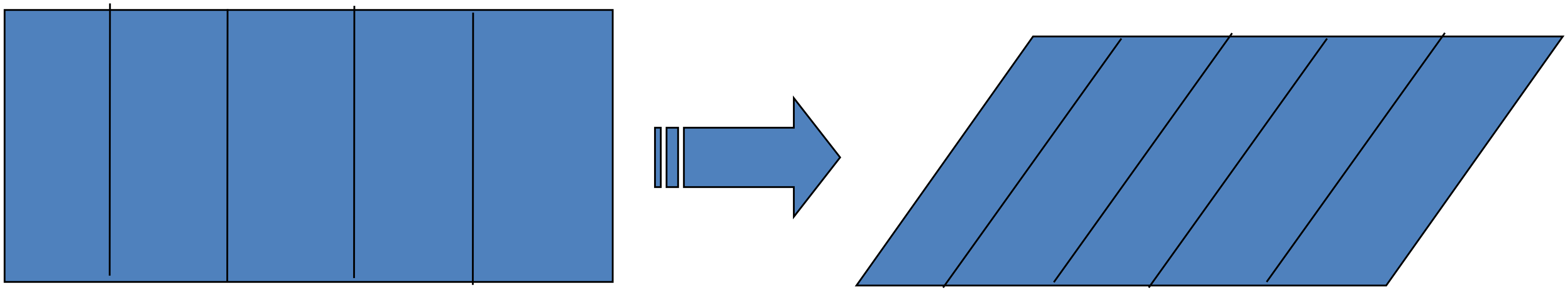

Shear testing

Intralaminar (τ_{23}) – no existing standard

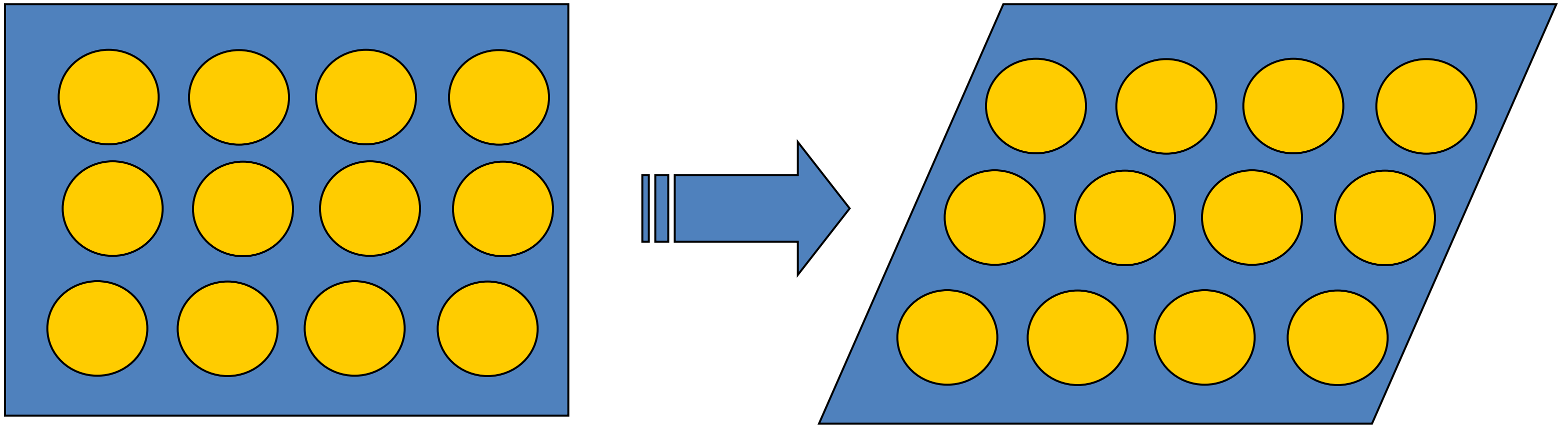

•Shear tests are difficult: Uniform stress field is hard to achieve

•Few standard tests. No universally accepted standards for all types and structures of long fibre composites

In-plane shear test methods:

•uniaxial tension of a ±45 laminate	•ISO 14129
•Iosipescu shear specimen (V-notched beam, VNB method)	•ASTM D5379M-98
•uniaxial tension of a 10^{o} off-axis specimen	•(None)
•two- and three-rail shear tests	•ASTM D4255M-83
•torsion of thin-walled tube	•ASTM D5448M-93
•twisting of a flat laminate	•ASTM D3044-94

±45° Test

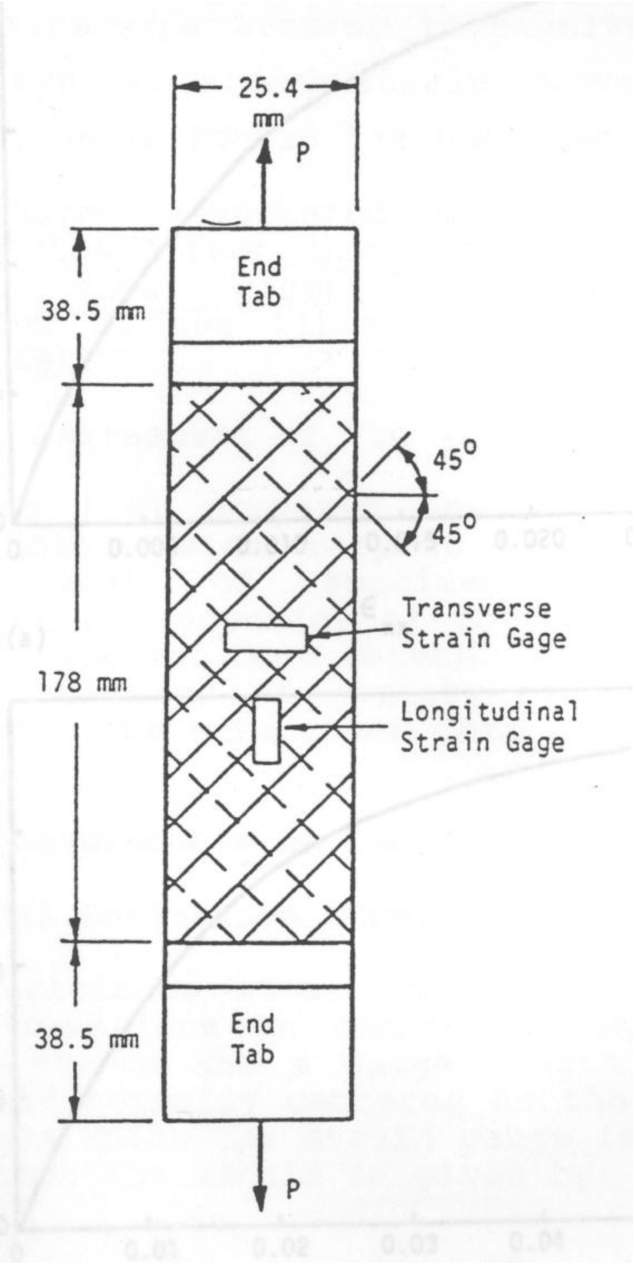

- Symmetric ±45° laminate in tension:
  - $\tau_{12} = 1/2\ \sigma_{xx}$
  - $\gamma_{12} = \varepsilon_{xx} - \varepsilon_{yy}$
- The test is accepted by all standards organisations
- Both for woven fabric and prepregs

±45° Test

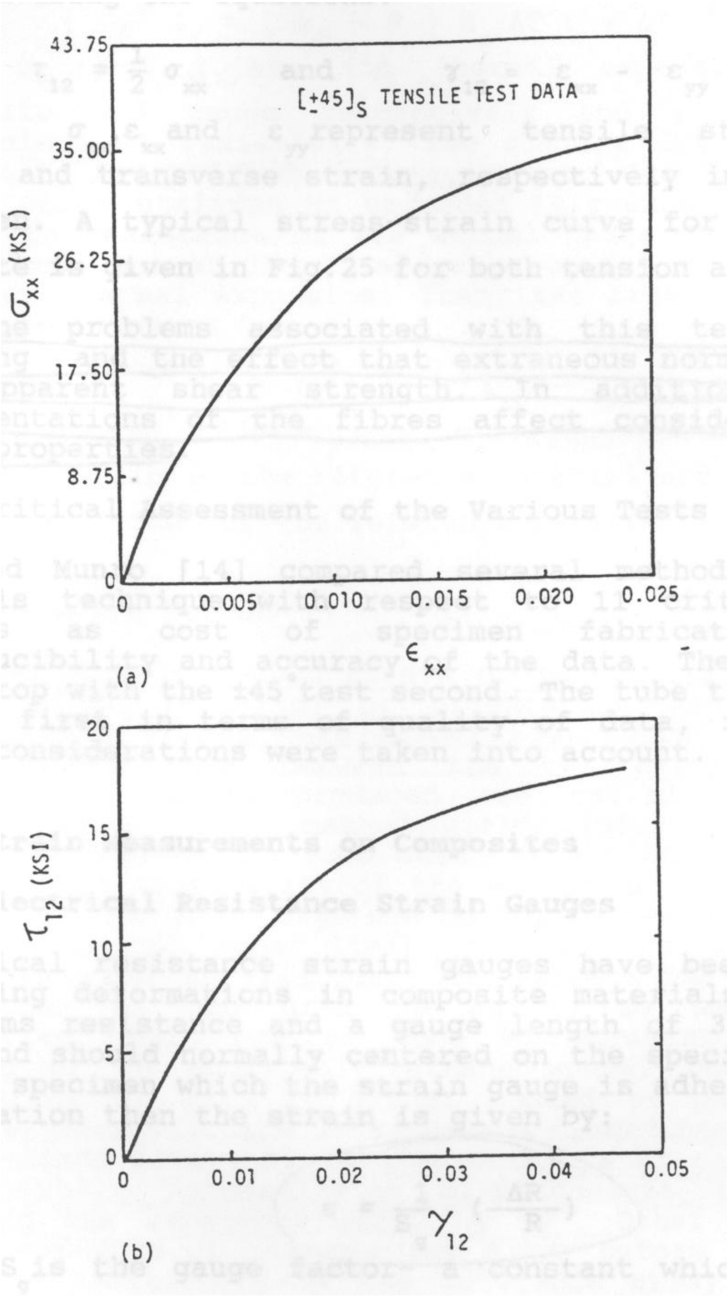

- Shear stress vs. shear strain is calculated by:
  - $\tau_{12} = 1/2\ \sigma_{xx}$
  - $\gamma_{12} = \varepsilon_{xx} - \varepsilon_{yy}$
- Typical curve for Boron / epoxy

Advantages

Simple coupon geometry

Easy to perform

Disadvantages

The coupling of the shear stresses between the laminae affect the measurements

Minor misalignment results to large deviations

double V notch – Isopescu test

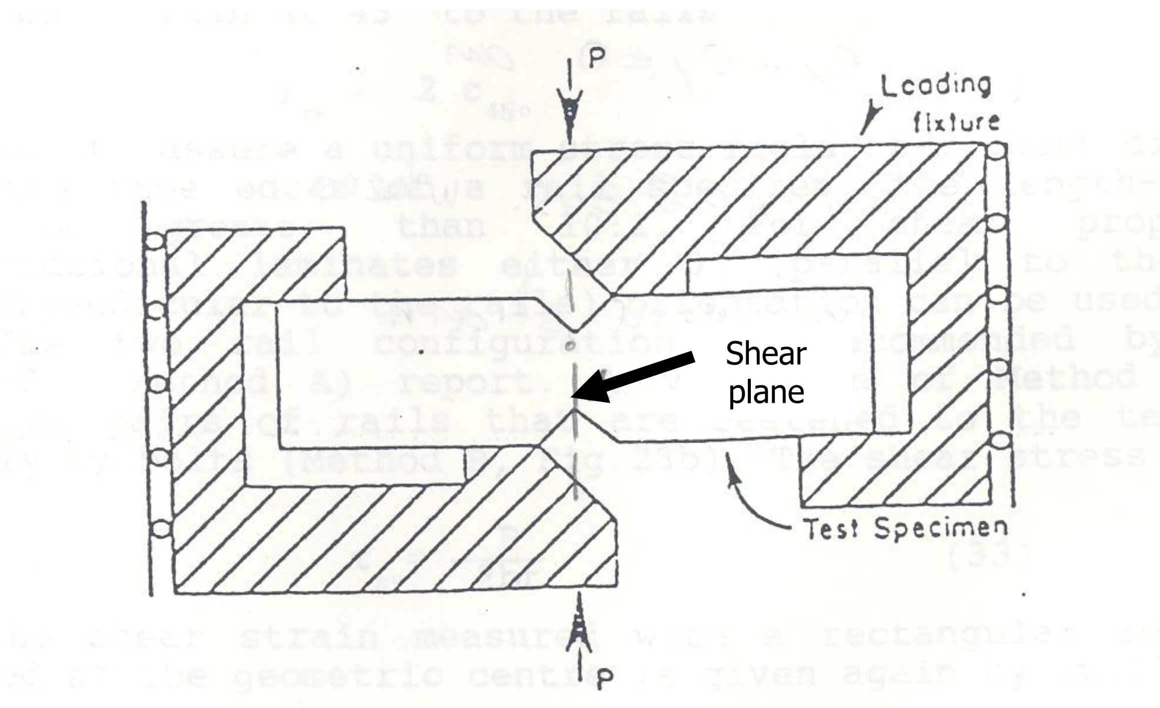

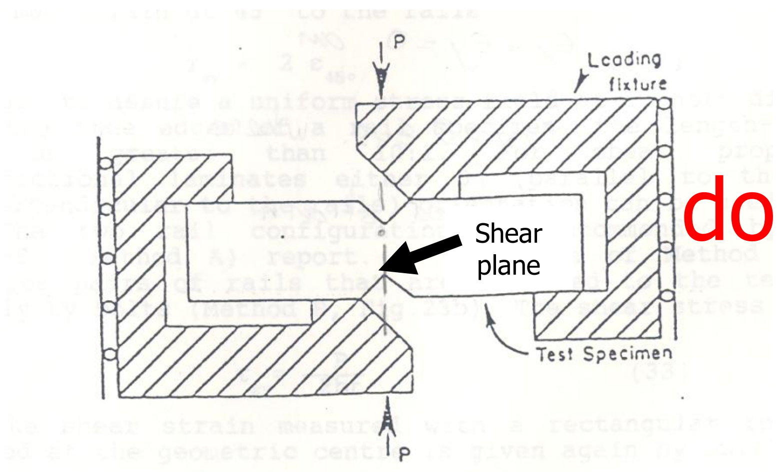

double V notch – Isopescu test

- Pure shear in the plane defined by the two notches
- Usually emplyed for 0° or 90° laminates
- For 90° laminates, it is very reliable
- Shear strength is derived by diviiding the load with the shear cross section
- The local stress field may lead to erroneous results
- The positioning of strain gauges is crucial
- Usually yields smaller values than the cylindrical beam

rail shear tests

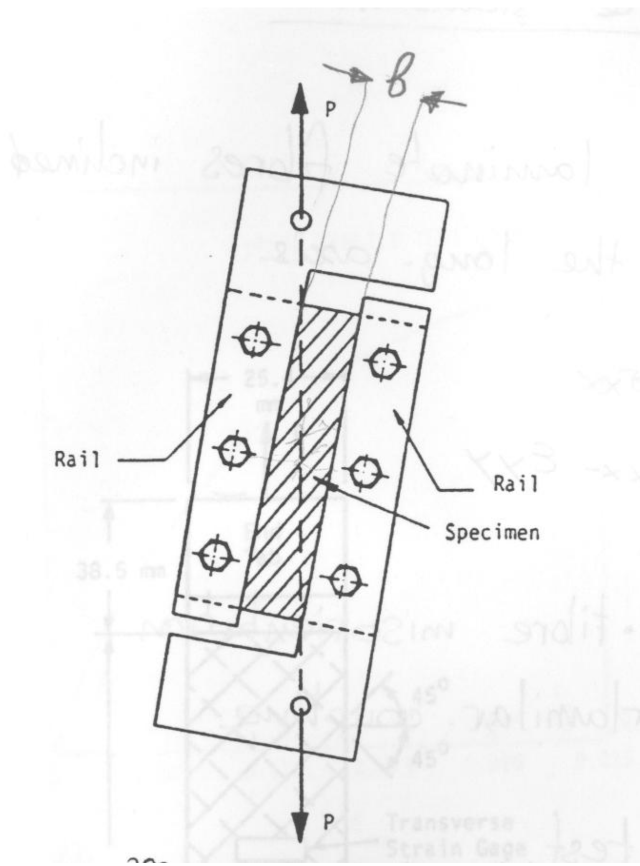

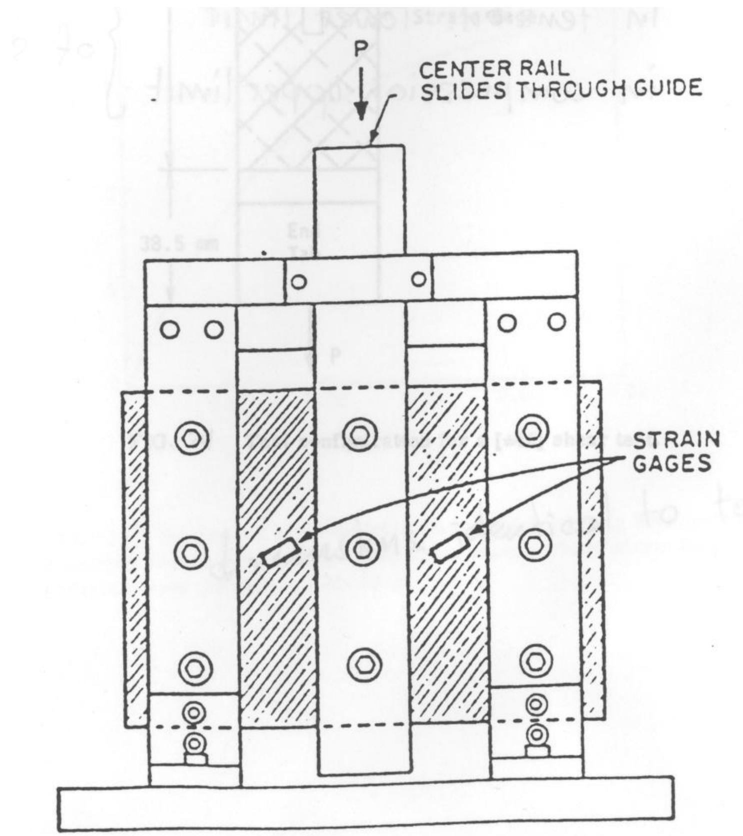

Fig. 23b. - Three-rail shear apparatus

rail shear test

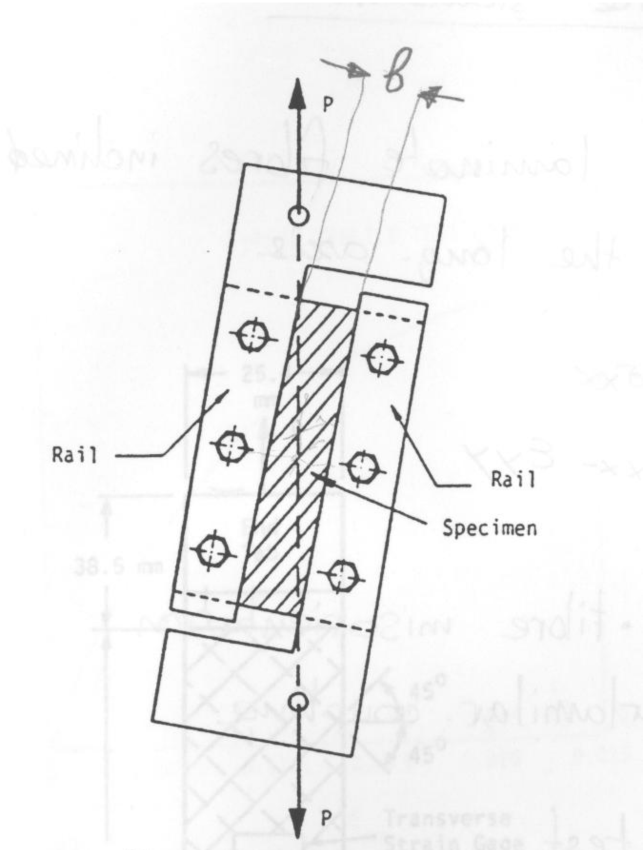

- A rectangular plate is fixed in side beams while the longitudinal direction is free
- The load induces shear stresses

For pure shear:

$$\varepsilon_{xx} = \varepsilon_{yy} = 0 \qquad \gamma_{xy} = 2\varepsilon_{45^\circ}$$

γ, the shear strain

The shear stress is :

- b width
- t thickness

$$\tau_{xy} = \frac{P}{bt}$$

Shear strain is measured at 45° to the rail

$$\gamma_{xy} = 2\varepsilon_{45^\circ}$$

Interlaminar shear: The ILSS test.

✓From the beam theory, flexural stress can be written as:

$$\sigma_{xx} = \frac{3P}{2wt}\left(\frac{S}{t}\right)$$

✓The maximum shear is

$$\tau_{xz} = \frac{3P_{\max}}{4wt}$$

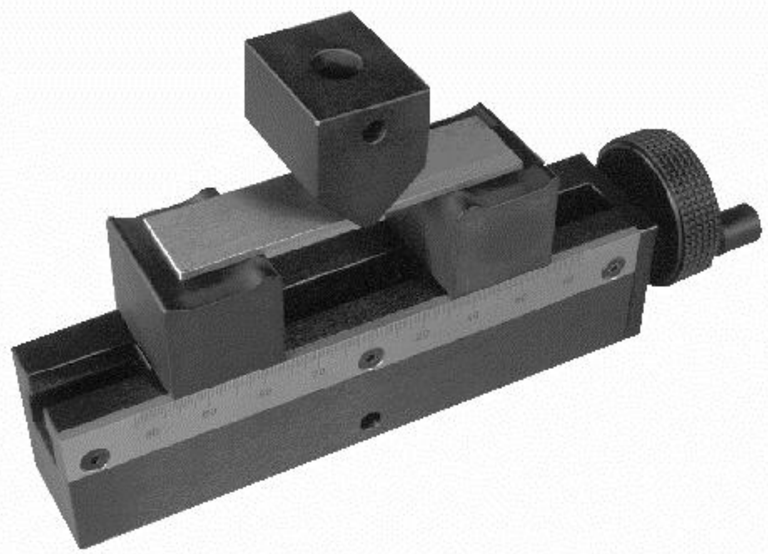

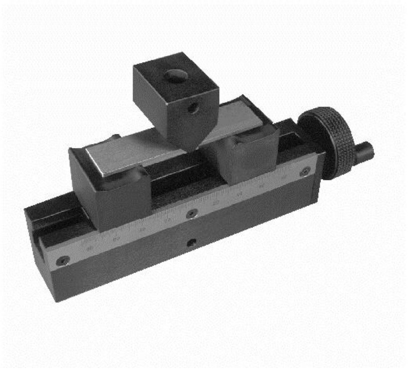

Interlaminar shear: The ILSS test.

✓Whereas the flexural stress decreases with s/t the maximum shear stress is independent of it.

$$\sigma_{xx} = \frac{3P}{2wt}\left(\frac{S}{t}\right) \qquad \tau_{xz} = \frac{3P_{\max}}{4wt}$$

For small S/t shear failure is more probable

Shear or Flexure;

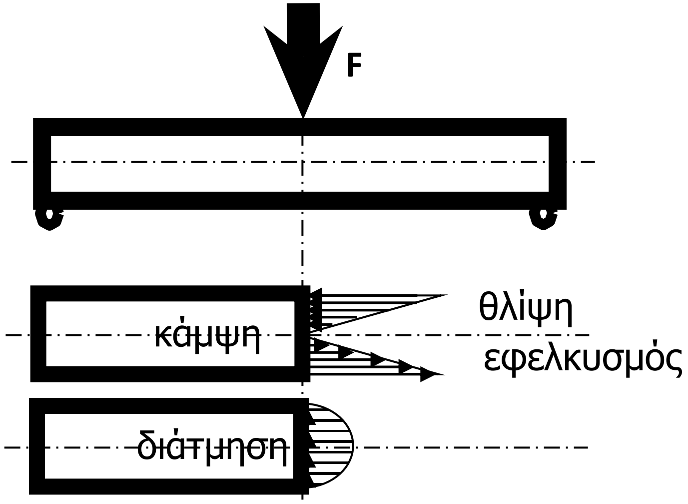

From the elastic beam theory:

- Maximum stress (compressive or tensile)-top and bottom surface respectively:

$$\sigma_{ult} = \frac{3P_{\max}S}{2wt^2}$$

- Maximum shear stress – neutral axis:

$$\tau_{ult} = \frac{3P_{\max}}{4wt}$$

- Maximum shear to maximum bending stress:

$$\frac{\tau_{ult}}{\sigma_{ult}} = \frac{S}{2t}$$

Shear or Flexure;

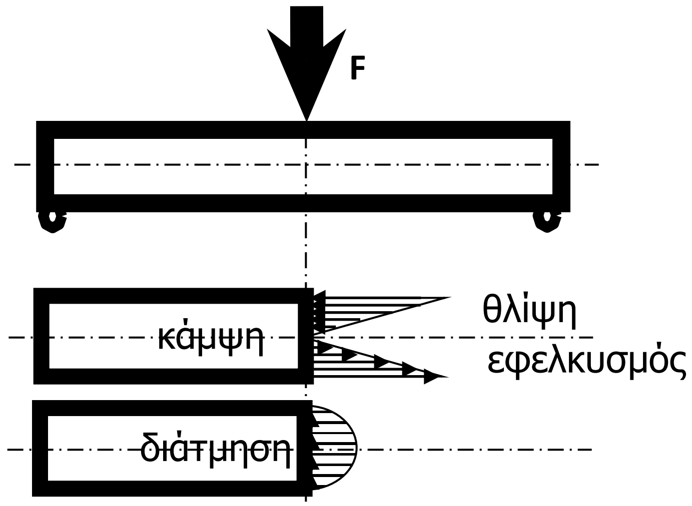

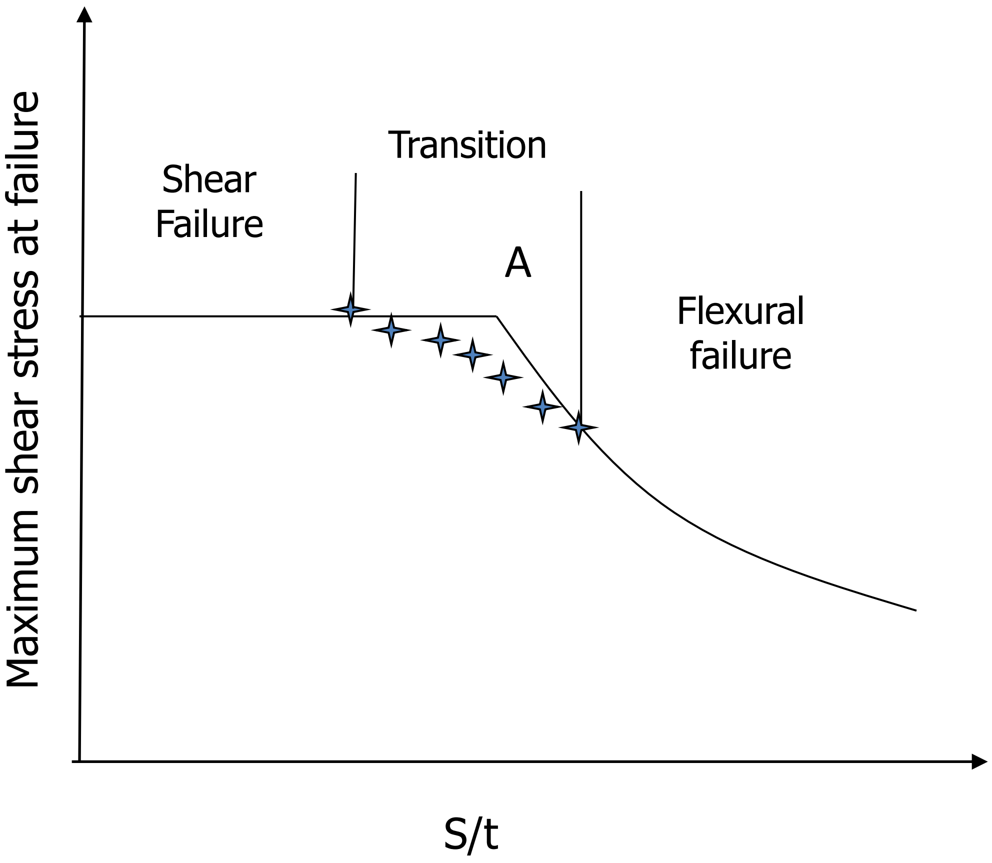

Shear strength:

- ✓For small S/t:

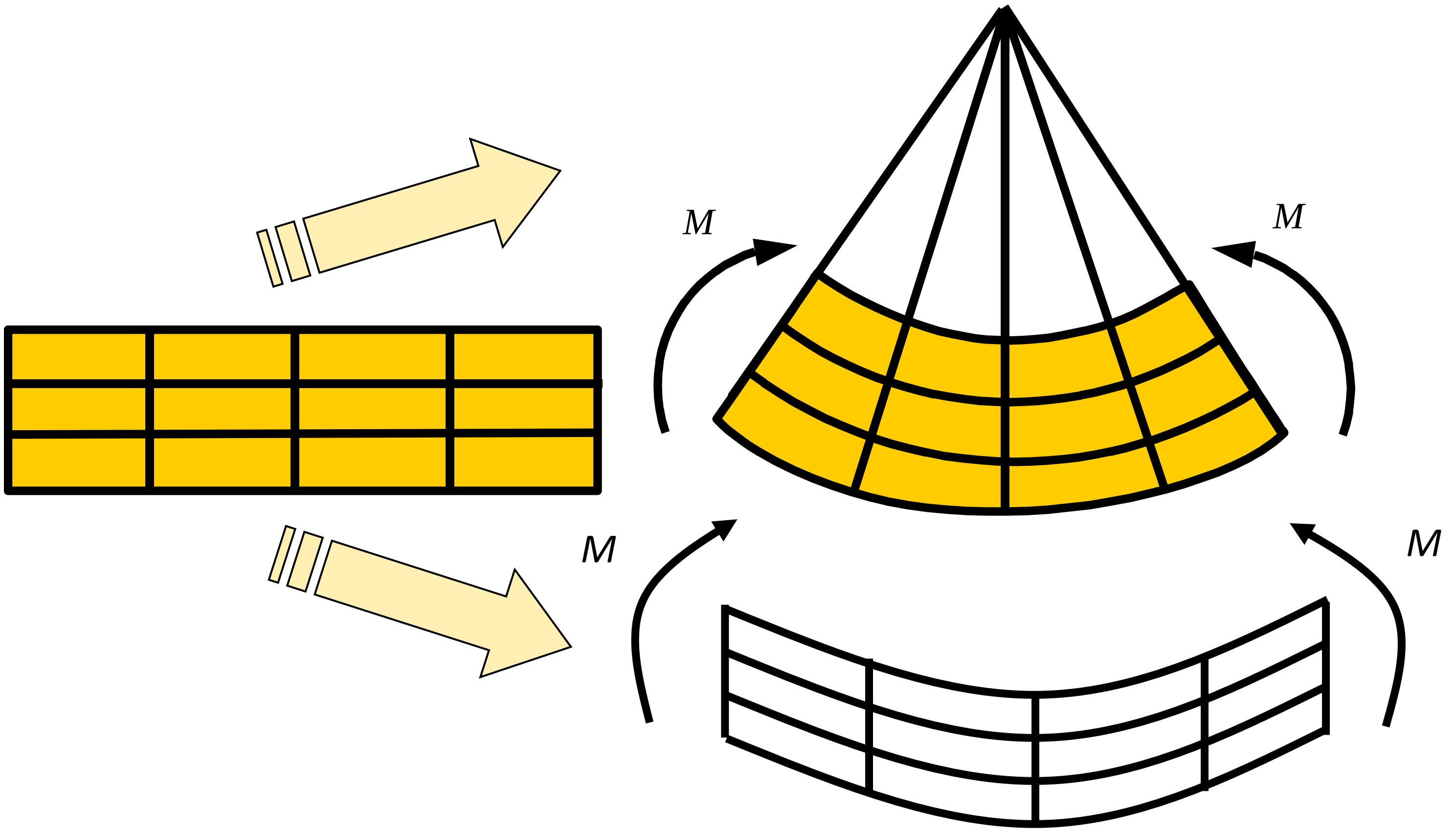

Shear strength:

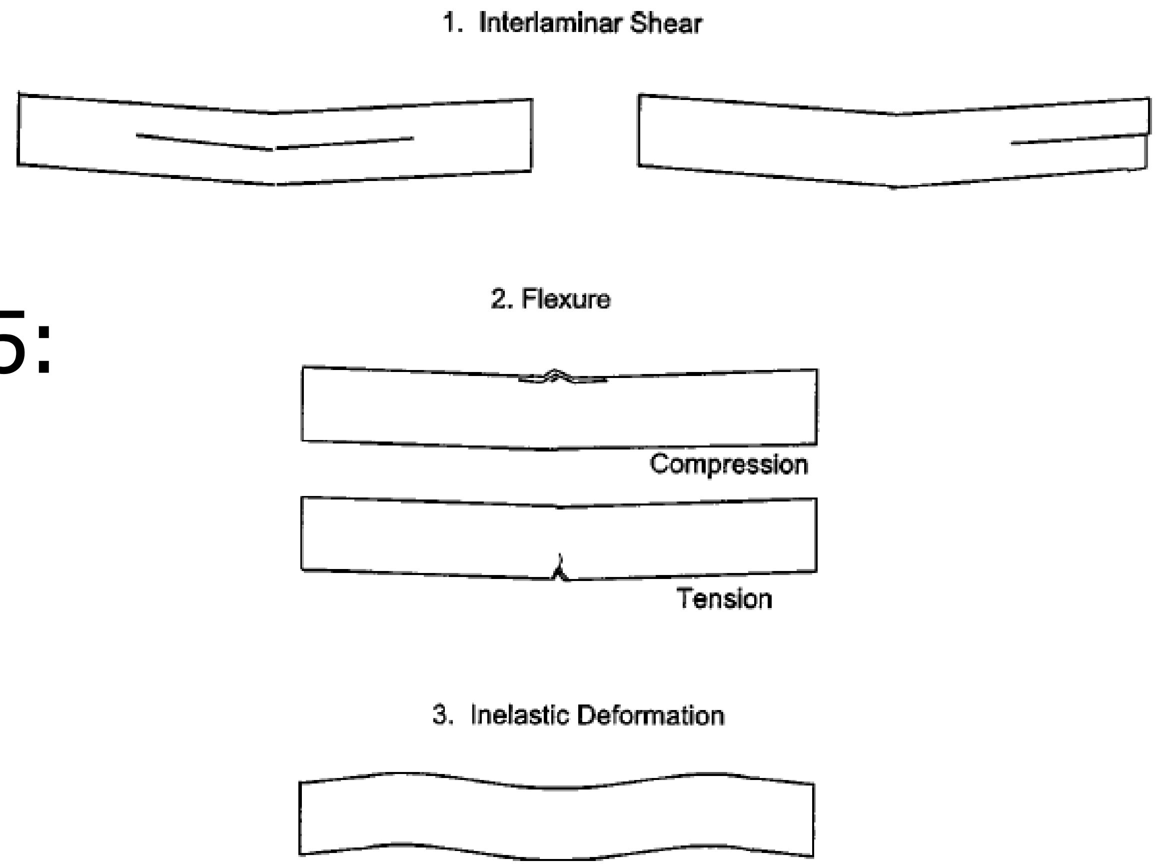

✓4 < S/t <5:

The coupon fails in shear

ILSS test:

- Two geometries
- (ASTM D3244):
  - Curved coupon
  - Flat coupon

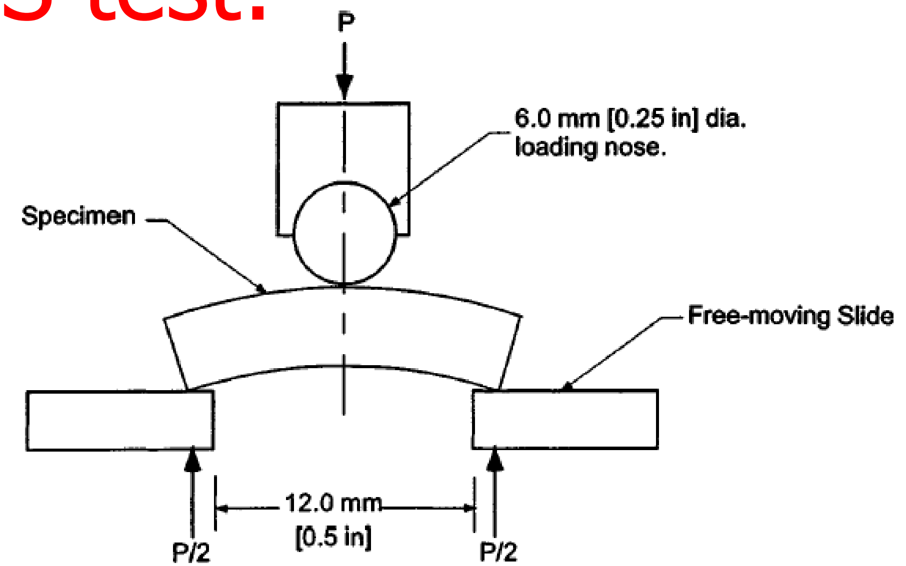

FIG. 5 Horizontal Shear Load Diagram (Curved Beam)

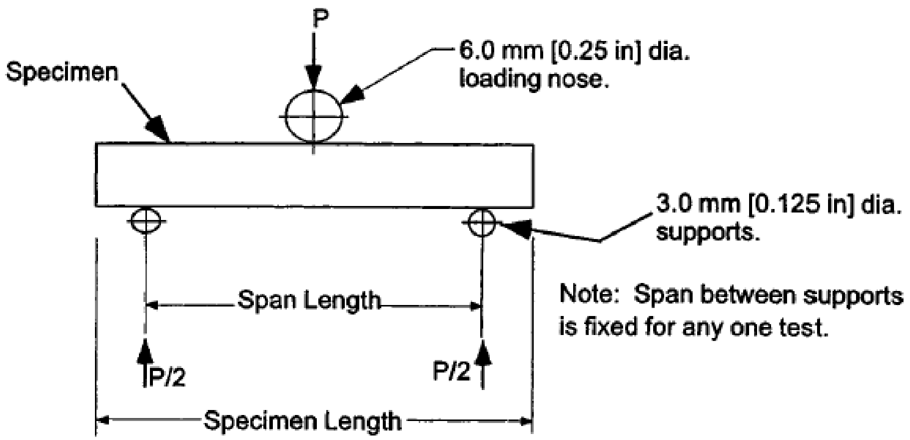

FIG. 6 Horizontal Shear Load Diagram (Flat Laminate)

ILSS tests:

Standards

Method	w	t	S/t	L	d_1	d_2	Speed (mm/min)
ASTM	10	2	5	14	3.2	6.4	1.3
BSI	»	»	»	12	6	6	1
CRAG	»	»	»	20	»	»	»

Advantages:

Simple to perform

Simple test configuration

Comparable data from all standards

Disadvantages

✓The geometry defines failure

The through thickness shear distribution is not parabolic

✓Difficult to assess acceptable failure mode

Fracture Testing

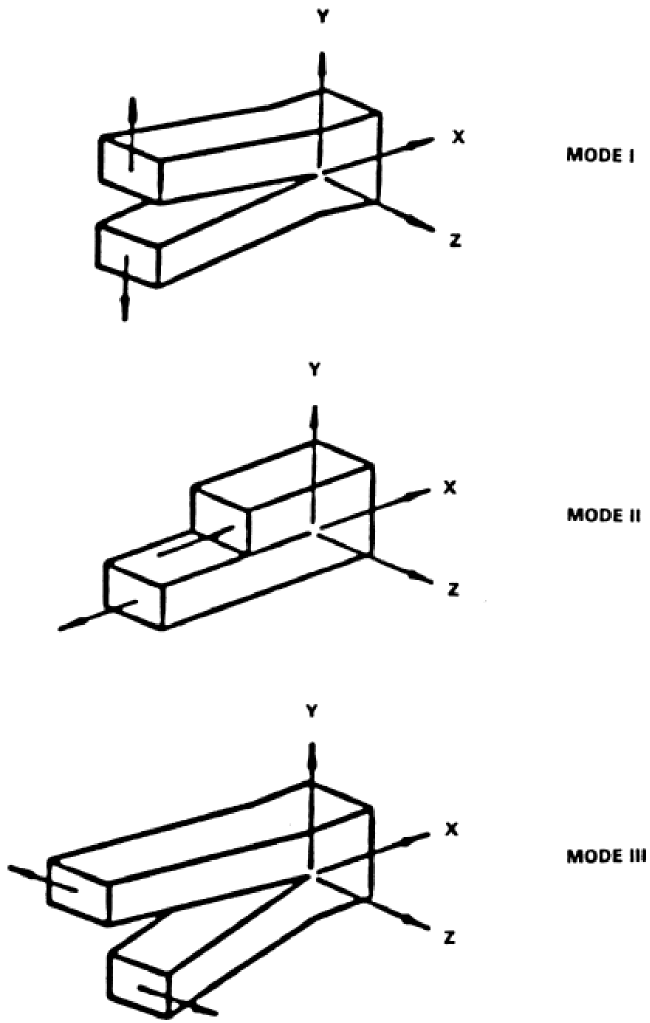

Opening mode

Shearing mode

Tearing mode

Figure 14 Fracture mechanics failure Modes I, II, and III.

DONALD F. ADAMS, University of Wyoming, Laramie, WY, USA, Volume 5, Ch 5.05 of Comprehensive Composite Materials

Fracture Testing

Double cantilever beam flexure test (tension)

End-notched flexure test (shear)

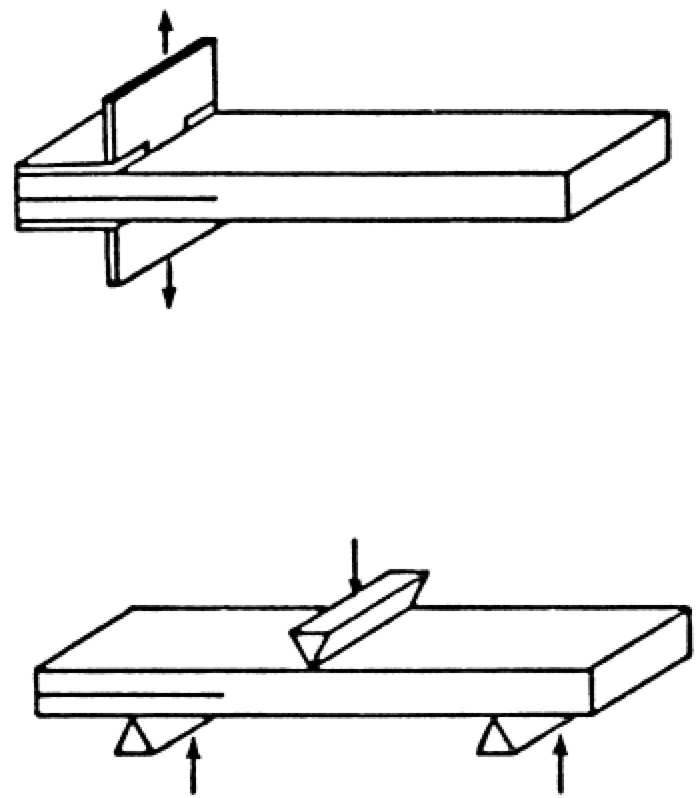

Figure 15 Interlaminar fracture toughness test methods for composite materials.

DONALD F. ADAMS, University of Wyoming, Laramie, WY, USA, Volume 5, Ch 5.05 of Comprehensive Composite Materials

Fracture Testing

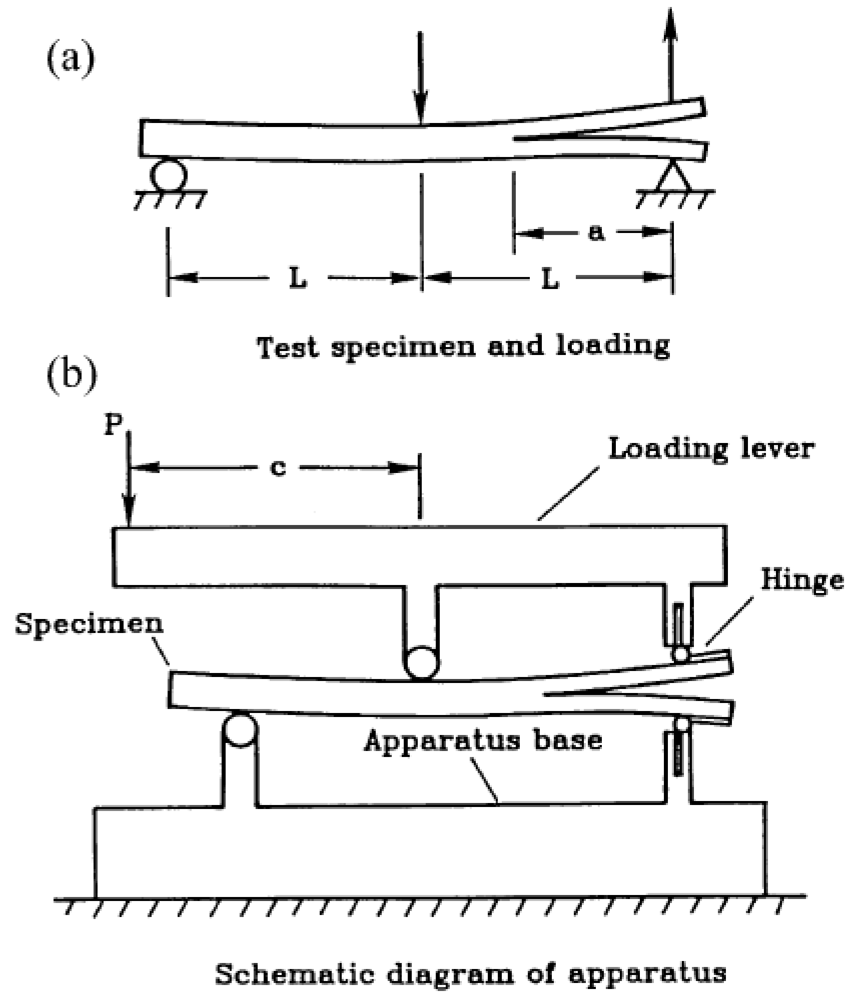

Figure 16 Mixed-mode interlaminar fracture toughness specimen and test fixture (after Crews and Reeder, 1988).

DONALD F. ADAMS, University of Wyoming, Laramie, WY, USA, Volume 5, Ch 5.05 of Comprehensive Composite Materials

Fracture Testing

- **Mode I - DCB Specimen**

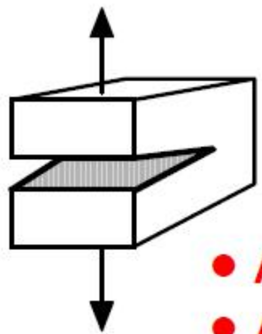

crack opening
mode I

- **ASTM D5528 - static**
- **ASTM D6615 - fatigue**

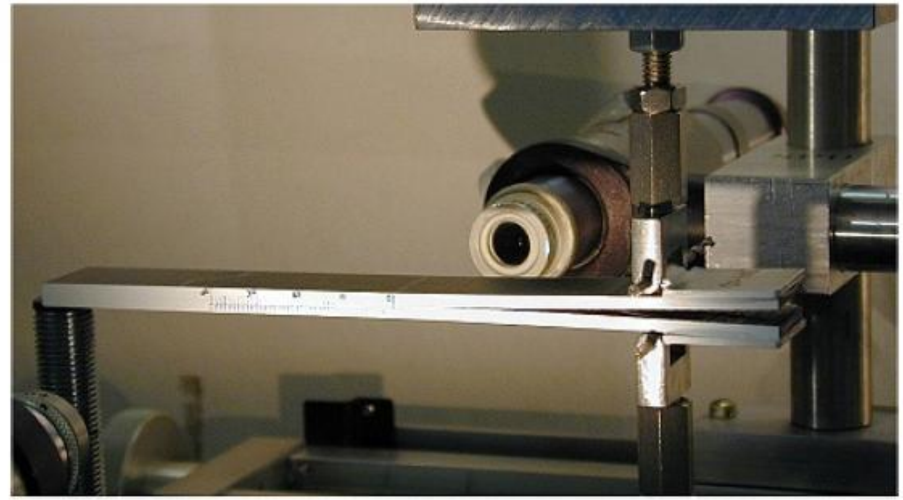

- **Mode II - 4ENF Specimen***

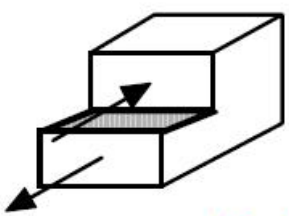

in plane shear
mode II

- **Standard in development**

*Rod Martin, MERL - Barry Davidson, Syracuse University

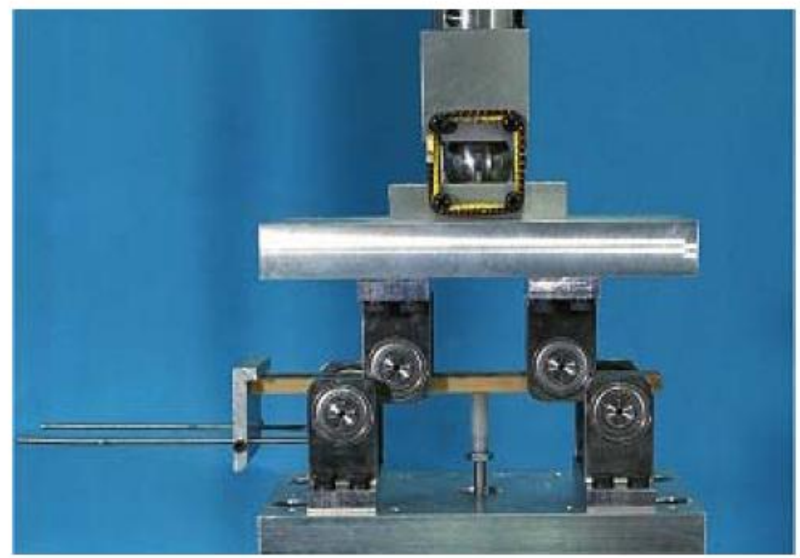

Fracture Toughness : mode 1

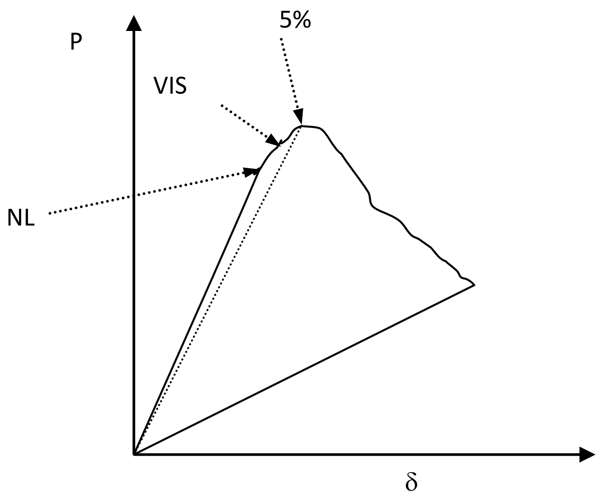

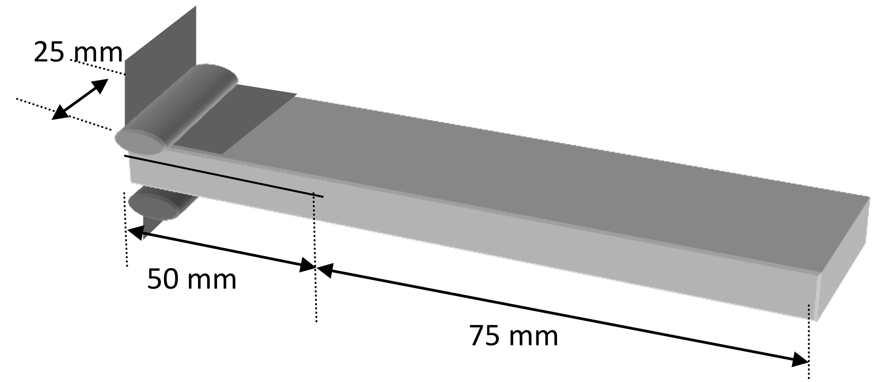

a

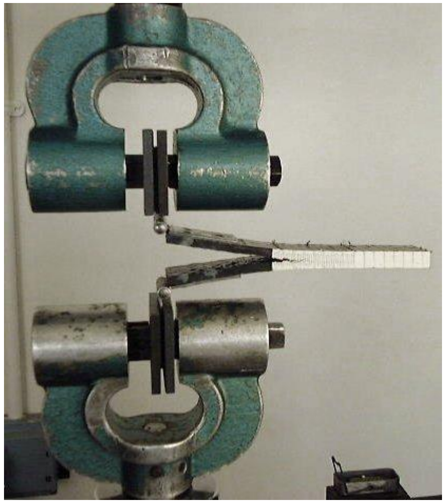

b

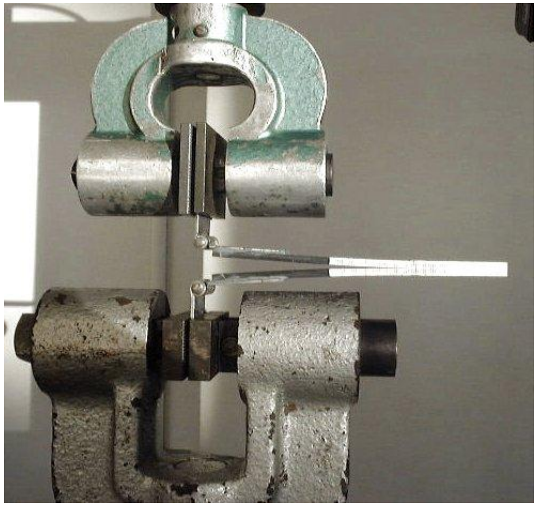

Carbon/nylon **Carbon**

Paul J. Hogg, NOVEL TOUGHENING CONCEPTS FOR LIQUID COMPOSITE MOULDING

Fracture Toughness : mode 1

Plain glass DCB test specimen

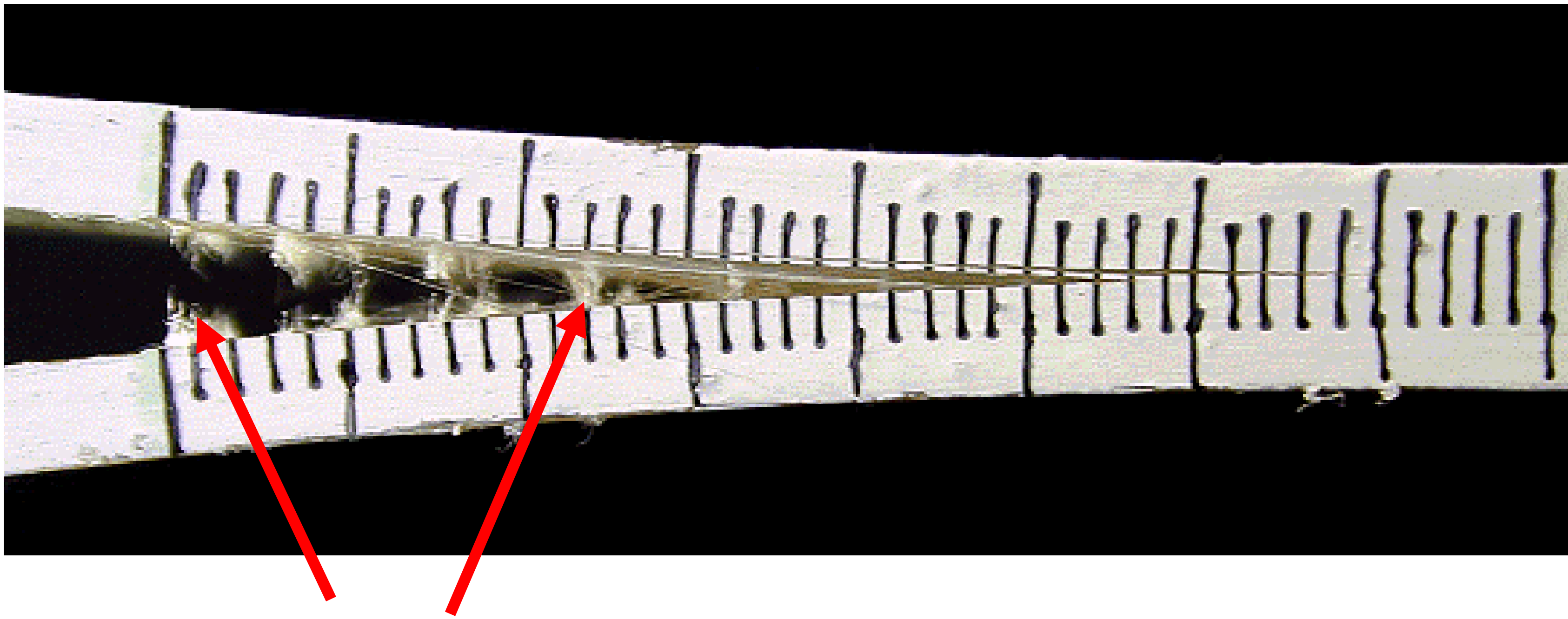

Fibre bridging mainly due to polyester stitching

Paul J. Hogg, NOVEL TOUGHENING CONCEPTS FOR LIQUID COMPOSITE MOULDING

Fracture Toughness : mode 1

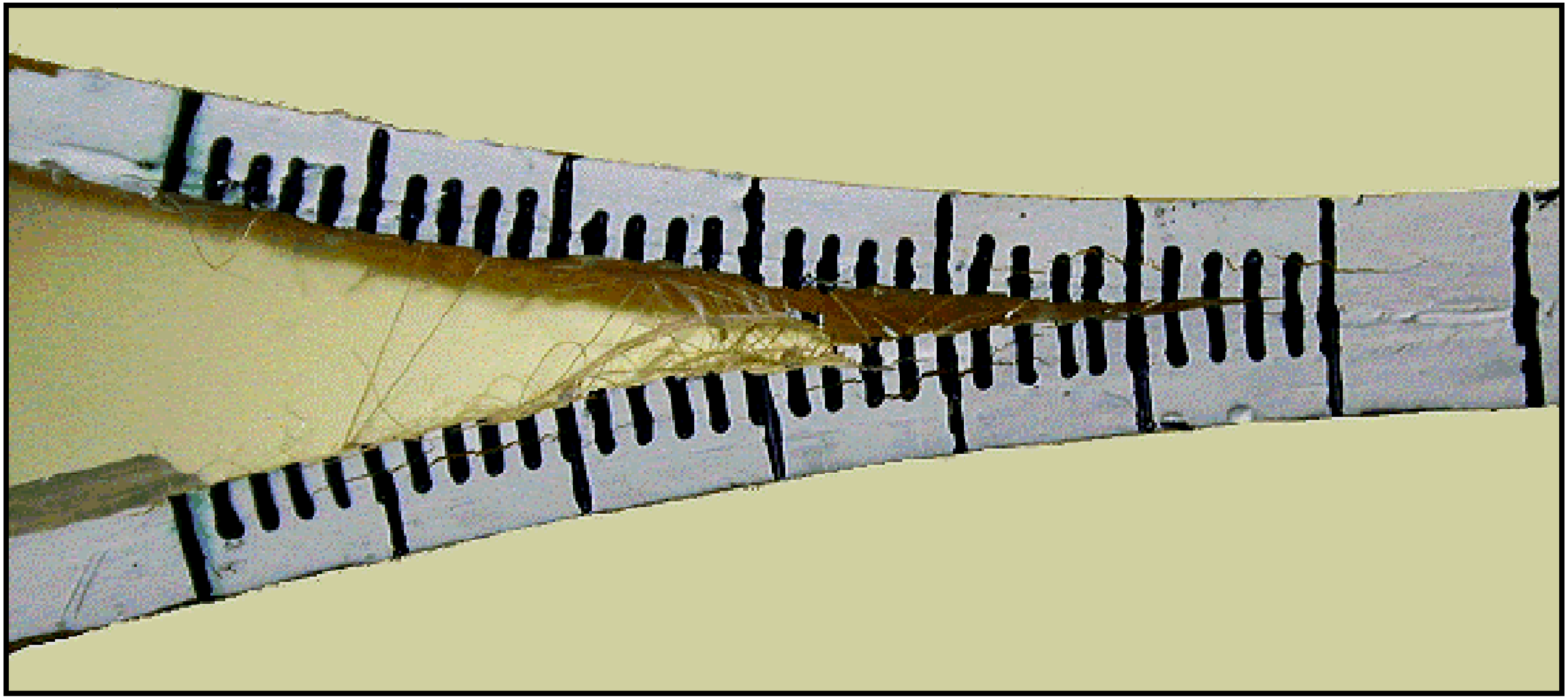

DCB test on Glass fibre : PP/Epoxy ep1

Paul J. Hogg, NOVEL TOUGHENING CONCEPTS FOR LIQUID COMPOSITE MOULDING

Fracture Toughness : mode 2

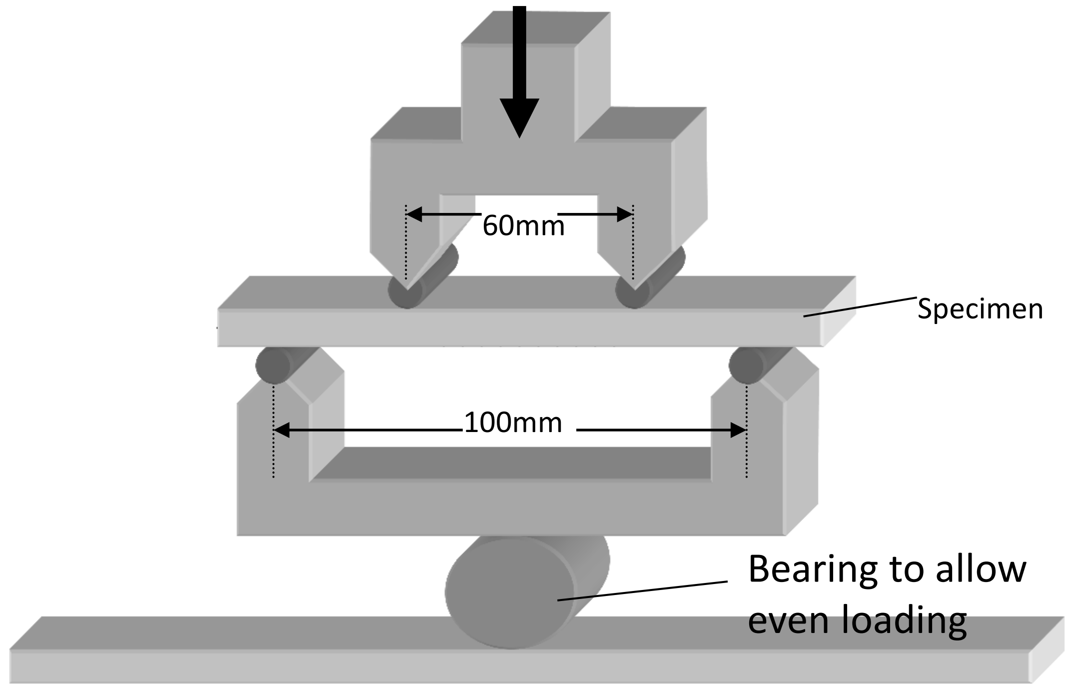

Four point end-notch flexure test

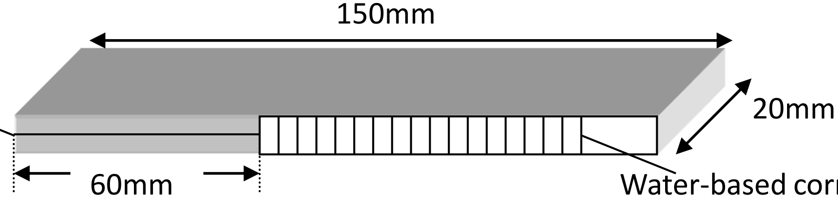

Paul J. Hogg, NOVEL TOUGHENING CONCEPTS FOR LIQUID COMPOSITE MOULDING

Fracture Toughness : mode 2

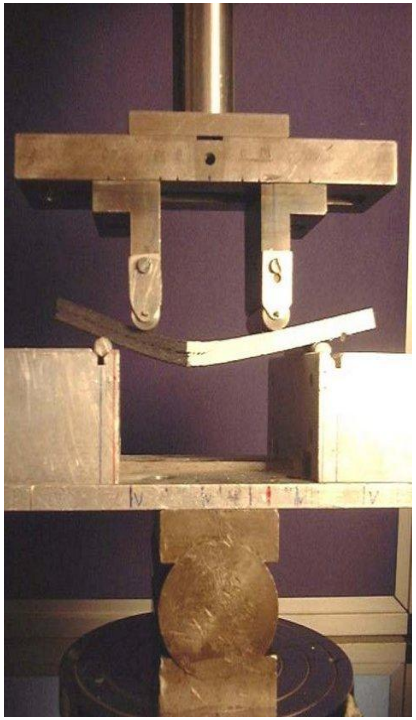

Carbon nylon

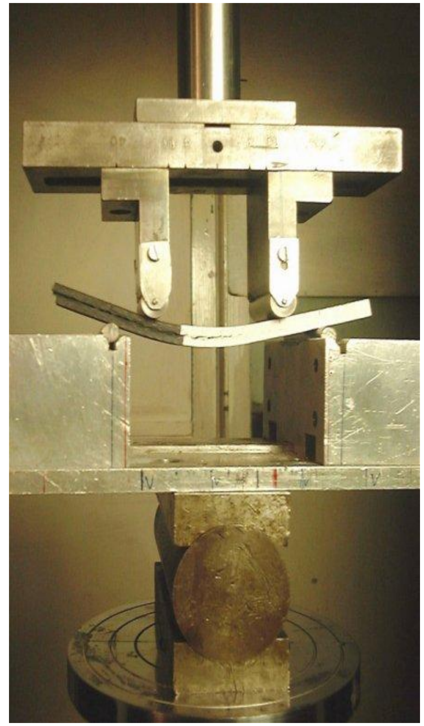

Carbon nylon (modified specimen)

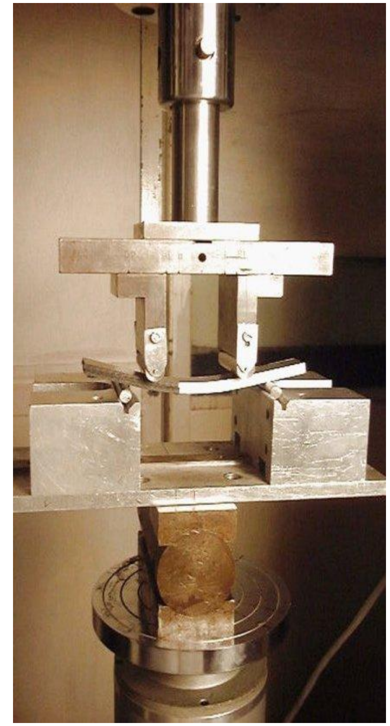

Carbon

Paul J. Hogg, NOVEL TOUGHENING CONCEPTS FOR LIQUID COMPOSITE MOULDING

Fracture mechanics

- **Mixed Mode I/II - MMB Specimen***

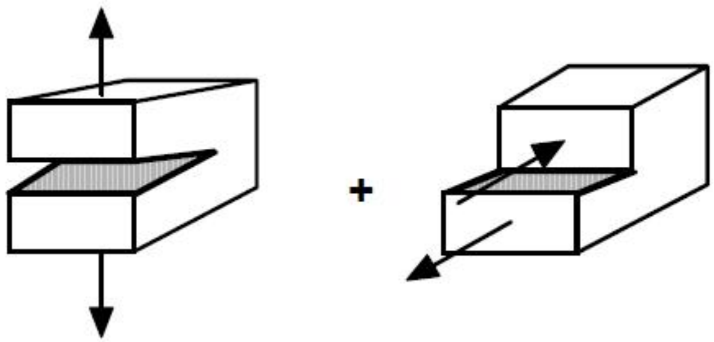

crack opening mode I + in plane shear mode II

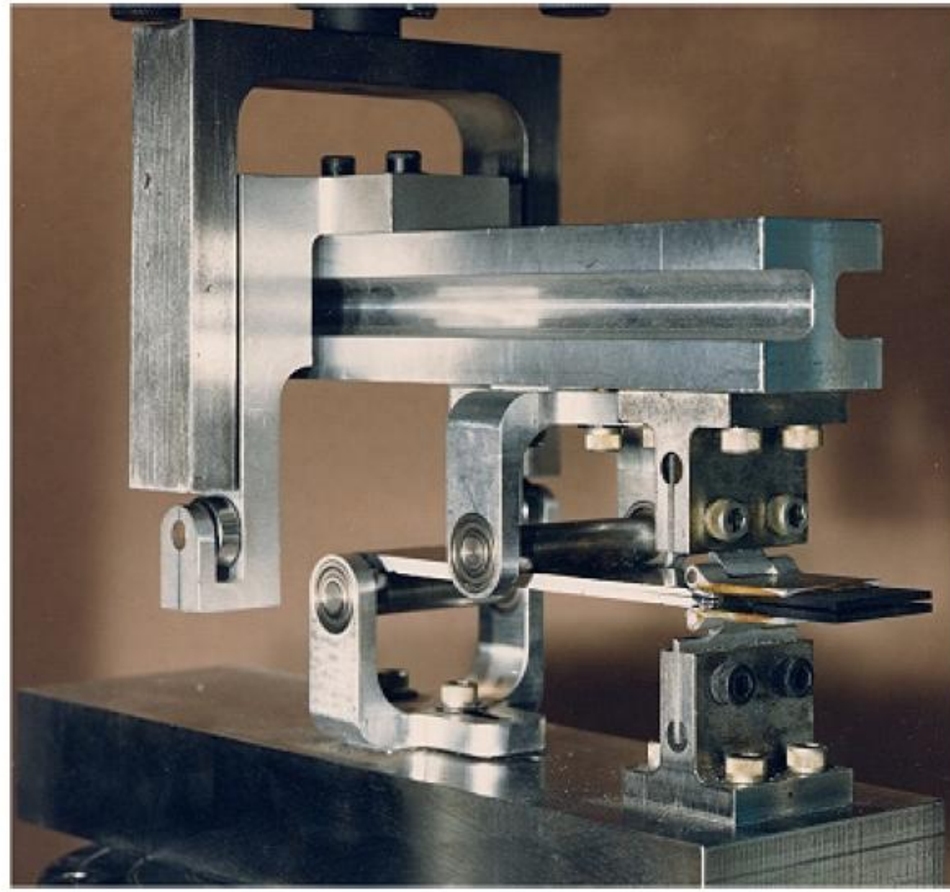

- **ASTM D6671**

*James Reeder, NASA Langley Research Center

Fracture mechanics

- **Mode III - ECT Specimen***

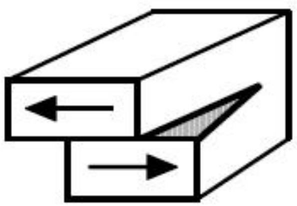

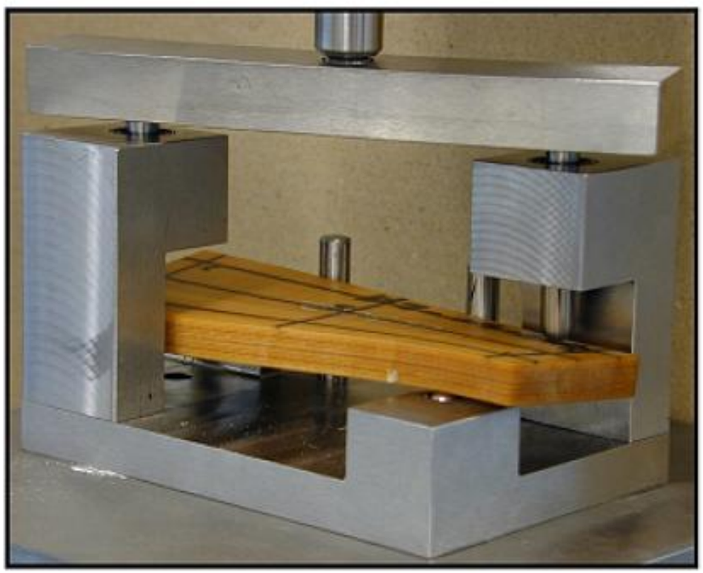

- **Standard in development**

*James Ratcliffe,NRC at NASA Langley Research Center

- **Failure surface $G_c = G_c(G_{Ic}, G_{IIc}, G_{IIIc})$****

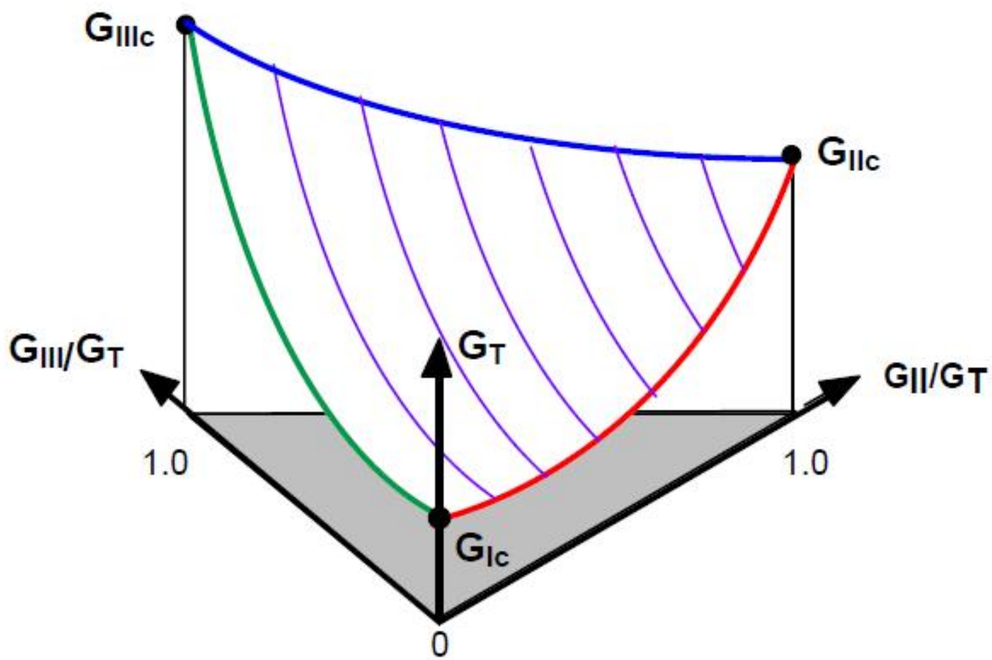

**James Reeder, NASA Langley Research Center

Durability Testing of Polymer Composites

PAUL T. CURTIS, DERA, Farnborough, UK

Volume 5, Ch 5.08 of Comprehensive Composite Materials

- FATIGUE TESTING
  - Tensile tests
  - Compression tests
  - Flexural tests
  - Shear tests
  - Biaxial fatigue testing
- Machines and Control Modes
- Presentation of Data
- Monitoring Fatigue Damage Growth
  - Microscopy
  - Ultrasonics
  - X-radiography
  - Thermography
- Potential Problems with Fatigue Testing
  - Stress concentrators
  - Frequency effects
  - Edge effects
  - Environmental effects
- IMPACT TEST METHODS
  - High-energy Impact Test Methods
  - Flexed-beam tests
  - The drop-weight impact test
  - Data analysis and failure modes
  - Low-energy Impact Test Methods
  - Ballistic impact tests
  - Drop-weight test
  - Residual Strength After Impact
  - Crashworthiness
- CREEP TEST METHODS
  - Creep Behavior of Polymer Composites
  - Creep Test Methods

Impact – Low velocity

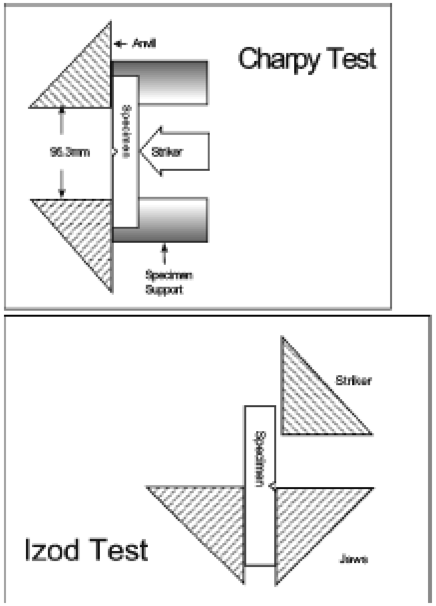

Figure 17 Schematic arrangements for Charpy and Izod impact tests.

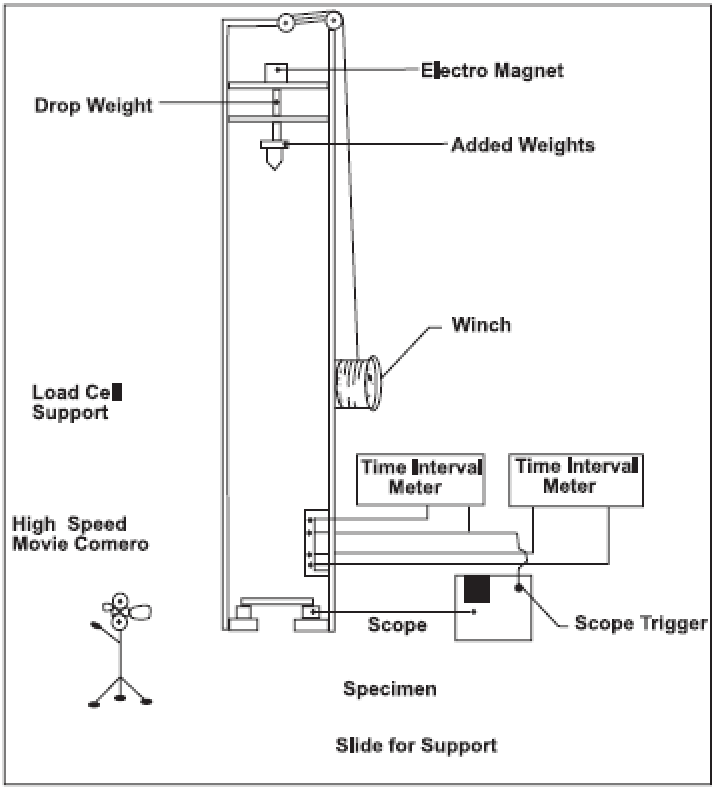

Figure 18 Schematic arrangement for drop-weight test.

PAUL T. CURTIS, DERA, Farnborough, UK, Volume 5, Ch 5.08 of Comprehensive Composite Materials

Impact – Low velocity

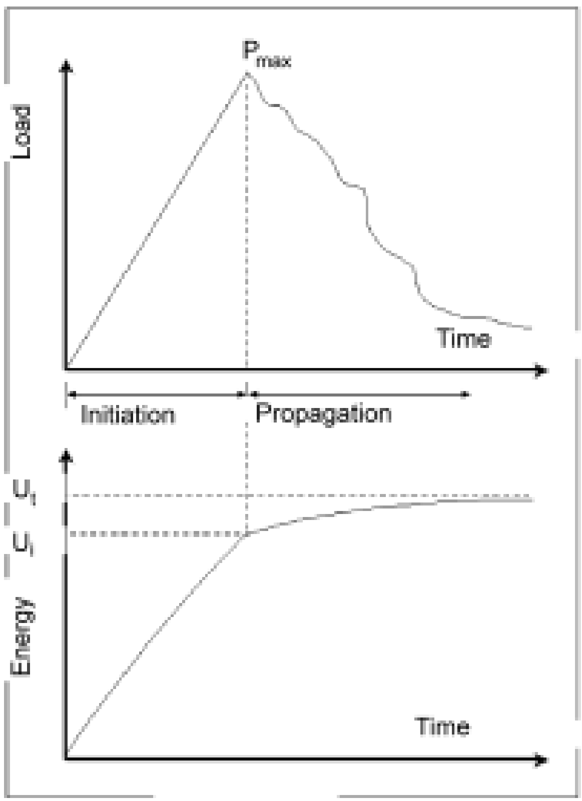

Figure 19 Schematic load–time and energy–time curves.

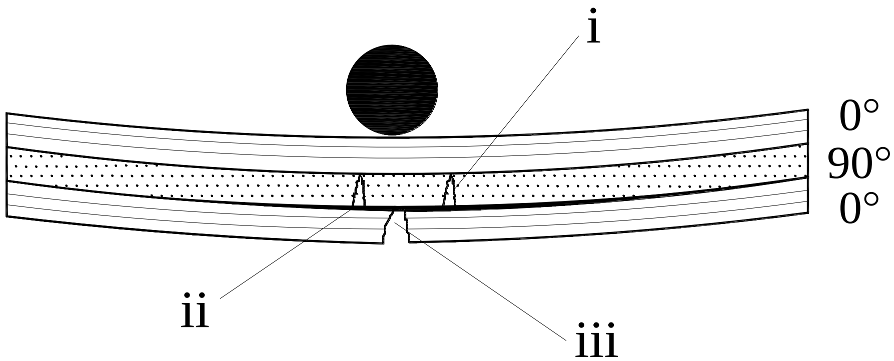

(Ellis 1996)

PAUL T. CURTIS, DERA, Farnborough, UK, Volume 5, Ch 5.08 of Comprehensive Composite Materials

Through penetration impact

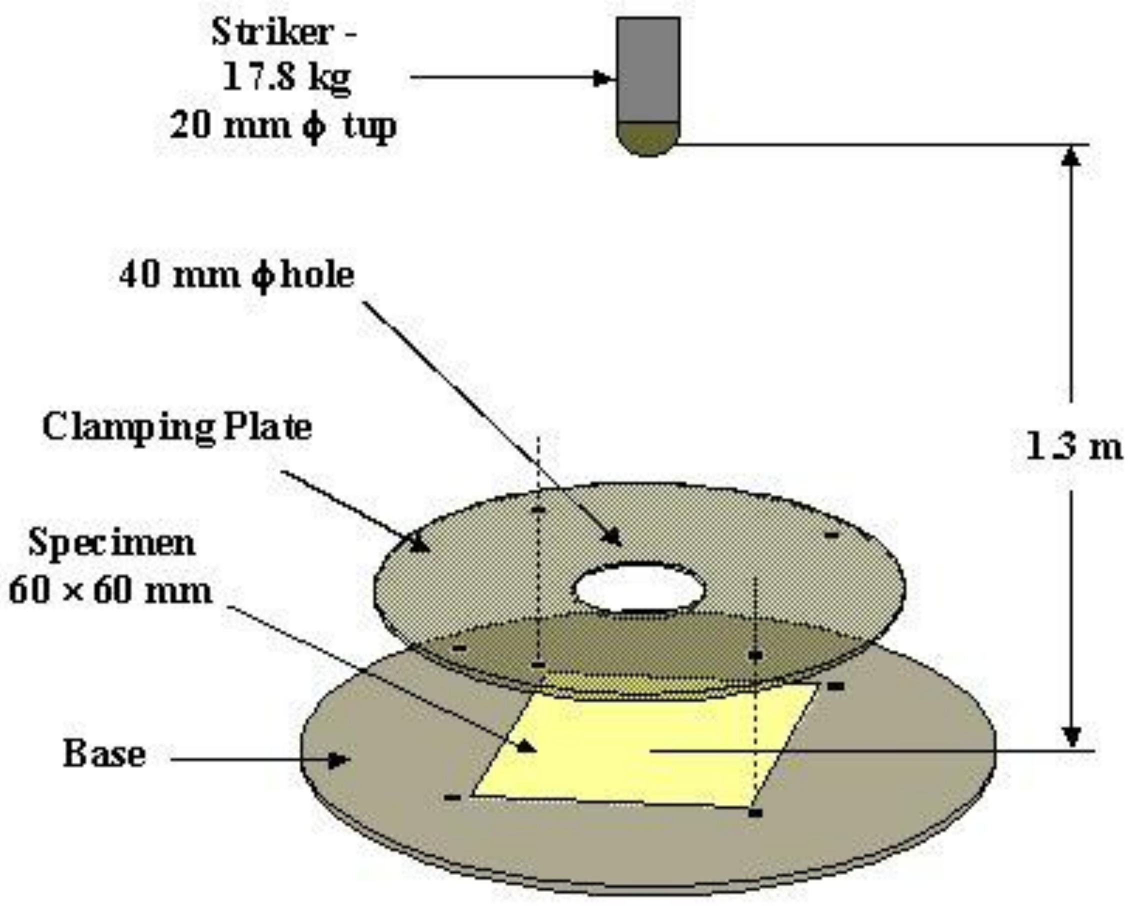

Paul J. Hogg, NOVEL TOUGHENING CONCEPTS FOR LIQUID COMPOSITE MOULDING

Through penetration impact

Impact energy = 227 J

Energy absorbed calculated

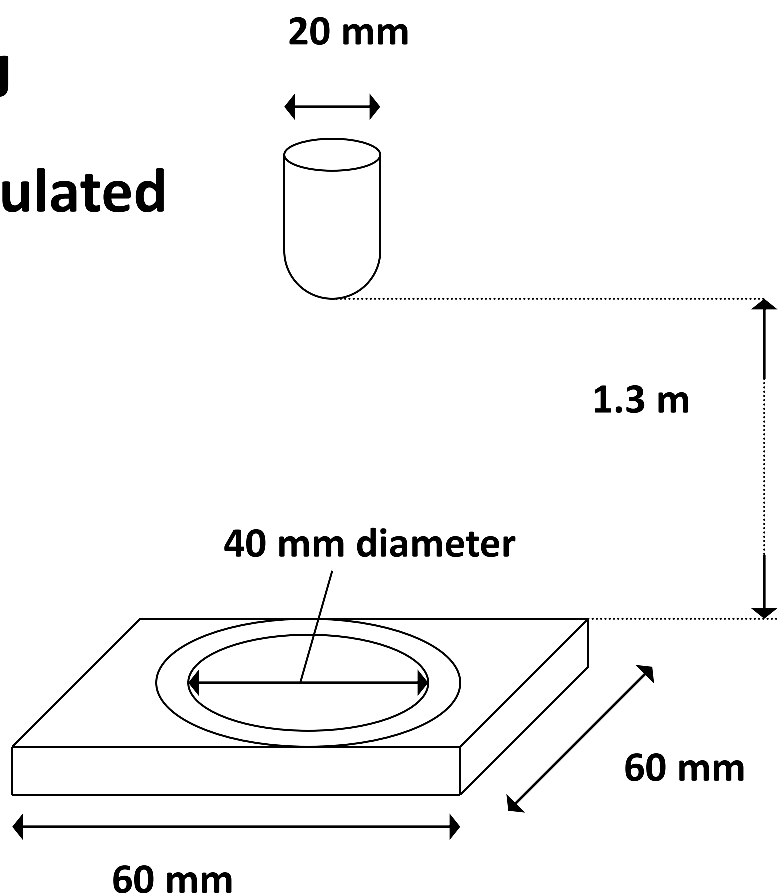

Paul J. Hogg, NOVEL TOUGHENING CONCEPTS FOR LIQUID COMPOSITE MOULDING

Through penetration impact

Impacted plain glass fibre specimens.

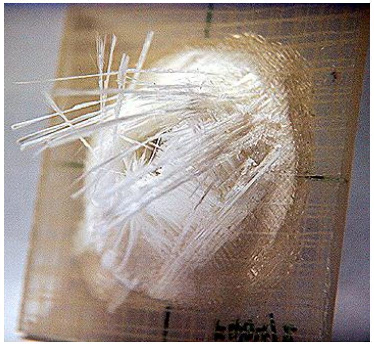

GF2/UP

GF1/EP1

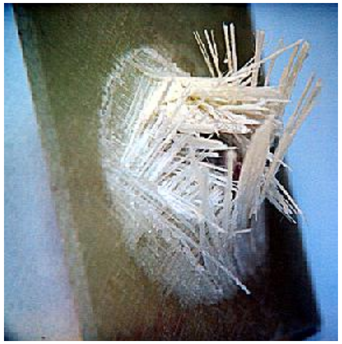

GF1/EP2

Paul J. Hogg, NOVEL TOUGHENING CONCEPTS FOR LIQUID COMPOSITE MOULDING

Through penetration impact

Impacted glass fibre/polypropylene specimens.

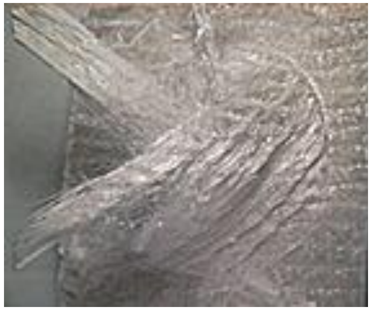

PP1/UP

PP1/EP1

PP1/EP2

Paul J. Hogg, NOVEL TOUGHENING CONCEPTS FOR LIQUID COMPOSITE MOULDING

Through penetration impact

Impacted polypropylene fibre/polypropylene specimens.

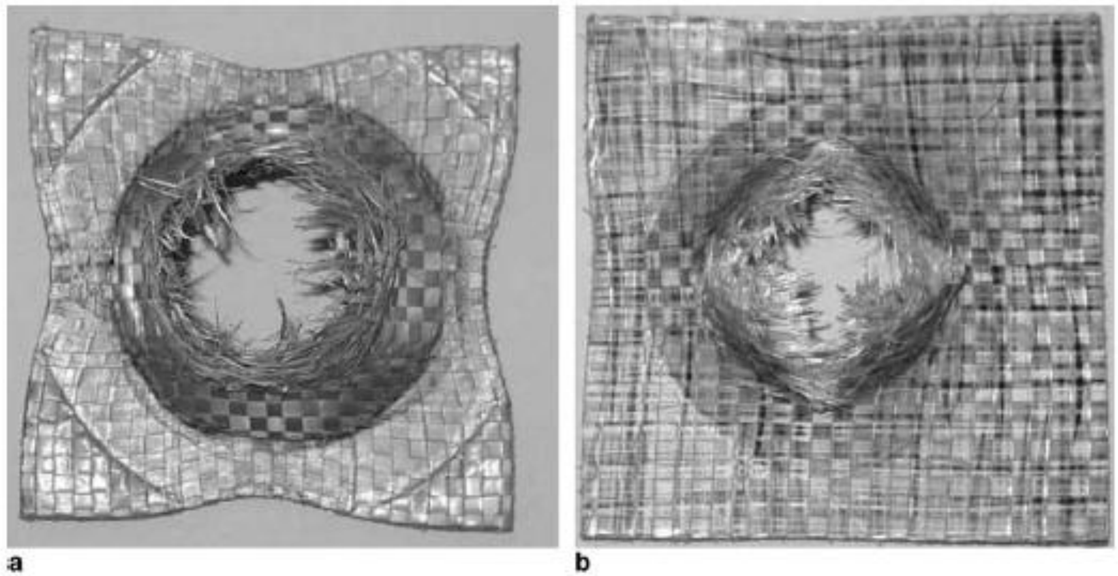

Fig. 10. Typical impact penetration damage at different compaction temperatures and pressures. Specimen (a) consolidated at lower temperature and pressure (140 °C, 0.1 MPa), shows large amounts of fibrillation and delocalised deformation giving a circular hole, while specimen (b) consolidated at higher temperature and pressure (160 °C, 11.4 MPa) shows very localised damage and breakage along tape boundaries giving a characteristic star-shaped hole.

B. Alcock et al. / Composites Science and Technology 66 (2006) 1724–1737

Through penetration impact

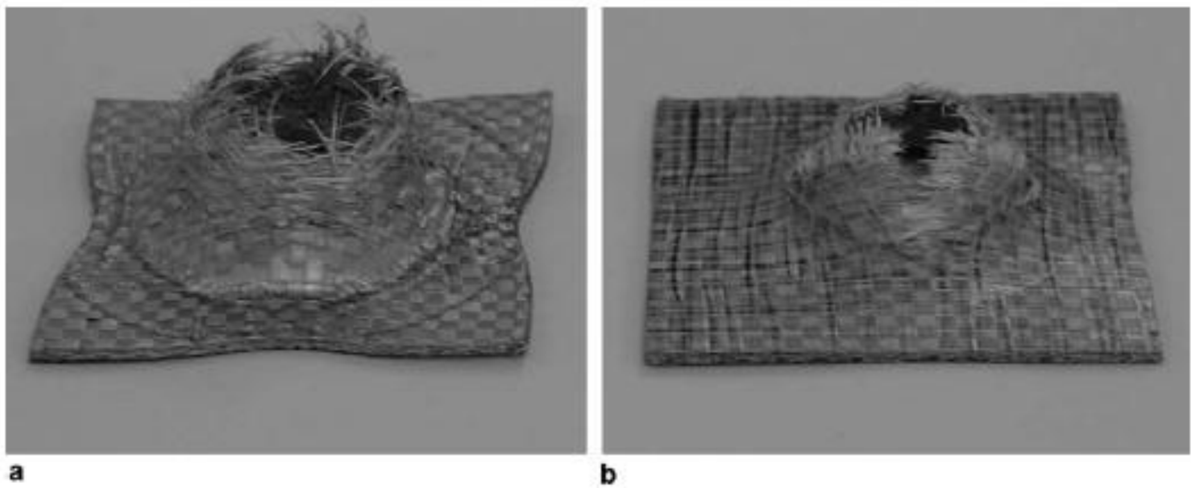

Fig. 12. Illustration of the out of plane deformation of all-PP composites. Specimen (a) consolidated at lower temperature and pressure (140 °C, 0.1 MPa), shows large amounts out of plane deformation and tape pull through, while specimen (b) consolidated at higher temperature and pressure (160 °C, 11.4 MPa) shows very localised damage and limited out of plane deformation.

B. Alcock et al. / Composites Science and Technology 66 (2006) 1724–1737

Through penetration impact

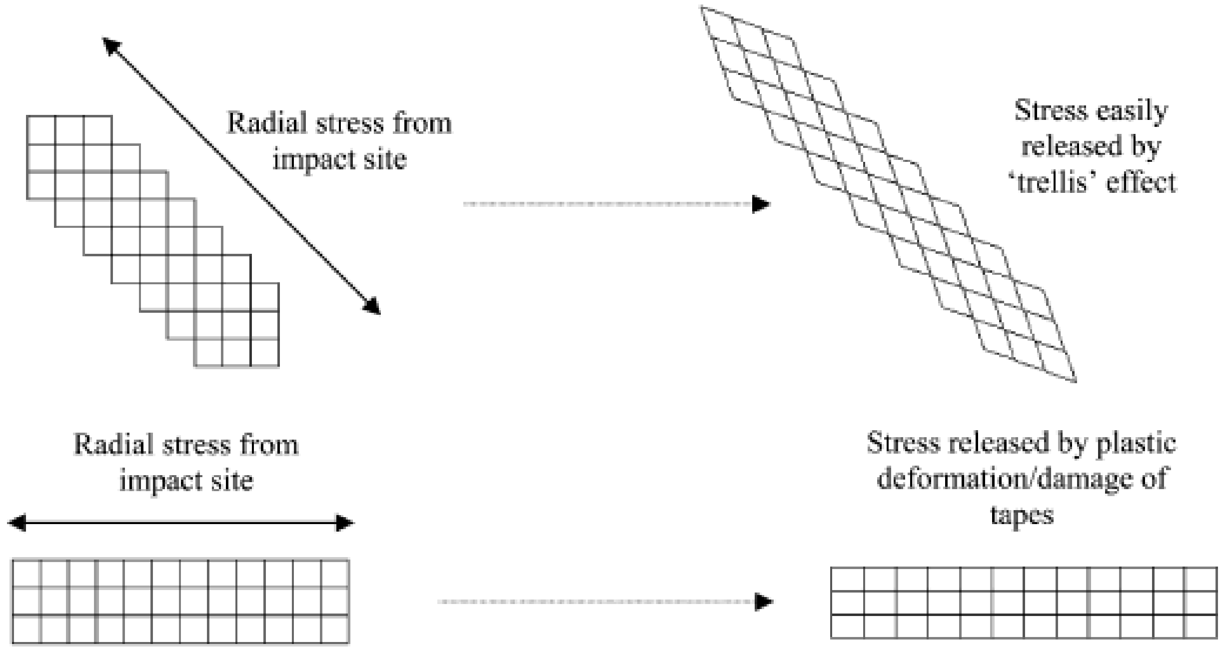

Fig. 14. Stress dispersion in different angles to tape direction showing the ease of plastic deformation during loading at ±45° to tape direction.

B. Alcock et al. / Composites Science and Technology 66 (2006) 1724–1737

Impact – Ballistic

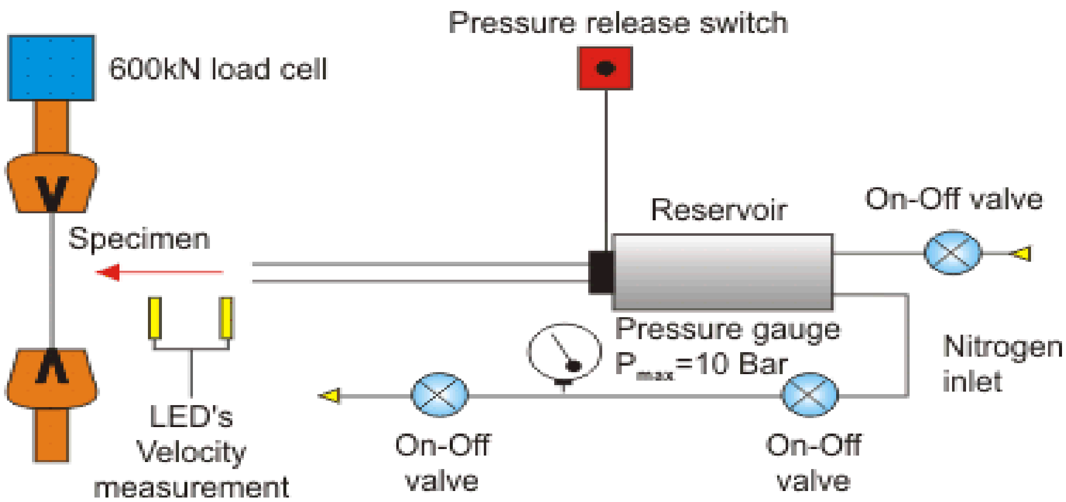

Neil Hancox 1996

shear plug

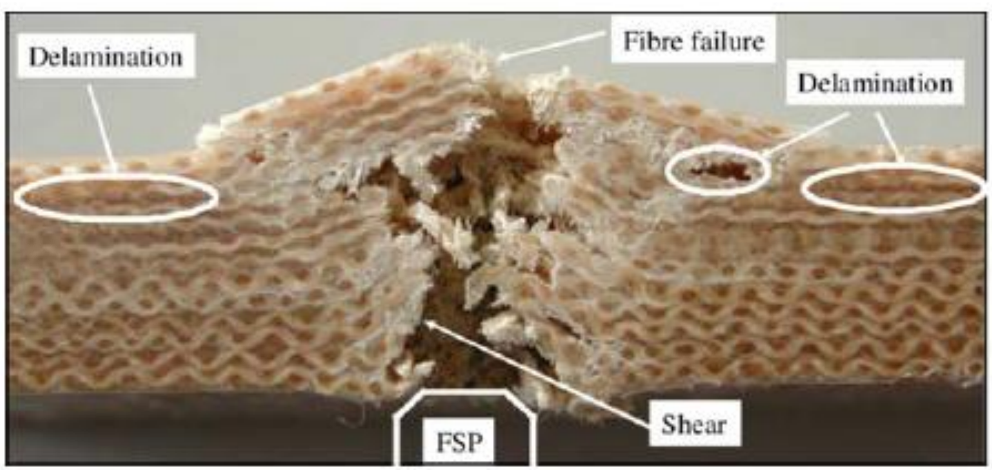

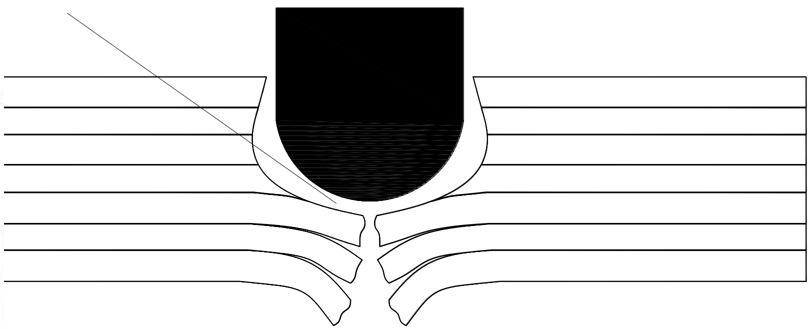

Ellis 1996

Wambua et al 2005

Impact – Ballistic

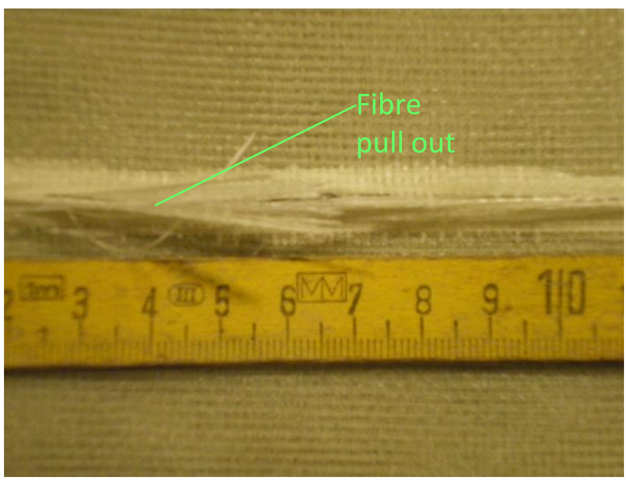

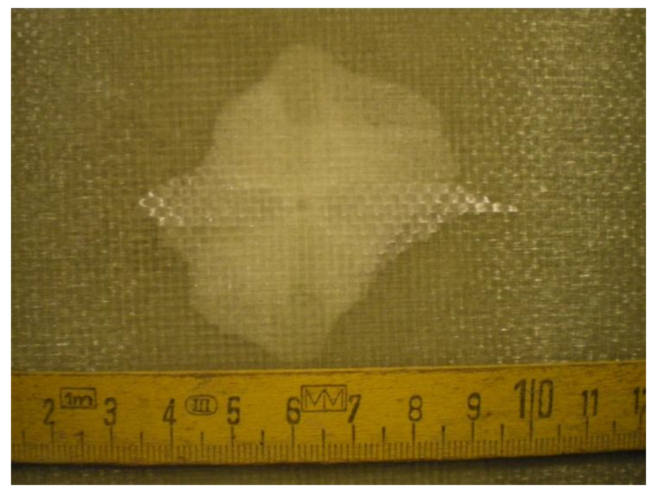

Degradation due to solid particle erosion

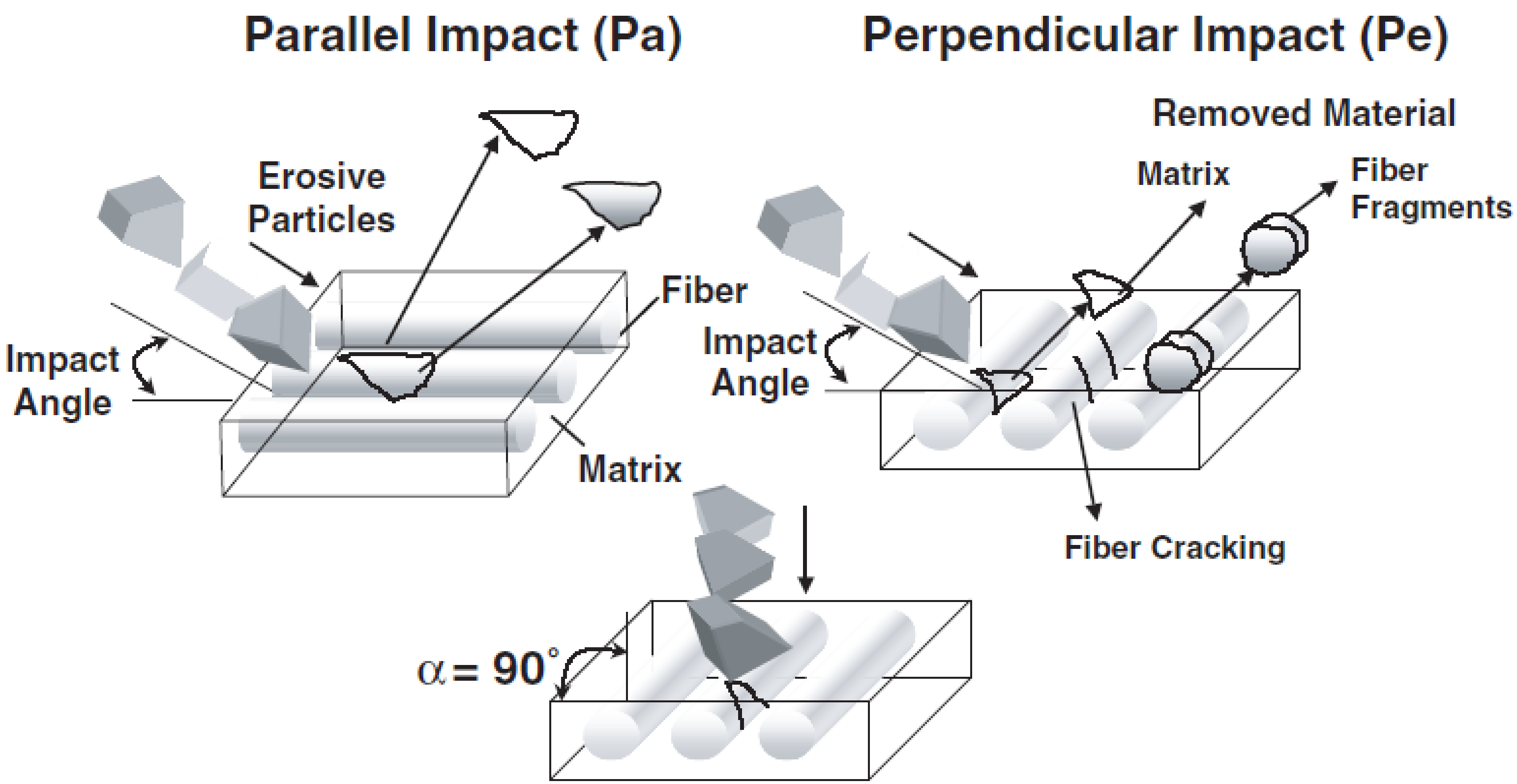

Figure 5. *Scheme of the role of the interface on the erosion of UD fiber-reinforced composites under parallel (Pa) and perpendicular (Pe) impact conditions.*

Journal of Reinforced Plastics and Composites, *Vol. 21, No. 15/2002*

Degradation due to solid particle erosion

(a)

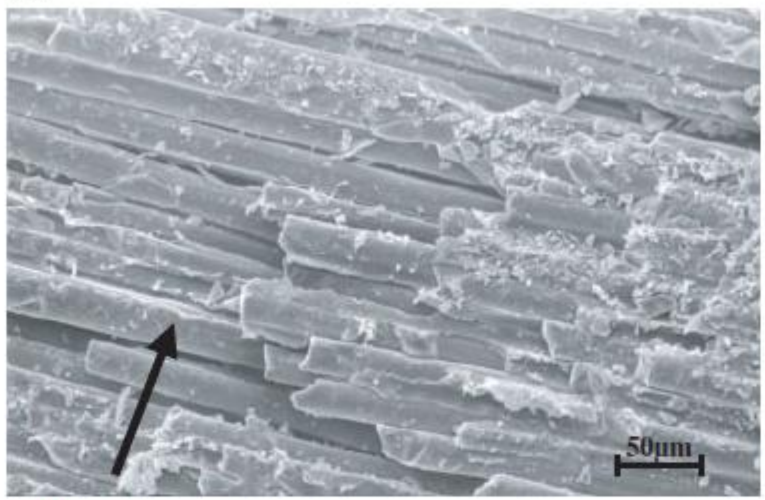

(b)

SEM micrographs taken on the eroded surface of composites impacte

Journal of REINFORCED PLASTICS AND COMPOSITES, *Vol. 21, No. 15/2002*

Degradation due to solid particle erosion

(a) (b)

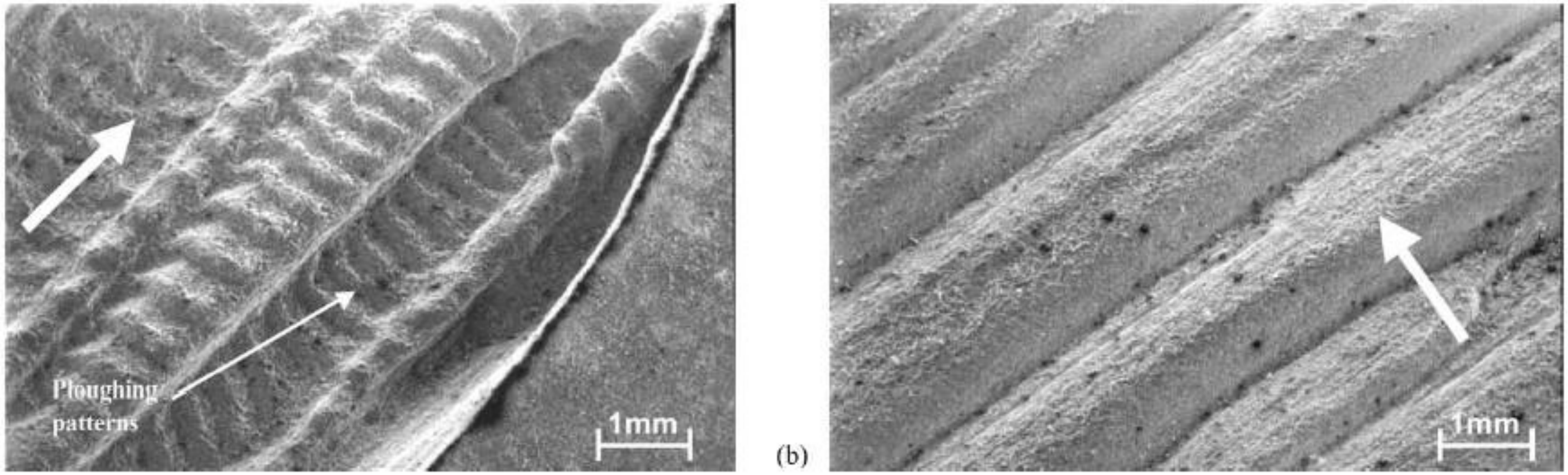

Fig. 4. Scanning electron micrographs taken on the eroded surfaces of GF/PP composites with 40 wt.% fibre content (erosion at 30° angle for 600 s)—illustration of orientation influence on surface topography: (a) parallel (Pa) erosion direction and (b) perpendicular (Pe) erosion direction.

N.-M. Barkoula, J. Karger-Kocsis / Wear 252 (2002) 80–87

Degradation due to solid particle erosion

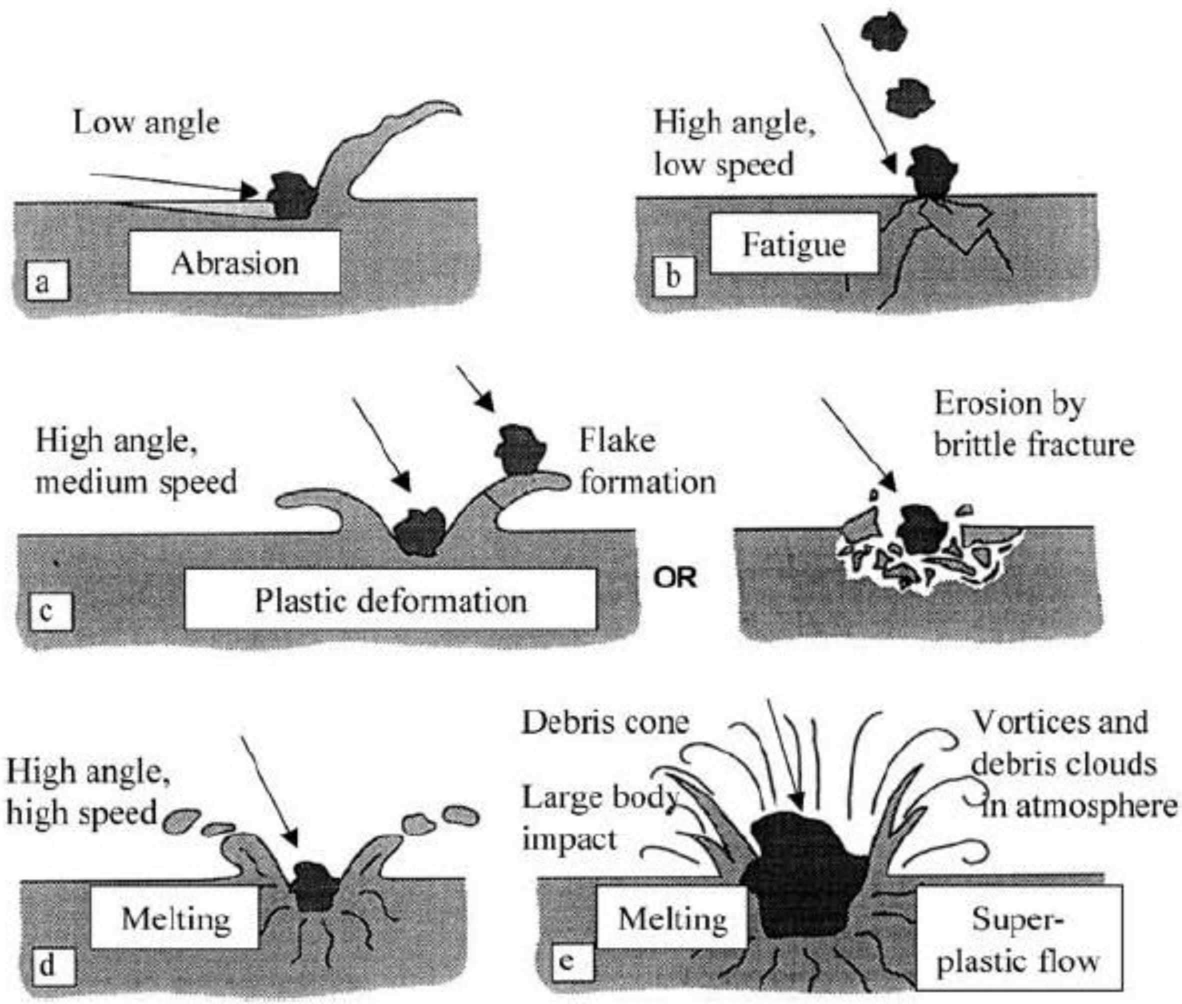

Figure 2 Possible mechanisms of solid particle erosion; (a) abrasion at low impact angles, (b) surface fatigue during low speed, high impingement angel, (c) brittle fracture or multiple plastic deformation during medium speed, large impingement angle, (d) surface melting at high impact speeds, (e) macroscopic erosion with secondary effects (after [12]).

Compression after impact

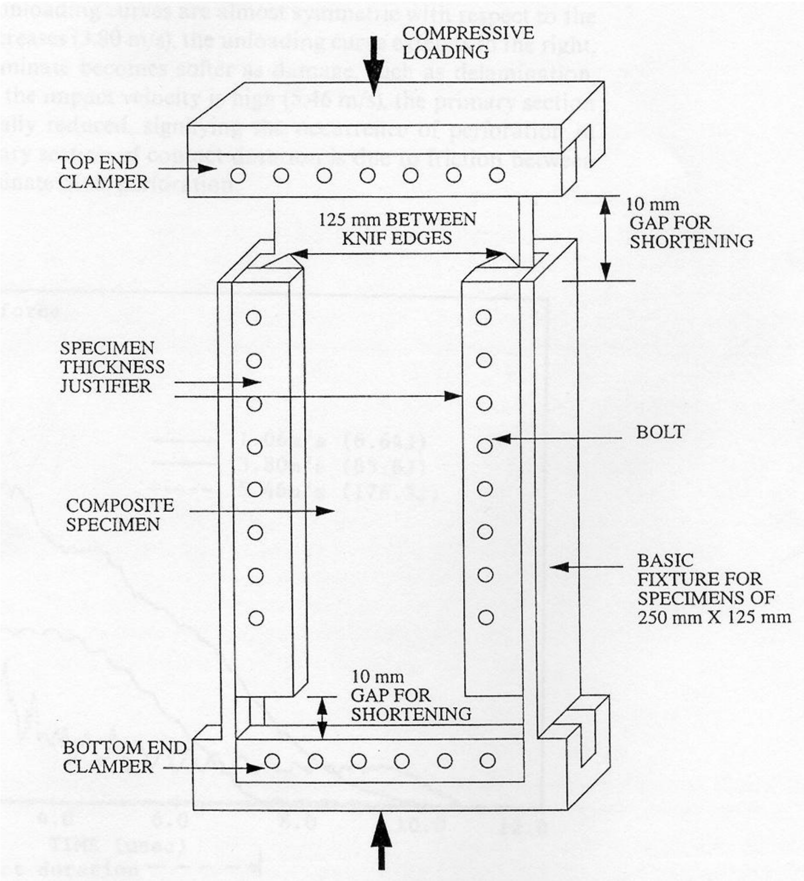

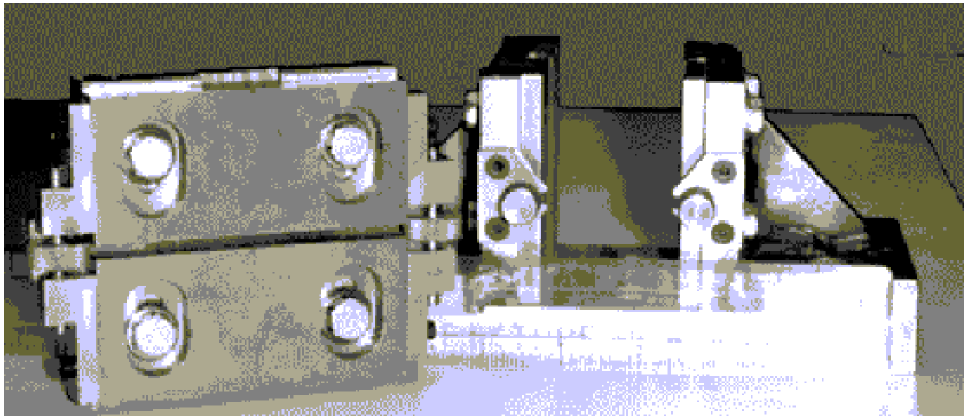

Paul J. Hogg, NOVEL TOUGHENING CONCEPTS FOR LIQUID COMPOSITE MOULDING

Compression after Impact : specimens and jig

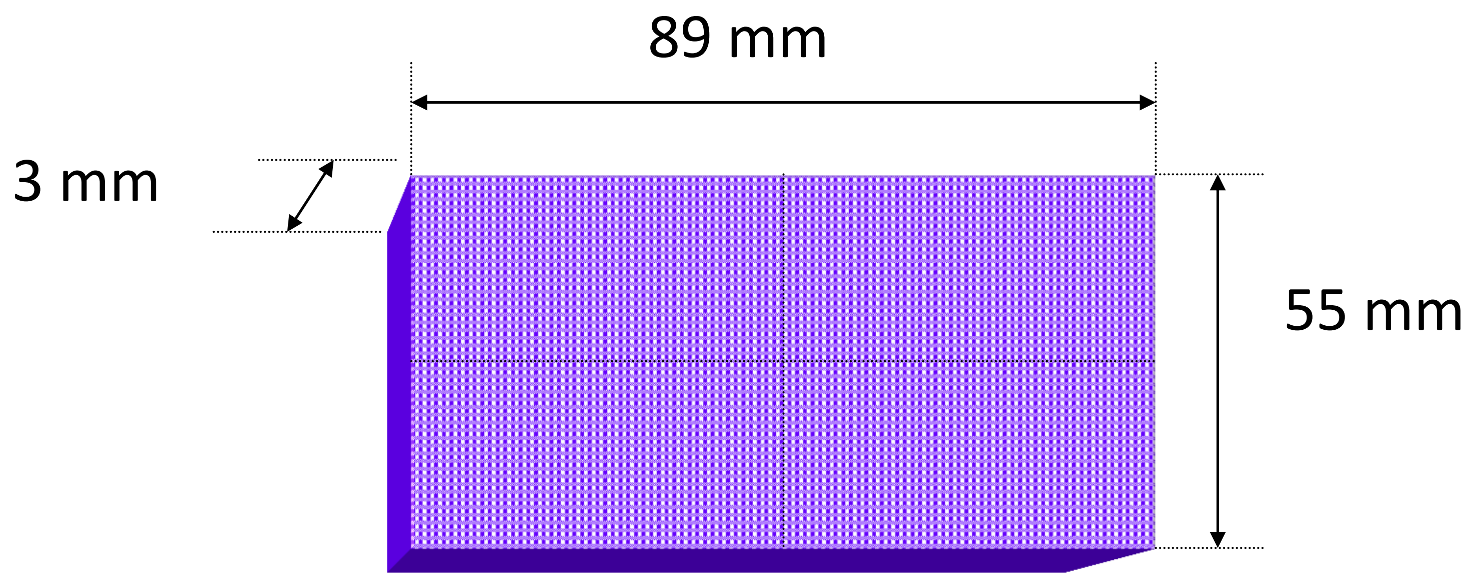

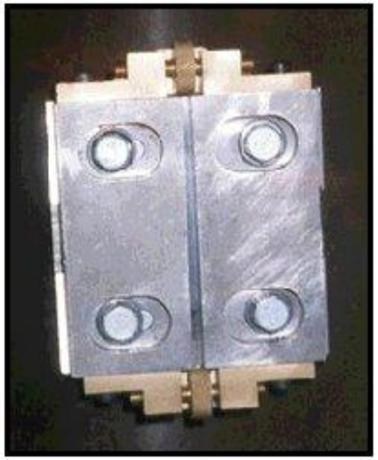

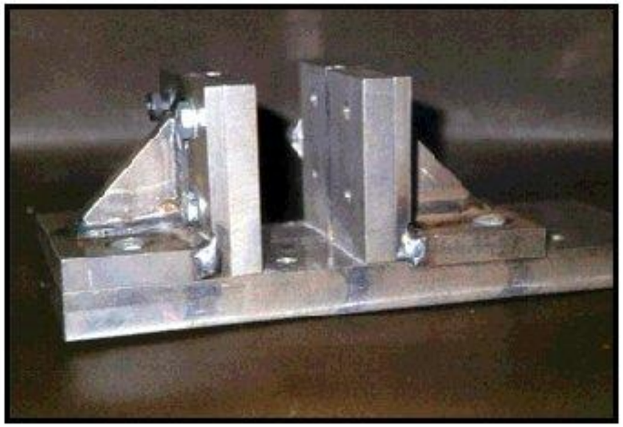

Paul J. Hogg, NOVEL TOUGHENING CONCEPTS FOR LIQUID COMPOSITE MOULDING

Residual strength after impact

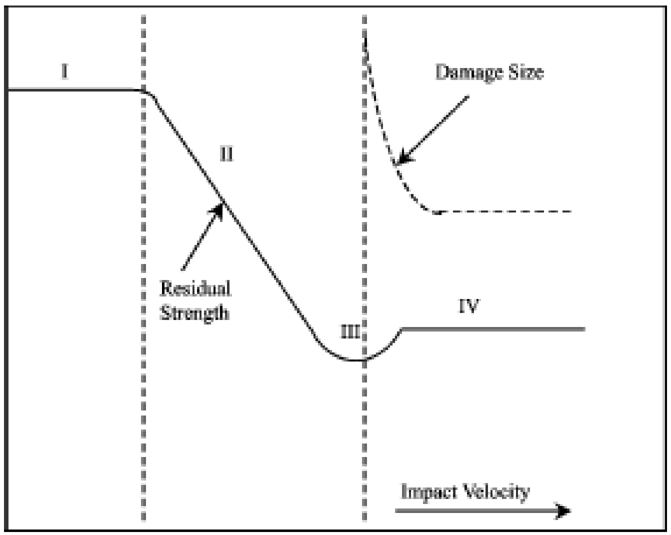

Figure 20 Schematic representation of the residual static strength in an impact damaged laminate.

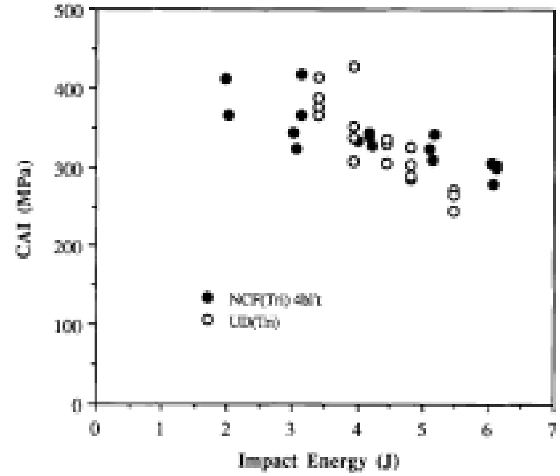

Figure 21 Typical residual compressive strength data vs. impact energy for a noncrimp fabric and comparable UD carbon fiber/epoxy quasi-isotropic laminate (after Kemp and Curtis, 1996).

PAUL T. CURTIS, DERA, Farnborough, UK, Volume 5, Ch 5.08 of Comprehensive Composite Materials

Residual strength after impact

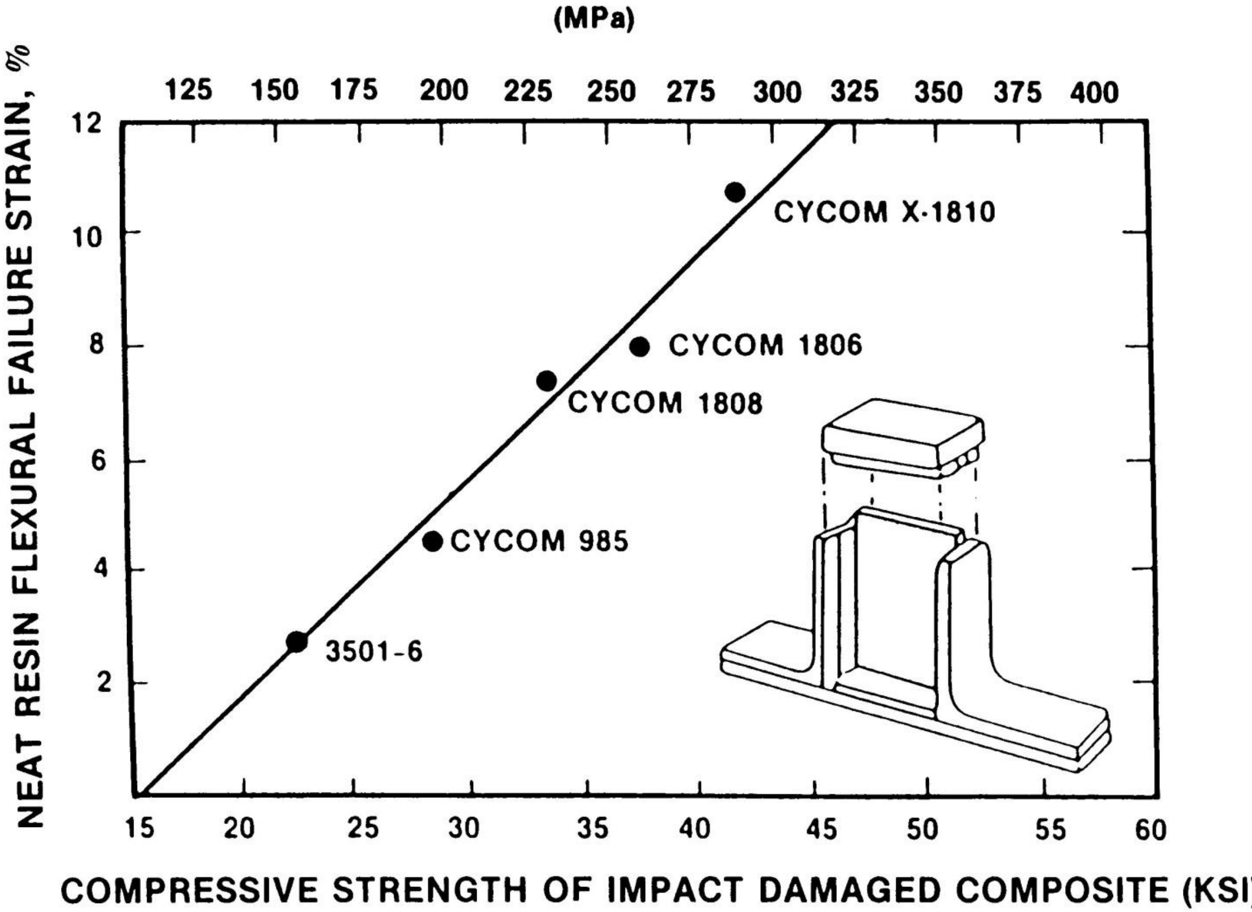

Key resin properties.....strain to failure

Paul J. Hogg, NOVEL TOUGHENING CONCEPTS FOR LIQUID COMPOSITE MOULDING

Fatigue

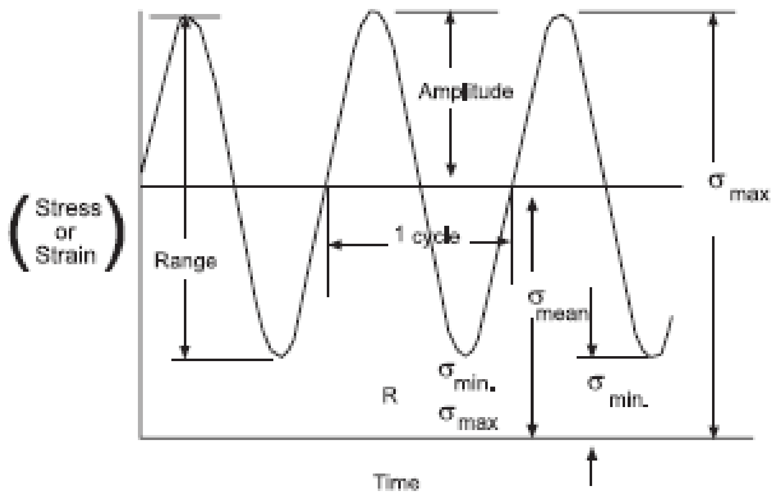

Figure 1 Typical applied stress–strain–time diagram for fatigue loading.

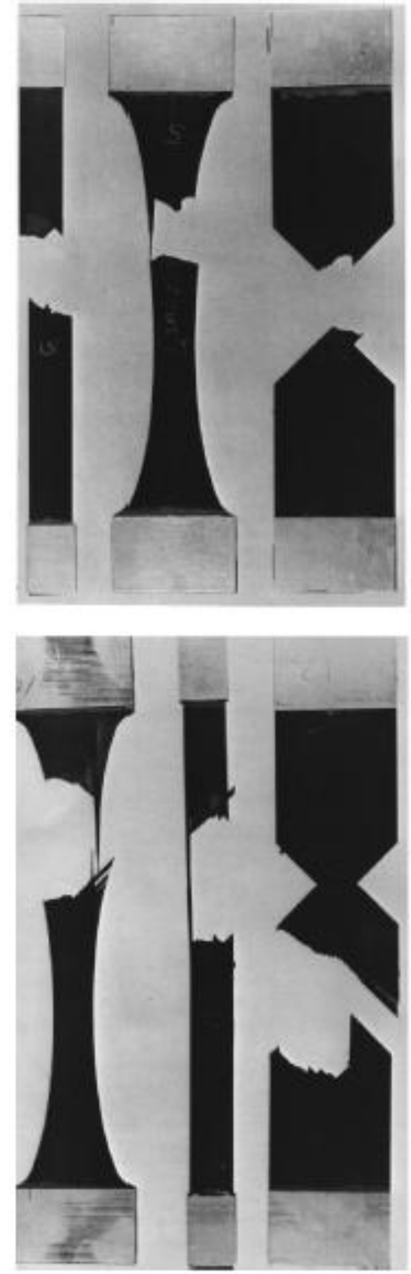

Figure 2 Coupons with varying gauge profiles tested: (a) statically, (b) fatigue.

PAUL T. CURTIS, DERA, Farnborough, UK, Volume 5, Ch 5.08 of Comprehensive Composite Materials

Fatigue

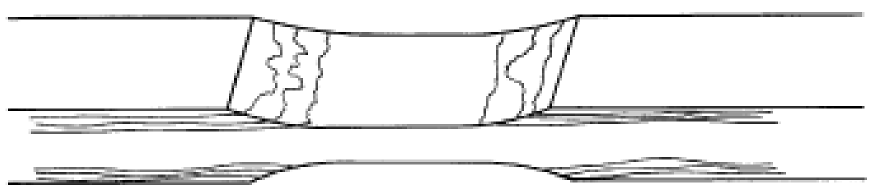

Figure 4 UD fatigue coupon—schematic showing split growth back to grips.

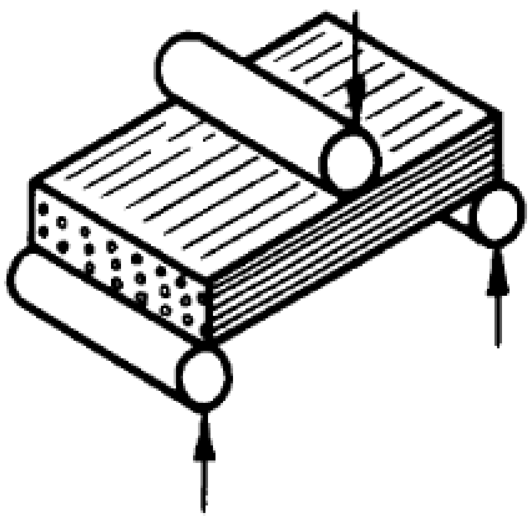

Figure 7 Interlaminar shear test specimen.

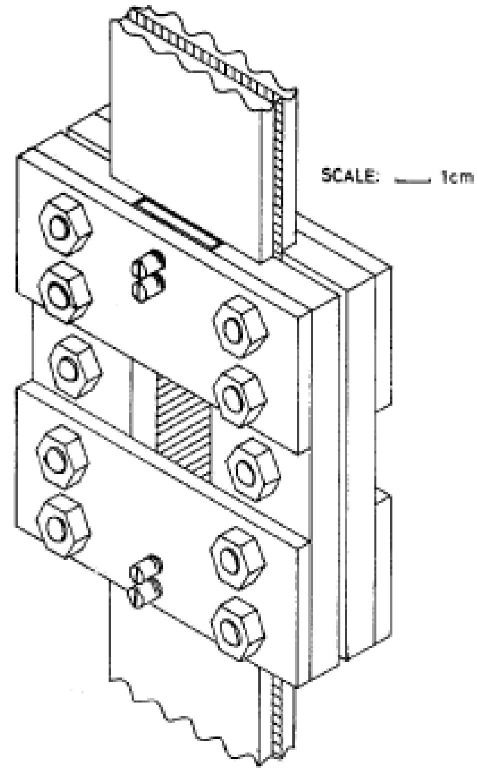

Figure 6 Typical antibuckling guide.

PAUL T. CURTIS, DERA, Farnborough, UK, Volume 5, Ch 5.08 of Comprehensive Composite Materials

Fatigue

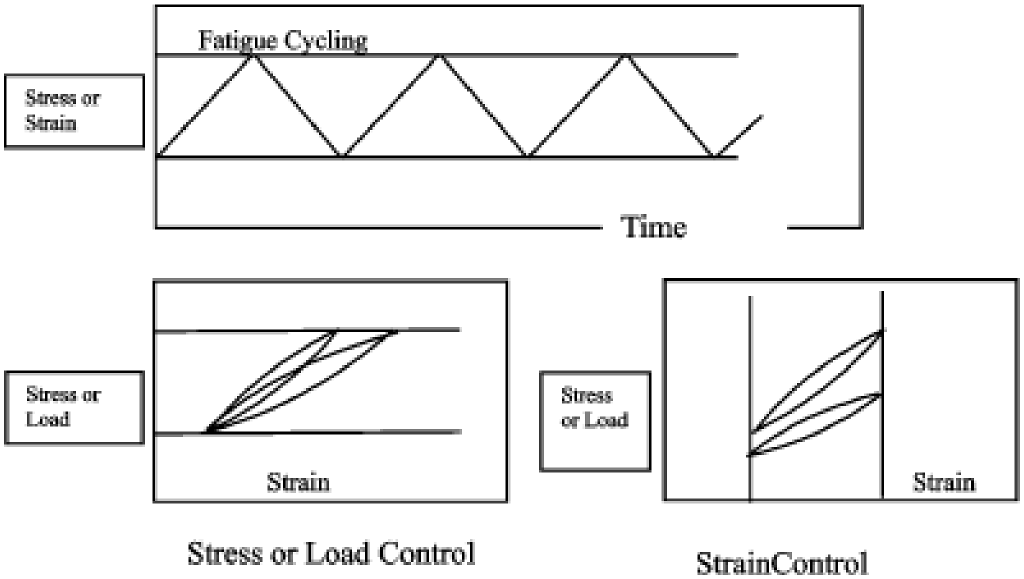

Figure 9 (a) Fatigue cycling under stress or strain. Differences in (b) stress-controlled and (c) strain-controlled fatigue tests of polymeric composites.

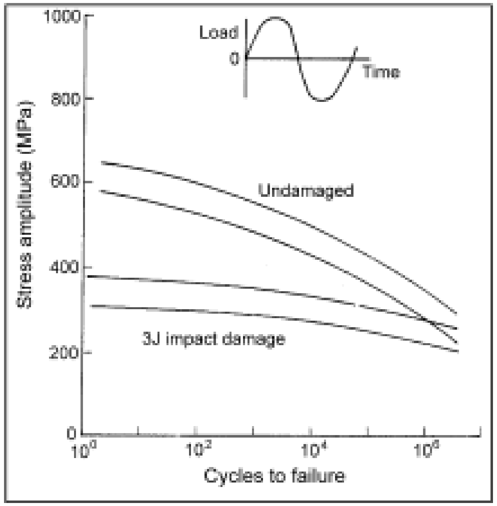

Figure 15 Convergence of S–N behavior for undamaged and impact damaged materials in fatigue at long lifetimes.

PAUL T. CURTIS, DERA, Farnborough, UK, Volume 5, Ch 5.08 of Comprehensive Composite Materials

Creep

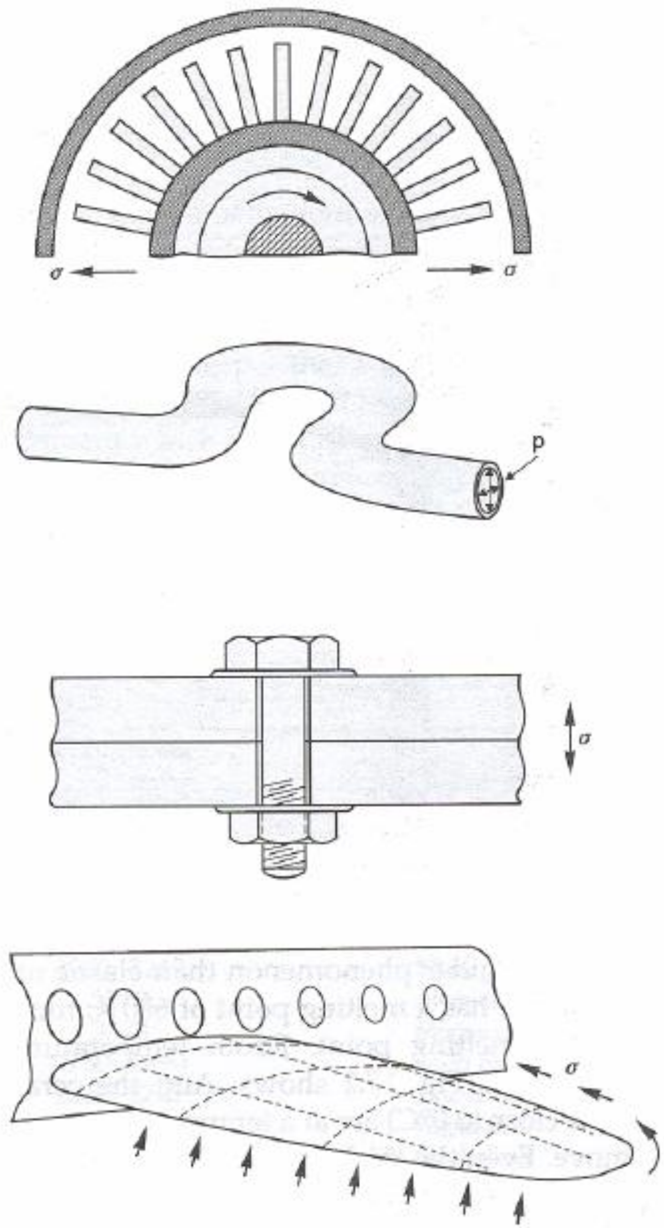

Four Design Classes

where creep is important

- Displacement-limited applications,
in which precise dimensions must be maintained (the disks and blades of turbine)
- Rupture-limited applications,
in which dimensional tolerance is relatively unimportant, but fracture must be avoided (as in pressure-piping)
- Stress-relaxation-limited applications,
in which an initial tension relaxes with time (as in the pretensioning of cables or bolts)
- Buckling-limited applications,
in which slender columns or panels carry compressive load
(upper wing skin of an aircraft)

Creep

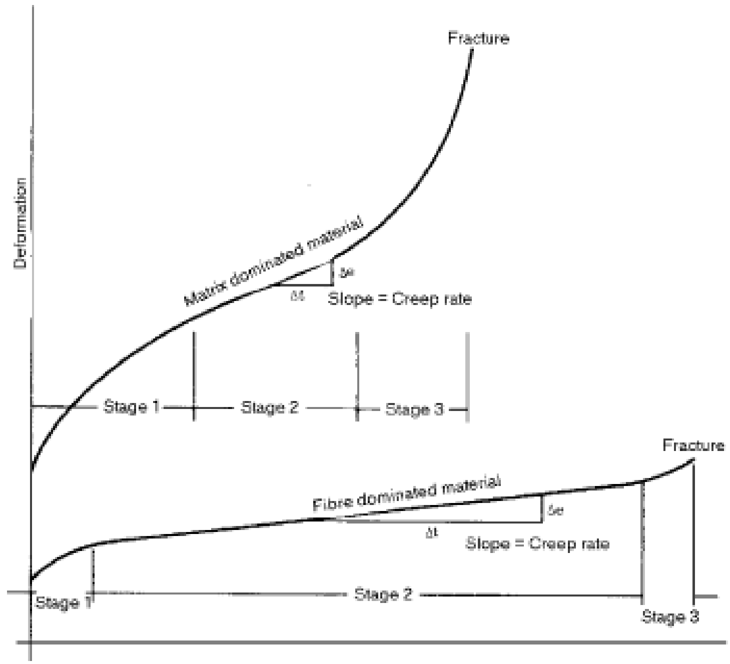

Figure 23 Schematic creep rupture behavior of a polymer matrix composite showing deformatic

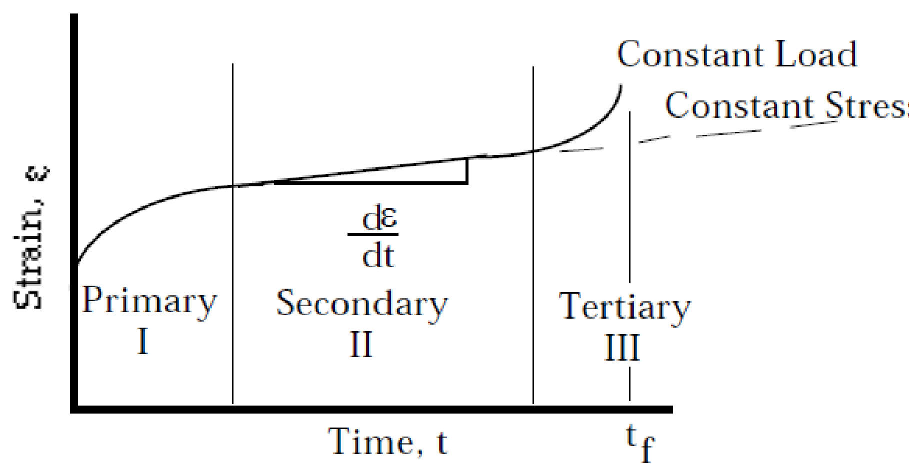

Figure 8.3 Strain time curve for a creep test

PAUL T. CURTIS, DERA, Farnborough, UK, Volume 5, Ch 5.08 of Comprehensive Composite Materials

Creep

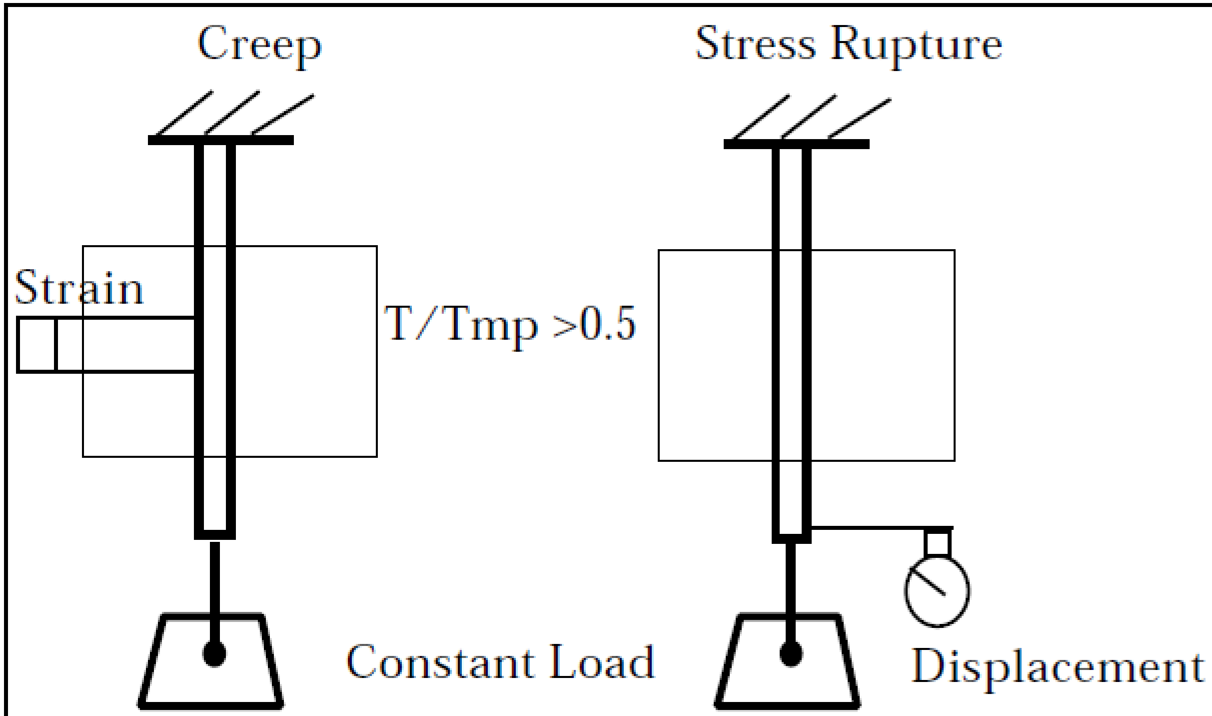

- Low Loads
- Precision Strain Measurement (ε f<0.5%)
- Long term (2000-10,000 h)
- Expensive equipment

Emphasis on minimum strain rate at stress and temperature

- High Loads
- Gross Strain Measurement (ε f up to 50%)
- Short term (<1000 h)
- Less expensive equipment

Emphasis on time to failure at at stress and temperature

Creep

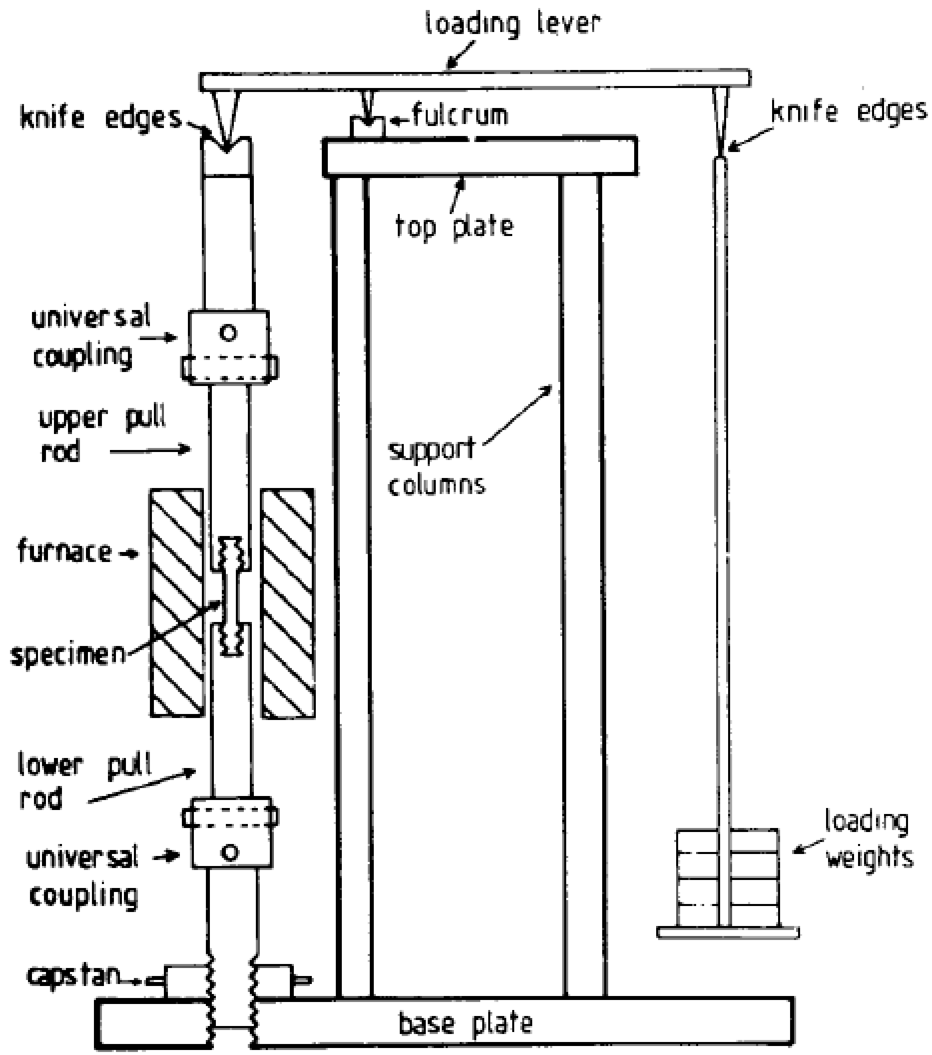

Figure 8.2 Typical creep test set-up

Test Methods for Physical Properties

MARK J. PARKER, BAE SYSTEMS (Warton), Lancashire, UK

Volume 5, Ch 5.09 of Comprehensive Composite Materials

FIBER/VOID VOLUME FRACTIONS AND FIBER DIRECTION

MOISTURE ABSORPTION AND CONDITIONING OF COMPOSITE MATERIALS

Mechanism of Moisture Absorption

Effects of Moisture Absorption

THE GLASS TRANSITION

DIFFERENTIAL SCANNING CALORIMETRY

DYNAMIC MECHANICAL ANALYSIS

THERMOPHYSICAL PROPERTIES

POLYMER COMPOSITE MATERIAL DEGRADATION

FIBER/VOID VOLUME FRACTIONS AND FIBER DIRECTION

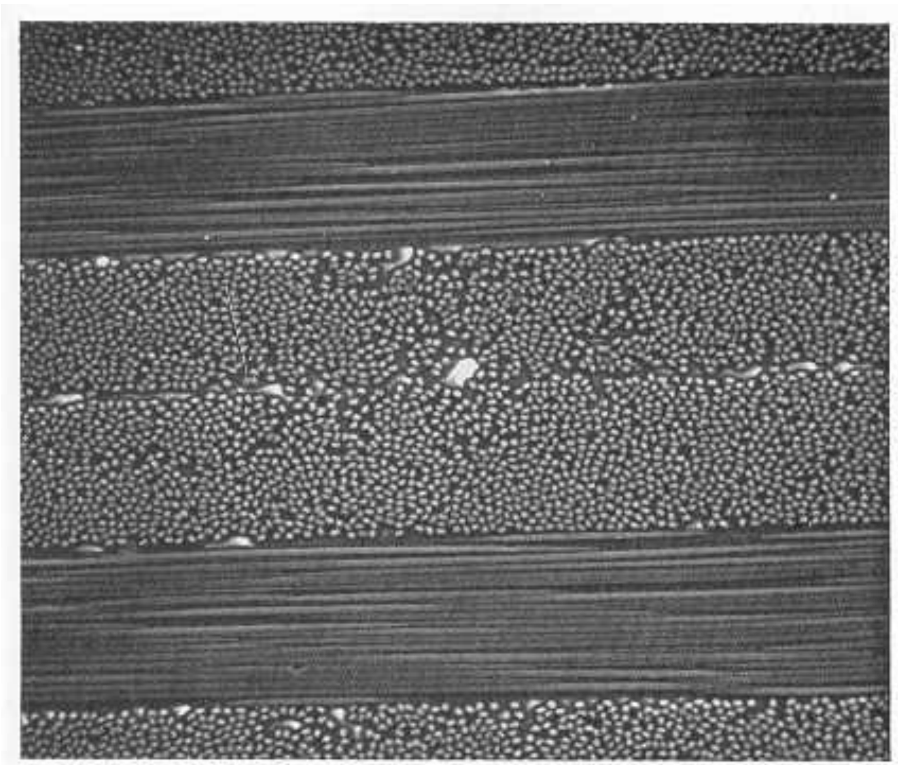

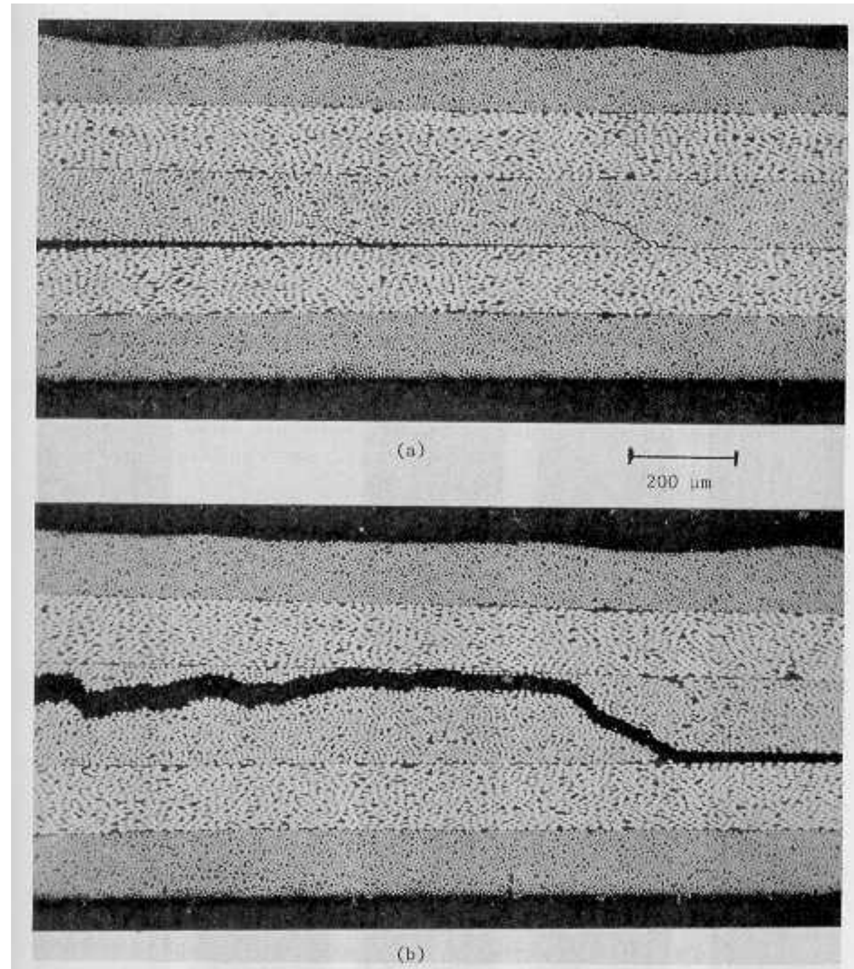

FIBER/VOID VOLUME FRACTIONS AND FIBER DIRECTION

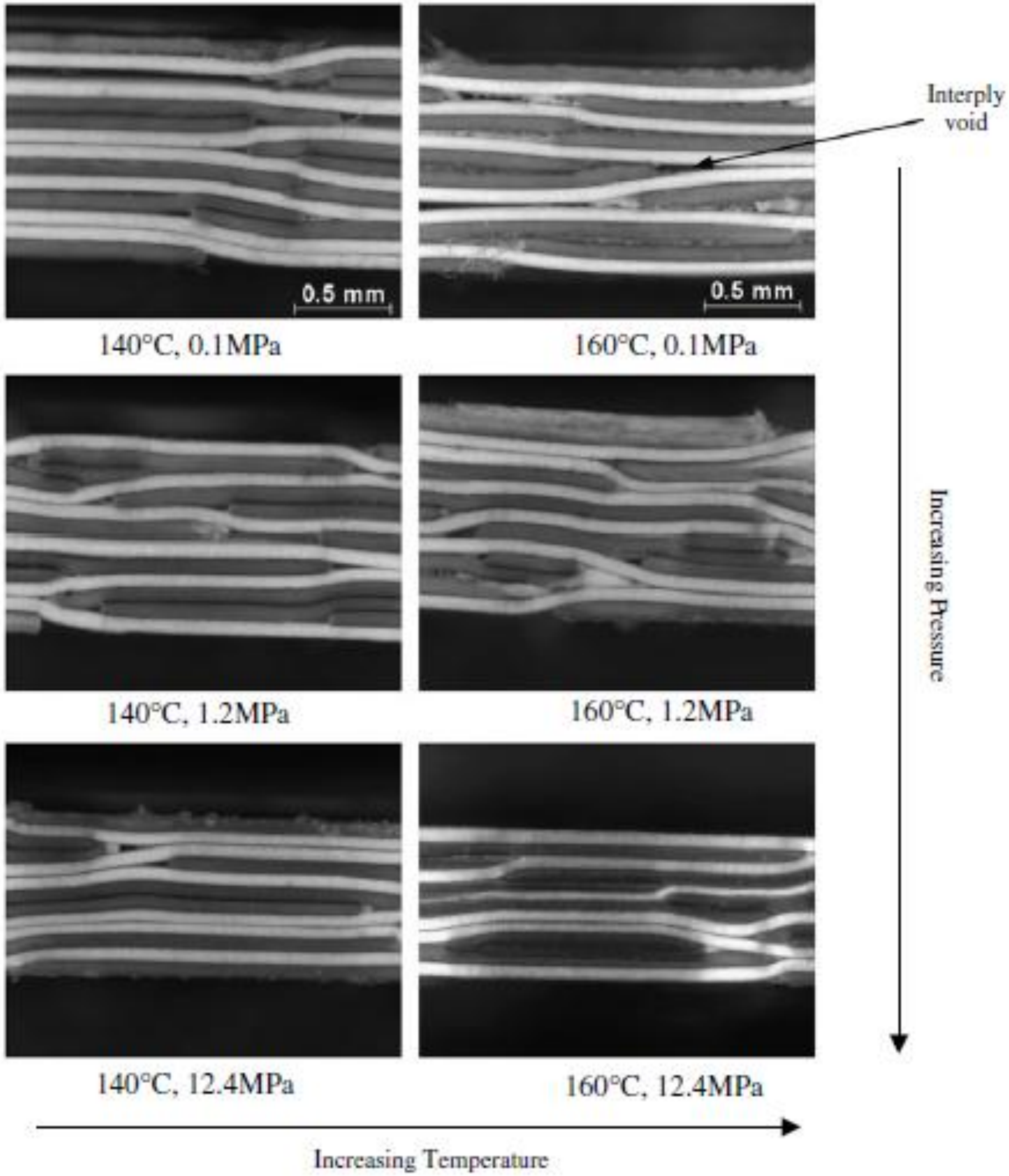

Moisture absorption

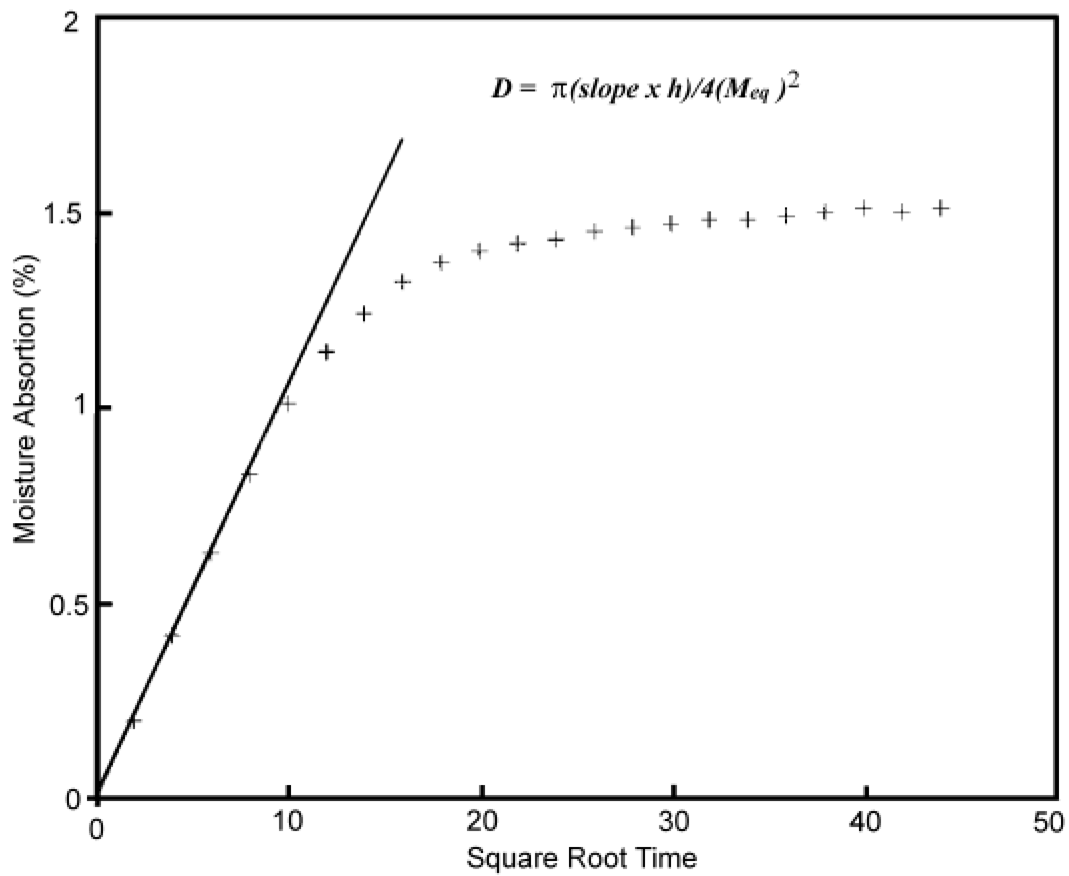

Figure 1 Plot of moisture content vs. time$^{1/2}$ (and determination of diffusion constant) for a material obeying Fick's law.

MARK J. PARKER, *Volume 5, Ch 5.09 of Comprehensive Composite Materials*

Moisture absorption

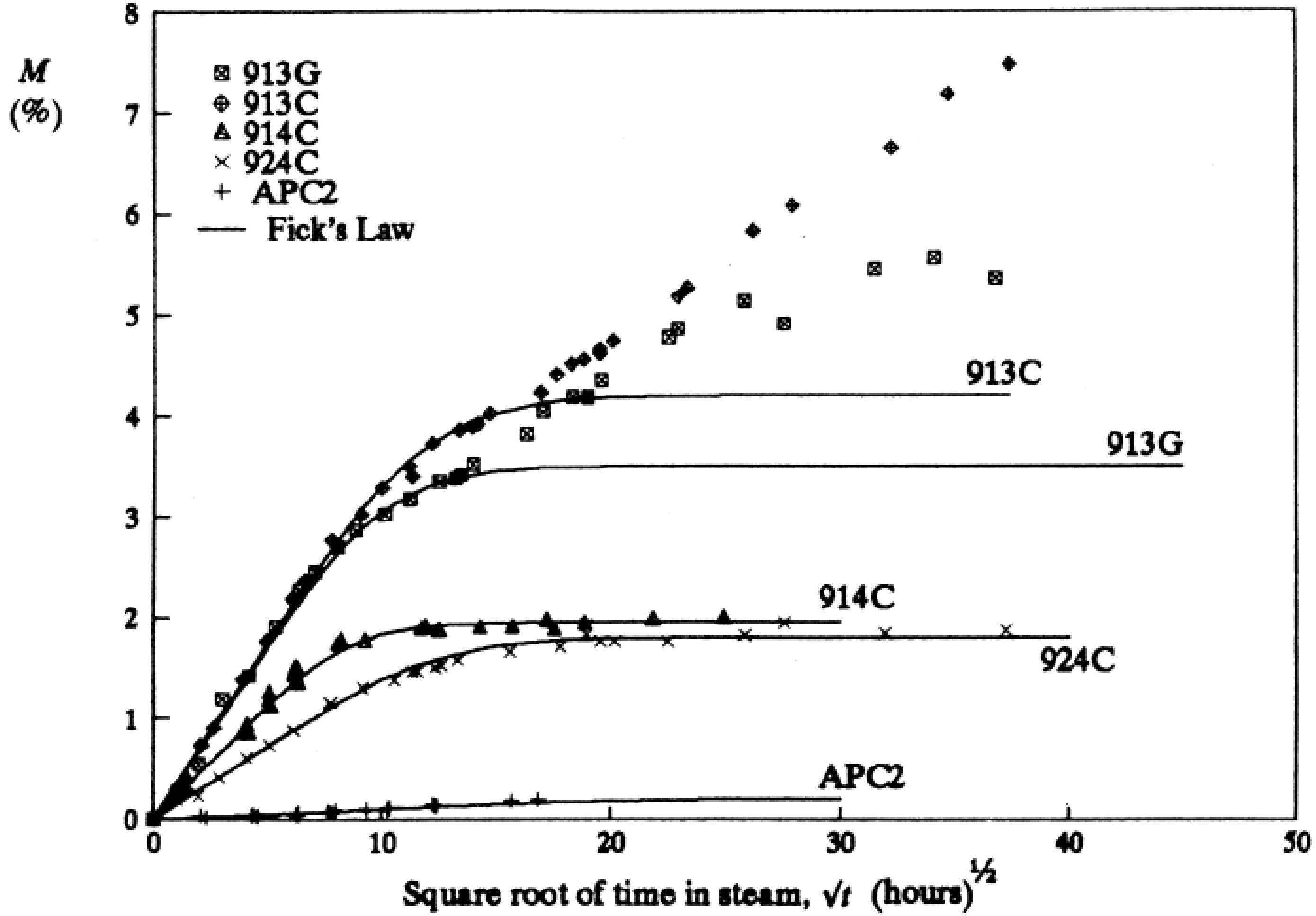

Figure 2 Percentage mass increase for five composite materials in steam as a function of the square root of time (*Comp. Sci. and Tech.*, 1996, **56**, 977, reproduced by permission of Elsevier).

MARK J. PARKER, *Volume 5, Ch 5.09 of Comprehensive Composite Materials*

Environmental testing

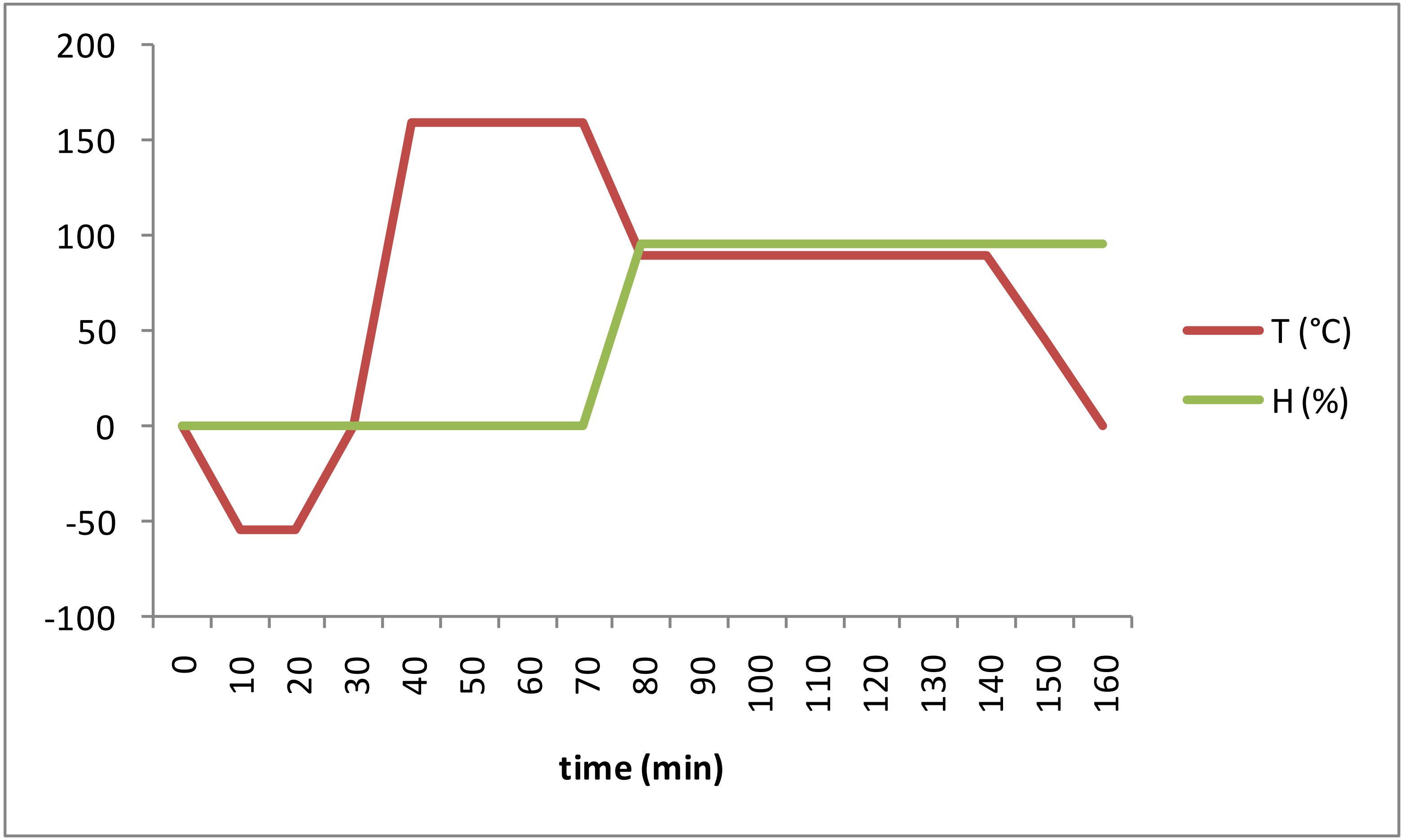

Temperature and relative humidity representative cycles reproduced after Reynolds and Mc Manus (Reynolds and Mc Manus 2000)

Environmental testing

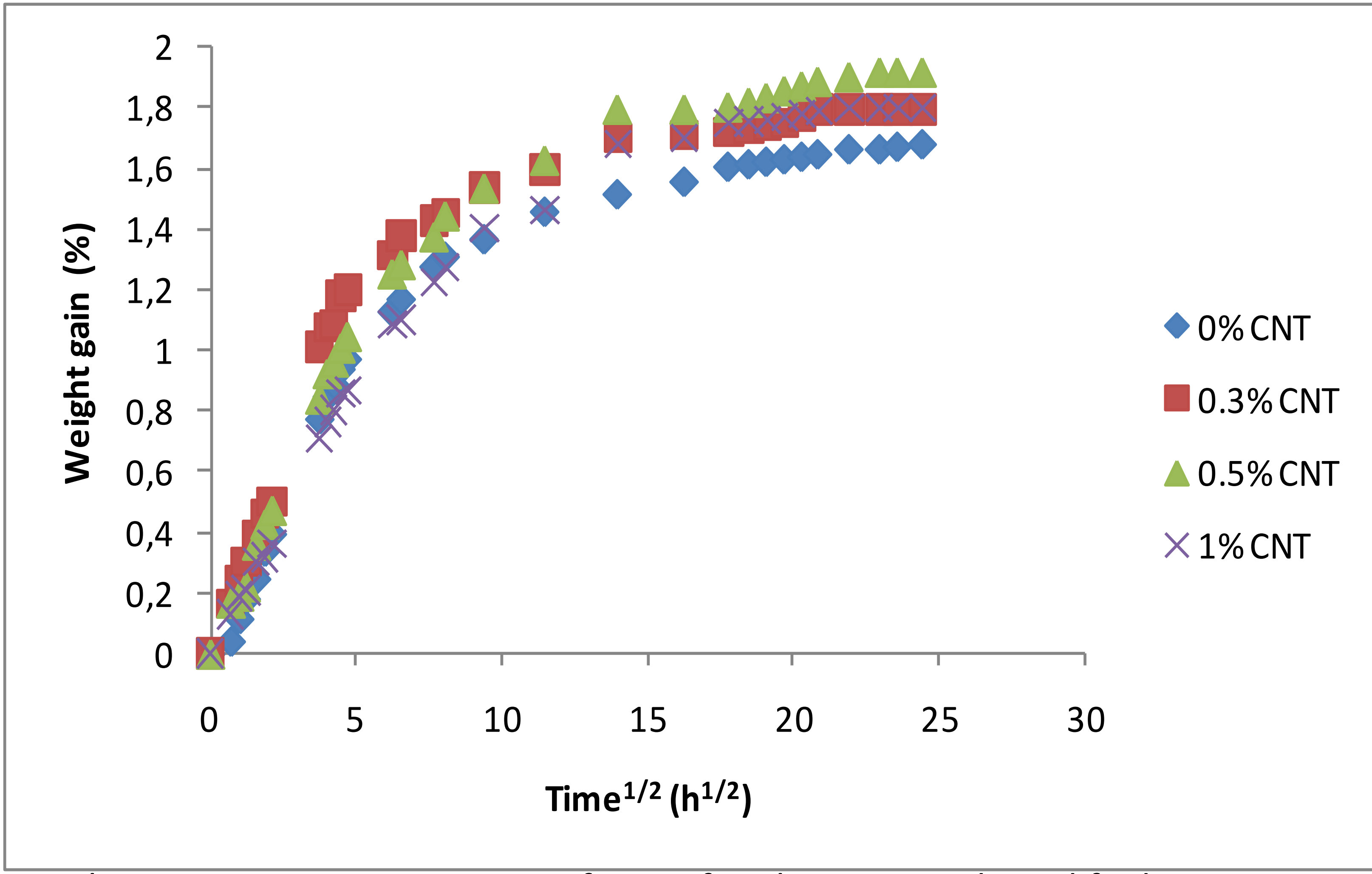

Weight gain versus square root of time for the neat and modified epoxy matrices reproduced after Barkoula et al. (Barkoula et al. 2009)

DSC

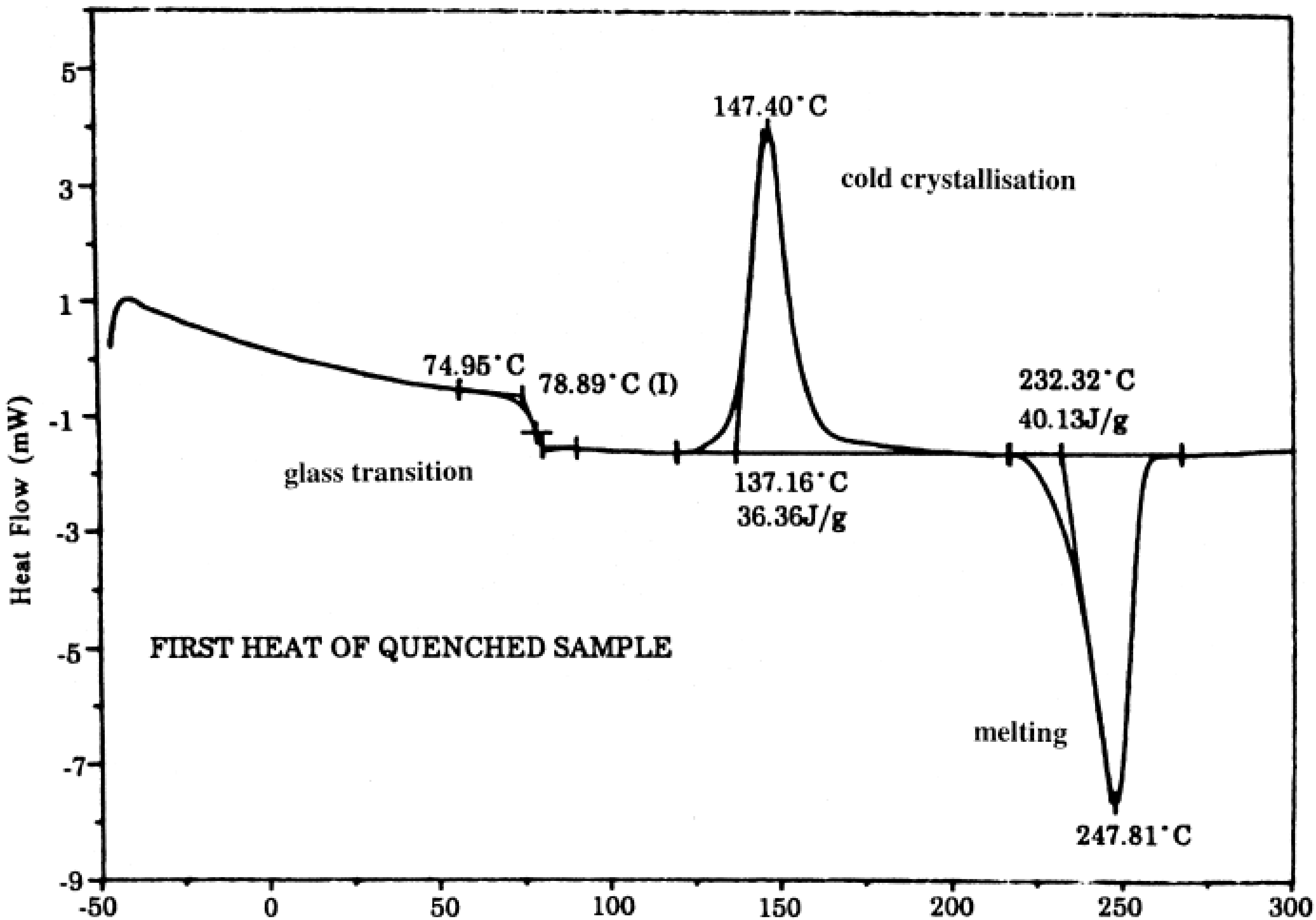

Figure 6 A DSC thermogram showing three transitions for a polyethyleneterephtalate specimen under dynamic heating (recreated with permission from TA Instruments Ltd.).

MARK J. PARKER, *Volume 5, Ch 5.09 of Comprehensive Composite Materials*

DSC

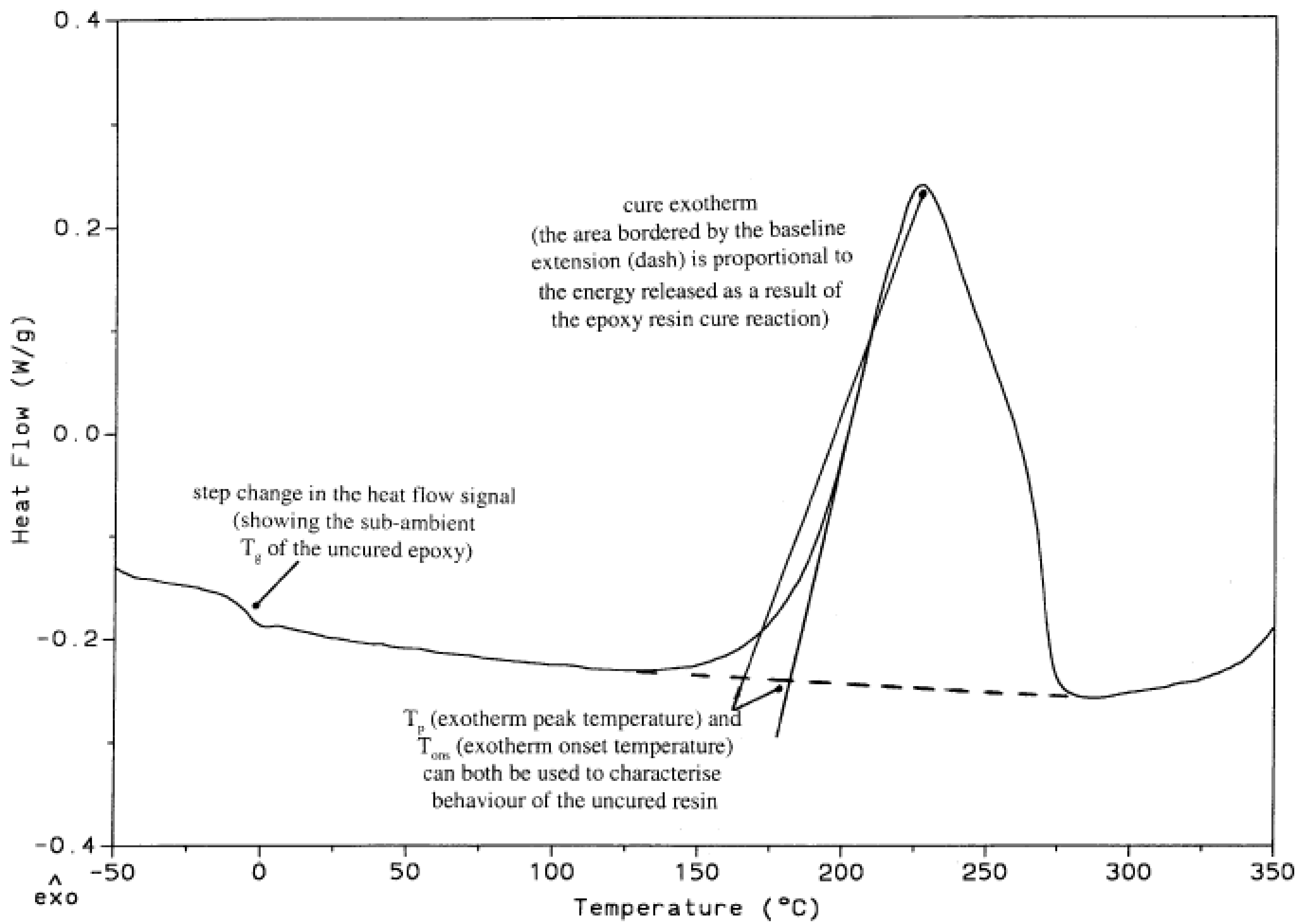

Figure 7 DSC thermogram of a high-temperature epoxy/carbon fiber prepreg (using EFA-CFC-TP-017), indicating the key thermal transitions.

MARK J. PARKER, *Volume 5, Ch 5.09 of Comprehensive Composite Materials*

DMA

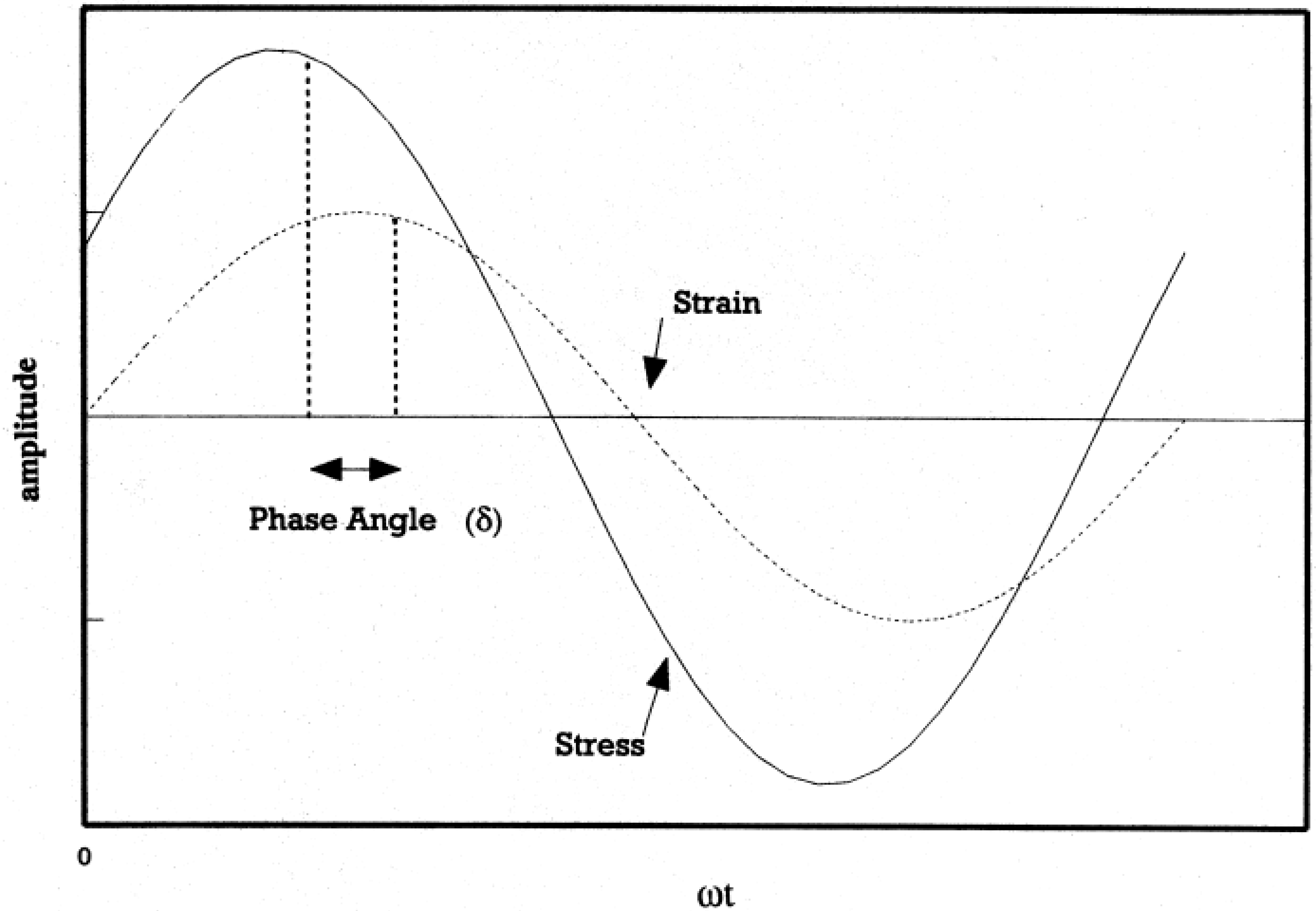

Figure 13 Diagram showing the phase angle between stress and strain in a viscoelastic material.

MARK J. PARKER, *Volume 5, Ch 5.09 of Comprehensive Composite Materials*

DMA

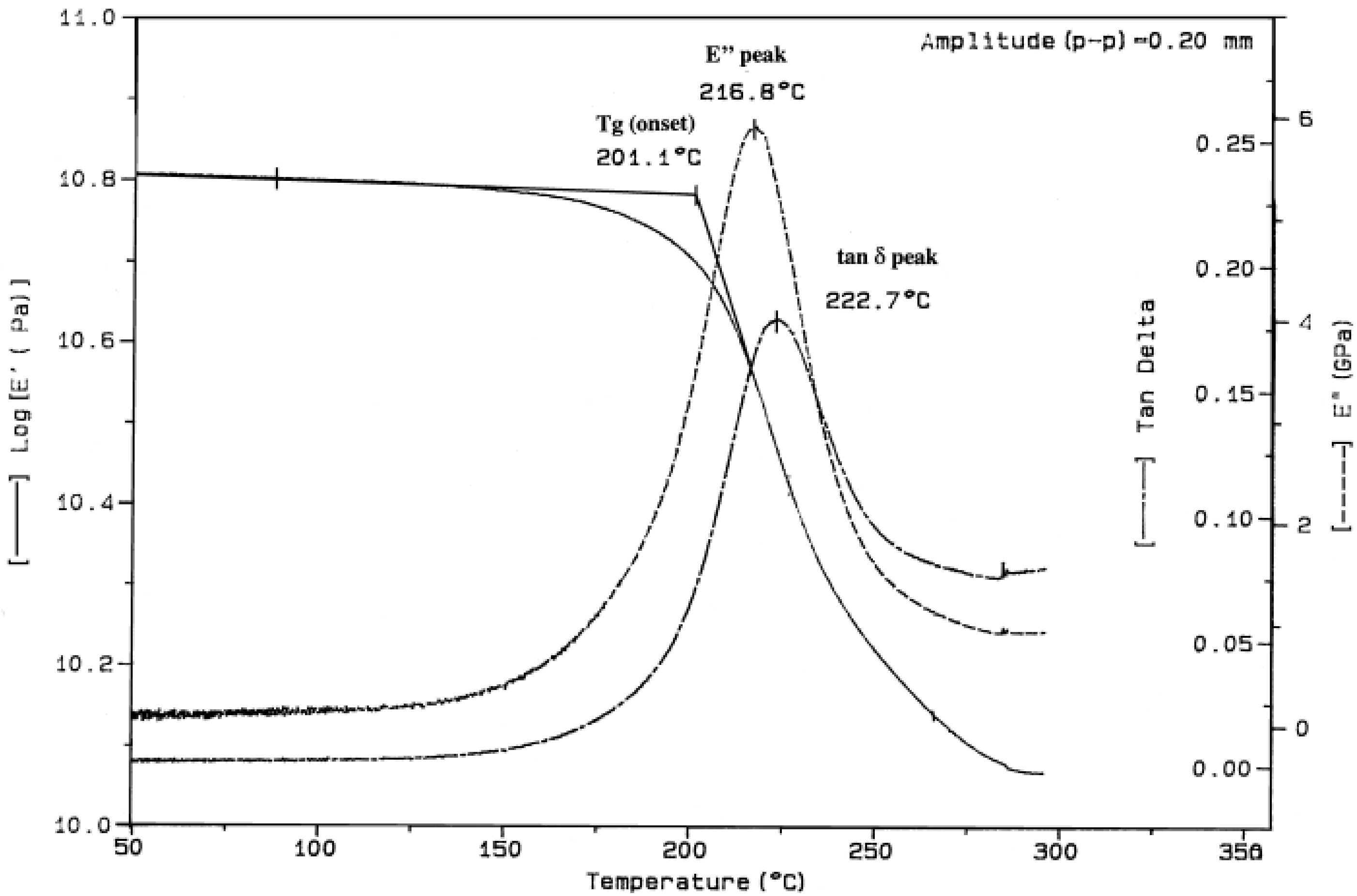

Figure 3 Dynamic mechancial analysis of a carbon/epoxy specimen showing the major response curves and the determination of T_g (onset), peak E" and peak tan δ.

MARK J. PARKER, *Volume 5, Ch 5.09 of Comprehensive Composite Materials*

DMA

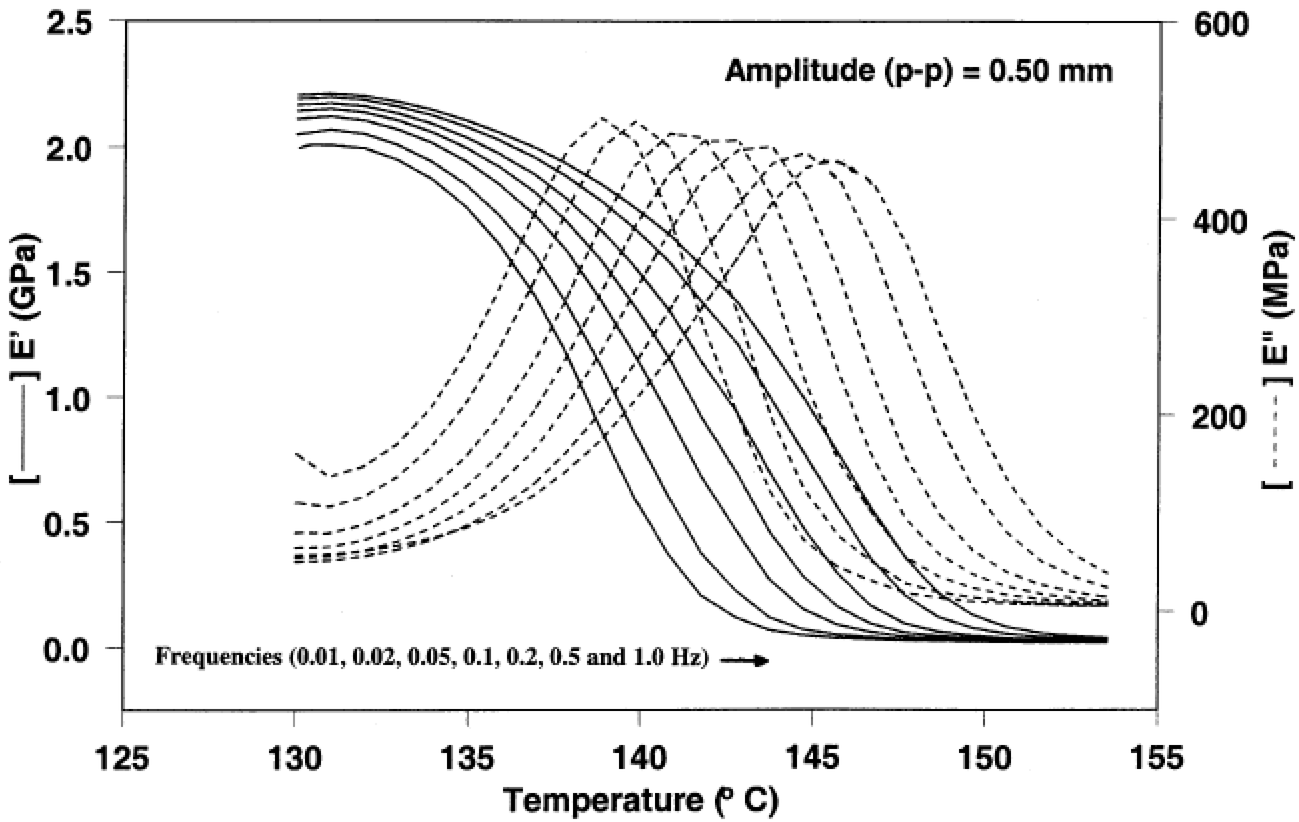

Figure 14 DMA thermograms of polycarbonate showing the variation in *E'* (drop off) and *E''* (peak) with the test frequency (recreated with permission from TA Instruments Ltd.).

MARK J. PARKER, *Volume 5, Ch 5.09 of Comprehensive Composite Materials*

DMA

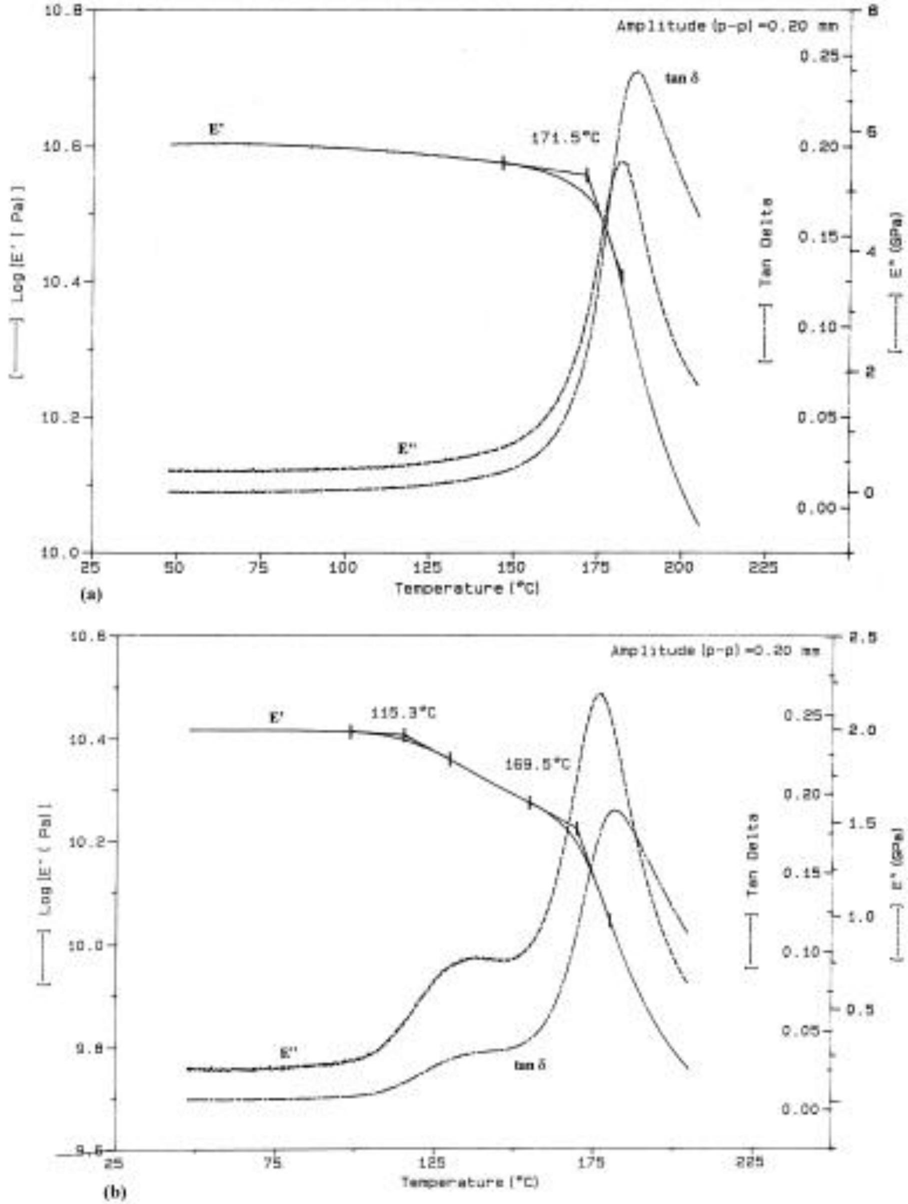

Figure 20 DMA thermograms showing the testing of wet conditioned specimens of an RTM laminate (a) without binder and (b) including a binder system.

MARK J. PARKER, *Volume 5, Ch 5.09 of Comprehensive Composite Materials*